DEPARTMENT OF MOLECULAR AND CLINICAL PHARMACOLOGY,
INSTITUTE OF TRANSLATIONAL MEDICINE,
UNIVERSITY OF LIVERPOOL

THE POTENTIAL ROLE OF LIVER SINUSOIDAL ENDOTHELIAL CELLS IN DRUG-INDUCED LIVER INJURY

Thesis submitted in accordance with the requirements of the University of Liverpool for the degree of Doctor in Philosophy

James Adebola Akingbasote

November, 2016

DECLARATION

This thesis is the result of my own work. The material contained within this thesis has not been presented, nor is currently being presented, either wholly or in part for any degree or other qualifications.

James Adebola Akingbasote

This research was carried out in the MRC Centre for Drug Safety Science, Department of Pharmacology and Therapeutics, The University of Liverpool.

TABLE OF CONTENTS

2.0 CHAPTER TWO: MATERIALS AND METHODS

3.0 CHAPTER THREE: CHARACTERISATION OF ISOLATED HUMAN LIVER SINUSOIDAL ENDOTHELIAL CELLS

4.0 CHAPTER FOUR: EFFECTS OF HEPATOTOXIC DRUGS ON HUMAN LIVER SINUSOIDAL ENDOTHELIAL CELLS *IN VITRO*

5.0 CHAPTER FIVE: LIVER SINUSODIAL ENDOTHELIAL CELLS IN A CO-CULTURE LIVER MICROTISSUE SYSTEM

6.0 CHAPTER SIX: OVERALL DISCUSSION

LIST OF TABLES

LIST OF FIGURES

CHAPTER ONE: GENERAL INTRODUCTION

CHAPTER THREE: CHARACTERISATION OF ISOLATED HUMAN LIVER SINUSOIDAL ENDOTHELIAL CELLS

CHAPTER FOUR: EFFECTS OF HEPATOTOXIC DRUGS ON HUMAN LIVER SINUSOIDAL ENDOTHELIAL CELLS IN VITRO

CHAPTER FIVE: LIVER SINUSODIAL ENDOTHELIAL CELLS IN A CO-CULTURE LIVER MICROTISSUE SYSTEM

CHAPTER SIX: OVERALL DISCUSSION

ABSTRACT

Liver sinusoidal endothelial cells (LSEC) constitute a unique population of endothelial cells with specialised liver-specific morphologic features and functions. LSEC are the only endothelial cells with fenestrations and which lack an organised basement membrane. They are involved in hepatic stellate cell (HSC) quiescence, endocytosis of small particles, selective transfer of substances from the blood, in the hepatic sinusoid, to the parenchymal cells and in liver regeneration. As the group of cells that form the inner lining of the capillaries of the liver sinusoids, and being the first to be in contact with blood-borne particles, pathogens, and xenobiotics, they are prone to the deleterious effects of these. The aims of this thesis were to investigate the unique features of human liver sinusoidal endothelial cells (HLSEC) in comparison with endothelial cells from other vascular beds, evaluate the sensitivities of HLSEC to a range of hepatotoxic drugs, including small-molecule receptor tyrosine kinase inhibitors (RTKIs), such as regorafenib, and to explore the role of HLSEC in a triculture human liver microtissue.

Results obtained from this study showed that HLSEC expressed phenotypic features of vascular and lymphatic endothelial cells, particularly vascular endothelial growth factor receptor 2 (VEGFR-2) which could be activated by VEGF-A to stimulate cell proliferation, migration and tubular morphogenesis. HLSEC also expressed functional VEGFR-3. Transcriptomic analysis indicated that HLSEC expressed specialised genes, such as *plasmalemma vesicle associated protein (PLVAP*), that support its liver-specific structure and functions. HLSEC were more sensitive to a range of small-molecule receptor tyrosine kinase inhibitors than other hepatic cells

(primary human hepatocytes [PHH] and human hepatic fibroblasts [HHF]) and endothelial cells from other vascular beds (human dermal microvascular endothelial cells and human dermal lymphatic endothelial cells). Regorafenib inhibited the activation of VEGFR-2 thereby abrogating cell proliferation, migration, tubular morphogenesis as well as upregulation of angiocrine factors involved in liver regeneration following activation by vascular endothelial growth factor A (VEGF-A). Regorafenib also caused a disruption of cytoskeletal structure of HLSEC and induced apoptosis via activation of caspase 3. Triculture liver microtissues formed with PHH, HLSEC and HHF were vascularised with higher expression of liver-specific drug-metabolising enzymes in comparison with the same combination of cells cultured as a monolayer. However, metabolic competence of triculture liver microtissues was significantly lower than in their monoculture counterparts (consisting of PHH only).

This study has further confirmed the uniqueness of HLSEC as a specialised endothelial cell adapted to its anatomical role, which could respond to a range growth factors to initiate endothelial cell-specific functions. It has also been demonstrated that HLSEC are a direct target of hepatotoxic drugs. Triculture liver microtissues generated with PHH, HLSEC and HHF showed less metabolic competence than their PHH-only counterparts. Future studies need to investigate the role of RTKIs in vascular toxicity using *in vivo* models of sinusoidal obstruction syndrome (SOS) and liver regeneration. Finally, it would be informative to investigate the possibility of identifying HLSEC-specific biomarkers of liver toxicity.

LIST OF ABBREVIATIONS

ALT: Alanine transaminase
ANOVA: Analysis of variance
APAP: Acetaminophen (paracetamol)
AST: Aspartate transaminase
ATP: adenosine triphosphate

BCA: Bicinchoninic Acid
BEC: Biliary epithelial cells
BSA: Bovine serum albumin

Ca2+: Calcium
cDNA: complementary DNA
CPT-1: Carnitine palmitoyltransferase-1
CYP: Cytochrome P450
CYP2C9: Cytochrome P450 family 2 subfamily C member 9
CYP2D6: Cytochrome P450 family 2 subfamily D member 6
CYP2E1: Cytochrome P450 family 2 subfamily E member 1
CYP3A4: Cytochrome P450 family 3 subfamily A member 4

DE: differentially-expressed
DILI: drug-induced liver injury
DMEM: Dulbecco's modified Eagle's medium
DMSO: Dimethyl sulphoxide
DNA: Deoxyribonucleic acid
dNTP: Deoxyribonucleotide triphosphate

EC: Expression console
ECM: Extracellular matrix
EDTA: ethylenediaminetetraacetic acid
EGF: epidermal growth factor
eNOS: endothelial nitric oxide synthase
EP-CAM: epithelial cell adhesion molecule
ERK: extracellular signal–regulated kinase

FAK: focal adhesion kinase
FBS: Fetal bovine serum
FDR: False discovery rate
FGF: fibroblast growth factor
FGFR: fibroblast growth factor receptor
GAPDH: Glyceraldehyde 3-phosphate dehydrogenase

h: hour
H_2O: water
HDLEC: Human dermal lymphatic endothelial
HDMEC: Human dermal microvascular endothelial cells
HGF: Hepatocyte growth factor
HHF; human hepatic fibroblasts
HHSEC: Human hepatic sinusoidal endothalial cells

HLSEC: human liver sinusoidal endothelial cells
HRP: horseradish peroxidase
HSC: hepatic stellate cell
HTA: Human transcriptome array
HUVEC: Human umbilical vein endothelial cell

ID1: DNA-binding protein inhibitor
IF: immunofluorescence
IFN-γ: Interferon-γ
iNOS: inducible nitric oxide synthase
KC: Kupffer cell

L: Litre
LC-MS/MS: Liquid chromatography coupled with mass spectrometer
LDS: Lithium dodecyl sulphate
LSEC: liver sinusoidal endothelial cells
LSIGN: Liver/lymph node-specific intercellular adhesion molecule-3-grabbing integrin
LYVE-1: Lymphatic vessel endothelial hyaluronan receptor 1

m: Milli
min: Minutes
miRNA: microRNAs
MMP-9: Matrix metalloproteinase protein-9
mRNA: Messenger RNA

NAFLD: Non-alcoholic fatty liver disease
NAPDH: Nicotinamide adenine dinucleotide phosphate
NAPQI: N-acetyl-p-benzoquinone imine
NASH: Steatosis leading to non-alcoholic steatohepatitis
NHDF: Normal human dermal fibroblast

NO: nitric oxide
NPC: non-parenchymal cells
NRTKI: Non-receptor tyrosine kinase inhibitor

OCT: optimal cutting temperature

PBS: Phosphate-buffered saline
PCA: principal component analysis
PCR: Polymerase chain reaction
PDGF: platelet-derived growth factor
PDGFR: platelet-derived growth factor receptor
PFA: paraformaldehyde
PHH: primary human hepatocyte
PHX: Perhexiline
PIGF: placenta growth factor
PLVAP: Plasmalemma vesicle associated protein
POD: Podoplanin
PROX-1: Prospero homeobox protein 1

RIPA: Radioimmunoprecipitation assay
RMA: Robust Multi-array Average
RNA: Ribonucleic acid
rpm: revolutions per minute
RTKI: receptor tyrosine kinase inhibitor

s: second
SD: Standard deviation of the mean
SDS: Sodium dodecyl sulphate
SEM: scanning electron microscopy
SOS: Sinusoidal obstruction syndrome

TAC: transcriptome analysis console
TBS: Tris-buffered saline
TBST: Tris-buffered saline + tween
TEM: transmission electron microscopy
TKI: tyrosine kinase inhibitor
TRAIL: TNF-related apoptotic-inducing ligand

UK: United Kingdom
ULA: Ultra-low attachment
URAT1: Urate transporter 1
UGT1A1: uridine diphosphate glucuronosyltransferase family 1 polypeptide 1

v/v: volume/volume
VEGF: Vascular endothelial growth factor
VEGF-A: Vascular endothelial growth factor A
VEGF-B: Vascular endothelial growth factor B
VEGF-C: Vascular endothelial growth factor C
VEGF-D: Vascular endothelial growth factor D
VEGF-E: Vascular endothelial growth factor E
VEGFR-1: Vascular endothelial growth factor receptor 1
VEGFR-2: Vascular endothelial growth factor receptor 2
VEGFR-3: Vascular endothelial growth factor receptor 3

w/v: weight/volume
WB: western blot
wnt2: Wingless-type MMTV integration site family, member 2

ZO-1: zona occludins-1
µ: micro
2-ME: 2-mercaptoethanol
5-HT: 5-hydroxytryptamine

ACKNOWLEDGMENTS

I would start by thanking the ONE WHO CAUSES TO BECOME – JEHOVAH GOD—for HIS loving kindness and mercy in seeing me through this herculean PhD task. It wouldn't have been possible without YOU. I cannot be grateful enough to my primary supervisor—Dr Michael Cross—for his supervision, attention to details, fatherly support, dogged determination to see everything work smoothly, and his unflinching confidence in me. Without your support, the story would be different today. I look forward to advancing the LSEC story with you. My unreserved appreciation goes to Dr James Sidaway, who remained within a helping distance to pay attention to and proffer needed ideas to this brainchild of his, despite being busy with many other projects. I just do not know where to start in expressing the profoundness of my gratitude to a rare scientist, Professor Christopher Goldring for his peerless supervision. Your timely intervention in times of need, your open-door approach, your robust scientific ideas, your constructive criticism, the vastness of your scientific knowledge, your problem solving skills and your tactful but firm approach in addressing conflicting ideas are but a few of the things that endear you to me. I look forward to exciting years of research with you. I would like to say a very big thank you to my industrial supervisor, Dr Dominic Williams, for his help and invaluable contribution towards this project. My deep appreciation also goes to my industrial line manager, Mrs Alison Foster, for playing a very strategic role all through this project. You have proven to be there and ensured the project ran smoothly, making sure all the logistics were taken care of. Your efficiency is unparalleled. Thank you very much, Alison. My deep and sincere gratitude goes to Dr Neil Kitteringham for his time, ideas and help during this project. This altogether has added depth to this project. I would like to thank Dr Neil French for his help in coordinating the 'MIP-DILI' angle of the project. I need to express my unreserved appreciation to Dr Ian Wilson and Dr Gerry Kenna, who supervised my Masters project at AstraZeneca. Your insightful words of advice have spurred me on during this tough PhD sojourn.

I must show my sincere gratitude to AstraZeneca and Institute of Translational Medicine, University of Liverpool for funding this project as this wouldn't have been possible without your full support.

I would like to appreciate members of the MJC-ANGIO group, past and present—Dr Maxine Seaton, Dr Gopika Nithianandarajah-Jones, Dr Emma Wilkinson, Dr Mohammed Aljasir, Miss Awel Williams, Miss Beth Wilkinson, Mr Matthew Ryan and Mr Ahmed Alrumayh. Thank you very much, Dr Ahmad Alghanem, for your brotherly help and continued assurances in the early days of my project. I cannot forget you. How can I forget the members of the Team Liver, past and present—Dr James Heslop, Dr Rob Hornby, Dr Rowena Sison-Young, Dr Laleh Kamalien, Dr Carol

Jolly, Mr Lawrence Howell, Mr Christopher Pridgeon. I didn't omit Dr Fang Zhang, who was very selfless in her support during the late isolation nights. Your refusal to back down, even when it seemed too late to collect and isolate cells has really helped to push my project through to completion. When I become an expert in Cantonese and Mandarin, we should write a book on DILI. I must appreciate our links to the liver surgery team – Mr Mohamed Elmasry, Mr Jonathan Evans, Mr David Bowden, Mr Nick Bird. The Aintree surgical team, Mr Hasan Malik, Mr Stephen Fenwick, Mr Edward Alabraba, are central to the success of this project. Without them, there would be no liver tissue, without which I would basically have no project. I would like to appreciate Dr Mark Bayliss for his expertise during the drug metabolism studies. Thanks to Mrs Alison Beckett of the electron Microscopy Unit for her help and patience. The Liver Research Team at the Institute of Biomedical Research at the University of Birmingham is appreciated for their help in training me in the isolation of human liver sinusoidal endothelial cells. I would like to specifically thank Dr Patricia Lalor and Mrs Gill Muirhead for making this possible.

I cannot forget those who have become like a family to me in Sherrington Building—Dr Adedamola Olayanju, Dr Monday Ogese and Dr Mohammed Amali. You have always proven to be there for me at the nick of time. I wouldn't be able to tell how things would have been without you. My dear friends, Adeniyi Olagunju, Ajala Adeola and Jude Akinwale, thanks for always being there for me too. To my mentor, Dr Ejaife Agbani, words will certainly fail if I attempt to fully thank you for your unfailing help and support.

My Dear wife Patience Akingbasote, how can I claim I possess the right word to thank you for your unflinching support for me during these years? Your understanding is just amazing, especially during those long lab hours. You lifted me up in moments of depression and uncertainty. I couldn't have asked for a better wife and partner. Better times are beckoning at us. I love you. My dear son, Tiwalolu, you have brought sunshine into my life. I am quite amazed at your rapid development and understanding. I enjoyed the moments we spent together in my office while writing up this thesis, and your enthusiasm in shouting to hear your own voice echo back to you in the foyer. That's the sign of a little scientist budding. I look forward to teaching you scientific concepts.

I must thank my mum, Mrs Abigail Akingbasote, who took out time to come look after our little Tiwalolu. Your prayers have gone a long way, mummy. To my dear brothers John and Olusola, I say a very big thank you, for being a very solid rock behind me. Your examples and inspirational words have kept me going. I feel proud to share same parents with you. My sisters, Esther and Oluwatoyin, I am indebted to you for your support. You were never too tired or too busy to listen and support me during these years. I look forward to spending time with you guys in the nearest future. I must also thank my brothers- and sisters-in law, Nyedoki, Ruth, Abiola and

Moses for being there for me. Finally, I must thank all those who have taught me valuable life lessons during these years; namely, what doesn't kill you makes you stronger.

LIST OF PUBLICATIONS

A. Research articles

1. **Akingbasote, J**., Foster, A. J., Jones, H. B., David, R. M., Gooderham, N., Wilson, I. D. & Kenna, G. (2016). Improved hepatic physiology in hepatic cytochrome P450 reductase null (HRN^{TM}) mice dosed orally with fenclozic acid. Toxicol Res. doi**:** 10.1039/C6TX00376a.

2. **James A. Akingbasote**, Alison J. Foster, Ian Wilson, Sunil Sarda, Huw B. Jones, J. Gerry Kenna (2016). Hepatic effects of repeated oral administration of diclofenac to hepatic cytochrome P450 reductase null (HRN™) and wild-type mice. Arch Toxicol. 90(4):853-62. doi: 10.1007/s00204-015-1505-x.

3. Aderounmu, A., Omonisi, A., **Akingbasote, J.**, Makanjuola, M., Bejide, R., Orafidiya, L., & Adelusola, K. (2013). Wound-Healing and Potential Anti-Keloidal Properties of the Latex of Calotropis Procera (Aiton) Asclepiadaceae in Rabbits. *Afr. J. Trad. Comp. Alt. Med.* 10(3), 574–579.

4. Salawu, Oluwakanyinsola A, Tijani, Adeniyi Y., **James A Akingbasote** and Oga Florence E. (2010)**:** Subacute Toxicity Study of Ethanolic Extract Of the Stem Bark of *Faidherbia albida* (Del) (Mimosoidae) in Rats**.** *Afr. J. Biotech*. 9(8): 1218-1224.

5. Tijani A. Y, Okale S.E., Salawu T. A., Onigbanjo H. O., Obianodo L. A., **Akingbasote J. A,** Salawu O. A, Okogun J. I., Kunle F. O., and Emeje M. (2009). Antidiarrhoeal and Antibacterial properties of crude aqueous stem bark extract and fractions of *Parkia biglobosa* (Jacq.) R. Br. Ex G. Don. *Afr. J. of Pharm. Pharmacol*. 3(7): 347-353.

6. Salawu O.A., B. A. Chindo., A. Y. Tijani., I. C. Obidike, T. A. Salawu and **A. James Akingbasote**. (2009). Acute And Sub-Chronic Toxicological Evaluation of the Methanolic Stem Bark Extract of *Crossopteryx febrifuga* in rats. *Afr. J. Pharm. Pharmacol*. 3(12):621-626.

7. Tijani A. Y, Uguru M. O, Salawu O. A, Abubakar A., Onyekwelu N. O. and **Akingbasote J. A.** (2009). Effect of *Faidherbia albida* on some biochemical parameters of rats infected with *Trypanosoma brucei brucei*. *Afr. J. Pharm. Pharmacol*. 3(1): 026-030.

B. Book Chapter

8. Edward L. LeCluyse, Leah M. Norona, **James A. Akingbasote**, Lawrence S. Howell, Jeffrey L. Woodhead, Michael J. Cross, Adrian B. Roth, and Christopher E. Goldring. (2016). Leading-Edge Approaches For In Vitro Hepatotoxicity Evaluation**. Chap 4.** *Comprehensive Toxicology, Third Edition.* (undergoing editorial review)

C. Referenced Conference papers

9. **James Akingbasote**, Alison Foster, Sunil Sarda, Huw Jones, Ian Wilson, Gerry Kenna. (2014). Utility of the HRN™ (hepatic cytochrome P450 reductase null) mice for investigating mechanisms of liver toxicity of carboxylic-acid-containing drugs. *Toxicology letters*. 229: S40. *Abstracts of the 50th Congress of the European Societies of Toxicology (EUROTOX)*

CHAPTER ONE

GENERAL INTRODUCTION

1.1 DRUG-INDUCED LIVER INJURY

Drug-induced liver injury (DILI) ranks high among the causes of drug attrition during development and withdrawal from clinical use (Gahr *et al.*, 2016) with about 20 new cases per 100,000 persons in the overall population being reported annually (Leise *et al.*, 2014). Research geared towards the understanding of DILI have placed the focus of attention mostly on hepatocytes, being the most abundant cell type of the liver and responsible for most liver functions. However, DILI events involve a complex, finely-orchestrated interplay between resident cell types. Moreover, non-parenchymal cells (NPCs), including liver sinusoidal endothelial cells (LSECs), hepatic stellate cells (HSCs), Kupffer cells (KCs) and biliary epithelial cells (BECs), play key roles in maintaining normal liver function. Only recently have we begun to appreciate the numerous and diverse functions of NPCs in shaping the liver's response to injury and involvement in precipitating adverse outcomes and response to compound exposure. NPCs also have been recognized to be both direct and indirect targets of liver toxins and their metabolites. This thesis focuses attention on the role of liver sinusoidal endothelial cells (LSEC) in DILI. The sections that follow in this chapter will address the role of LSEC in liver physiology and pathology, as well as its use in organotypic liver microtissues. A brief review of endothelial cell physiology and drugs which affect this will be made. Finally, hepatotoxic drugs with potential to cause LSEC injury will be reviewed with a view to setting the background for what will be addressed in the experimental chapters that follow.

1.2 THE LIVER

The liver is the largest mammalian organ which performs both exocrine and endocrine functions. Located in the right hypochondriac and epigastric region of the abdominal cavity, and attached to the diaphragm and protected by the ribs, the liver accounts for 2%–5% of the total body weight in the adult human (Si-Tayeb *et al.*, 2010, Haschek *et al.*, 2010, McCuskey, 2012).

1.2.1 Structure and cell types

The liver is divided into right and left lobes which are separated by the falciform ligament. The right lobe is posteriorly and inferiorly subdivided into the *caudate* and *quadrate lobes* (Figure 1.1). The liver receives a dual blood supply by means of the hepatic artery and the portal vein via its hilus, also the exit point for efferent bile ducts and the lymphatics. About 80% of blood supply to the liver is via the portal vein which supplies poorly-oxygenated venous blood from the intestines, pancreas, spleen and gallbladder. The remaining 20% comes from the hepatic artery. The basic subunit of the liver is a hexagonal structure called the lobule which hosts the central vein by means of which blood supply into the hepatic sinusoids is emptied (Haschek et al., 2010). In the angles of the lobules are the portal tract which contains bile ducts, hepatic artery, branches of the portal veins, nerves and lymphatics. The sinusoid, which separates hepatic plates, serves as a channel for blood flow from the portal tracts to the central vein.

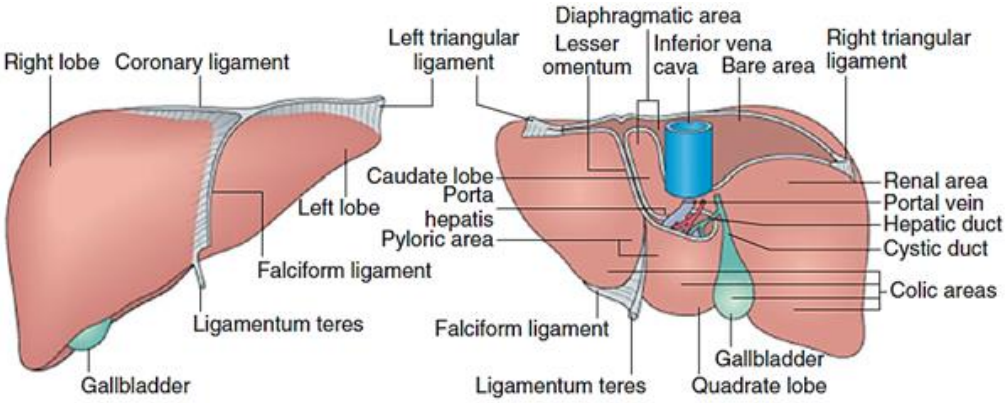

Figure 1.1: Anterior (left) and posteroinferior (right) views of the human liver showing Lobes, surfaces, and ligaments. Adapted from McCuskey (2012)

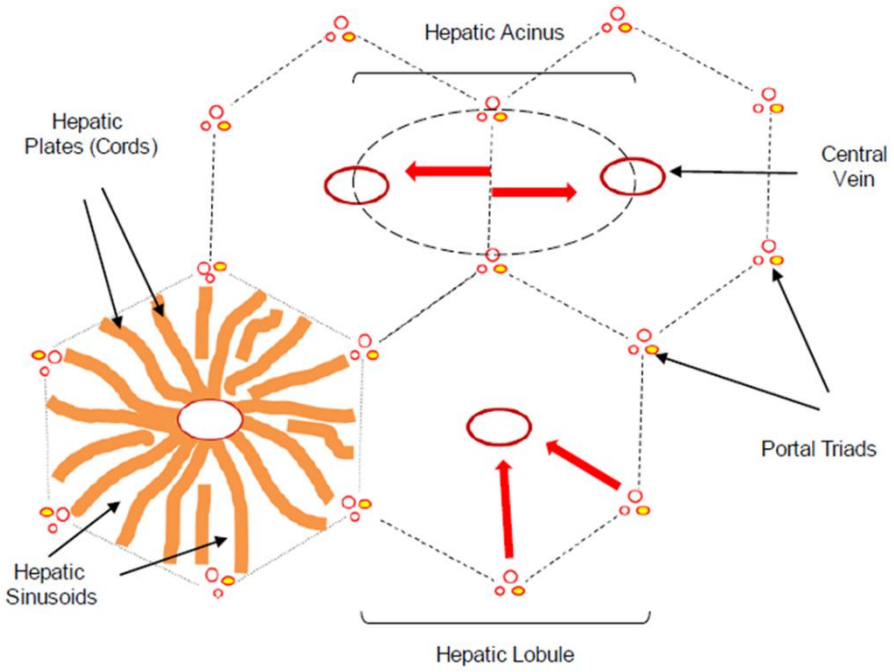

Figure 1.2: Representation of the liver microstructure.
Diagram of the basic hepatic lobule and acinus substructure showing the relative direction of blood flow from periportal microvasculature towards the central veins (red arrows). Adapted from LeCluyse *et al.* (2012a)

1.2.2 Embryonic development of the mammalian liver

Liver organogenesis in humans commences in week 3 of gestation. This begins as an endodermal bud from the ventral foregut. The bud develops into the hepatic diverticulum and forms a cavity contiguous with the foregut. Within this time period, the hepatic diverticulum forms the septum transversum which has three portions namely: the *hepatic portion* which forms the hepatic parenchymal cells and intrahepatic bile ducts, the *cystic portion* which forms the gall bladder, while the *ventral portion* forms the head of the pancreas (McCuskey, 2012). Week 4 marks the formation of blood vessels (Figure 1.3). From the hepatic diverticulum arise buds of epithelial cells which extend into the mesenchyme of the septum transversum and make thick multicellular anastomosing cords. This develops into the close association between the sinusoids and the parenchymal cells. On week 7, vitelline veins form the portal vein while the hepatic artery derives from the celiac axis and after the formation of bile ducts, ingrowths of the hepatic artery into the hepatic primordium take place. Between this period and birth, the foetal liver performs haematopoietic functions until the development of mature bone marrow that takes over as the main site of haematopioesis. In addition, the main serum protein *in utero* is alpha fetoprotein up until the end of the first trimester, while at 16 weeks of gestation albumin is synthesised (McCuskey, 2012, Si-Tayeb et al., 2010)

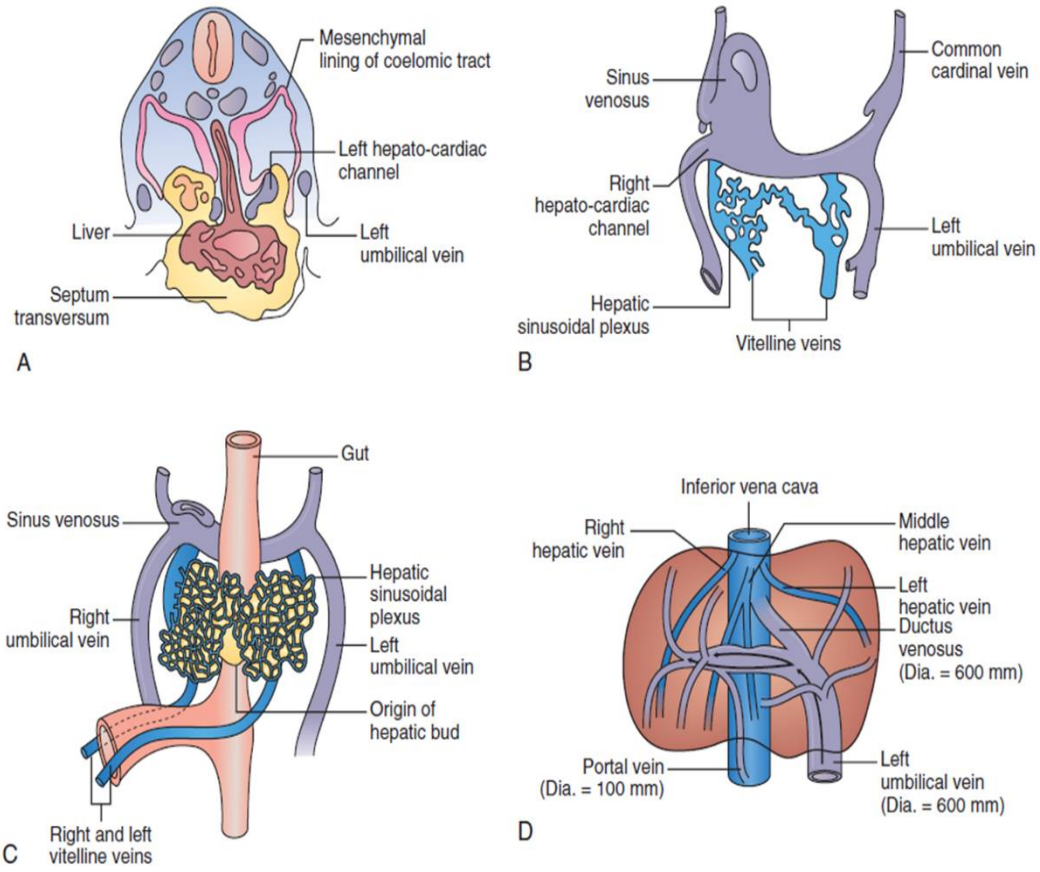

Figure 1.3: Embryonic development of the liver.

(A) Section through the region of the hepatic bud of a 26 day-old human embryo. (B) Vascular channels associated with the developing liver in a human embryo of 30 somites. (C) Vascular channels at a later stage showing development of the sinusoidal network. (D) Portal hepatic circulation in a human embryo of 17 mm (7 weeks). Adapted from *McCuskey (2012)*

1.2.3 Hepatic cell types and their physiological functions

The main cell type of the liver is the hepatic parenchymal cells or the ***hepatocytes*** which constitute about 80% of total liver volume and 60% of total cell population. Polyhedral in shape, the hepatocytes have two surfaces: the sinusoidal surface and

the basolateral canalicular surface. Blood from the portal vein and hepatic artery flows over the sinusoidal surface (Beath, 2003). Organised into plates or laminae, hepatocytes form tight junctions which create a canaliculus surrounding each hepatocyte and which collects bile and bile acids that are transported into the apical surface of the hepatocyte (Rogers & Dintzis, 2012). Microvilli on the hepatocytes protrude into the space of Disse and through the fenestrations on the sinusoidal endothelial cells (Haschek et al., 2010, Stolz, 2011b). The space of Disse which lies between sinusoidal endothelial cells and the hepatocyte also contains the stellate cells. The Küpffer cells are attached to the sinusoidal endothelium. (Figure 1.4). Additionally, hepatocytes are oriented in cords which are made up of a single row of cells demarcated by the sinusoidal endothelial cells (Haschek et al., 2010). There is a variation in the distribution of hepatocytes along sinusoids along the gradient of blood flow from the periportal to the centrilobular regions. This is a reflection of the physiological variation due to adaptation of hepatocytes to difference in the concentration gradient of nutrients, oxygen tension and other relevant substances along the sinusoids. Variation in hepatocyte distribution has resulted in the division of the hepatic lobule into three zones (1-3); zone 1 being in the periportal area with the highest oxygen supply, and zones 2 and 3 are in the order of decreasing oxygen tension towards the centrilobular area (Figure 1.4). Consequently, the hepatocytes in the centrilobular area are larger and richer in smooth endoplasmic reticulum than the periportal end of the sinusoid. Hepatocytes are responsible for energy storage in the form of glycogen, biotransformation of xenobiotics and endogenous chemicals required for regulation of physiological processes. In addition, they regulate the synthesis and transportation of

cholesterol, urea metabolism and the production of a vast array of plasma proteins, including albumin and Apo lipoproteins (Cattley & Cullen, 2013). **Kupffer cells**, which make up about 20% of non-parenchymal cells, are the macrophages of the liver (Wisse & Knook, 1977). They form the first line of defense in the liver which serves in the elimination of infectious bacterial materials via the blood supply from the gastrointestinal tract. Although they are ubiquitous within the lobule, Kupffer cells are more concentrated in the portal area to enable them to interact with incoming foreign bodies (Stolz, 2011b). They have also been reported to migrate along the surface of the sinusoidal endothelial cells (SEC), effecting a temporary blockage of blood flow, thereby facilitating an interaction between non-parenchymal cells and leukocytes in circulation (MacPhee *et al.*, 1995). **Stellate cells** (also called Ito cells, lipocytes, fat storing cells, or perisinusoidal cells) are fat-storing cells that make up about 15% of non-parenchymal cells. They are resident in the space of Disse (between the LSEC and the hepatocytes). Because they envelop the endothelial cells and are capable of contraction, they are often referred to as sinusoidal pericytes (Sato *et al.*, 2003). When quiescent, they store retinoids, triglycerides, cholesterol and other free fatty acids, but upon activation they lose these lipid stores, and secrete cytokines and proteins of the extracellular matrix (ECM). Changes in composition of the ECM and deposition of ECM into the space of Disse result in capillarisation or pseudocapillarisation (loss of LSEC fenestration). Stellate cells are reportedly responsible for liver fibrosis and cirrhosis (Yin *et al.*, 2013). **Pit cells** form part of the resident hepatic leukocyte population and make up about 2% of the total non-parenchymal cell population. They are resident in the

sinusoidal lumen and kill tumours as well as virally-infected cells (Nakatani *et al.*, 2004).

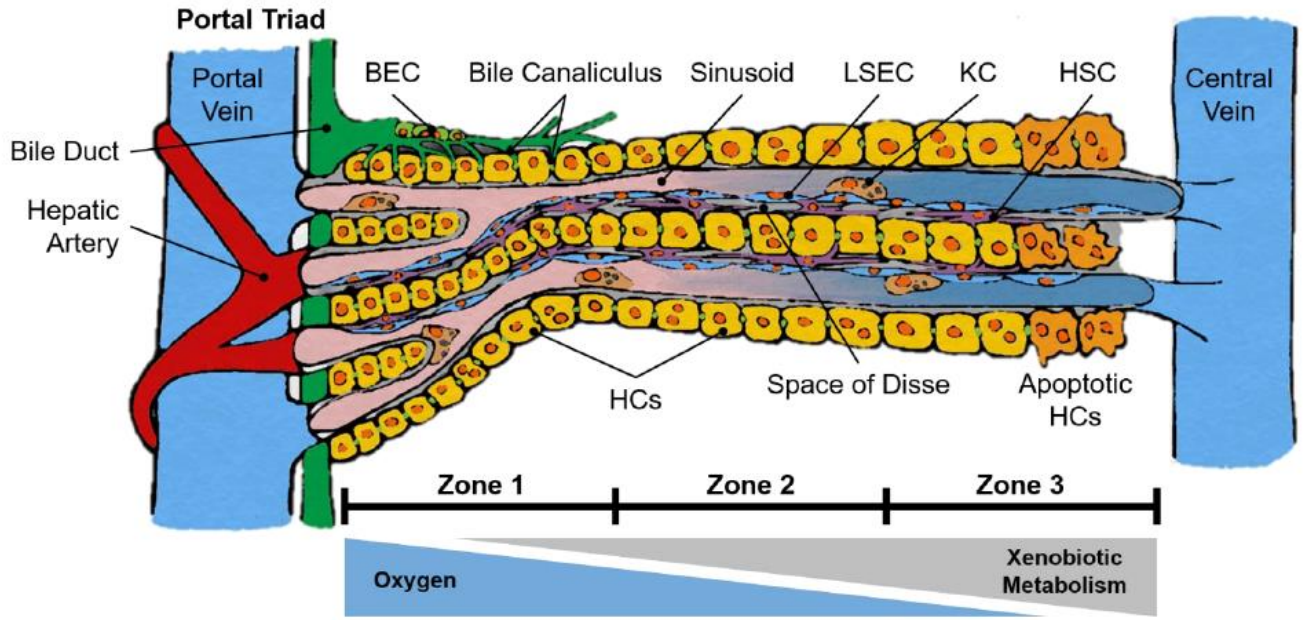

	Periportal	Transitional	Pericentral
Primary Function	β-Oxidation, Gluconeogenesis, Glycogen Synthesis (from lactate), Cholesterol Biosynthesis	Mixture of Zone 1 and Zone 3 functions	Glycogen Synthesis (from glucose), Glycolysis, Lipogenesis, Ketogenesis, Bile Acid Synthesis, Glutamine Synthesis, Heme Synthesis, Xenobiotic Metabolism

Figure 1.4: Structural zonation of the liver.

Discrete microenvironments or zones of the liver between the portal triad (periportal region) and central vein (pericentral region) illustrating the differences in hepatocyte (HC) size and ploidy (diploid→tetra/octaploid). Due to the flow of mixed blood from the portal vein and hepatic artery towards the central vein, inherent gradients are formed that vary in oxygen tension, nutrient concentrations and the levels of other soluble and bound factors. These gradients are thought to play a role in the creation of localized differences in HC gene expression profiles and phenotypes, including the uptake and metabolism of both endogenous and exogenous substrates. Note that the greatest capacity for lipid uptake and metabolism is exhibited in HCs in zone 1 and the greatest capacity for xenobiotic uptake and metabolism is exhibited in HCs in zone 3. Adapted from (Turner et al., 2011). BEC: biliary epithelial cells, LSEC: liver sinusoidal endothelial cell, KC: Kupffer cell, HSC: hepatic stellate

1.3 LIVER SINUSOIDAL ENDOTHELIAL CELLS

Liver sinusoidal endothelial cells (LSECs) are highly specialised cells that form the basic tubular vessel for transvascular exchange between blood flowing in the sinusoid and the surrounding parenchymal cells (PC). In the early 1970s, by the use of electron microscopy, Wisse successfully characterized LSECs as the cell type on the surface of the liver sinusoid and distinguished them from Kupffer cells, thus ending the assumption that endothelial cells could develop into Kupffer cells (Wisse, 1970, Wisse, 1972). LSECs make up about 50% of the total number and volume of non-parenchymal cells (DeLeve, 2011). Lining the capillaries of the microvasculature, LSECs are unique to the liver as they are the only mammalian endothelial cells with open fenestrae and which lack an organized basement membrane (Hang *et al.*, 2012). Hence it is the most permeable of all mammalian endothelial cells (DeLeve, 2011). These fenestrae (170 nm in diameter) lack diaphragms and are assembled in groups referred to as sieve plates. Due to their strategic location, LSECs are essentially the first cells to be in contact with blood flowing into the hepatic sinusoid (Figure 1.4). They are involved in the selective transfer of substances from the blood in the hepatic sinusoid to the parenchymal cells, hepatic stellate cell (HSC) quiescence, endocytosis of small particles, and liver regeneration. This section will focus on the embryological development of LSEC, role of LSEC in liver physiology and pathology as well as models that have been developed to study the involvement of LSEC in drug-induced liver injury (DILI).

1.3.1 LSECS in liver organogenesis

The liver sinusoids are the first blood vessels to be formed during hepatogenesis and arise from septum transversum mesenchyme (STM) (Collardeau-Frachon & Scoazec, 2008, Couvelard *et al.*, 1996). Precursory to the functional liver sinusoidal endothelial cells (LSEC) are angioblasts (Matsumoto *et al.*, 2001) and these intercede between the thickening endoderm and the STM. Sinusoids are believed to be formed via angiogenesis as well as by introduction of endothelial cells of mesothelial origin (Perez-Pomares *et al.*, 2004). Klein *et al.* (2008) have shown that Wnt2 signalling plays a key role in the proliferation and differentiation of the liver sinusoid. In a murine study, they demonstrated that Wnt2, which is expressed in rat LSEC has the potential to promote LSEC proliferation via β-catenin signalling. They concluded that an autocrine activity of Wnt2 cooperates with *VEGF* signalling to regulate LSEC growth. This was further confirmed when depletion of *Wnt2* resulted in a reduction of the expression of VEGF receptor-2 (VEGFR-2) on rat LSECs. It has been shown that LSEC and their main signalling receptor, VEGFR-2, are required during organogenesis of the liver (Matsumoto et al., 2001). These nascent endothelial cells create the pattern for the lobular organization of the liver by directing the migration of the liver into cords (McLin & Yazigi, 2011). Interactions between newly-specified hepatic endoderm cells and LSECs are crucial for the endoderm's subsequent growth and morphogenesis into a liver bud (Figure 1.3). Therefore, these nascent cells are key in the provision of required growth stimulus needed by the hepatic bud even before formation of local vessels that supply blood

and oxygen. A similar interplay between LSECs and hepatocytes via VEGF signalling occurs during liver regeneration (Ding et al., 2010b, Rafii *et al.*, 2016).

1.3.2 Role of LSECs in liver physiology

LSECs form the basic tubular vessel for transvascular exchange between blood flowing in the sinusoid and the surrounding parenchymal cells (Figure 1.9), recently reviewed by Sorensen *et al.* (2015). This unhindered access to circulating blood enables hepatocyte oxygenation, movement of substrates and lipoprotein to and from hepatocytes, and a more efficient clearance of xenobiotics (DeLeve *et al.*, 2004, Fraser *et al.*, 1995). In healthy individuals, LSECs generally lack a basal lamina which enables solutes and small particles to have direct access to the perisinusoidal space where hepatic stellate cells (HSCs) and hepatic microvilli are found. This ensures an unhindered exchange of these substances (solutes and small particles) between the blood and the hepatic parenchymal cells.

1.3.2.1 Delivery of oxygen

Because only ~30% of the blood supply to the hepatic sinusoid is oxygen-rich, oxygenation of the hepatocytes is facilitated by the architectural and cytoplasmic features of the LSECs, such as the presence of fenestrations, a very narrow and spread cytoplasm, and the lack of an organized basement membrane, which reduce the distance required for oxygen diffusion. (DeLeve, 2011). In capillarised and pseudocapillarised livers, where there is a loss of fenestrations and alterations in the basement membrane, hepatocyte hypoxia ensues (Le Couteur *et al.*, 2001).

There is also evidence that there is a correlation between oxygen diffusion through the sinusoid and oxidative drug metabolism as Hickey *et al.* (1995) and Le Couteur *et al.* (1999) have demonstrated the re-establishment of drug metabolism in cirrhotic rat liver following oxygen supplementation.

1.3.2.2 Nitric oxide production and signalling

LSECs produce nitric oxide (NO) via endothelial nitric oxide synthase (eNOS) and inducible nitric oxide synthase (iNOS), the former being restricted to LSECs in the liver (Perri & Shah, 2005a). NO in the hepatic endothelium serves in the regulation of vascular tone in response to shear stress and other factors that cause a constriction of the hepatic sinusoids resulting in local dilation of the vascular bed and an enhancement of blood flow (Figure 1.6) (Shah *et al.*, 1997). Endothelial NOS can also drive the production of NO by the action of agonists such as vascular endothelial growth factor (VEGF) and oestrogen. LSECs can also generate NO via the induction of iNOS in response to cytokines (*e.g.*, interferon-γ [IFN-γ] and to lipopolysaccharides [LPS]) (Rockey & Chung, 1996). In capillarised liver, there is a perturbation of the NO-dependent pathway which disrupts the LSEC phenotype, a predisposing factor to liver fibrosis (reviewed in DeLeve (2015) and Greuter and Shah (2016)).

1.3.2.3 Stellate cell quiescence

In vivo, LSECs help maintain hepatic stellate cell (HSC) phenotype and quiescence through NO signalling (DeLeve et al., 2004, 2008). In a quiescent state, HSCs are

responsible for the storage of triglycerides, retinol (vitamin A), cholesterol retinoids, and free fatty acids. However, upon activation, these lipid stores become depleted and HSCs proliferate and secrete a variety of cytokines and extracellular matrix (ECM) proteins and enzymes that modulate the external ECM composition, such as matrix metalloproteinase protein-9 (MMP-9). This change in ECM composition results in capillarisation or pseudocapillarisation which leads to fibrosis (Bosch, 2007, Iwakiri & Groszmann, 2007). Deleve *et al.* (2008) have demonstrated that LSECs in a differentiated state maintain HSC quiescence and can even revert activated HSCs towards a quiescent state via VEGF-stimulated nitric oxide (NO) production (Figure 1.6).

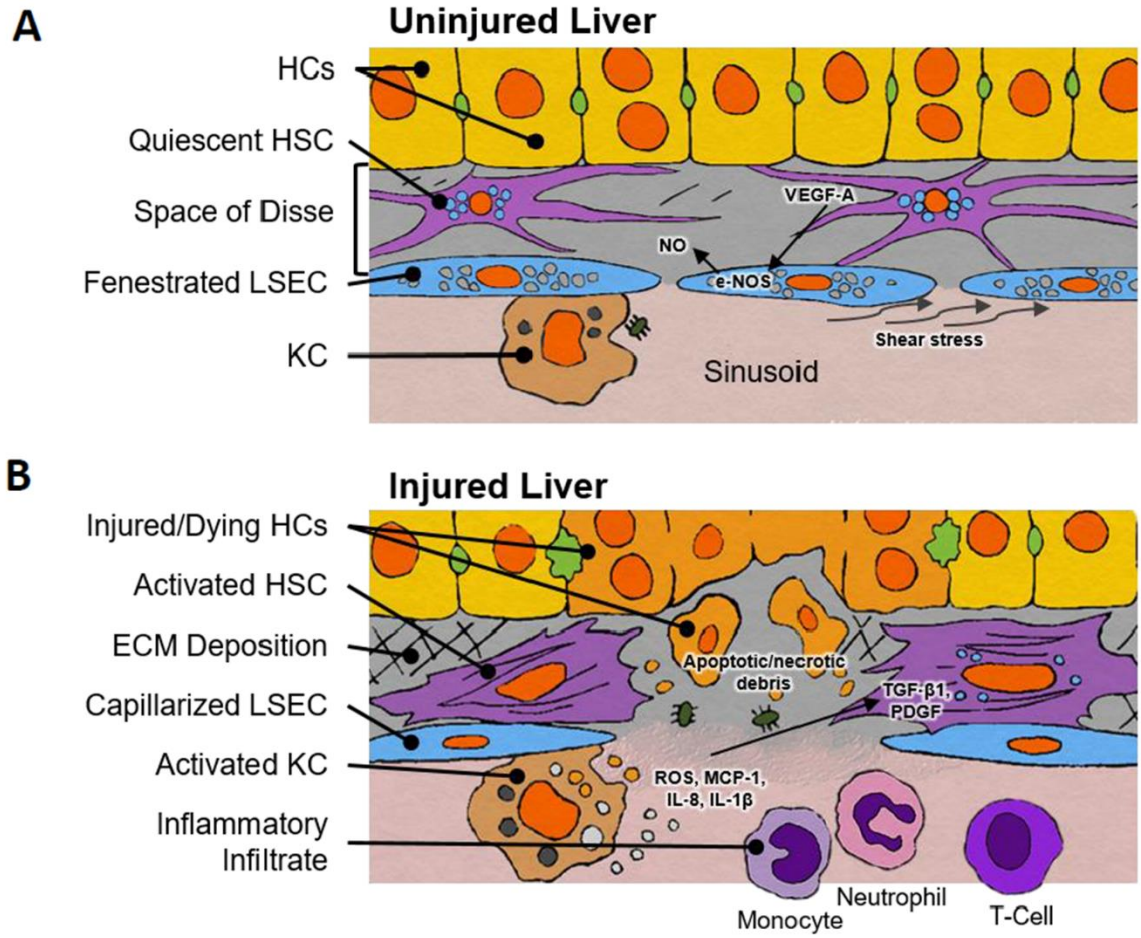

Figure 1.6: Liver sinusoidal endothelial cells in regulating stellate cell quiescence.

(A) In uninjured liver, shear stress or vascular endothelial growth factor-A (VEGF-A) act directly on liver sinusoidal endothelial cells (LSECs) to generate nitric oxide (NO) via endothelial nitric oxide synthase (eNOS) activity. NO produced via this process can help maintain hepatic stellate cells (HSCs) in a quiescent state. Furthermore, VEGF production by quiescent HSCs is an important factor in maintaining the differentiated or fenestrated phenotype of LSECs. (B) In the absence of this crosstalk (*e.g.*, in the event of livery injury), HSCs become activated and transdifferentiate to myofibroblasts, resulting in the deposition and accumulation of extracellular matrix (ECM) within the space of Disse. Furthermore, LSEC fenestrae are compromised leading to capillarisation of the liver and an impedement of oxygen and nutrient delivery to the parenchymal cells. The activation of resident macrophages, or Kupffer cells (KCs), causes a myriad of proinflammatory and chemotactic cytokines to be released that modulate the phenotypic features of other cell types and influence the liver's response to injury, including recruitment of extrahepatic inflammatory cells to the site of injury. This wound-healing response is dependent on a finely orchestrated balance and interplay between resident and recruited cell types. When this balance is disrupted (*i.e.*, during chronic liver injury) excessive ECM deposition occurs and ultimately disrupts normal liver architecture and function, which over time become the hallmarks of liver fibrosis and cirrhosis. IL-1β, interleukin-1β; IL-8, interleukin-8; MCP-1, monocyte chemoattractant protein-1; PDGF, platelet-derived growth factor; TGF-β1, transforming growth factor-β1; ROS, reactive oxygen species.

1.3.2.4 Scavenger function

As the first checkpoint for macromolecules and antigens entering the portal circulation from the intestine, LSECs play a complementary role to Kupffer cells (KCs) as a scavenger system in the clearance of these foreign waste products. While KCs phagocytose larger particulate matters and insoluble wastes, LSECs remove colloids, macromolecules and soluble components which are less than 0.23 μm in size from the blood (Smedsrod *et al.*, 1990, Shiratori *et al.*, 1993, Elvevold *et al.*, 2008). This function is enhanced by the slow and intermittent blood flow through the sinusoids, the large surface area of the LSEC, positively-charged coated pits that facilitate endocytosis of negatively charged particles, presence of the endocytic surface receptors and the highly-specific lysosomal enzymes which aid in the disposal of waste products (Knook & Sleyster, 1980, Sorensen *et al.*, 2012). The main scavenger receptors on LSECs are the hyluronan/scavenger receptors, SR-H (Stabilin-1 and -2). These are responsible for the clearance of hyluronan, chondroitin sulphate, formaldehyde-treated serum albumin (employed as a test ligand for scavenger receptor-mediated endocytosis) (Blomhoff *et al.*, 1984) and internalization of phosphorothioate-modified antisense oligonucleotides (ASO) (Miller *et al.*, 2016). A second endocytosis receptor system on the LSEC is the CD206 (collagen-α-chain/mannose) receptor which clears denatured collagen alpha chains in circulation (Malovic *et al.*, 2007). The LSEC Fc receptor FcγIIb2 (CD32b or SE-1), clears immune complexes formed with IgG (March *et al.*, 2009). Very recently, the scavenger receptor B1, an HDL receptor involved in cholesterol metabolism, has been shown to be highly expressed on LSECs (Ganesan *et al.*, 2016). During

capillarisation, there is deterioration in LSEC-mediated endocytic functions (Ito *et al.*, 2007).

Table 2.1: Some markers present on the LSEC

Marker	Description
CD31 or PECAM-1	Cell surface marker on all endothelial cells but expressed in the cytoplasm in LSEC. It is involved in transendothelial leucocyte migration.
Stabilin-2	LSEC-specific scavenger receptor
CD33	A myeloblast antigen also present on LSEC surface
CD4	Present on T cell monocytes, dendritic cells and LSEC
Fcγ receptor IIb_2	Involved in the endocytosis of immune complex
CD36	Thrombospondin-1 receptor
CD45	A leucocyte common antigen present on about 90% LSECs isolated by elutriation
Integrin $\alpha_1\beta_1$	Binds collagen preferentially
Integrin $\alpha_5\beta_1$	Binds fibronectin preferentially
LYVE-1, CD46, CD 80, CD86	Clearance of hyaluronan and other waste products from connective tissues

Source: DeLeve (2011)

1.3.2.5 Clearance of drugs and small particles

Protein-bound drugs pass through the fenestrations on the LSECs into the space of Disse; thus free drug can be cleared by adjacent hepatocytes. This allows bound drug to re-equilibrate with free drug thereby enabling newly-formed free drug to be cleared by the hepatocytes (DeLeve, 2011). This process accelerates the removal of free drug from circulation via the liver. Consequently, due to an appreciable drop in

oxidative drug metabolism and loss of fenestrae in capillarised and pseudo-capillarised livers, drug disposition is expectedly compromised in fibrotic and aging liver. In a similar manner, chylomicron remnants are transported into the space of Disse when they are of smaller size than the fenestral diameter to be cleared by the hepatocytes. Chylomicrons are lipoprotein particles made up primarily of triglycerides, phospholipids, cholesterol and proteins (Hussain, 2000). Because they contain about 90% triglyceride, chylomicrons serve as a vehicle for the transport of triglycerides. In ageing- or fibrosis-related capillarisation, where there is a considerable loss of LSEC fenestrations, chylomicron and hence triglyceride clearance is impaired. This phenomenon is related to the initiation of atherosclerosis and hyperlipidaemia (Botham & Wheeler-Jones, 2007). Species with smaller fenestral diameter and lower sinusoidal porosity (*e.g.*, chicken and rabbit) tend to develop atherosclerosis (Braet & Wisse, 2002).

1.3.2.6 Liver regeneration

LSECs have been reported to be involved in liver regeneration (reviewed in DeLeve (2013) and Forbes and Rosenthal (2014)). In a mouse model of partial hepatectomy, activation of vascular endothelial growth factor receptor 2 (VEGFR-2) on LSECs was observed to induce the upregulation of transcription factor Id1 which causes a release of angiocrine factors Wnt2 and hepatocyte growth factor (HGF) which are required for hepatocyte proliferation (Figure 1.7) (Ding *et al.*, 2010a). This observation is not only limited to partial hepatectomy, Ding *et al.* (2014) have also shown induction of liver regeneration in acetaminophen (APAP)- and carbon-

tetrachloride (CCl_4)-induced liver injury. This observation highlights the importance of LSECs in effecting a cascade of events that begins with the initial release of vascular endothelial growth factor A (VEGF-A). This was first observed with a 30-fold elevation of hepatic VEGF-A after administration of toxic doses of APAP in a rat study, whereas an exogenous administration of VEGF-A to another group of rats resulted in the abrogation of the hepatocellular necrosis observed in APAP overdose (Donahower *et al.*, 2010b, Donahower *et al.*, 2006). Because hepatocytes release VEGF-A that acts in an autocrine fashion to enchance LSEC survival, migration and proliferation (DeLeve et al., 2004), it is therefore conceivable that during liver injury and/or hepatectomy, hepatocytes release VEGF-A which activates the VEGFR-2 on LSECs and initiates the cascade of events that results in liver repair and regeneration. Also, liver regeneration is dependent on angiogenesis, which when inhibited, prevents liver regeneration (Drixler *et al.*, 2002, Greene *et al.*, 2003, Taniguchi *et al.*, 2001), a process mediated by the anigiogenic factor VEGF-A (Taniguchi et al., 2001).

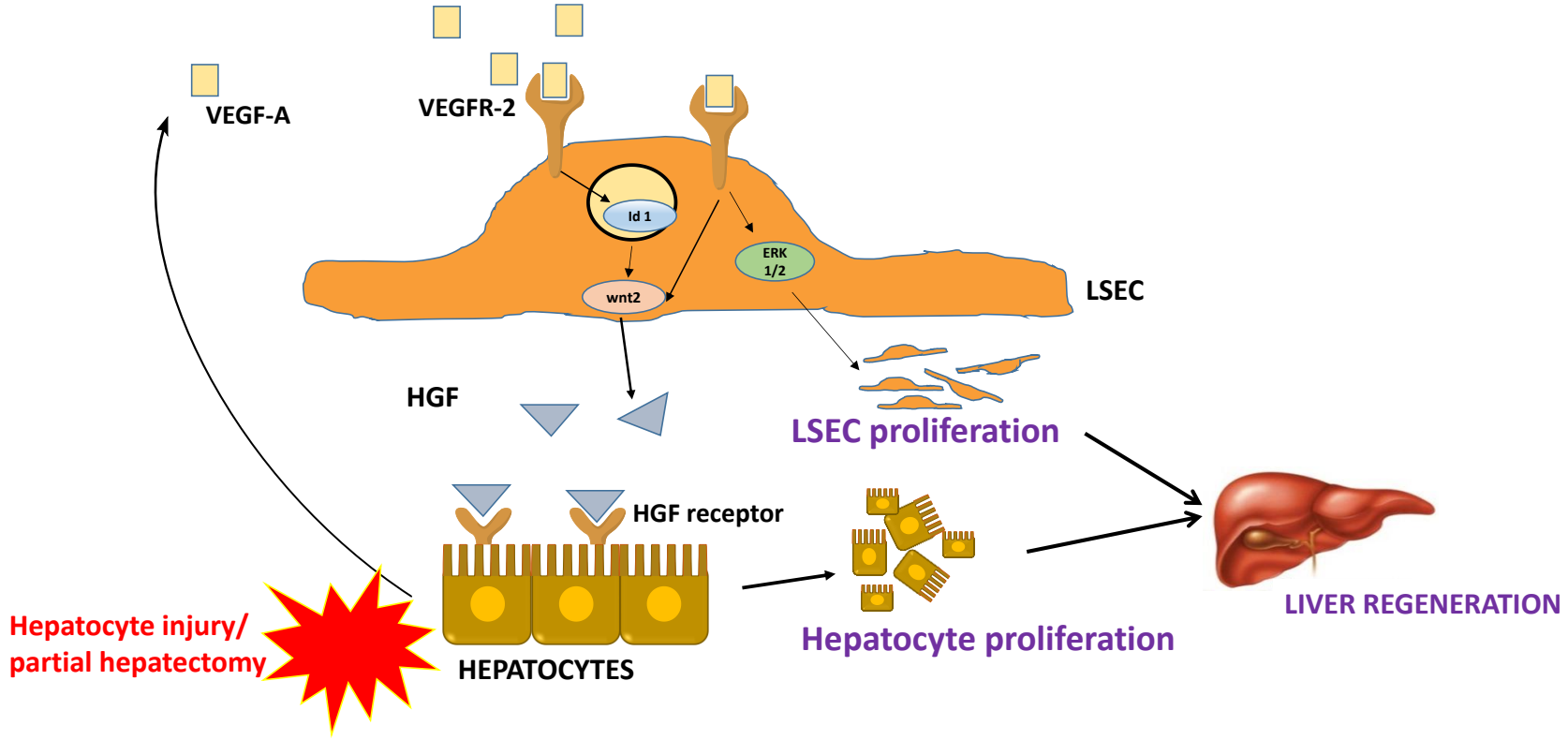

Figure 1.7: Role of liver sinusoidal endothelial cells (LSECs) in liver regeneration*:*
A simplified diagram showing the role of LSECs during liver injury and regeneration. After partial hepatectomy or toxic injury, hepatocytes release vascular endothelial growth factor A (VEGF-A), which causes activation of the VEGF receptors (VEGFR-2) in LSECs, resulting in the upregulation of transcription factor Id1 and release of Wnt2. The release of Wnt2 triggers the release of hepatocyte growth factor (HGF) from LSECs, which then activates its receptor, HGFR, on the hepatocyte surface and promotes hepatocellular proliferation and reconstitution of liver mass. Simultaneous, activation of VEGFR-2 on LSECs initiates a cascade of intracellular signalling that involves cell survival and proliferation. This also helps form tracts to guide the arrangement of the newly-formed hepatocytes into a lobular pattern and facilitate their vascularization (Ding *et al.*, 2010b). It is important to note that this is not the sole pathway involved in liver regeneration. There are other cells and signalling molecules involved in liver regeneration including macrophages, hepatic stellate cells (HSCs), TGF-β1, angiopoietin-2, and progenitor cells (reviewed in (Forbes & Parola, 2011)).

1.3.2.7 LSEC fenestrations

One of the principal hallmarks of the LSEC is its fenestrae. These transcellular pores span 50-150 nm in diameter and are collected into groups of 10-100 called sieve plates (Figure 1.8 and Figure 1.9). (Svistounov *et al.*, 2012). Making up about 7% of the total endothelial surface area, the fenestrae form a selective barrier between the blood and hepatocytes. As discussed earlier, they also help in the clearance of colloids and soluble macromolecules from the circulation (Elvevold et al., 2008, DeLeve, 2011). Forced sieving and 'LSEC massage' have been described as being involved in the transendothelial movement of particulates somewhat larger than the size of the fenestrae (Wisse *et al.*, 1996). Just as there is a variation in size and metabolic capabilities of hepatocyte from the periportal (zone 1) to centrilobular (zone 3) regions, there is also an increase in fenestral diameter and porosity along this gradient (Wack *et al.*, 2001). Controlled by the actin cytoskeletal network, the diameters of the fenestrae can be adjusted by the pressure of blood flowing through the lumen, and in presence of vasoactive substances, alcohol, drugs, and toxins in the bloodstream (Braet *et al.*, 1996). Fenestral diameter is also suggested to be regulated by serotonin (5-hydroxytryptamine, 5-HT) via the 5-HT_2 receptor on LSECs. As a result of an influx of calcium, following 5-HT_2 receptor activation, there is a phosphorylation of the myosin light chains resulting in an increase in actin-activated myosin ATPase activity in areas surrounding the fenestral opening. This results in contraction which can be reversed by calcium channel blockers (Gatmaitan *et al.*, 1996). Fenestrae can be induced by such microfilament inhibitors such as latrunculin A, cytochalasin B, and misakinolide (Braet & Wisse, 2002). LSEC

porosity is also known to be regulated by VEGF. Constitutively produced by contiguous hepatocytes and hepatic stellate cells (HSCs), VEGF stimulates an autocrine production of NO which serves to maintain fenestral integrity (DeLeve et al., 2004).

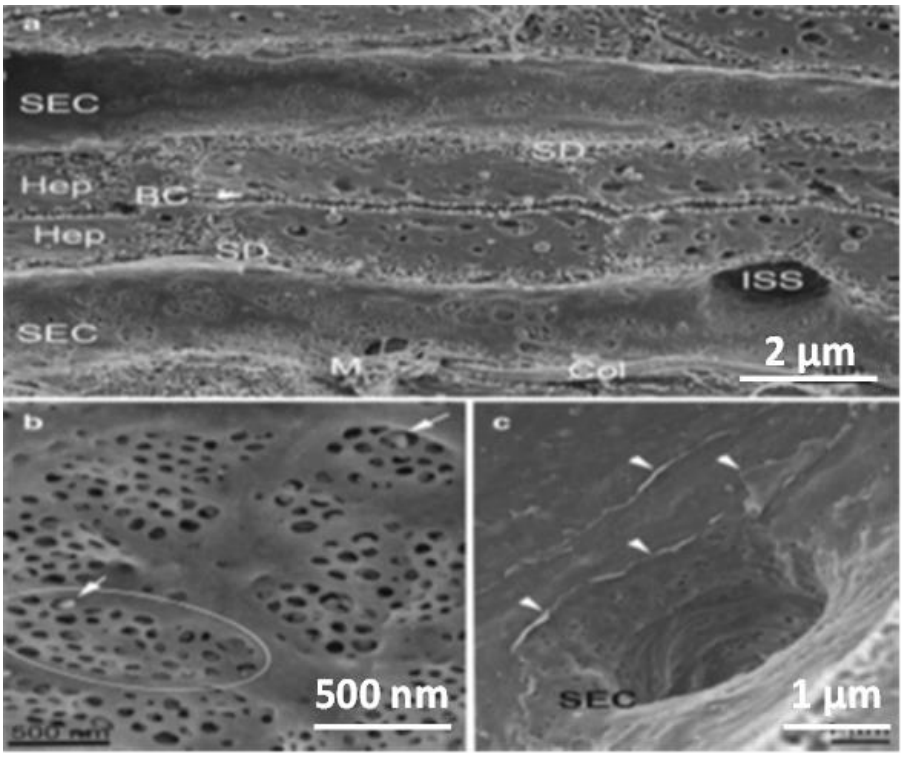

Figure 1.8: Scanning electron micrographs of a section of mouse liver sinusoidal endothelial cells.

*(*a) A low magnification image accentuating the anatomy of the hepatic plate bounded by sinusoids. (b) A high magnification micrograph of a sinusoid highlighting sieve plates (c) Transition of the portal venule into the sinusoid (SEC). There is an abrupt change of non-fenestrated to fenestrated endothelium from the portal venule to the sinusoid. SEC, sinusoidal endothelial cell; Hep, hepatocyte; BC, biliary cells; SD, space of Disse. Source: Stolz, 2011

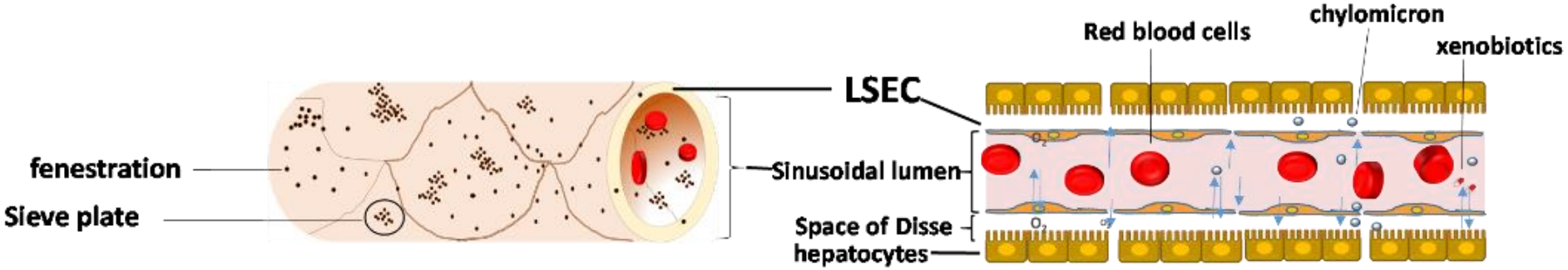

Figure 1.9: Exchange of oxygen and soluble substances between blood and the perisinusoidal space

LSECs play an important role in the transport of oxygen from the sinusoidal blood to the hepatocytes (HCs). This is facilitated by their fenestrations, thin cytoplasm, and a lack of organised basement membrane. These features enable the passage and clearance of protein-bound drugs and phospholipids to and from the circulating blood. Loss of fenestrae (capillarisation) results in the inability of LSECs to clear lipoproteins, which is an important factor in the initiation of atherosclerosis.

1.3.3 Role of LSECS in liver pathology

Given the physiological roles of LSECs which includes barrier function, scavenger function, clearance of small particles and hepatic stellate cell (HSC) quiescence, any interference with these could adversely affect hepatocytes and liver function, resulting in a liver disease. This section discusses some conditions that affect the LSECs with a consequent adverse effect on the liver in general.

1.3.3.1 Capillarisation of the LSEC

Capillarisation is a dedifferentiation process in which the LSEC phenotype is converted to a vascular phenotype, marked by defenestration and formation of an organized basement membrane (DeLeve et al., 2004). *In vivo*, capillarisation occurs as an onset of alcoholic liver disease, fibrosis, cirrhosis and ageing. However, the changes seen as a result of aging, are more significantly a loss of fenestration with partial changes in the basement membrane. Hence, this phenomenon in an ageing liver is more appropriately termed pseudocapillarisation (McLean *et al.*, 2003). In capillarisation and pseudocapillarisation, clearance of lipoproteins is impaired leading to hyperlipidaemia and atherosclerosis. Other factors that contribute to defenestration as seen in these phenomena include generation of reactive oxygen species (ROS) and some toxins (Stolz, 2011b). In an *in vivo* study, Straub *et al.* (2007) have shown that a daily five-day administration of sub-lethal doses (250 parts per billion) of trivalent arsenic could cause capillarisation in rat LSECs. This observation was due to superoxides generated from NADPH oxidase (NOX), whereas NOX-knockout mice did not experience this defenestration phenomenon (Straub *et al.*,

2008). Oxidative stress and depletion of endogenous antioxidants (*e.g.*, glutathione) also have been associated with capillarisation (Cogger *et al.*, 2004).

1.3.3.2 Alcoholaemia

As mentioned above, alcohol induces an increase in fenestral diameter (Wisse et al., 1996). On the other hand, chronic alcohol intake has been implicated in LSEC capillarisation, commonly associated with reduction in diameter and number of fenestrae and formation of basement membrane as seen in liver cirrhosis (discussed below). However, this is reversible upon abstinence from alcohol (Fraser et al., 1995). Acute alcohol consumption impairs the scavenger function of LSECs, while chronic alcoholic intake reduces receptor-mediated endocytosis. This means that bacterial antigens are not efficiently removed and this may lead to immune stimulation, and thus increased liver inflammation (Thiele *et al.*, 1999).

1.3.3.3 Liver cirrhosis

In a cirrhotic liver, there is a general scarring of the liver accompanied by damage to the hepatic architecture. There is impedance to the hepatic circulation mainly due to a decline in the nitric oxide (NO) production that is brought about by an enhanced expression of nitric oxide synthase (NOS) inhibitory proteins and decreases in endothelial nitric oxide synthase (eNOS) phosphorylation (Perri & Shah, 2005a, Fulton *et al.*, 2001). As discussed above, there is a shrinkage of and dramatic reduction in the number of fenestrae in LSECs which marks sinusoidal capillarisation. With the loss of NO, there is activation of hepatic stellate cells (HSCs) leading to the

production of ECM and fibrosis of the liver, which is correlated with a rise in serum hyaluronate. Although LSECs are involved in HSC quiescence, when stimulated by transforming growth factor-β1 (TGF-β1), they can produce ECM components like laminin, fibronectin, and collagen type IV (Rieder *et al.*, 1993). A consequence of ECM production in cirrhotic liver is the poor oxygenation of the parenchyma which leads to hepatocellular hypoxia and necrosis.

1.3.3.4 Sinusoidal obstruction syndrome

Sinusoidal obstruction syndrome (SOS) is the pathological condition which leads to LSEC injury and obstruction of sinusoidal flow (Tallman *et al.*, 2013). SOS takes place mainly in two settings: ingestion of pyrrolizidine alkaloid as well as chemotherapy alone or in combination with irradiation of the liver (Deleve, 2008a). This has been reported to be associated with an incidence of 70% morbidity and 67% mortality (Nakamura *et al.*, 2012). Understanding the mechanism of LSEC injury in SOS has been enhanced by the use of a rodent model of the disease which exhibits similar symptoms of the disease in humans. Monocrotaline is activated by CYP3A4 to its pyrrole derivative which is electrophilic (DeLeve *et al.*, 2003, Wang *et al.*, 2005). It readily targets and depolymerizes the F-actin cytoskeleton, and activates matrix metalloproteinase-9 (MMP-9) which digests the extracellular matrix (ECM) of the LSECs. This results in a compromise of the tight junctions between LSECs which form the endothelial barrier of the hepatic microcirculation, paving the way for red blood cells to pass through the gap formed into the space of Disse. There occurs an embolism of the LSECs lining the sinusoids leading to obstruction of the hepatic

microcirculation, ischemic damage, centrilobular haemorrhagic necrosis (DeLeve, 2011), coagulative necrosis of hepatocytes, and loss of LSECs (Nakamura et al., 2012). Loss of LSECs is accompanied by a corresponding drop in number of KCs in the liver. Additionally, the loss of LSECs leads to a drop in the level of NO which tonically inhibits the synthesis of MMP-9. Because monocrotaline pyrrole is electrophilic, it causes a depletion of glutathione (GSH), and enhances the activities of MMP-9. Hence supplementation with GSH or N-acetyl cysteine inhibits MMP-9 activity (DeLeve et al., 2003). Drugs that have been reportedly implicated in SOS in the clinic include oxaliplatin, busulfan, cyclophosphamide, 6-thioguanine, and actinomycin D (Robinson *et al.*, 2013, Vreuls *et al.*, 2016). This has recently been reviewed by Valla and Cazals-Hatem (2016).

1.3.3.5 Non-alcoholic fatty liver disease

As mentioned previously, LSECs are involved in the modulation of hepatic stellate cell (HSC) phenotype. Compromises of the LSEC-HSC nitric oxide (NO) signalling results in HSC activation, a prominent event in which the overproduction and deposition of ECM eventually leads to fibrosis (DeLeve, 2015). Activation of HSCs is common in non-alcoholic fatty liver disease (NAFLD) which is also preceded by excessive fat accumulation in hepatocytes (steatosis and phospholipidosis). This process begins with simple steatosis leading to non-alcoholic steatohepatitis (NASH), and may further progress into cirrhosis and hepatocellular carcinoma in the absence of chronic alcohol intake (Ashtari *et al.*, 2015, Angulo & Lindor, 2002, Bellentani *et al.*, 2010). The link between LSEC injury and NAFLD was established in a recent study

published by Miyao *et al.* (2015) using a choline-deficient, L-amino-acid defined and high diet fat mouse model of NAFLD. The authors showed that LSEC capillarisation occurs during the early stages of this disease followed by inflammatory cell infiltrate, fibrosis, cirrhosis, and hepatocellular carcinoma.

1.3.3.6 LSECs in drug-induced liver injury

There have been several reports identifying LSECs as targets of hepatotoxic drugs. Dimethyl nitrosamine (DMN) has been reported to cause LSEC necrosis (very often with localized haemorrhage) in the centrilobular zone (Wang *et al.*, 2012a) which is posited to be caused by toxic metabolites that diffuse from the hepatocyte towards the sinusoidal space (Cattley & Cullen, 2013). DMN is also known to cause hepatic fibrosis (Wang *et al.*, 2012b). Microcystin-LR, an algal toxin produced by *Mycrocystis aeruginosa* found in drinking water in some parts of the world (Wei *et al.*, 2008, Mereish *et al.*, 1991), causes rapid destruction of the LSECs. Reports have shown that LSEC injury is followed by damage to the hepatocyte cytoskeleton, which in turn leads to blebbing and rounding of the hepatocytes, and liver necrosis (Hooser *et al.*, 1991). In APAP toxicity, LSEC injury precedes hepatocellular injury as early as 30 minutes after exposure (Holt *et al.*, 2010), which might be due to both direct and indirect metabolism-dependent effects (DeLeve *et al.*, 1997) and, in either case, leads to hepatic congestion *in vivo*. Swelling of the LSECs, gap formation, fenestral coalescence leading to red blood cell infiltration and accumulation into the space of Disse have been reported (McCuskey *et al.*, 2005, Ito *et al.*, 2003, Ito *et al.*, 2004, Walker *et al.*, 1983). The molecular mechanism of LSEC-specific cell death in APAP

toxicity has been described to be through TNF-related apoptotic-inducing ligand (TRAIL) activation (Badmann *et al.*, 2012). Other drugs known to cause LSEC injury include antimycin A (Braet *et al.*, 2003), diclofenac (Triebskorn *et al.*, 2004), and small molecule tyrosine kinase inhibitors (Koudelkova *et al.*, 2015).

1.3.4 LSECs in organotypic co-culture systems

In an attempt to recapitulate a liver-like organotypic system, *in vitro* pharmacological, toxicological and drug metabolism studies have increasingly incorporated non-parenchymal cells (NPCs) including LSECs. These efforts have been geared towards creating more *in vivo*-relevant experimental models to better mimic and predict biological processes and response to xenobiotics (reviewed in Handa *et al.* (2014), Godoy *et al.* (2013) and Bale *et al.* (2014). Furthermore, because cell-cell interactions and paracrine signalling between constituent cells is necessary for maintenance of liver physiology (Patel *et al.*, 2012, Bhatia *et al.*, 1999) and primary human hepatocytes de-differentiate when cultured *in vitro* (Heslop *et al.*, 2016), attention has been paid to a multicellular co-culture system with the goal of enhancing hepatocellular function. Several options have been explored, including a sandwich configuration where hepatocytes are cultured with endothelial cells and/or other NPCs in different layers (Kim *et al.*, 2012), a scaffold system (Kostadinova *et al.*, 2013), and a monolayer co-culture of endothelial cells and hepatocytes (Nelson *et al.*, 2015). In order to recreate the native environment of the liver, and enhance hepatic functionality, 3D co-cultures of hepatocytes and endothelial cells has been attempted using different methods and materials (Inamori *et al.*, 2009, Takezawa *et*

al., 1992, Takebe *et al.*, 2014, Miyamoto *et al.*, 2015, Otsuka *et al.*, 2013, Messner *et al.*, 2013, Chan *et al.*, 2016, Kang *et al.*, 2015). These have been found to be more functional and more predictive of *in vivo* liver physiology compared to their 2D counterparts (reviewed in Achilli *et al.* (2012)). For example, Takebe *et al.* (2013) created vascularized 3D liver buds using induced pluripotent stem cells (iPSCs), human mesenchymal stem cells and human umbilical vein endothelial cells. These authors observed a self-organization into a 3D system with a highly vascularized organoid. Not only did they demonstrate an expression of albumin and CYP enzymes, these liver organoids metabolized CYP-specific substrates.

A major shortcoming of these models developed so far is the fact that they are not made up exclusively of primary liver cells. Also, the endothelial cells included in these studies were neither microvascular nor were they of liver origin. Whereas LSECs are unique in their expression of phenotypes of both vascular endothelial and lymphatic endothelial cells (Sorensen et al., 2015, Rafii et al., 2016), they are better suited in multicellular organotypic hepatic models. Owing to the fact that primary human hepatocytes de-differentiate in culture and are not readily available/accessible coupled with the effect of inter-individual variability, alternative sources of hepatocyte or hepatocyte-like cells are desirable (Nelson et al., 2015). Using stem-cell-derived hepatocytes and immortalized cell lines like HepaRG makes for easy accessibility, availability, and reproducibility (Marion *et al.*, 2010, Du *et al.*, 2014).

1.3.5 LSECs in the future of toxicity testing

Being the first point of contact with xenobiotics, antigens, and other foreign particles in blood flowing into the liver, LSECs are equipped with a robust system that protects the liver against such harmful agents. A compromise to this system as described above results in injury to both the LSECs and ultimately the liver parenchyma, resulting in liver injury. A very important factor in the regulation and function of LSECs in the liver is growth factor signalling. VEGF, which specifically acts on endothelial cells, is also involved in their pathophysiology and in the survival of the liver from toxic insults by known hepatotoxins (Donahower et al., 2010b, Ding et al., 2014, Ding et al., 2010a). These effects are known to be mediated via the activation of the VEGFR-2 which leads to a series of intracellular signalling cascades that results in cell survival, proliferation, and migration (Holmes et al., 2007). It is therefore plausible that inhibition of these pathways might partly explain why certain small molecule tyrosine kinase inhibitors have caused liver toxicity in cancer patients (Shah *et al.*, 2013, Weng *et al.*, 2015, Karczmarek-Borowska & Sałek-Zań, 2015). This hypothesis is yet to be to confirmed and reported in the literature. Equally, LSECs have been reported to selectively express VEGFR-3 which gives them a unique phenotype in comparison to vascular endothelial cells (Ding et al., 2010a). It would be informative to explore the physiological role of this receptor and its activation on LSECs. Finally, in view of the role of LSECs in liver physiology, building an organotypic *in vitro* model of drug-induced liver injury (DILI) should ideally include primary LSECs alongside freshly isolated primary hepatocytes and other liver cell types derived from

the same species. The following section focusses on the regulation of endothelial cell physiology by means of the tyrosine kinases.

1.4 TYROSINE KINASES IN ENDOTHELIAL CELL PHYSIOLOGY

1.4.1 Tyrosine kinases

Tyrosine kinases are a family of enzymes that catalyse the phosphorylation of tyrosine residues present on proteins (Nelson *et al.*, 2008). Phosphorylation involves the transfer of the γ-phosphate group from a high-energy nucleoside phosphate donor such as adenosine triphosphate (ATP) to the hydroxyl group of the tyrosine residue on the target protein substrate, thereby effecting a functional change of the protein (Hubbard & Till, 2000, Nelson et al., 2008, Ségaliny *et al.*, 2015). Tyrosine kinases can be broadly grouped into receptor and non-receptor tyrosine kinases (Krause & Van Etten 2005, Hubbard & Till, 2000). Non-receptor tyrosine kinases (NRTKs) are cytoplasmic kinases which, after receiving signals originating from extracellular cues, phosphorylate tyrosine residues on intracellular proteins in order to modulate their functions (Paul & Mukhopadhyay, 2004, Wan *et al.*, 2014, Gocek *et al.*, 2014). NRTKs can be grouped into nine distinct families, categorised on the basis of the similarity of their domain structure in relation to the catalytic Src Homology 1

(SH1), p-Tyr binding Src Homology 2 (SH2), and protein-protein interaction Src Homology 3 (SH3) domains which share a high degree of homology. This has been comprehensively reviewed by Gocek et al. (2014). They lack characteristic features of receptors tyrosine kinase which include an extracellular ligand-binding domain, a transmembrane and an intracellular portions, described below. Some NRTKs are attached to the plasma membrane via amino-terminal modifications such as palmitoylation (Hubbard & Till, 2000). In general, NRTKs are involved in diverse signalling processes including regulation of the immune system, cytoskeletal remodelling and oncogenesis (Paul & Mukhopadhyay, 2004). On the other hand, a receptor tyrosine kinase is a transmembrane glycoprotein that are activated following binding with its specific ligands (cytokines, growth factors etc). This results in the generation of an extracellular signal which is transduced to its cytoplasmic domain, resulting in the phosphorylation of specific tyrosine residues on themselves or other intracellular proteins, thereby setting up a cascade of signalling events that result in such cellular processes as cell proliferation, migration, differentiation, and survival (Schlessinger & Ullrich, 1992). Receptors tyrosine kinase (RTKs) are broadly divided into 20 distinct subfamilies, among which are epidermal growth factor receptor (EGFR), fibroblast growth factor receptor (FGFR), and vascular endothelial growth factor receptor (VEGFR) families (Robinson *et al.*, 2000). RTKs are made up of three main parts; an N-terminal extracellular domain, a transcellular domain and a C-terminal intracellular domain (Ségaliny et al., 2015) (Figure 1.10). For example, VEGFR-2 is a dimer containing an N-terminal extracellular domain made up of 7 immunoglobulin-like domains; domains II and III are responsible for ligand binding, such that after ligand binding and dimerization with another receptor, domain VII in

the two receptor monomers are held together to bring about stability of the receptor dimer (Ruch *et al.*, 2007). More importantly, this process helps hold the intracellular kinase domain in order to effect autophosphorylation (Holmes et al., 2007). The intracellular part of VEGFR-2 consists mainly of kinase domains 1 and 2, between which there is a kinase insert domain. Then there is a C-terminal tail at the end of the receptor.

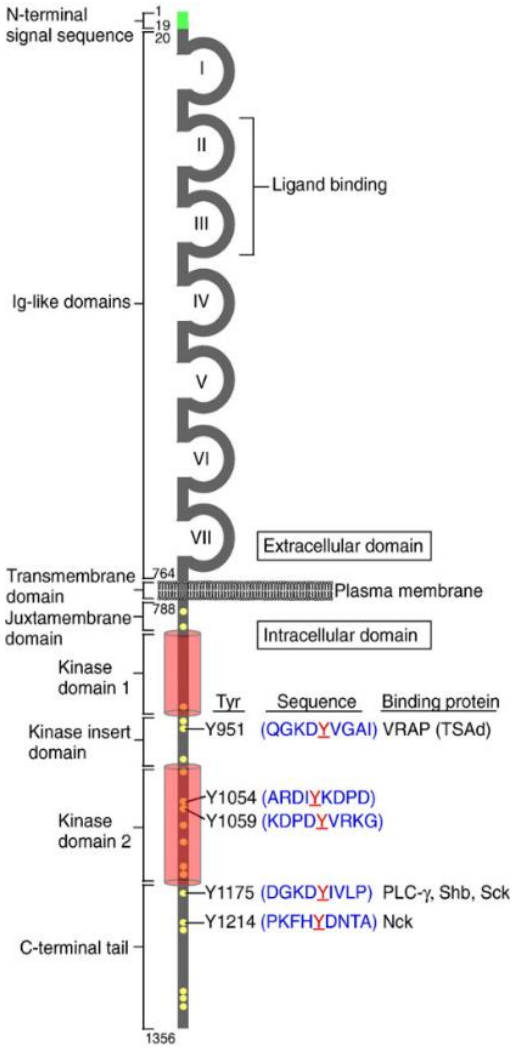

Figure 1.10: Structure of a human VEGFR-2 showing phosphorylation sites

Receptor consists an extracellular N-terminal consisting a 7 Ig-like domains and an intracellular C-terminal consisting of different phosphorylation sites. The Ig-like domains II and III are suited for ligand recognition and binding while the domain VII helps hold the two monomers together. The different phosphorylation sites are denoted by yellow dots showing the position of tyrosine along the amino acid sequence. The different tyrosine residues on the sequence have their specific roles and proteins they bind to in order to initiate a cascade of intracellular signalling with their cellular responses as shown in Figure 1.11 below. Source: Holmes *et al.* (2007)

Phosphorylation of specific tyrosine residues on the receptor kinase domain initiates a series of events that brings about the recruitment of certain intracellular proteins;

this triggers the pathway that the recruited protein is associated with (Figure 1.12). In a general sense, for endothelial cells, this results in the main endothelial physiological responses namely survival, permeability, proliferation and migration; all of these contribute to formation or maintenance of vasculature. Meanwhile, the next section focusses on vascular endothelial growth factor receptor family.

1.4.2 Vascular endothelial growth factor ligands and their receptors

1.4.2.1 Vascular endothelial growth factors

Vascular endothelial growth factors are a group of glycoproteins which act on three related receptors tyrosine kinase denoted vascular endothelial growth factor receptors (VEGFR) -1, -2, and -3. The VEGF ligands are generally called VEGF-A, VEGF-B, VEGF-C, VEGF-D, placenta growth factor (PIGF) (Zhuang & Ferrara, 2015). These ligands bind and activate the different receptors in distinctive manners. **VEGF-A** is the main ligand involved in the regulation of development and growth of blood vessels (Ferrara *et al.*, 2003). VEGF-A is required for physiologic angiogenesis during embryogenesis. The lack of a single *vegf-a* allele in mice has been shown to be embryonically lethal due to inability to form a functional vasculature (Carmeliet *et al.*, 1996). On the other hand, there is an overexpression of this growth factor in inflammation and tumour, leading to angiogenesis—abnormal vascularisation arising from a pre-existing blood vessels (Chung *et al.*, 2010). Splice variations of VEGF-A and how they affect specificity and catalytic properties of VEGF-A has been reviewed by

Ferrara et al. (2003), Holmes et al. (2007) and Zhuang and Ferrara (2015). **VEGF-B**, is a growth factor critical for endothelial cell survival (Zhang *et al.*, 2009a) rather than angiogenesis (Li *et al.*, 2009). It bears 88 % amino acid sequence homology to VEGF-A and selectively binds to VEGFR-1 for its action (Sun *et al.*, 2006, Olofsson *et al.*, 1998). Unlike VEGF-A, it does not play a critical role in vascular development. During embryogenesis, VEGF-B knockout mice manifest cardiac malformation (Aase *et al.*, 2001). **VEGF-C** and **VEGF-D** are ligands required for lymphangiogenesis and angiogenesis during embryonic development. Their angiogenic and lymphangiogenic effects are mediated via activation of VEGFR-2 and VEGFR-3 respectively (Joukov *et al.*, 1996). A complete absence of VEGF-C is embryonically lethal as shown in a murine study (Karkkainen *et al.*, 2004) while VEGF-D is not as critical (Baldwin *et al.*, 2005).

1.4.2.2 Vascular endothelial growth factor receptor family

All vascular endothelial growth factor receptors belong to the receptor tyrosine kinase family. They are generally subdivided into three groups comprising VEGFR-1, VEGFR-2 and VEGFR-3. Just as described above, they all possess an N-terminal extracellular ligand recognition and binding domain, as well an intracellular C-terminal catalytic domain (Ségaliny et al., 2015). **VEGFR-1** is a 151 KDa protein expressed on vascular endothelial cells, monocytes (Sawano *et al.*, 2001), dendritic cells and haemopoietic stem cells (Dikov *et al.*, 2005). While not essential for vascular development, VEGFR-1 is required for vascular organisation during embryonic development, as shown in a study with

vegfr$^{-/-}$ mice. Lethality was observed due to the inability of the endothelial cells to organise into functional vascular channels but they were excessive and disorganised (Fong *et al.*, 1995). It has been suggested that, in the vascular endothelium, VEGFR-1 might actually play a negative regulatory role in vascular development. Hiratsuka *et al.* (1998) deleted the kinase domain in the *vegfr-1* in a mouse embryonic model without affecting the recognition and ligand binding extracellular domain. VEGF-A-induced macrophage migration was supressed. However, the mice survived and developed normal vasculature. This suggests that VEGFR-1 might be involved in reducing the sheer amount of VEGF-A available for binding with VEGFR-2 during vascular development in order to regulate angiogenesis; this is reasonable as it is has also been shown that VEGFR-1 has a higher binding affinity for VEGF-A than VEGFR-2 (Kendall & Thomas, 1993). VEGFR-1 might also play a role in liver regeneration as shown by LeCouter *et al.* (2003). **VEGFR-2** is a 225 KDa receptor tyrosine kinase with binding affinity for VEGF-A, VEGF-C and VEGF-D (Figure 1.11). Unlike VEGFR-1, VEGFR-2 is a key element in embryonic vasculogenesis. Shalaby *et al.* (1995) have demonstrated lethality in *vegfr-2*$^{-/-}$ mice as early as day 8.5. This was due to a defective haematopoietic and vascular formation. VEGFR-2 signalling is responsible for most of the downstream effects that characterise VEGF-A and which drive vascular endothelial cell physiology. These will be discussed in the next section. It also worth noting that liver repair and regeneration secondary to partial hepatectomy or hepatotoxin exposure involves VEGF-A/ VEGFR-2 signalling as already discussed above (section 1.3.2.6). **VEGFR-3** is a 153 KDa monomeric RTK which can dimerise with itself, VEGFR-2 or neuropilin-2 (Zhuang & Ferrara, 2015). VEGFR-3 shows ligand affinity with VEGF-C and VEGF-D to effect lymphangiogenesis. It is expressed in lymphatic endothelial cells and fenestrated vascular endothelial cells such

as LSEC. Paavonen *et al.* (2000) and Dumont *et al.* (1998) have shown that a knockout of VEGFR-3 is embryonically lethal. Since VEGFR-3 has been shown to be crucial for lymphangiogenesis (Zhang *et al.,* 2010) the physiological relevance of its presence on liver sinusoidal endothelial cells remains to be understood.

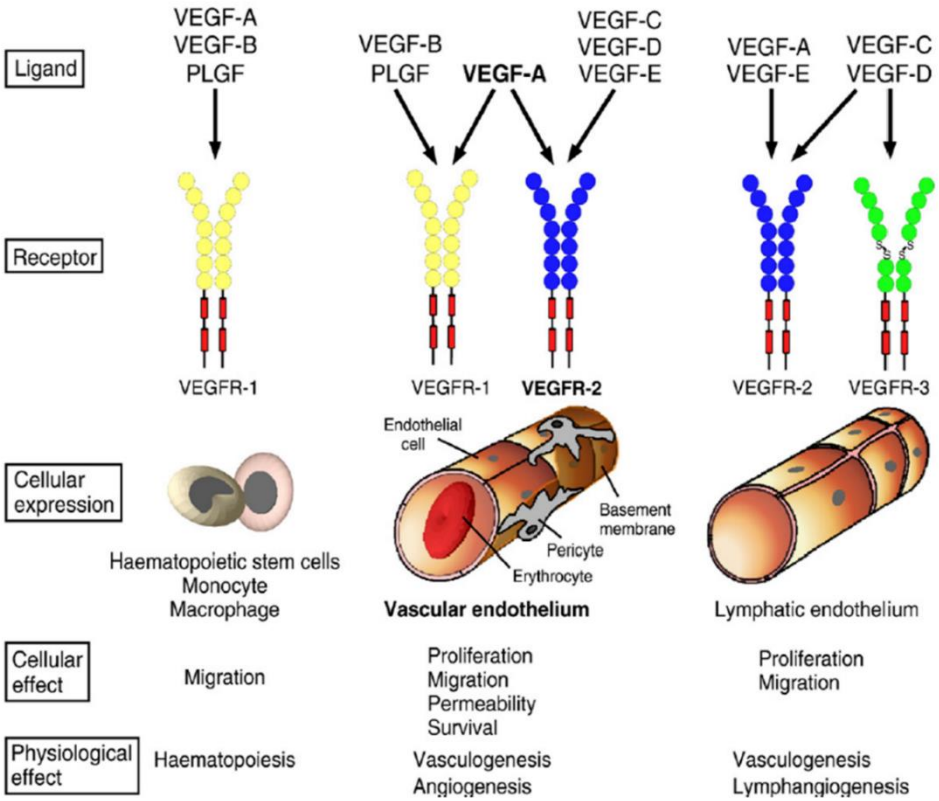

Figure 1.11: Ligand-binding specificities of different vascular endothelial growth factor receptors.

Broadly, the VEGF receptors are divided into receptors -1, -2 and -3. VEGFR-1 is mainly located on haematopoietic stem cells, monocytes, microphages and vascular endothelium; ligand-binding specificity includes VEGF-A, VEGF-B and PLG mainly leading to cell migration during haematopoiesis, while it is involved in mediating vascular endothelium-specific cellular and physiological effects. VEGFR-2 is located on the vascular and lymphatic endothelia; while it mediates proliferation, migration, permeability and survival on the vascular endothelium resulting in vasculogenesis and angiogenesis, it is more suited to cell proliferation and migration in the lymphatic endothelium, resulting in vasculogenesis and lymphangiogenesis. Ligand specificity is shown in the schematic diagram. VEGFR-3 is exclusively found on lymphatic endothelium and some specialised vascular endothelium like the LSEC. Upon binding with VEGF-C or VEGF-D, VEGFR-3 mediates cell proliferation and migration leading to vasculogenesis and lymphangiogenesis in the lymphatic endothelium, while it promotes vasculogenesis and angiogenesis in the LSEC. *Source: Holmes et al. (2007)*

1.4.3 Cellular effect of VEGF-induced VEGFR activation

As briefly mentioned earlier, the cellular effect of stimulation of VEGFR-2 leads to cell migration, permeability and survival. The section that follows shows the signalling cascades that bring about these effects.

1.4.3.1 Cell proliferation

Activation of VEGFR-2 after VEGF-A binding stimulates cell proliferation via the RAS/RAF/ERK/MAPK pathway (Meadows *et al.*, 2001). This takes place following phosphorylation of the Y1175 tyrosine residue which in turn phosphorylates PLCγ and a subsequent activation of PKC (Takahashi *et al.*, 2001). This takes place when the phosphorylated PLCγ induces the hydrolysis of the membrane phospholipid phosphatidylinositol (4, 5)-bisphosphate (PIP_2) which results in the generation of diacylglycerol (DAG) and inositol 1, 4, 5-trisphosphate (IP_3). The latter—IP_3— effects an increase in intracellular Ca^{2+} while DAG activates PKC which has been implicated in the regulation of VEGF-A mediated proliferation (Wellner *et al.*, 1999). Activation of PKC causes an activation of protein kinase D (PKD) which has been reported to induce the translocation of histone deacetylases (HDACs) 5 and 7 into the nucleus (Ha *et al.*, 2008, Wang *et al.*, 2008). Both the activation of PKD and ERK ultimately lead to cell proliferation (Koch & Claesson-Welsh, 2012) (Figure 1.12).

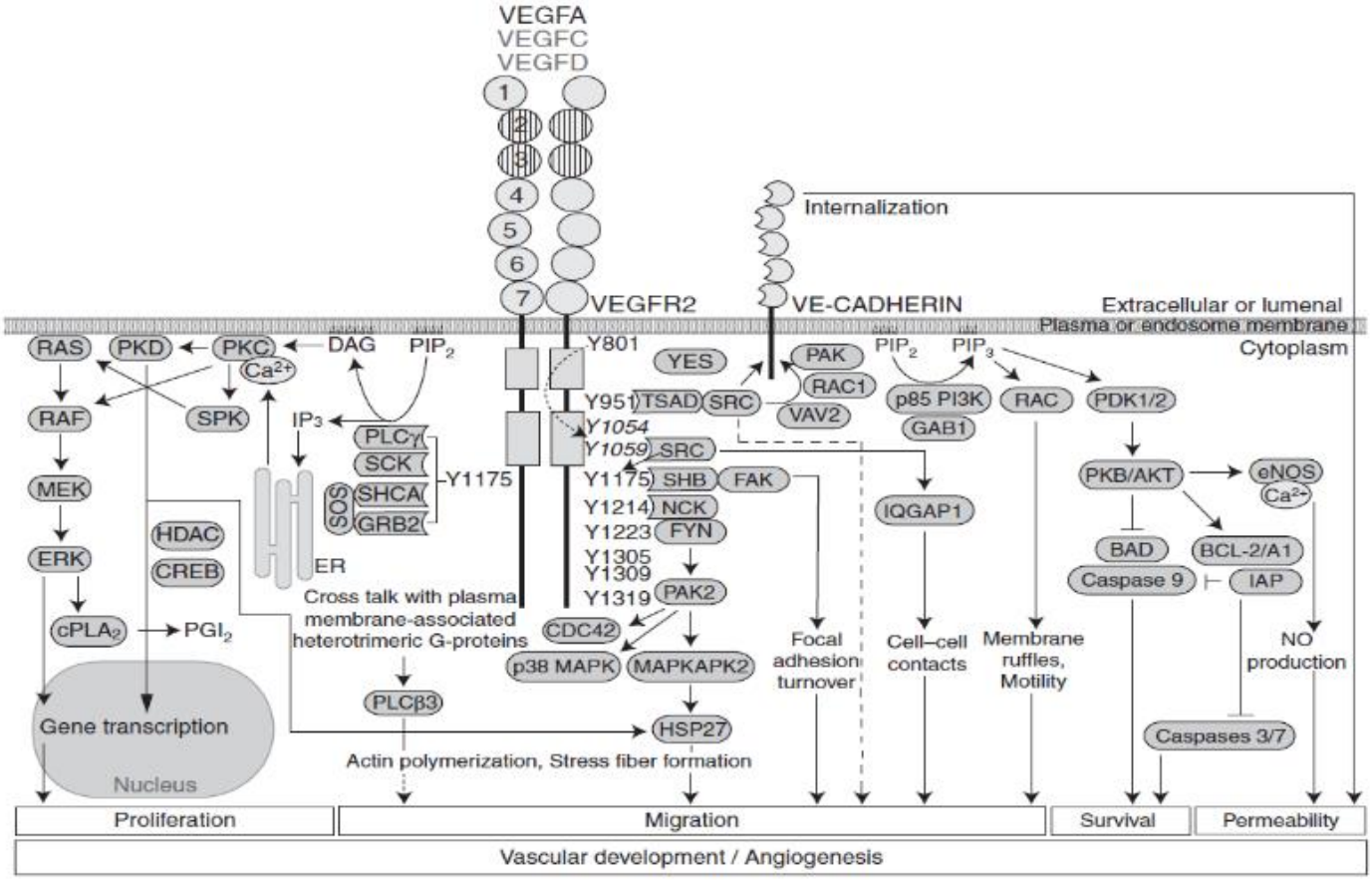

Figure 1.12: Signal transduction following VEGFR-2 activation

As a result of a complex series of intracellular signalling mediated by VEGF-A, -C and –D, VEGFR-2 is activated via tyrosine phosphorylation at intracellular resulting in the activation of different pathways that mediate different endothelial cell responses. These include cell proliferation, migration, survival and permeability, and are required for the formation and/ or maintenance of endothelial vascular structures. *Source: Koch and Claesson-Welsh (2012)*

1.4.3.2 Cell migration

In order for endothelial cells to form new vascular structure, they need to migrate in response to and towards the relevant stimulant (e.g. growth factor like VEGF-A) (Gerhardt & Betsholtz, 2005). This they do by migrating through basement membrane that has been previously degraded by proteases (e.g. matrix metalloproteinases; MMPs). As illustrated in Figure 1.12**,** quite a few tyrosine residues (e.g. Y951, Y1175, and Y1214) are phosphorylated to effect endothelial cell migration. For example, phosphorylated Y1175 binds to SHB in an SRC-dependent manner; and SHB further binds to focal adhesion kinase (FAK) (Holmqvist *et al.*, 2004). This process has been described in the regulation of cell migration and attachment (Parsons, 2003). Other intracellular proteins and pathways are illustrated in Figure 1.12 and have also been reviewed (Holmes et al., 2007, Lamalice *et al.*, 2007, Koch & Claesson-Welsh, 2012).

1.4.3.3 Cell Survival

Cell survival occurs following receptor activation and phosphorylation which in turn activates PI3K activation. This is accompanied by the generation of membrane-bound PIP3 which initiates the recruitment of PKB/AKT towards the membrane and its phosphorylation by phosphoinositide-dependent kinases 1 and 2 (PDK1 and PDK2). AKT phosphorylates BCL-2-associated death promoter (BAD) and caspase 9 in order to inhibit their apoptotic activity (Cantley, 2002, Cardone *et al.*, 1998), which results in cell survival. Also, VEGF-A activation of VEGFR-2 induces the expression of BCL-2

and A1, inhibitors of apoptosis (IAP) and survivin, which block the activation of pro-apoptotic proteins caspases 3 and 7 (Gerber *et al.*, 1998, Deveraux *et al.*, 1998, Li *et al.*, 1998).

1.4.3.4 Cell permeability

In order to ensure neovascularisation or angiogenesis, VEGF-A induces endothelial cell permeability. The process that results in vascular permeability involves the formation of transcellular endothelial pores and the transient opening of the endothelial cell-cell junction (Bates & Harper, 2002, Garrido-Urbani *et al.*, 2008). Endothelial nitric oxide synthase (eNOS), can give rise to production of nitric oxide (NO) which induces cell permeability due to VEGF-A exposure. Prior to this, eNOS can be activated either by PLC-induced Ca^{2+} influx or AKT-mediated phosphorylation which results in production of NO and the subsequent induction of cell permeability. Other factors that impact on cell permeability are the presence of tight junction and adherens junction proteins on endothelial cells (Dejana *et al.*, 2008, Tornavaca *et al.*, 2015). Adherens junction are made up of proteins belonging to the cadherin family. An important member of this family is VE-cadherin which is located at endothelial cell-cell junction which is important for the formation new vasculature during angiogenesis. Its main function is in the maintenance of regulation of endothelial junction, while still enabling movement of molecules though the junction (Vestweber, 2008). On the other hand, the tight junctional proteins responsible for the formation of a tight barrier between endothelial cells are required for endothelial cell integrity (Tornavaca et al., 2015). The main protein involved in this is the *zonas*

occludins-1 (ZO-1). The molecular mechanism underlining its regulation of cell permeability has been reviewed by (Wallez & Huber, 2008).

1.4.4 Tyrosine kinase inhibitors

Tyrosine kinase inhibitors (TKIs) are a group of antineoplastic drugs that inhibit the growth and progression of cancer cells by interfering with specific pathways required for the growth and development of tumours (Krause & Van Etten 2005). Unlike the mainstream cytotoxic drugs which are non-selective and are toxic to all rapidly-dividing cells, TKIs are designed to be targeted towards specific molecules that are highly expressed in or mutated in tumour cells (Gharwan & Groninger, 2016). A hallmark of cancer is angiogenesis (Hanahan & Weinberg, 2000) which is the formation and development of new vessels from extant vasculature (Bergers & Benjamin, 2003). Angiogenesis helps to provide nutrients and oxygen to tumours beyond 1-2 mm^3 to help sustain proliferation and metastasis (Verheul *et al.*, 2004). The vascular endothelial growth factor (VEGF) pathway is one crucial pathway required for angiogenesis and is the main target of antiangiogenic TKIs (Gotink & Verheul, 2010a)

1.4.4.1 Mechanisms of action of tyrosine kinase inhibitors

Receptor tyrosine kinase inhibitors are small molecules which act by competitively targeting the ATP-binding site of a kinase in the intracellular domain of the receptor tyrosine kinase (Gotink & Verheul, 2010a). In fact, some of them bear structural

similarity to the adenine ring of ATP which makes them act like antimetabolites which were among the first class of chemotherapeutic agents that interfere with cellular functions due to their structural similarity to endogenous molecules required for nucleic acid synthesis (Parker, 2009). An example is illustrated in Figure 1.13 below.

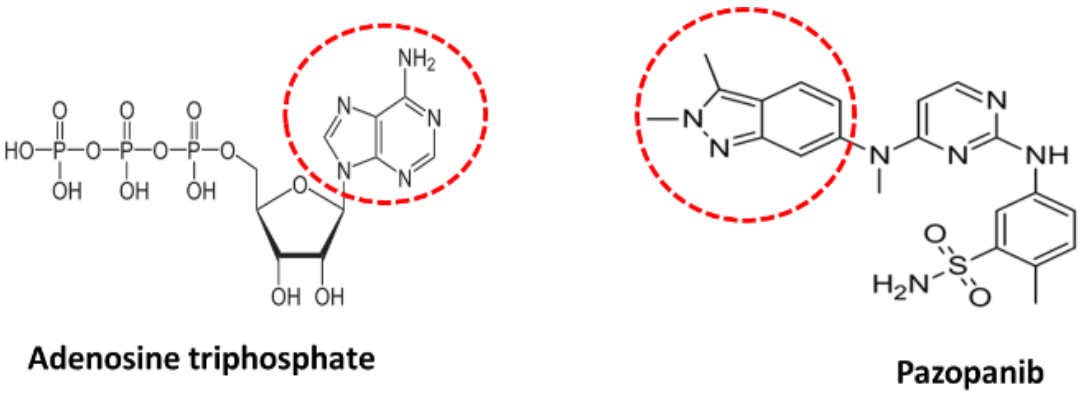

Figure 1.13: Structural similarity between ATP and tyrosine kinase inhibitors.
Structural similarity is one of the conditions that enhance the inhibitory activities of tyrosine kinase inhibitors. This, in part, enable them to form hydrogen bond with the kinase domain in a manner similar to ATP in order for them compete with it.

Tyrosine kinase inhibitors can act via different mechanisms, which includes binding to the ATP-binding site by means of hydrogen bond in a manner similar to ATP, thereby competing with ATP. Other TKIs indirectly compete with ATP by binding to the allosteric site directly adjacent to the ATP-binding site, thereby modulating a kinase activity in an allosteric manner, blocking phosphorylation of the receptor and no signal transduction (Wan *et al.*, 2004). Some other TKIs can covalently bind with cysteine at specific sites on the kinase. This covalent binding takes place when electrons are shared between the electron-rich sulphur group of the cysteine residue

of the kinase and the electrophilic group in the TKI. This prevents the formation of hydrogen bonds required for ATP to bind to its site on the kinase, thereby leading to inhibition of kinase activation (Kwak *et al.*, 2005). The mechanism of action of TKIs via competitive inhibition of the ATP-binding on the kinase domain has been comprehensively reviewed by Zhang *et al.* (2009b). In terms of spectrum of activity and anti-kinase actions, small molecule TKIs target a number of kinases which are involved in different angiogenic and oncogenic pathways. For example, the TKIs discussed below target not only the angiogenic pathway. They also target pathways that enhance tumour growth, thereby effecting a 'silver-bullet' response in cancer chemotherapy. Also, in terms of the anti-angiogenic effect of TKIs, a drug that targets the activation of VEGFR, FGFR and PDGR also seem to be a good fit as it can affect key pathways that are involved in formation and stability of blood vessels.

1.4.4.2 Tyrosine kinase inhibitors and liver toxicity

As earlier noted, many TKIs target multiple pathways and in some cases these may be the unintended ones. While the primary target of anti-angiogenic TKIs are tumour vasculature, the pathways they inhibit are also required for the physiology of blood vessels both in the vascular bed where the tumours are situated and in other organ-systems. The inability of TKI to differentiate non-tumour-associated vasculature to vasculatures in tumours is a potential for drug toxicity (Widakowich *et al.*, 2007, Gotink & Verheul, 2010a). There have been reported cases of vascular disorders even in patients receiving non-antiangiogenic TKIs (Valent *et al.*, 2015, Pasvolsky *et al.*, 2015). Other effects reported for TKIs include cardiovascular, haematological,

gastrointestinal, dermatologic and hepatic toxicities, which could range from mild to fatal (Gharwan & Groninger, 2016). Hepatotoxicity has also been reported for this class of drugs. Imatinib, which targets BCL-Abl in chronic myelogenous leukaemia (CML) was discontinued as a result of hepatotoxicity owing to reports of severe cytolytic hepatitis with necrosis resulting in acute liver failure (Cross *et al.*, 2006, Ohyashiki *et al.*, 2002).

1.5 DRUG-INDUCED LIVER INJURY AND HEPATOTOXIC DRUGS

As indicated in the introduction of this chapter, most studies intended to understand the mechanisms of DILI have focussed primarily on the hepatocytes, being the main cell types of the liver, and being at the centre of most liver functions (LeCluyse *et al.*, 2012b). However, the fact that other cells – for example, LSEC – play critical roles in liver functions also suggest toxic events that affect their physiology might also contribute to DILI. This has been highlighted in section 1.3.3.6. As revealed in section 1.4.4.2 above, DILI events might be due to on-target effect, wherein the toxicity is due to cellular interaction that affects the physiology of the cell. On the other hand, it might affect a target different from the intended one, resulting in toxicity. In some cases, toxicity might arise from the physicochemical property of the xenobiotic thereby impacting on cellular components or processes (Rudmann, 2013). As earlier noted, hepatotoxicity has been reportedly responsible for the withdrawal of drugs during development. In addition, some drugs were withdrawn during post-marketing

surveillance. There are some other drugs currently in clinical use which cause toxicity in selected population, or those that are toxic due to repeated use, over-dosage or as a result of metabolic bio-activation.

1.5.2 Adverse reactions – types and classification

The description of drug toxicities described above fits well with the well-documented classification of adverse drug reactions (ADRs) which can be grouped as types A, B, C , D, E and F as reported by Edwards and Aronson (2000). **Class A** ADRs are dose-related and somewhat on-target. Toxic effects can be abrogated with withdrawal of the drug. Examples include cardiac glycosides like digoxin. **Class B** ADRs are non-dose-related and are characteristic of idiosyncratic and immunological reactions as reported for β-lactam antibiotics (Amali *et al.*, 2016) and which could lead to organ damage (Meng *et al.*, 2016). **Class C** ADRs are dose-related and time-related. Toxicity results from chronic exposure to the drug of interest. Examples include hypothalamic-pituitary-adrenal axis suppression by corticosteroids. **Class D** ADRs are the uncommon types which are often delayed and uncommon, characteristic of carcinogenic drugs. **Class E** ADRs are also uncommon and often occur as a result of withdrawal of treatment as in myocardial ischaemia due to withdrawal of β-adrenergic blockers. Finally, **Class F** ADRs occur as a result of failure of drug therapy. This is common with drug-drug interaction and often dose-related. It can be reversed with dosage increase. The next subsection focuses on drugs of different therapeutic classes and varied mechanisms of DILI. Attention is paid to anti-angiogenic small molecule tyrosine kinase inhibitors which have been reported to induce liver toxicity,

which may also have potential for LSEC toxicity. Also, other drugs – clinically used or withdrawn due to adverse drug reactions – will be briefly reviewed.

1.5.1 Small molecule tyrosine kinase inhibitors

1.5.1.1 Regorafenib

Regorafenib (Stivarga®) is a multikinase inhibitor which targets oncogenic, angiogenic, and stromal receptors tyrosine kinase (Wilhelm *et al.*, 2011). It has been registered in the United States of America for the treatment of metastatic colorectal cancer and non-surgically removable advanced gastrointestinal stromal tumour (Strumberg *et al.*, 2012, FDA, 2013)

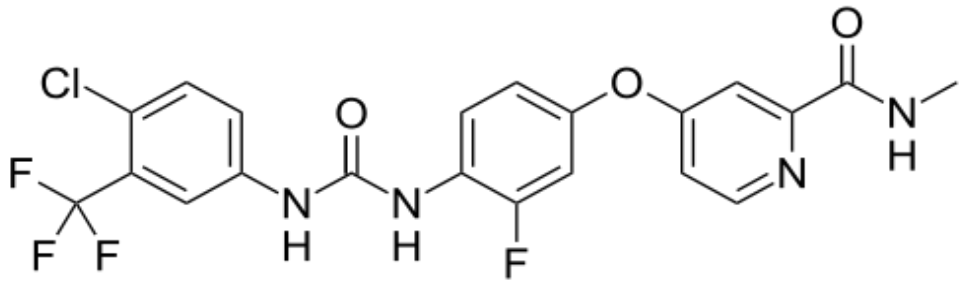

Figure 1.14: Regorafenib

Regorafenib inhibits the activation of VEGFR -1, -2 and -3, PDGFR-β, FGFR and tie-2 (Wilhelm et al., 2011, Waddell & Cunningham). Accordingly, it has been experimentally proven to be a potent inhibitor of VEGFR-2 and -3 mediated auto-phosphorylation, migration and intracellular signalling in human umbilical vascular

and lymphatic endothelial cells, and has been effective in blocking the proliferation of a metastatic colorectal cancer liver metastasis model (Schmieder *et al.*, 2014b). Regorafenib is metabolised by CYP3A4 to N-oxide and demethylated N-oxide derivatives that have been claimed to have similar molecular targets and potency as the parental compound (Zopf *et al.*, 2014). However, regorafenib has been associated with elevated liver transaminases, bilirubin and fatalities secondary to liver damage (Grothey *et al.*, 2013, Demetri *et al.*, 2013, Sacre *et al.*, 2016). In fact, there was a clinical case of sinusoidal obstruction syndrome in a patient managed with regorafenib (Takahashi *et al.*, 2016a)

1.5.1.2 Pazopanib

Pazopanib (Votrient®) is a multi-targeted TKI which targets VEGFR -1, -2 and -3, PDGFR and c-kit (Kumar *et al.*, 2009). It has demonstrated efficacy against renal cell carcinoma, lung and breast cancer, soft tissue sarcoma and pancreatic neuroendocrine tumours (Sloan & Scheinfeld, 2008, Motzer *et al.*, 2013,

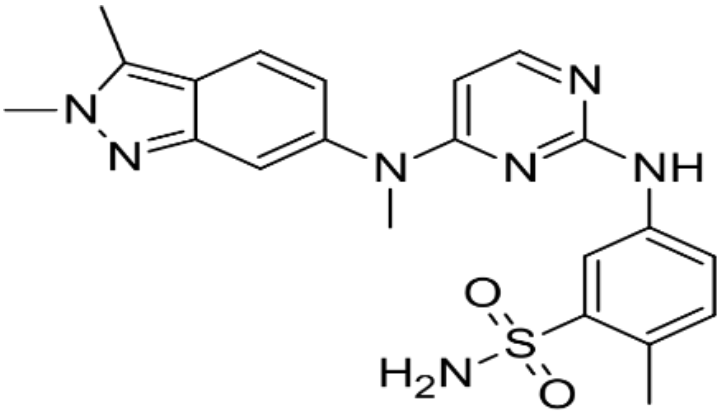

Figure 1.15: Pazopanib

Kwekkeboom, 2015). In a preclinical study, Kumar *et al.* (2005) demonstrated that pazopanib could inhibit VEGF-A-induced cell proliferation in HUVEC as well as inhibit tumour growth in a murine model. In addition to inhibiting cell proliferation and tube formation in HUVEC, Podar *et al.* (2006) have demonstrated the efficacy of pazopanib in growth inhibition and induction of apoptosis in a multiple myeloma model. Pazopanib also prolonged survival of a xenograft model of this cancer. Pazopanib is orally absorbed, metabolised mainly by CYP3A4 with minimal contributions from CYPs 1A2 and -2C8 (Deng *et al.*, 2013). Like regorafenib, pazopanib has been associated with increased levels of transaminases during clinical trials (Zivi *et al.*, 2012, Kapadia *et al.*, 2013, Phan *et al.*, 2015).

1.5.1.3 Axitinib

Axitinib (Inlyta®) is another anti-angiogenic multi-targeted small molecule TKI with potency against VEGFR-1, -2 and -3 as well as PDGFR and c-kit (Inai *et al.*, 2004). It has been approved for the treatment of renal cancer carcinoma and has demonstrated clinical efficacy in advanced pancreatic cancer in combination with gemcitabine (Spano *et al.*, 2008). It has also been used in the treatment of advanced thyroid cancer (Cohen *et al.*, 2008). Like regorafenib and pazopanib above, axitinib possesses the ability to inhibit both cancer cells and the growth of their vasculature.

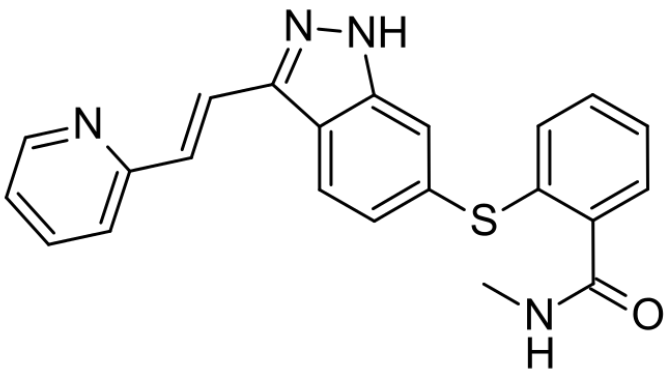

Figure 1.16: Axitinib

For example, in a study reported by Zhu *et al.* (2006), axitinib was shown to inhibit PDGR-β and VEGFR-2 phosphorylation with a corresponding reduction in inhibition of vasculature formation. Also, they demonstrated its ability to induce a regression of a human bladder cancer xenograft. In a sensitivity testing of patient-derived cancer cells, axitinib induced an inhibition of BCR-ABL 1 fusion gene, an oncogene implicated in chronic myeloid leukaemia and acute lymphoblastic leukaemia (Pemovska *et al.*, 2015). Axitinib is metabolised by CYP3A4/5 and UGT1A1 to form a sulphoxide derivative and a glucuronide conjugate respectively; neither of these is pharmacologically active (Chen *et al.*, 2013, Smith *et al.*, 2014). During clinical trials, there have been reported cases of elevated serum transaminases in a quarter of patients (Rini *et al.*, 2013) with only less than 5 % having alanine transaminase (ALT) and aspartate transaminase (AST) values greater than 5 times the upper limit of normal. However, there have been no instances of liver failure or fatality induced by liver injury reported (Shah et al., 2013).

1.5.1.4 Sunitinib

Sunitinib is a TKI approved for the treatment of renal cell carcinoma and imatinib-

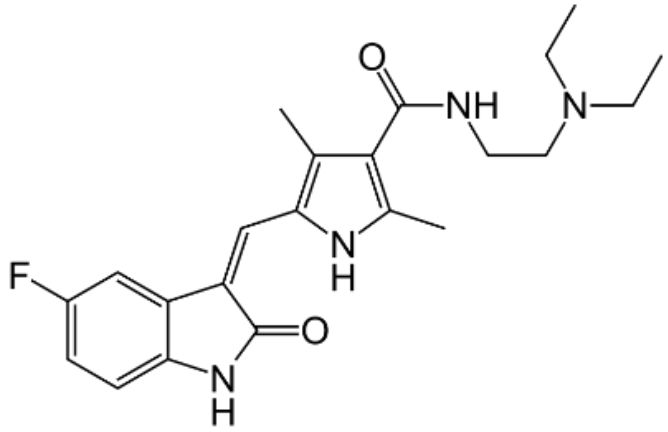

Figure 1.17: Sunitinib

resistant gastrointestinal carcinoma (Demetri *et al.*, 2006). It has also shown efficacy against breast, lung and colon cancers (Mena *et al.*, 2010) Sunitinib blocks the phosphorylation of VEGFR-1, -2, and -3 (Christensen, 2007). Osusky *et al.* (2004) have shown the efficacy of sunitinib in the inhibition of cell migration and tube formation in an *in vitro* assay, while Abrams *et al.* (2003) demonstrated its inhibitory activity against the activation of c-kit and PDGFR. Sunitinib was shown to display anticancer activity against a range of tumours in xenograft studies (Mendel *et al.*, 2003). Sunitinib is metabolised mainly via cytochrome P450-mediated routes; inducing N-de-ethylation and N-oxidation of the indolylidene and dimethylpyrrole groups on the molecule (Speed *et al.*, 2012). Sunitinib had been associated with fulminant hepatic failure—elevated AST, ALT and bilirubin—which was managed and reversed in the case of a patient being treated for renal cell carcinoma with sunitinib (Mueller *et al.*, 2008)

1.5.2 Other hepatotoxic compounds

1.5.2.1 Paracetamol

Paracetamol (acetaminophen) is a widely used analgesic, anti-pyretic drug, discovered over a century ago but extensively for used some 50 years. Despite its widespread clinical use, its mechanism of action remains an enigma. Compared to non-steroidal anti-inflammatory drugs, the safety profile of paracetamol, explains why it is an extensively used over-the-counter medication. However, in the biomedical research community, paracetamol is rather infamous for its liver toxicity as clinical and experimental research data have shown. In fact, paracetamol is at the fore-front of acute liver failure in such western nations as Great Britain (40 %) (Hawton *et al.*, 2013) and the United States (45%) (Larson *et al.*, 2005) as a result of its overdosage or chronic use.

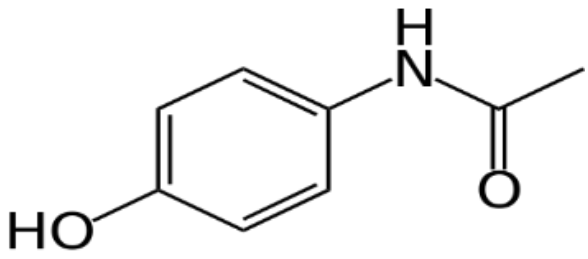

Figure 1.18: Paracetamol

Briefly, paracetamol has been commonly known to cause toxicity in high doses as a result of a rapid depletion of hepatic glutathione. Also, the detoxification pathways

involving glucuronidation and sulphation are overwhelmed. This shifts metabolism to cytochrome P450 pathways— principally CYP 2E1—which results in the generation of a toxic and highly reactive nucleophilic metabolite N-acetyl-p-benzoquinone imine (NAPQI) (Figure 1.19) (Dahlin *et al.*, 1984). NAPQI covalently binds with cellular proteins, notably on the cysteine residue; this NAPQI-protein adduct can be highly immunogenic (Roberts *et al.*, 1991). Following hepatocyte lysis, these adducts are released into circulation and can be measured (Roberts *et al.*, 2016). Also, depletion of glutathione, an antioxidant tripeptide, readily predisposes the liver to oxidative stress and further production of other free radicals that might progressively cause lipid peroxidation, and hepatocellular damage (Muriel, 2009). This explains why sylimarin—a naturally-occurring antioxidant flavonoid—has been used as an adjunctive measure in paracetamol toxicity (Feher & Lengyel, 2012). The hepatic effect of paracetamol is not restricted to the hepatocyte as has already been reviewed (Section 1.3.3.6). In fact, LSEC have been found to be early targets of paracetamol toxicity (McCuskey, 2006). Also, in a murine model of paracetamol toxicity, increased serum levels of VEGF-A were detected, whereas an intraperitoneal administration of recombinant VEGF-A effected a significant reduction in paracetamol-induced hepatic necrosis (Donahower et al., 2006, Donahower *et al.*, 2010a). Since VEGF-A is involved in the pathophysiology of endothelial cells, LSEC is evidently a target of paracetamol and other hepatic toxicant.

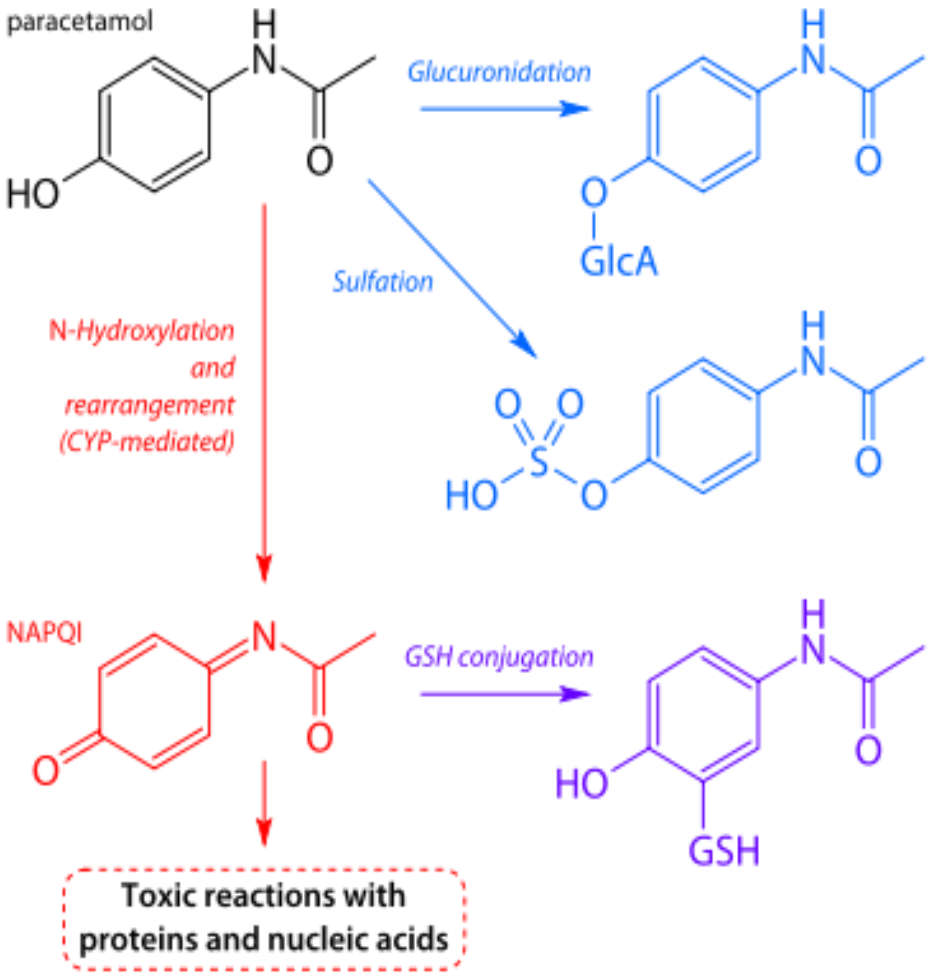

Figure 1.19: metabolism of paracetamol

Paracetamol is metabolised via the bioactivation route denoted in red colour and deactivated via the glucuronidation route denotes in blue. Paracetamol is metabolised principally by CYP2E1 and proceeds via N-hydroxylation to form NAPQI which is highly nucleophilic and highly reactive; it forms a conjugate with glutathione. On the other hand, paracetamol can be concomitantly glucuronidated or sulphated to render the parent compound more hydrophilic and extractable.

1.5.2.2 Benzbromarone

Benzbromarone is a uricosuric drug developed four decades ago and widely used in gout patients (Lee *et al.*, 2008). In gout or hyperuricaemia, there is an impairment in the excretion of uric acid whereby uric acid is reabsorbed into systemic circulation, mainly via urate transporter 1 (URAT1) (Ichida *et al.*, 2004).

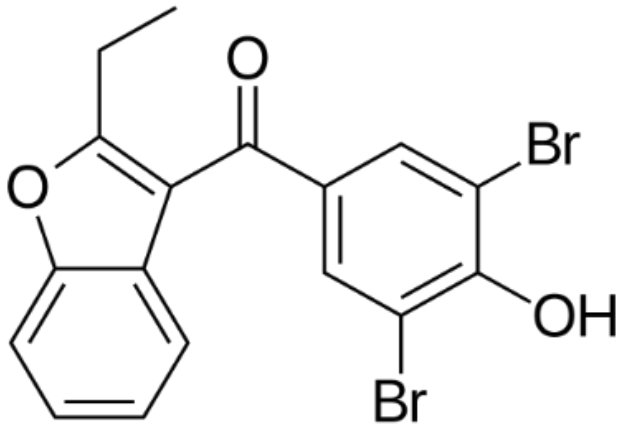

Figure 1.20: Benzbromarone

This results in a high plasma concentration of uric acid which gets deposited as crystals in the joints, kidneys and soft tissues (Daskalopoulou *et al.*, 2005, Eggebeen, 2007). Uricosuric — or antihyperuricaemic— drugs including benzbromarone largely act on the proximal tubules in the kidney to inhibit the reabsorption of uric acid, thereby enhancing its renal excretion (Becker *et al.*, 2005). The angiotensin II inhibitor losartan blocks URAT1 (Hamada *et al.*, 2008). Benzbromarone can be classed as a prodrug as the parental compound has a half-life of 3 hours, while its 6-hydroxy metabolite is the main uricosuric agent (Lee et al., 2008). Despite its potent

anti-gout activity and high clinical tolerability, benzbromarone was withdrawn from Europe in 2003 following four cases of hepatotoxicity which culminated in the death of two patients (Jansen *et al.*, 2004). The likely mechanism of benzbromarone toxicity has been elucidated by McDonald and Rettie (2007) after incubation of a pool of human liver microsomes from 13 different liver samples with benzbromarone. They found out that benzbromarone is sequentially metabolised by CYP2C9 to 6-hydroxybenzbromarone which is further metabolised to a 5, 6-dihydroxybenzbromarone—a catechol. Incubation of this product with human liver microsomes in the presence of glutathione formed a glutathione adduct. The two hydroxyl groups on the catechol were likely oxidised to form a quinone intermediate which is highly reactive, and which could have adducted with other cellular proteins (Figure 1.21). Prior to this study, Kaufmann *et al.* (2005) have shown the production of reactive oxygen species in HepG2 cells incubated with benzbromarone. Further, this study demonstrated mitochondrial toxicity, apoptosis and necrosis in rat liver treated with benzbromarone. It has also been shown in a study also involving HepG2 that benzbromarone is an uncoupler of the electron transport chain; it is also mitotoxic (Felser *et al.*, 2014).

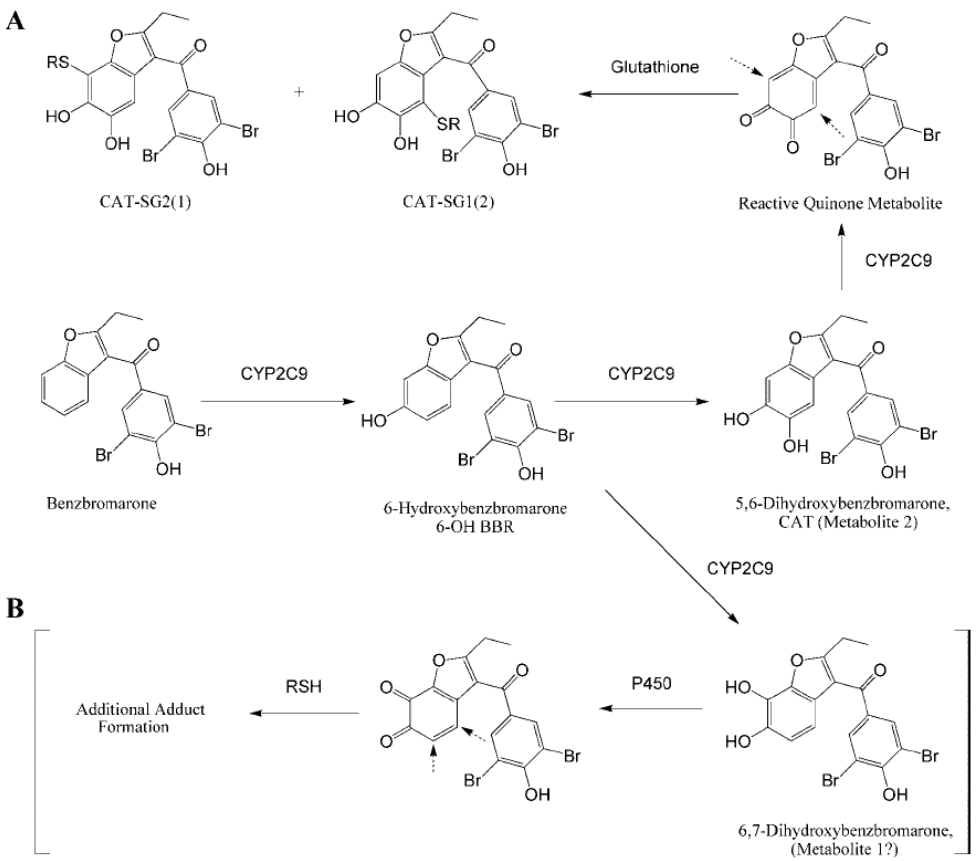

Figure 1.21: metabolism and bioactivation of benzbromarone

Benzbromarone (BBR) is metabolised by CYP2C9 to 6-hydrxybenzbromarone (6-OH BBR) which is further hydroxylated to a dihydroxy product (5,6-OH BBR or 6,7-OH BBR). The OH groups of either of these products can be oxidised to form a quinone which is highly reactive and can covalently bind with cellular protein or nucleic acid and might deplete cellular glutathione. *Adapted from McDonald and Rettie (2007)*

1.5.2.3 Desipramine

Desipramine (Norpramin®) is a tricyclic antidepressant which is formed by N-demethylation of imipramine—another tricyclic antidepressant (Linnet, 2004, Lemoine *et al.*, 1993). It mainly acts by inhibiting the reuptake of noradrenaline and serotonin (5-hydroxytryptamine) from the post synaptic neuron in the brain, thereby prolonging the central excitatory effect of noradrenaline and/ or serotonin. In addition, desipramine has been shown to have affinity for and can activate the δ- and κ-opioid receptors in the basal ganglia and neocortical regions of the brain (Peppin & Raffa, 2015), implicating its reported antinociceptive properties (Onali *et al.*, 2009). It is interesting to note that opiates like tramadol have been considered as antidepressants due to the fact that activation of the δ- and κ-opioid receptors enhance mood (Berrocoso *et al.*, 2009).

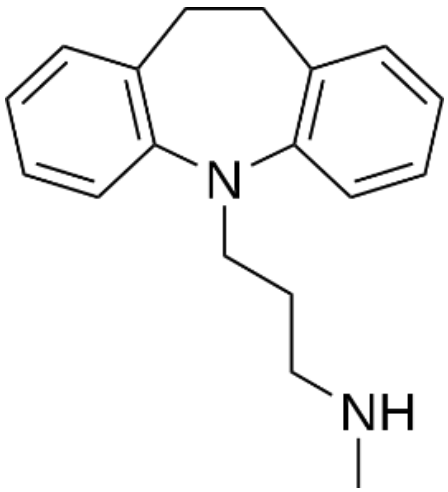

Figure 1.22: Desipramine

Desipramine is a potent inhibitor of CYP2D6 which coincidentally metabolises it (Hara *et al.*, 2005, Shin *et al.*, 2002, Reese *et al.*, 2008). This is a potential for interaction with drugs that are metabolised by this enzyme. The first case of liver toxicity in desipramine was reported by Powell *et al.* (1968) who observed midzonal and central hepatic necrosis in a patient post-mortem. Later, another case hepatitis was reported (PRICE *et al.*, 1983). There is paucity of data on the exact mechanism of desipramine-induced liver toxicity. Its inclusion in this study was to investigate its toxicity in LSEC in comparison with primary human hepatocyte and other endothelial cell types.

1.5.2.4 Perhexiline

Perhexiline (Pexsig®) is an antianginal drug developed about half a century ago (Ashrafian *et al.*, 2007). Angina pectoris occurs when myocardial oxygen supply does not meet requirement at a given point in time due to physical exertion among other factors. In most cases, this arises from myodardial ischaemia due to a reduction in blood flow to the heart, reduced oxygen-carrying capacity of the blood or reduction in vascular tone of cardiac arteries (Hung *et al.*, 2014). This results in chest pain in patients. Perhexiline is a highly hydrophobic molecule with pharmaceutical preparations existing as a racemic mixture of the (+) and (-) enantiomers (Davies *et al.*, 2007). Biochemically, perhexiline is a fatty acid oxidation inhibitor owing to its ability to inhibit the metabolism of fatty acid in the myocardium. Specifically, perhexiline is a

potent competitive inhibitor of carnitine palmitoyltransferase-1 (CPT-1) in the myocardium. (Kennedy *et al.*, 1996).

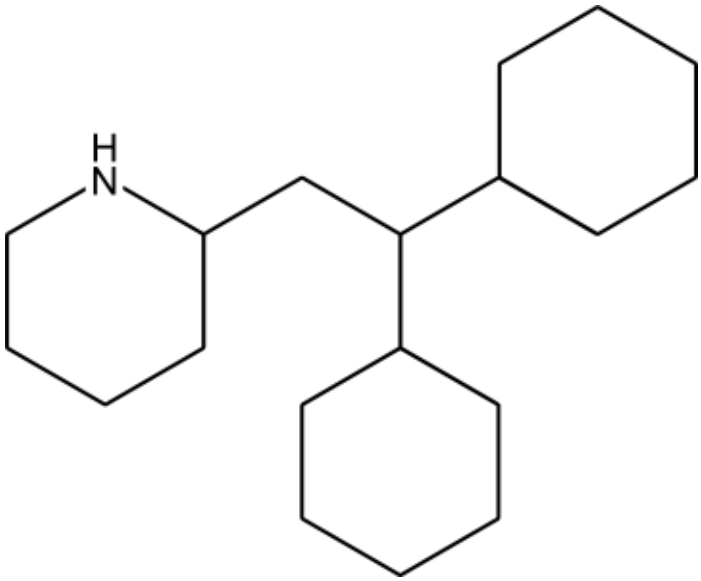

Figure 1.23: Perhexiline

This is to improve efficiency as fatty acids consume more oxygen per unit of ATP generated in the mitochondrion. Inhibition of fatty acid oxidation switches myocardial energy generation to carbohydrate metabolism which consumes less oxygen. The 30 % increase in oxygen production improves the symptoms of angina (Essop & Opie, 2004, Ashrafian et al., 2007). However, perhexiline is hepatotoxic in a selected population; its toxicity is linked to its metabolism. Perhexiline is metabolised by CYP2D6 which is highly polymorphic (Sørensen *et al.*, 2003, Gardiner & Begg, 2006). The link between metabolism and toxicity of perhexiline will be discussed in chapter 5.

1.5.2.5 Aflatoxin

Aflatoxin belongs to a class of toxic and carcinogenic chemicals derived from mold of the *Aspergillus* family, which grows on eggs, milk, meat, grains, decaying vegetation and in the soil (Baydar *et al.*, 2005). Aflatoxin B1 is of interest in this study due its reported liver toxicity (Neal *et al.*, 1998, Hamid *et al.*, 2013). Aflatoxin B1 is metabolised by CYP3A4 to form several products, one of which is an 8, 9-epoxide. This product is highly reactive and has hepatocarcinogenic potential (Guengerich *et al.*, 1996, Ramsdell *et al.*, 1991).

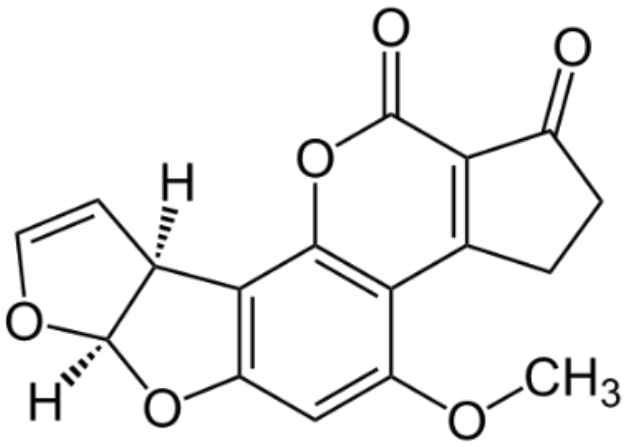

Figure 1.24: Aflatoxin B1

The table below is a summary of the drugs reviewed in the sections above

Table 1.3: Summary of drugs

Test Compound	Pharmacological class	Therapeutic dose	Plasma Cmax	Molecular target	Mechanism of liver toxicity
Paracetamol	Analgesic, antipyretic	1 g oral dose, maximum of 4 times daily	20 µg/ml	unknown	Mitochondrial toxicity, metabolic bioactivation, cytolysis, lipid peroxidation etc
Benzbromarone	Uricosuric	50-200 mg oral daily dose	3.51 µg/ml	Inhibition of urate transporter (URAT1), and xanthine oxidase.	Mitochondrial toxicity, metabolic bioactivation and covalent binding with cellular proteins etc.
Desipramine	Tricyclic antidepressant	25-300 mg/day oral	11.8 ng/ml (after 50 mg oral dose)	Inhibition of reuptake of noradrenaline and serotonin	Not characterised but may be due to inhibition of CYP 2D6 which also metabolises it.
Perhexiline	Antianginal	100- 500 mg oral daily	0.6 mg/l	Inhibition of fatty acid oxidation (inhibition of palmitoyltransferase-1 inhibition).	Mitochondrial toxicity—uncoupling of complexes I and II of oxidative phosphorylation.

Aflatoxin	Food contaminant	Not applicable	Not applicable	DNA adduction	Metabolic bioactivation to epoxides which are carcinogenic by adduction to DNA.
Regorafenib	Tyrosine kinase inhibitor antiangiogenic, antocancer.	160 mg	2.5 µg/ml	Inhibits VEGFR-1, -2 and -3. PDGFR-β, FGFR and Tie-2	Uncharacterised. May be on-target, following inhibition of signalling pathways implicated in cell physiology.
Pazopanib	Tyrosine kinase inhibitor antiangiogenic.	200-800 mg daily	58.1 µg/ml	Inhibits VEGFR-1, -2 and -3. PDGFR-β, and c-kit.	Uncharacterised. May be on-target, following inhibition of signalling pathways implicated in cell physiology
Axitinib	Tyrosine kinase inhibitor antiangiogenic, anticancer.	10 mg	27.8 ng/ml	Inhibits VEGFR-1, -2 and -3. PDGFR-β, and c-kit.	Uncharacterised. May be on-target, following inhibition of signalling pathways implicated in cell physiology
Sunitinib	Tyrosine kinase inhibitor antiangiogenic, anticancer.	37.5 mg daily	69 ng/ml	Inhibits VEGFR-1, -2 and -3. PDGFR-β and c-kit,	Uncharacterised. May be on-target, following inhibition of signalling pathways implicated in cell physiology

1.6 AIMS OF THESIS

This project was conceptualised following reports that paracetamol overdose in rats induced elevation of VEGF-A and that an exogenous administration of VEGF-A to paracetamol-intoxicated mice resulted in improved liver physiology (Donahower et al., 2010a, Donahower et al., 2006). Further, liver sinusoidal endothelial cells were damaged in paracetamol toxicity, even prior to hepatocyte damage (Walker et al., 1983, Ito et al., 2003, Ito et al., 2004, McCuskey et al., 2005). Other studies have demonstrated that liver sinusoidal endothelial cells were integrally involved in liver regeneration following partial hepatectomy and toxic injury (Ding et al., 2010b, Ding et al., 2014). Finally, some antiangiogenic receptor tyrosine kinase inhibitors are hepatotoxic (Shah et al., 2013)

Consequently, this thesis is aimed at;

1. Characterising human liver sinusoidal endothelial cells (HLSECs) and evaluating their phenotypic and functional difference to vascular and lymphatic endothelial cells from a different vascular bed.
2. Examining the sensitivity of LSEC to a broad range of hepatotoxic drugs with focus on small molecule receptor tyrosine kinase inhibitors.
3. Developing a triculture liver micro-tissue model in order to test the effect of liver sinusoidal endothelial cells on the physiology of the hepatocyte.

The main hypotheses of the thesis are:

1. Liver sinusoidal endothelial cells are a unique endothelial cell population with phenotypes that better suit them to their liver micro environment;
2. Liver sinusoidal endothelial cells are direct targets of hepatotoxins.
3. There is a direct link between the toxicity of small-molecule receptor tyrosine kinase inhibitors and their inhibition of physiology of liver sinusoidal endothelial cells.
4. Inclusion of liver sinusoidal endothelial cells in a tri-culture liver micro-tissue, helps retain the physiology of hepatocytes which de-differentiate in culture.
5. Presence of liver sinusoidal endothelial cells in liver micro-tissues protect the hepatocyte from hepatotoxicity, especially in the presence of VEGF-A and/ or VEGF-C.

CHAPTER TWO

MATERIALS AND METHODS

2.1 MATERIALS AND REAGENTS

Unless otherwise stated, all reagents were purchased from Sigma-Aldrich, (MO, USA).

2.1.1 Reagents and buffers

Fibronectin from human plasma (F0895), Collagenase type IV (C5138), Dexamethasone (D1756-100MG), Paracetamol (A7085), Collagen-I coated plates (Corning, 356400), Sterile water (Kays Medical, WAT230S), Williams E medium(W1878-6X500ML), L-glutamine (G7513-100ML), Pen/strep (P0781-100ML), Insulin-Transferrin-Selenium (Life Technology, 41400045), Calcium Chloride (Fisher Scientific, 10171800), Dimethyl sulfoxide (DMSO) (Fisher Scientific, 10080110), D-Glucose (Fisher Scientific, 10141520), HEPES (H3375-100G), Potassium Chloride (Fisher Scientific, 10375810), Sodium Chloride (1Kg) (Fisher Scientific, 10428420), Human collagen solution (Vitrocol® Advanced BioMatrix, 5007-A), Sodium chloride, Tris base, Glycine, polyoxyethylenesorbitan monolaurate (Tween-20), Sodium dodecyl sulfate (SDS), were purchased from Fisher Scientific. Ammonium persulfate (APS), ammonium chloride, Triton X-100, ethidium bromide, Tris-EDTA (TE) buffer solution (pH8.0), Dimethyl sulfoxide (DMSO). Dulbecco's Phosphate-Buffered Saline (PBS) without Ca^{2+} and Mg^{2+} (BE17-212F, Lonza, Switzerland),

Dulbecco's Phosphate-Buffered Saline (PBS) with Ca^{2+} and Mg^{2+} (17-513F, Lonza, Switzerland). 0.5% (w/v) Gelatin solution containing 0.1% (w/v) gelatin from porcine skin, (type A, cell culture tested) (Sigma-Aldrich (Poole, UK) in ddH_2O and autoclaved. Acetonitrile (MeCN)(Thermofisher, 10616653, LC-MS grade), Formic Acid (FA) (Sigma-Aldrich, 56302, LC-MS grade), Water (H_2O) (Thermofisher, 10777404, LC-MS grade), Dimethylsulphoxide (DMSO), (Sigma-Aldrich, D8418, MOL BIO grade), Acetic Acid (AcOH), (Sigma-Aldrich, 49199, LC-MS grade), Acetone (ACE), (Thermofisher, 10131560, HPLC grade), Methanol (MeOH), (Thermofisher, 10653963, LC-MS grade).

2.1.2 Growth factors

SDF-1, VEGF-A165, VEGF-C, VEGF-D, FGF-2, PDGF-BB, EGF, and HGF were purchased from Peprotech EC (Rocky Hill, NJ, U.S.A).

2.1.3 Test Compounds and compounds for LC-MS/MS

Sunitinib maleate (S1042), lapatinib GW-572016 (S2111), and staurosporine (S1421) were purchased from Selleckchem (U.S.A). Cytochalasin D (1233) was purchased from R&D systems. Aflatoxin-B1 (A6636-1MG), Benzbromarone (B5774-1G), Desipramine-HCL (D3900-1G). Fluconazole (F8929, SIGMA-ALDRICH), D_4-Fluconazole (F421002, Toronto Research Chemicals), Perhexiline

Maleate (FP27567, CARBOSYNTH), Perhexiline-d11 Maleate, (Mixture of Diastereomers), (P287322, Toronto Research Chemicals), cis-Hydroxy Perhexiline (H948905, (Mixture of Diastereomers), Toronto Research Chemicals

trans-Hydroxy Perhexiline(Mixture of Diastereomers) (H948910, Toronto Research Chemicals), cis-Hydroxy Perhexiline-d11(Mixture of Diastereomers) (H948907, Toronto Research Chemicals)

2.1.4 Protein extraction and Western blot kits

Bicinchoninic acid solution, copper (II) sulfate solution, Aprotinin, leupeptin, pepstatin, phenylmethylsulfonyl fluoride (PMSF), sodium orthovanadate (Na3VO4), paraformaldehyde, 2-mercaptoethanol, Nu-PAGE® 4-12% Bis-Tris gels, 1.5mm cassettes, 4X lithium dodecyl sulfate (LDS) sample buffer, Full-range rainbow molecular weight marker (12-225kDa), Hybond® ECL® nitrocellulose membrane, enhanced chemiluminescence (ECL) were purchased from GE healthcare (Amersham, U.K). Agarose (electrophoresis grade), NuPAGE® MES SDS Running Buffer (20X) (ThermoFisher Scientific).

2.1.5 RNA extraction, cDNA synthesis and real-time PCR kit

RNeasy RNA extraction kit (74106), sterile RNase and DNase free water, fibrous tissue RNA extraction kit (7404), DNase I, were purchased from Qiagen

Sciences (MD, USA).Oligo dT (Life technologies), dNTP mix (10 mM), 5X first strand buffer, DTT (0.1 M), of RNaseOUT (40 unit/ µl), M-MLV reverse transcriptase (200 units/µl) were purchased form Invitrogen, (Canada). 96 well semi-skirted PCR plates, 384 well PCR plates, clear polypropylene sealing film for PCR were purchased from Starlab, UK. 96-well Ultra-Low Attachment Plate (7007, Corning Life Sciences, UK). DreamTaq Green PCR Master Mix (2X) [Thermo Scientific. #K1081]

2.1.6 Animal sera

Goat serum (005-000-121) and donkey serum (017-000-121) were purchased from Jackson ImmunoResearch Laboratories (USA),

2.1.7 Human liver sinusoidal endothelial cell isolation and culture kit

PERCOLL (170891-01, GE Health Care, Buckinghamshire, UK), Mouse Monoclonal EP-CAM antibody (HEA 125) (61004, Progen Biotechnik GmbH, Heidelberg, Germany), Goat anti-Mouse IgG Dynabeads. (11033, Life Technologies LTD, UK), Mouse antihuman Dynabeads® CD31 Endothelial Cell. (11155D, Life Technologies LTD, UK), Pooled Human AB Serum (IPLA-SERAB, Innovative Research, Inc, Michigan, USA), TrypLE™ Express Enzyme (12605-010, Life Technologies LTD, UK.)

2.1.8 Cell culture media

Endothelial full growth medium: Endothelial Cell Basal Medium MV2 C-22221 (PromoCell, Heidelberg, Germany) supplemented with Foetal calf serum (5 %), Epidermal growth factor (recombinant human) 5 ng/ml, Basic fibroblast growth factor-A (recombinant human) 10 ng/ml, Insulin-like growth factor (long R3 IGF) 20 ng/ml, Vascular endothelial growth factor 165 (recombinant human) 0.5 ng/ml, Ascorbic acid 1 μg/ml, Hydrocortisone 0.2 μg/ml. **Fibroblast Full growth media**: Fibroblast Basal Medium 3 C-23230 (PromoCell Heidelberg, Germany) supplemented with Foetal calf serum 0.1 ml/ml, fibroblast growth factor (recombinant human) 1 ng/ml, Insulin (recombinant human 5 μg/ml). **DMEM Full growth media**: Dulbecco's Modified Eagle's Medium – High Glucose (DMEM) D6429 Sigma-Aldrich (Poole, U.K), supplemented with Glucose, L-glutamine, Sodium pyruvate, Sodium bicarbonate 4500 mg/L, Fetal calf serum 0.1 ml/ml. **Low serum endothelial cell medium**: Endothelial Cell Basal Medium MV2 C-22221 (PromoCell, Heidelberg, Germany) supplemented with foetal bovine serum (1 %). **HLSEC medium**: Human endothelial SFM (Invitrogen, UK) supplemented with 10% (v/v) heat-inactivated human serum [Human Serum, Innovative Research Inc.], 60 μg/ml benzyl penicillin, 100 μg/ml streptomycin and [all from Sigma, UK] and 10 ng/ml of vascular endothelial growth factor (VEGF) and hepatocyte growth factor (HGF) [both from Peprotech, UK]). **ScienCell HLSEC Medium**: Endothelial cell medium (1001, ScienCell Research Laboratory (Carlsbad, USA)), FBS (10%), penicillin-Streptomicin (1%), Endothelial cell growth

supplement (1%). **Upcyte HLSEC Medium**: Endothelial basal medium (ML 5003, Upcyte Technology GmbH, Hamburg, Germany), FBS (10 %), HGF, VEGF-A. **Primary Human hepatocyte complete medium**: Williams E medium supplemented with 1 % insulin–transferrin–selenium [Life Technologies, Carlsbad, CA], 2 mM L-glutamine [Sigma-Aldrich, St. Louis, MO], 10−7 M dexamethasone and penicillin [100 units/ml] /streptomycin [100 µg/ml] [Sigma-Aldrich, St. Louis, MO]).

2.1.9 Other reagents

Hoechst 33342 purchased from Molecular Probes Europe BV (Leiden, The Netherlands). Prolong gold anti-fade reagent purchased from Life Technologies (Paisley, U.K).

Table 2.1: Primary antibodies

Antibody	Vendor	Catalogue #	Dilution Factor	Application
R α Albumin	Abcam	Ab135575	1:50, 1:500	WB, IF
Sh α CD-31	R & D	AF806	1:1000, 1:200	IF, IHC
G α CD-31	SCBT	sc-1506	1:500	WB
R α Actin	SCBT	sc-1615	1:1000	WB
R α Anti-ZO-1	CST	40-2200	1:400	IF
R α GAPDH	CST	5174	1:2000	WB
M α Collagen 1	SCBT	sc-59772	1:100, 1:1000	IF
R α Caspase-3	CST	9662	1:1000	WB
R α AKT	CST	9272	1:1000	WB
R α P-AKT (Ser473)	CST	4060	1:2000	WB
R α VEGFR-2	CST	2479	1:1000	WB
R α P-VEGFR-2	CST	3770	1:1000	WB
R α VEGFR-3	SCBT	sc-321	1:1000	WB, IF
R α CYP 2D6	Abcam	Ab62204	1:200	WB
R α CYP 3A4	Millipore	Ab1254	1:1000	WB
R α CYP 2E1	Abcam	Ab19140	1:3000	WB
G α UGT 1A1	R&D Systems	AF6490	1:1000	WB
R α Albumin	Abcam	Ab135575	1:50, 1:500	WB, IF

Species in which antibodies were raised are indicated as: R, rabbit; M, mouse; sh, sheep; G, goat. Vendors are abbreviated as: CST, cell signalling technologies (UK); SCBT, SantaCruz biotechnology (USA).

Table 2.2: Secondary antibodies used for western blotting

Antibody	Catalogue Number	Dilution Factor
HRP Goat anti-Rabbit	111-035-144	1:5000
HRP Goat antimouse	115-035-166	1:5000
HRP Donkey antigoat	705-035-147	1:5000

All antibodies were supplied by Jackson ImmunoResearch Laboratories (USA)

Table 2.3: Secondary antibodies used for Immunofluorescence staining

Antibody	Catalogue Number	Dilution Factor
Alexa Fluor® 568 Phalloidin	A12380	1:300
Alexa Fluor® 488 Donkey anti-mouse IgG (H+L)	A21202	1:1000
Alexa Fluor® 488 Donkey anti-sheep IgG (H+L)	A11015	1:1000
Alexa Fluor® 568 Donkey anti-rabbit	A10042	1:1000
Alexa Fluor® 568 Donkey anti-mouse	A10037	1:1000
Alexa Fluor® 680 Donkey anti-mouse	A10038	1:1000
Alexa Fluor® 680 Donkey anti-rabbit	A10043	1:1000
Alexa Fluor® 488 Donkey anti-rabbit	A21206	1:1000
Hoechst 33342	H-21492	1:5000

All Antibodies were supplied by Invitrogen (Paisley, U.K).

Table 2.4: Externally sourced cells

Cell type	Source	Lot #, Catalogue #
HDMEC (Adult) #1	Abdomen of a 32-year old female, Caucasian.	0092101.2, C-12212
HDMEC (Adult) #2	Breast of a 44-year old female Caucasian.	406Z013.1, C-12212
HDMEC (Adult) #3	Temple of a 60-year old female Caucasian.	394Z028.3, C-12212
HDMEC (juvenile)	Foreskin of a 3-year old male Caucasian.	6060707.1, C-12210
HDLEC (juvenile)	Foreskin of a 4-year old male Caucasian.	2011204, C-12216
HDLEC Adult #1	Breast of a 46-year old female Caucasian.	394Z027.3, C-12217
HDLEC Adult #2	Temple of a 60-year old female Caucasian.	394Z016.2, C-12217
NHDF Juvenile	Foreskin of a 5-year old male, Caucasian.	0083002.2, C-12300
HLSEC SC		13884, 5000
Medicyte HLSEC		462-ULO-C00W0013.

All HDMEC, HDLEC and NHDF were supplied by PromoCell (Heidelberg, Germany), Human hepatic sinusoidal endothelial cells (HLSEC SC) were supplied by ScienCell Research Laboratory (Carlsbad, USA), Medicyte HLSEC were supplied by Upcyte Technology GmbH, Hamburg, Germany.

2.1.10 Human liver tissues for cell isolation

Liver tissues were obtained from liver resection following surgery at Aintree University Hospital, Liverpool, UK after full patient consent and ethical approval were obtained. Patients were adult males. For experiments reported in this study, cells were isolated from 10 different patient liver samples. Although the underlying liver pathology ranged from cholangiocarcinoma to rectal cancer, isolations were carried out on areas of the liver that were normal. All samples, cells isolated and products thereof were handled according to the Human Tissue Act of 2004.

2.2 METHODS

2.2.1 Isolation of human hepatic cells

2.2.1.1 Primary human hepatocytes

Primary human hepatocytes were isolated using a two-step collagenase method previously described by LeCluyse *et al.* (2005) and (Heslop et al., 2016). Tissues were kept stored in Hepes-buffered saline and transported on ice to the laboratory. Tissues were perfused at 37 ˚C with Hepes-buffered saline (HBS; 10 mM Hepes, 5 mM KCl, 136 mM NaCl, 5 g/l glucose), and digested with 0.2 mg/ml Collagenase A or IV (Roche, Basel, Switzerland or Sigma-Aldrich, St. Louis, MO) in HBS containing 700 µM $CaCl_2$. After digestion (noted by tenderness of the tissue), the capsule was cut open using a pair of

scissors and isolated cells were gently strained through a gauze into a sterile glass beaker. For complete and efficient cell recovery, the digested tissue matrix on the gauze was washed down the gauze using ice-cold Williams E medium (Sigma-Aldrich, St. Louis, MO, USA). The resulting cell suspension was centrifuged twice at 80g for 5 mins at 4 ˚C and resuspended in Williams E medium. Cell viability was determined using the trypan blue exclusion method. Cell viability of 89 % and above was considered suitable for experiments. Hepatocytes were resuspended at a density of 10^6 cells/ml in primary human hepatocyte complete medium. For monoculture monolayer experiments, cells were plated on collagen-coated cell culture plates (Corning, UK) at 250,000 cells/cm^2 to achieve full confluency and incubated at 37 ºC and 5 % CO_2 for 3 h after which medium was changed to remove dead, non-attached cells.

2.2.1.2 Human liver sinusoidal endothelial cells

Human LSEC and HHF were isolated using a modified version of the method previously described (Lalor *et al.*, 2002). Briefly, supernatants obtained from digested liver tissue from primary human hepatocyte isolation were spun down at 2000 rpm and 4˚C. Pellets formed were resuspended in ice-cold PBS and centrifuged 3-4 times as above and the resulting final pellets were suspended and made up to 18 ml with ice-cold PBS. Approximately 3 mls of suspension containing a mixture of non-parenchymal cells was layered on 6

mls of 33 % - 77 % Percoll gradient in 15 ml centrifuge tubes and centrifuged at 2000 rpm using minimum acceleration and deceleration for 25 min at 4 ˚C. The resulting top-layer was tipped off and the band of cells at the interphase was removed and transferred to a 50 ml centrifuge tube and made up to 50 ml with ice-cold PBS. This was centrifuged at 2000 rpm for 5 min at 4 ˚C to remove any residual Percoll. This step was repeated 2-3 times on the ensuing pellets. The final pellet was resuspended in 500 µl of PBS and incubated with 50 µl of monoclonal mouse anti-human epithelial cell adhesion molecule antibody (EP-CAM) (Progen) at 37 ˚C for 30 min with intermittent agitation. Thereafter, 14 ml of ice-cold PBS was added to the cell mixture and centrifuged at 2000 rpm for 5 min at 4 ˚C. The resulting pellet was resuspended in 500 µl ice-cold PBS and 10 µl ice-cold goat anti-mouse Dynabeads (Invitrogen) was added and incubated for 30 min at 4 ˚C with constant agitation. Ice-cold PBS (5 mls) was added to the cell mixture and placed in a magnet (DynaMag™-15, Invitrogen) for 2 min to remove biliary epithelial cells which been had bound to the magnetic bead. The supernatant was carefully removed and transferred to a fresh tube. The supernatant was placed in the magnet for 2 mins to remove any residual beads. The resulting supernatant was centrifuged at 2000 rpm for 5 min and the pellets formed were resuspended in 500 µl of ice-cold PBS. Thereafter, 10 µl of CD31-conjugated Dynabeads (Invitrogen) was added and allowed to incubate for 30 min at 4 ˚C with continual mixing on a rocking platform. Then, 5 mls of ice-cold PBS was added and the mixture was placed in the magnet for 2 min after

which the supernatant was removed. The magnetic beads were washed in 5 ml of ice-cold PBS and the above step was repeated twice more. Finally, the magnetic beads (containing CD-31-positive cells) were resuspended in 5 ml of HLSEC medium and transferred to a 25 cm^2 tissue-culture flask and incubated at 37 ˚C in a humidified incubator at 5 % CO_2. Cells were not used beyond 5 passages for all experiments.

2.2.1.3 Human Hepatic fibroblast

To isolate human hepatic fibroblasts, the supernatant generated from the separation of LSEC was decanted into a 15 ml centrifuge tube and volume was made up to 14 ml and centrifuged at 2000 rpm for 5 min at 4 ˚C. The supernatant was decanted and the pellet resuspended in fibroblast medium in a 25 cm^2 cell culture flask (Corning, UK) and incubated at 37 ˚C and 5% CO_2.

2.2.2 Cryopreservation and recovery of liver sinusoidal endothelial cells and human hepatic fibroblasts

Medium was aspirated off cells in a 75 cm^2 flask and cells were washed with about 5 mls of Versene solution (PBS without Ca^{2+}/Mg^{2+} containing 0.5 µM EDTA). Then 2 mls of Tryp-LE™ (Life Technology, UK) was added to the cells and the flask was placed in the incubator at 37 ˚C for about 5 min to allow cells

to dissociate from the surface of the flask. Cells were further suspended using about 5 ml of medium and transferred into a 15 ml centrifuge tube. Cells were counted using a haemocytometer. The cell suspension was spun down at 1500 rpm for 5 min, medium taken off and the cells were resuspended (2 X 10^5 cells/ ml for LSEC and 5 X 10^5 cells/ ml for HHF) in 10% DMSO/ 90% foetal bovine serum. Aliquots of 1 ml were carefully transferred into cryovials which were then placed into Mr Frosty™ Freezing containers which enabled the cells to freeze at a constant rate of -1 ˚C / min when placed in a -80 ˚C ultra-freezer. Thereafter, cells were cryo-stored in liquid nitrogen at -196 ˚C. To recover cryopreserved cells, vials of cells were taken out of liquid nitrogen, placed in a water bath at 37 ˚C to thaw the contents and these were transferred into about 8 ml of cell culture medium. The cells were then plated out in collagen-coated 25 cm^2 cell culture flasks (or uncoated flasks for HHF) and allowed to attach for 3 h after which the medium was taken off to remove traces of DMSO, and fresh medium added. Cells were then grown on as required.

2.2.3 Cell culture

In general, cell culture was performed in an Airstream® Class II biological safety cabinet (ESCO GB Ltd, UK) with lamina airflow (inflow: 0.54 m/s, Downflow 0.37 m/s). The working surface was disinfected with 70 % iso-propanol before and after cell work. Similarly, materials used in the safety cabinet were carefully sprayed with 70 % iso-propanol and allowed to dry

before commencement of cell culture. Cells were passaged by aspirating off the culture medium, washing cells with Versene and incubating cells with the appropriate volume of Tryp-LE™ (Invitrogen, UK) for a maximum of 4 min to allow cells to fully detach from surface of the tissue culture flask or dish. Cells were then observed under microscope to confirm detachment, suspended with culture medium, counted (if needed) and reseeded on appropriate vessels. For the duration of all experiments, cells were grown in a humidified cell incubator maintained at 37 °C and 5% CO_2 level.

2.2.4 Coating of dishes

A 1.7 % (v/v) [a 1:58 dilution] solution of Human **collagen** type I (Advanced BioMatrix) was made in PBS with Ca^{2+}/Mg^{2+} and 4 ml transferred to a 75 cm^2 tissue culture flask (volume depends on size of dish or flask in use) and allowed to adhere for 30 min at 37 ^oC. The collagen solution was aspirated immediately prior to adding cells and cell media. Alternatively, after aspirating off the collagen solution, coated flasks were left with lid open in the cell culture safety cabinet for up to 8 h to dry up the flask and stored, preferably at 4°C for future use. When the coating agent was **gelatin**, a 0.5 % (v/v) solution of sterile gelatin was used as described above**. Coating with fibronectin**: flasks were coated with human fibronectin (Sigma-Aldrich, MO, USA) at a surface density of 2 µg/cm^2 overnight (37 °C, 5 % CO_2).

2.2.5 Preparation of liver microtissues

This followed a modified version of the method described by Bell *et al.* (2016). Isolated primary human hepatocytes were plated at a density of 1500 cells per well in a round-bottom 96-well ultra-low attachment (ULA) plate (Corning Life Sciences, UK). Cells were allowed to settle in the plate for approximately 10 min and then centrifuged at a speed of 130 g for 3 min at 25 ^{o}C. Plates were then placed in a humidified incubator (37 ^{o}C, 5 % CO_2) to allow cells to self-aggregate. After 96 h, cells were microscopically observed at a magnification of X 10 to check for formation of microtissues after which the medium was changed. After another 72 h, liver microtissues were harvested and further processed as required. In order to prepare tri-cellular micro-tissues, the procedure above was repeated with cells as follows: (PHH: LSEC: HHF at a ratio of 8:2:2). Other experiments were based on cell ratios 2:1:1, 4:1:1, 10:7:2—based on literature (Takebe et al., 2013, Takebe et al., 2014) or based on the hepatocyte cell ratios

2.2.6 Protein analysis

2.2.6.1 Preparation of protein lysate from liver microtissues

Liver microtissues were harvested into a clean reagent reservoir kept on ice, transferred into a 15 ml centrifuge tube, centrifuged at 130 g for 5 min at 4 ^{o}C

to allow them to collect at the bottom of tube. Medium was removed and the micro-tissues washed with ice-cold PBS and spun down as above. The process was repeated with micro-tissues transferred to a 1.5 ml centrifuge tube, spun down as above, PBS was carefully removed and 150 µl of RIPA lysis buffer (Sigma-Aldrich, St. Louis, MO) was added. Micro-tissues were sonicated on a Soniprep 150 Plus ultrasonic Disintegrator (Henderson Biomedical, UK) 3 times at an amplitude of 5 and nominal frequency of 23 KHz for 5 s. Lysates were centrifuged at 17,000 g (14,000 rpm) for 20 min at 4 ^{o}C and the supernatant containing the whole cell contents were collected in a new centrifuge tube and assayed for total protein as described below.

2.2.6.2 Preparation of liver homogenates

About 0.5 mg of tissue was weighed out, placed in a sterile 2 ml centrifuge tube, 600 µl RIPA lysis buffer added and a sterile sharp-edge metal ball bearing was placed in the tube. Tubes were placed in a Retsch Mixer Mill MM400 (Cole-Parmer, UK) and tissues were homogenised at 30 oscillations / sec for 3 mins. Homogenates were aliquoted into a fresh tube and centrifuged at 17,000 g (14,000 rpm) for 20 mins at 4 ˚C and the supernatant containing the tissue protein contents were collected in a new centrifuge tube and assayed for total protein as described below.

2.2.6.3 Protein determination in whole cell lysate and whole liver homogenates

Protein contents in whole cell or tissue lysates were quantified using the BCA assay (Smith *et al.*, 1985) which is a colourimetric method based on the protein-induced biuret reaction that causes a reduction of Cu (II) to Cu (I) and a subsequent chelation of Cu (I) by two molecules of bicinchoninic acid (BCA) to form a water-soluble purple-coloured complex that absorbs strongly at 562nm, the intensity of which increases with increasing protein concentration. A 7-point standard curve (0 - 1 mg protein/ml) was produced by serially diluting the 1mg/ml bovine serum albumin protein standard using deionised water. Aliquots (20 µl) of both the protein standards and 10 µl of samples were pipetted into a clear-bottom 96-well plate and then 200 µl Working Reagent (WR; 50 parts of reagent A (sodium carbonate, sodium bicarbonate and sodium tartrate in 0.1 N sodium hydroxide) to 1 part reagent B (4% cupric sulphate)) was added. The plate was then incubated at 37°C for 30 min, cooled for 2-3 min and absorbance determined using an the Varioskan Flash plate reader (Thermo Scientific, USA) at a wavelength of 562 nm. A standard curve was constructed and protein concentration of samples calculated.

2.2.6.4 Western blotting

Whole cell lysates (20 µL containing approximately 10 µg of proteins) were added to 5 µL of sample loading buffer (4X LDS and 2-mercapto ethanol)

(Sigma, MO, USA). The sample was then heated up for 5 min at 90 ^{o}C to allow protein denature. 4 µL of the molecular weight marker (protein kaleidoscope standards or rainbow marker) and the whole denatured samples were loaded on a 15-well Bolt™ 4-12% Bis-Tris Plus polyacrylamide gel using Mini Gel Tanks and NuPAGE® MES SDS Running Buffer. Samples were run at 70 mA and 200 V for 45 min. The separated proteins in the gels were transferred onto hybond nitrocellulose paper (GE Healthcare, UK) at 230 mA for 120 min using a Mini Blot Module (ThermoFisher Scientific). Membranes were blocked for 1 h in 5 % w/v BSA solution or 10 % w/v non-fat milk (Bio-Rad) made up in TBST on an orbital shaker. Membranes were probed overnight with anti CYP 2D6 (Abcam, UK, 1:200 in 2% non-fat milk), CYP 3A4 (Millipore, UK. 1:8000 in 2 % w/v in non-fat milk), CYP 2E1 (Abcam, UK. 1:3000 in non-fat milk), UGT 1A1 (R&D Systems, UK. 1:1000 in 2% non-fat milk), anti-phospho-AKT473 (1:1,000 in TBS-Tween containing 2 % (w/v) BSA), caspase 3 (1:1,000 in TBS-Tween containing 2 % (w/v) BSA), phospo-Erk 1/2 (1:1,000 in TBS-Tween containing 2 % (w/v) BSA), anti-VEGFR-3 (1:1,000 in TBS-Tween containing 2 % (w/v)), anti CD-31 (1:500 in TBS-Tween containing 2% (w/v)and anti GAPDH (1:1,000 in TBS-Tween containing 2% (w/v) or anti β-actin (1:1,000 in TBS-Tween containing 2% (w/v) used as loading control. Membranes were washed for 6 x 10 min in TBS-Tween and probed for 1 h with the appropriate HRP-linked secondary antibody. The following secondary antibodies were used: goat anti-rabbit HRP (1:5,000 in TBS-Tween containing 2 % (w/v) BSA or 5 % w/v non-fat milk), rabbit anti-goat HRP (1:5,000 in TBS-Tween containing 2 % (w/v) BSA or

2 % (w/v) non-fat dry milk), goat anti-mouse HRP (1:5,000 in TBS-Tween containing 2 % (w/v) or 2 % w/v non-fat dry milk). Membranes were washed FOR 6 x 10 min in TBS-Tween and visualised in the dark by the addition of enhanced western lightening chemiluminescence reagents Hyperfill ECL (Perkin Elmer, UK) to the membrane, a film placed on the membrane to pick up bands and exposed to Kodak developer and fixer solutions in ratio 1:1. Band intensity was quantified and analysed using the Image-J software (NIH, USA).

2.2.7 Nucleic acid analysis

2.2.7.1 Primer design

In order to design primers to genes of interest its accession number was determined online from http://www.qiagen.com/products/quantifastprobeassay.aspx which was used to determine the correct mRNA sequence on http://www.ncbi.nlm.nih.gov/sites/entrez?db=Nucleotide. The sequence was pasted into the website http://tools.invitrogen.com/content.cfm?pageid=9716. A careful selection of the base pair was made using some stringent conditions of primer size (Min 18, Opt 20, Max 27), melting temperature (Min 57, Opt 60, Max 63), the percentage GC (Min 40, Opt 50, Max 60) in the sequence, product size and salt concentration. The selected pair was run through the website:

http://www.ncbi.nlm.nih.gov/tools/primer-blast/index.cgi?LINK_LOC=BlastHome to determine what set of genes they were specific for and the set of gene with the highest specificity and least self-complementarity and self-3' complementarity was selected and ordered online from ThermoFisher Scientific, UK. Upon receiving the primer pair, they were constituted to 100 µM using Tris-EDTA Buffer pH 8.0 (Sigma, UK). Thereafter, the primers were tested as below.

2.2.7.2 Primer testing by agarose gel electrophoresis

Reconstituted primers were tested using the DreamTaq Green PCR Master Mix kit (Thermo Scientific). Briefly, reaction mix was prepared in a PCR reaction tube with 10 µl of DreamTaq Green PCR Master mix, 4.4µl of nuclease-free water, 2 µl of forward primer, 2 µl of reverse primer and 1.6 µl of cDNA. The mix was run on a thermal cycler (GeneAmp® PCR System 9700, Applied Biosystems, UK) as follows: 95˚C for 10 min, 95˚C for 15 sec and 60˚C for 1 min over 30 cycles. A volume of 10 µl of the reaction mix was run on a 3% agarose gel mixed with 7.5 µl of ethidium bromide to a final concentration of 0.5 ug/ml. Quick-Load 100 bp DNA ladder (New England Biolab) was used as marker. Samples were run electrophorectically for 45 min at 100V and products formed were viewed using a transilluminator. Primers were deemed

good when a single band was formed; implying the absence of primer dimer and this was further confirmed by RT-PCR.

Table 2.5: List of PCR primers

Primer Name	Forward Sequence (5' to 3')	Reverse Sequence (5' to 3')
ALB	CCTGTTGCCAAAGCTCGATG	ATCTCCATGGCAGCATTCCG
UGT 1A1	TTAATCAGCCCCAGAGTGCT	AATGGCACATGTCATCCTGA
CYP2D6	TTCCCAAGGGGTGTTCCTGG	TCACGGCTTTGTCCAAGAGA
CYP2E1	ACCCTGAGATCGAAGAGAAGC	AAATGGTGTCTCGGGTTGCT
CYP3A4	AGAAATCTGAGGCGGGAAGC	GGAATGGAAAGACTGTTATTGAGAG
Stabilin-1	CTCTTCACAGCGGGTCTCTC	CCCCTCCTCAGAAATGTTCA
Stabilin-2	TTGGCAACAAACAATGGCTA	GGCCAGAAGAGAGTGACTGG
LYVE-1	GCTTTCCATCCAGGTGTCAT	GCCAAACTTAGTCCCAGCAG
Prox-1	CAAAAATGGTGGCACGGAG	CCTGATGTACTTCGGAGCCTGT
CD31	CAGGAGCACCTCCAGCCAACTT	ATCCTGGGCTGGGAGAGCATTTCG
ZO-1	GGAGAGGTGTTCCGTGTTGT	GGCTAGCTGCTCAGCTCTGT
PDGFR-β	GAGGAATCCCTCACCCTCTC	GGGTATATGGCCTTGCTTCA
VEGFR-1	TGTGCCAAATGGGTTTCATG	TGCAAGACAGTTTCAGGTCCTC
VEGFR-2	CAAACGCTGACATGTACGGTCT	CCAACTGCCAATACCAGTGGA
VEGFR-3	GCTCCTACGTGTTCGTGAGAGA	TCCTGTTGACCAAGAGCGTG
VEGF-A	CCTTGCTGCTCTACCTCCACC	TCCTCCTTCTGCCATGGG
VEGF-B	GGG CAC ACA CTC CAG GCC ATC	CCTTGACTGTGG AGCTCATGGGCC
VEGF-C	TCAGGCAGCGAACAAGACC	TTCCTGAGCCAGGCATCTG
VEGF-D	TCCAGGAACCAGCTCTCTGT	TTTTTGGGGTGCTGGATTAG
Id-1	CGGATCTGAGGGAGAACAAG	TCCCACCCCCTAAAGTCTCT
POD	CTGCTCTTCGTTTTGGGAAG	GGTTCCTGGAGTCACCACAT

2.2.7.3 RNA extraction from whole liver

This was done using RNA mini kit (Qiagen, UK) according to manufacturer's instruction. Approximately 30 mg of tissue was weighed out, rinsed 3 times in PBS and transferred into a sterile 2 ml centrifuge tube. A sterile sharp-edge metal ball bearing was placed in the tube and 300 µl of lysis buffer (300 µl of buffer RLT plus 3 µl of 2-mercaptoethanol) was added. Tubes were placed in a Retsch Mixer Mill MM400 (Cole-Parmer, UK) and tissues were homogenised at 30 oscillations / sec for 3 mins. Beads were removed with sterile tweezers which were cleaned with ethanol between each tube. RNase-free water (590 µl) and 10ul protinase K (Qiagen) were added to the lysate and vortex mixed. The mix was incubated at 55 ˚C for 10 min on a heater block (Grant-bio PCH1), centrifuged at 10,000 g for 3 min, and supernatant transferred into a new 2ml tube. A volume of 100 % ethanol which was half the volume of sample liquid was added (400 µl of ethanol was added to 800 µl of sample) and was pipette mixed. Then 700ul of sample was transferred to mini column and centrifuged at 8000 x g for 15 s, and flow through (liquid collected in bottom clear tube) was discarded. This was repeated until all sample had been passed through the column. Thereafter, 350 µl of RWI was buffer added and centrifuged at 8000 xg for 15 seconds, flow through discarded and 80 µl of DNase 1 master mix (10 µl of DNase with 70ul of buffer RDD (Qiagen)) was pipetted unto the silica surface of the column. This was incubated at room temperature for 15 min, 350ul RW1 buffer was added, centrifuged at 8000 g for 15 s, flow through discarded, 500ul buffer RPE added, centrifuged at 8000 g for 15 s, and flow

through discarded. Another 500 µl volume of buffer RPE was added and column centrifuged at 8000 g for 2 min, and flow through discarded. The collection tube was replaced by a 1.5 ml centrifuge tube, 50ul of RNase-free water was added unto the column and was centrifuged for 1 min at 8000 g. The eluted mRNA sample was quantified using the Nanodrop spectrophotometer (ND-1000, Thermo Scientific, UK).

2.2.7.4 RNA extraction from cells

Medium was aspirated off cells cultured in monolayer and were washed twice with ice-cold PBS. RNA lysis buffer (350 µl with 3.5 µl of 2-mercaptoethanol) was added to the cells on ice. After 15 min, cells were scrapped and using a cell scrapper and lysates transferred into a clean centrifuge tube. Thereafter, 245 µl of 100 % ethanol was added to the lysate and was mixed by pipetting up and down. Then 700ul of sample was transferred to mini column, centrifuged at 8000 g for 15 s, and flow through (liquid collected in bottom clear tube) was discarded. This was repeated until all sample had been passed through the column. Thereafter, 350 µl of RWI was buffer added and centrifuged at 8000 g for 15 s, flow through discarded and 80 µl of DNase master mix 10 µl of DNase [Qiagen] with 70ul of buffer RDD) was pipetted unto the silica surface of the column. This was incubated at room temperature for 15 mins, 350ul RW1 buffer was added, centrifuged at 8000 g for 15 s, flow through discarded, 500ul buffer RPE added, centrifuged at 8000 g for 15 s, and flow through discarded. Another 500 µl volume of buffer RPE was added and

column centrifuged at 8000 xg for 2 minutes, and flow through discarded. The collection tube was replaced by a 1.5 ml centrifuge tube, 50ul of RNase-free water was added unto the column and was centrifuged for 1 minute at 8000 g. The eluted mRNA sample was quantified using the Nanodrop spectrophotometer (NanoDrop™ 1000 Spectrophotometer, Thermo Fisher Scientific).

2.2.7.5 Reverse transcription of RNA

Messenger RNA extracted above was diluted to a concentration of 100 ng/µl with sterile RNase-free, DNase-free dH_2O to a total volume of 10 µl. This was followed by addition of 1 µl of Oligo dT and 1 µl of 10 mM dNTP mix, incubated at 70°C for 5 min and samples were rapidly cooled on ice to prevent formation of secondary structures. Then 8 µl of the master mix (containing 4 µl of 5X first strand buffer, 2 µl of DTT (0.1 M), 1 µl of 40 unit/ µl of RNaseOUT and 1 µl of 200 units/ µl of M-MLV reverse transcriptase) was added to the samples. This was followed by cycles of annealing (25 °C, 5 min), cDNA synthesis extension (37 °C for 60 min.), and reaction inactivation (70°C, 15 min.). Finally, 130 µl of RNase-free, DNase-free dH_20 was added to dilute cDNA to a final concentration of 6.66 ng/µl.

2.2.7.6 Real-time quantitative polymerase chain reaction

RT-PCR was performed according to the manufacturer's protocol using the SYBR Green master mix (Invitrogen). Briefly, 1.4 µL of cDNA (10 ng), 3 µL of nuclease-free dH_20, 12.5 µL of 2x SYBR Green, 4 µL each of both forward and reverse primers were mixed in a 500 µL centrifuge tube and centrifuged. From this, 10 µL was transferred in duplicates into a 384-well plate and sealed with an optically-clear QPCR adhesive seal sheet. This was centrifuged for 15 s at 700 g (1800 rpm) at 4 °C. Polymerase chain reaction was run using the ViiA 7 PCR machine (Life Technologies, UK) with 40 cycles of 95 ˚C for 15 s per cycle and 60 ˚C for 1 min per cycle. A dissociation curve was generated in order to determine the specificity of the primers and accuracy of the SYBR green fluorescence.

2.2.7.7 Relative quantitation of gene expression

From the Ct values obtained from the PCR run the relative gene expression was calculated using method described by Livak and Schmittgen (2001) as follows:

ΔCt = Ct target gene – Ct reference gene

$\Delta\Delta$Ct = ΔCt stimulated samples (sample of interest) - ΔCt Control sample (sample with lowest ΔCt value)

Fold change (gene expression) in relation to the control sample was calculated as:

Fold change relative to control = $2^{-\Delta\Delta Ct}$

2.2.8 Analysis of endothelial cell physiology

2.2.8.1 Co-culture angiogenesis assay

This was performed according to a method previously described by Hetheridge *et al.* (2011). Briefly, normal human dermal fibroblasts (juvenile) were seeded at 7.8 X 10^3 cells/ cm^2 on a gelatin-coated 24-well plate or on gelatin-coated glass coverslips in 1 ml fibroblast growth medium. Fibroblasts were grown for 72 h under standard conditions until confluent. Then, medium was aspirated, cell washed with PBS and endothelial cells at a density 2.1 x 10^4 cells/ cm^2 in 0.5 ml endothelial cell full growth media for 24 h. Then medium was aspirated from the wells, washed once with PBS. Endothelial cell media containing 1% FBS containing the growth factors or inhibitors required was added to a total volume of 0.5 ml/well for 72 h. Thereafter, medium was aspirated and replaced with fresh medium containing 1 % FBS and the growth factors/inhibitors for 48 h. Then, medium was aspirated and cells gently washed with PBS twice and fixed in 200 µl of 2% PFA for 15 min at room temperature on the rocker set at 30 rpm. Cells were washed in 1 ml PBS twice, permeabilised using 200 µl 0.25% (w/v) Triton X-100 for 10 min at room temperature. Cells were then washed twice in 1X TBS. Cells were blocked with 1 % BSA for 1 h at room temperature. After which primary antibody was added for 1 h, cells washed three times in TBST.

1. For colorimetric assay, anti-sheep IgG whole molecule alkaline phosphatase conjugate secondary antibody (diluted 1:200 in 1% BSA in TBST) was added for 1 h at room temperature on the rocker set at 30rpm. Then cells were washed in dH_2O 1ml per well three times. Then 200µl of substrate (1 SIGMA Fast BCIP/NBT tablet per 10 ml distilled water) was added per well and left at

37°C for 15 min. Cells were washed with dH_2O and about 300 µl of dH_2O was added and plates were either stored at 4 °C or imaged immediately on Nikon Microscope using 4X objective. Images were quantified using the Angioquant programme.

2. For immunofluorescent staining, secondary antibody diluted as instructed by manufacturer on 1% BSA in TBST for 1 h at room temperature on the rocker set at 30rpm. Thereafter Hoechst nuclear stain (diluted at 1:5000 in 1% BSA in TBST) was added and incubated at room temperature for 10 min on the rocker set at 30rpm. Cells were washed three times in 1 ml of TBST and mounted on slides after about 20 µL of prolong gold and sealed around with nail varnish.

2.2.8.2 Agonist stimulation of cells for intracellular signalling

Endothelial cells were seeded at a density of 2.1 X 10^4 cells/cm^2 in a 12-well plate for 48 h after which medium was removed and washed twice with sterile PBS and cells were incubated with medium containing 1 % FBS overnight. Cells were incubated with 50 ng/ ml of growth factor or basal medium for 10 min at 37 °C after which they were washed twice with ice-cold PBS on ice and lysed with 120 µl of modified RIPA lysis buffer for 15 min. Cells were scraped and assayed for protein contents as described.

2.2.8.3 Cell migration assay

Endothelial cells were seeded in a 12-well collagen-coated tissue culture plate until confluent. Medium was removed and cells washed twice with PBS and medium containing 1 % FBS was added overnight. A straight scratch was vertically drawn with a sterile 200 µl pipette tip using a ruler disinfected with 70 % iso-propanol. Medium was aspirated off to remove dead cells which were further washed once with PBS. Cells were pre-treated with the respective dilution(s) of inhibitor(s) or medium containing 1 % FBS for 30 mins. Thereafter, 50 ng/ml of growth factors diluted in medium containing 1 % FBS or medium containing only 1 % FBS was added. Images of scratches were taken using light microscope to mark time t= 0h. Then cells were incubated for 16 h 37C and 5 % CO_2. Then medium was aspirated off and cells washed twice with PBS at room temperature. Then they were fixed with 2 % paraformaldehyde for 15 min and washed twice with PBS before being stained with crystal violet. After the removal of PBS from the wells, 200 µl of crystal violet was added to each well, ensuring the surface of the well was covered and incubated for 15 min at room temperature. Cells were then washed with water in sink to remove all excess stain. Plates were stored in PBS at 4°C whenever storage was required before imaging using light microscopy.

2.2.8.4 Cell proliferation assay

Endothelial cells were seeded at 4, 000 cells per well in a collagen-coated 96-well plate and cultured for 48 h after which medium was removed and cells washed with

PBS. Medium containing 1 % FBS was added to the cells for 16 h after which cells were incubated with 50 ng/ml of growth factors constituted in medium containing 1% FBS for 72 h. Thereafter, cells were washed with ice-cold PBS which was aspirated off and 100 µl of PBS was added followed by 20 µl of Cell Titer Glo Reagent (Promega) per well. Plates were placed on a shaker for 20 min and allowed to stand for 10 min to allow luminescence signal to stabilise. Thereafter, 100 µl of cell lysates were transferred from each well into a white-bottomed 96-well plate (Greiner bio-one, UK) and plates were read for luminescence using Varioskan Flash plate reader (Thermo Scientific, USA) at a wavelength of 100 nm. Luminescence reading, proportional to ATP contents (a measure of cell viability) was recorded and represented as percentage of basal which was set at 100 %.

2.2.9 Cell and microtissue imaging

2.2.9.1 Immunofluorescent staining of cells

Cells grown on collagen-coated glass cover slips were fixed with 2% PFA/PBS for 15 min at room temperature. Cells were washed once in freshly made quench solution (50mM NH_4Cl in PBS) followed by a further 10 min incubation in the quench solution. Cells were washed three times in PBS and permeabilised for 10 min with a 0.2% Triton X-100 solution at room temperature. Cells were then washed two times in TBS followed by a 1 h block with 5 % serum (from animal source of 2° antibody) for 1 h at room temperature. Primary antibody (200 µL), diluted as optimised or instructed by manufacturer in TBS containing 1% BSA and 0.1% Tween-20, was added to the cells on cover slips. Sufficient volume of diluted antibody was added to cover the glass

region of the dish, and incubated for 1 h at room temperature. Cells were washed three times in TBST and incubated with fluorescently-labelled secondary antibody (diluted 1:1000) for 1 h at room temperature with dishes containing cells covered with foil in order to protect fluorescent dyes which are light sensitive. Then cells were washed twice in TBST and incubated with 2µg/ml Hoescht stain for 10 min and washed again three times in TBST. Coverslips were mounted by adding 10µl of Prolong Gold (Invitrogen) directly onto the glass slide and then any excess liquid gently blotted out and coverslips placed face down onto slide. Coverslips were gently pressed with forceps to remove any bubbles and were sealed with nail varnish. Cells on coverslips were then imaged using Zen Axio Observer Z.1 fluorescence microscope (Carl Zeiss, GmbH).

2.2.9.2 Immunofluorescent staining of liver microtissues

After 7 days in culture, liver microtissues were harvested in the ULA plates. Medium was carefully taken off to avoid losing the micro-tissues. Medium was replaced with PBS at room temperature until the well was clear, indicating a total removal of the culture medium. Microtissues were then fixed in 4% paraformaldehyde (PFA) for 1 h after which they were washed 3 times with PBS. Thereafter, micro-tissues were permeabilised overnight with 0.5% Triton X-100 in PBS, followed by a two-hour block step in 3 % bovine serum albumin (BSA) in TBST at room temperature. The primary antibody made up at the determined concentration in 1% BSA /TBST/0.1% Triton-X was added overnight at 4 ºC after which micro-tissues were washed 3 times (1 h per wash) with TBST/ 0.1% Triton-X at room temperature. Thereafter, fluorescently-

conjugated secondary antibody (usually diluted at 1:1000 in 1% BSA/ TBST/ 0.1% Triton-X) was added overnight at 4 ˚C. Micro-tissues were then washed with TBST/ 0.1 % Triton-X (once for 1 h.) followed by addition of Hoechst (diluted at 1:5000 in TBST/0.1% Triton-X) for 1 h. After the removal of Hoechst, micro-tissues were quickly washed with TBST/0.1% Triton-X and another one-hour wash. After much of the wash buffer was removed from the wells, micro-tissues were removed and transferred onto a microscope slide and excess buffer removed with a clinical tissue paper. Then a about 30 µl of Prolong Gold (Invitrogen) was added to cover the micro-tissues after which a cover slip was gently placed on top and sealed on the side with a transparent nail polish. Microtissues were imaged using a Zen Observer Z.1 fluorescence microscope (Carl Zeiss, GmbH).

2.2.9.3 Scanning electron microscopy

Endothelial cells were seeded on collagen coated glass slides in a 24-well tissue culture plate at a density of 1.1 X 10^6 cells/cm^2 for 24 h after which medium was replaced with LSEC full growth medium alone or supplemented with 50 ng/ml of VEGF-A or VEGF-C for 48 h. Thereafter, medium was removed and cell washed with PBS and fixed with 4% PFA and 2.5% glutaraldehyde in 0.1M phosphate buffer (pH 7.4) at room temperature for 2 h. Cells were washed for 3 min twice in 0.1M Phosphate buffer (pH 7.4) at room temperature. Cells were then incubated with reduced osmium staining [2% OsO_4 in H_2O + 1.5% potassium ferrocyanide in ddH_2O] (20s on-20s off-20s on-20s off. 20Hg). Cells were then washed for 3 min, three times in ddH_2O at room temperature and incubated with the mordant containing: 1%

thiocarbohydrazide (TCH) in ddH_2O (20s on-20s off-20s on-20s off. 20Hg). Thereafter, cells were washed in ddH2O three times and 3 min each at room temperature. Cells were exposed to a second osmium staining with 2% OsO_4 in ddH_2O (20s on-20s off-20s on-20s off. 20Hg) and washed ddH_2O five times for 3 min. each at room temperature. They were then stained with 1 % uranyl acetate in ddH_2O overnight at 4°C and washed with ddH_2O five times for 3 min each at room temperature. Cells were then dehydrated in graded ethanol (30, 50, 70, and 90 %) in ddH_2O for 5min each and then 3 times in 100% ethanol, followed by critical-point drying. Cells were then sputter coated with 10 nm of Au/Pd. Then cover glasses were placed on scanning electron microscope (SEM) stubs with conductive silver epoxy and left to dry overnight. Images were taken with FEI Quanta 250 scanning electron microscope (FEI UK Limited, Cambridge, UK). Fenestrations were quantified by manual counting and an average of four images were taken.

2.2.10 Transcriptomic analysis of endothelial cells

Human dermal microvascular endothelial cells, human dermal lymphatic endothelial cells or human liver sinusoidal endothelial cells were seeded at a density of 9.1×10^3 on a collagen-coated 10 cm plastic tissue culture dish for 48 h. Medium was aspirated off and cells washed two times with ice-cold PBS on ice. Thereafter, cells were lysed with 600 µl of RLT RNA lysis buffer (containing 600 µl of buffer RLT with 6 µl of 2-mercaptoethanol). RNA was extracted as described above (section 2.2.7.4) Then, RNA samples (free from genomic DNA) were quantified using the Qubit BR RNA kit, and the quality of the RNA assessed using the Agilent 2100 Bioanalyser and RNA Pico

chip. Samples were prepared for hybridisation onto Affymetrix Human Transcriptome (HTA 2.0) arrays, following the WT Plus labelling kit version 3 protocol. 100 ng of total RNA was used as input into the labelling reactions. Amplification of cRNA was checked by bioanalyser before proceeding to ss-cDNA. 5.5 µg of ss-cDNA was fragmented and labelled, prior to hybridisation onto HTA 2.0 arrays and hybridised for 16 h at 45˚C, 60 rpm in a GeneChip Hybridization Oven 645. Following hybridisation, the arrays were washed on a GeneChip® Fluidics Station 450 using the GeneChip Hybridisation, Wash and Stain kit and fluidics script FS450_0001 and scanned using the GeneChip® Scanner 3000 7G.

2.2.10.1 Bioinformatics analysis

The resulting gene expression intensity data obtained from the GeneChip® Scanner above was analysed with the Expression Console® (EC) software (Affymetrix, UK) which was used to estimate and normalise gene expression using the SST-RMA mode. The data thus generated was an estimate of the expression of the genes of interest converted to $\log_2$. The EC software enabled the generation of a PCA plot. The output from this analysis was further analysed using the Transcriptome Analysis Console (TAC) software (Affymetrix, UK). TAC was used to identify the differentially-expressed genes, the signal intensities of any particular gene in the sample of interest. Using signal intensity data generated, each group was compared with the other to generate the linear fold change (FC) in gene expression relative to the other. The estimated $\log_2$ fold change (logFC) in the genes of interest were compared between the groups of interest using t-test. The estimated p-values for each logFC

values were adjusted for multiple testing using the False Discovery Rate (FDR) method. Significantly differential expression were those whose FDR had adjusted p-value < 0.05. The number of differentially-expressed genes in each paired comparison and the direction of the expression were plotted into an MA plot. The TAC software was also used to generate a heatmap that helps to visually identify the signal intensities of the genes of interest in the samples.

2.2.11 Drug metabolism in liver microtissues

2.2.11.1.1 Preparation and treatment of liver microtissues

Liver micro-tissues were made as previously described above (section 2.2.6.1). After 7 d, micro-tissue were dosed with 5 µM of perhexiline for 24 h following which drugs were taken off and transferred into another set of 96-well plates and rapidly frozen on dry ice. Samples were stored at -80˚ C until required for analysis as described below.

2.2.11.2. Analysis of metabolite formation by LC-MS/MS

2.2.11.2.1. Stock solutions

Stock solutions of hydroxy-perhexiline (PHX-OH) metabolites and internal standards were prepared in DMSO/Methanol (50/50 v/v). All other stock solutions were prepared in DMSO. The solutions were prepared and stored in glass vials.

2.2.11.2.2. Working solutions

All working solutions were prepared in glass vials using positive displacement pipettes. The fluconazole (Fluc) stock was diluted with MeCN to give a solution containing 1 µg/mL. This was followed by a dilution of the D_4-fluconazole (D_4-Fluc) stock with MeCN/water (25/75, v/v) to give a solution containing 1 µg/mL. Then the perhexiline parent compound, metabolites and internal standards were prepared in MeCN/water (50/50, v/v) as follows:

- PHX : 0.05, 0.5 & 5 µM
- cis-PHX-OH: 0.005, 0.05, 0.5 µM (total concentrations)
- trans-PHX-OH: 0.005, 0.05, 0.5 µM (total concentrations)
- D_{11}-PHX & D_{11}-cis-PHX-OH: 0.5 µM

In order to test extraction recoveries of the test compounds from medium, medium validation samples were prepared by spiking incubation medium with concentrations of analytes corresponding to the low, medium and high calibration standards, after dilution, using positive displacement pipettes.

2.2.11.2.3. Calibration standards

Independent calibration lines were prepared for PHX, cis-PHX-OH and trans-PHX-OH, directly in a 2mL 96-deep well analysis block, using the following solutions and volumes. 0.1% FA reduces otherwise significant carry/over and buildup of the analytes in the LC-MS/MS system.

2.2.11.2.4. PHX calibration standards

std	Conc (µM)			Vol (µL)			
no	CAL	WS	WS	IS	diluent A	diluent B	total
1	0.0010	0.05	10.0	10.0	230	250	500
2	0.0020	0.05	20.0	10.0	220	250	500
3	0.0040	0.05	40.0	10.0	200	250	500
4	0.0100	0.5	10.0	10.0	230	250	500
5	0.0200	0.5	20.0	10.0	220	250	500
6	0.0400	0.5	40.0	10.0	200	250	500
7	0.1000	5	10.0	10.0	230	250	500
8	0.1500	5	15.0	10.0	225	250	500
9	0.2000	5	20.0	10.0	220	250	500

IS = corresponding internal standard
Diluent A = MeCN/water (50/50, v/v)
Diluent B = Diluent A containing FA (0.2%, v/v)
Metabolite calibration standards were prepared using the same volumes as tabulated above except that the concentrations of the calibration standards and the working solutions were 10-fold lower and diluent B contains FA (0.2%, v/v) in water.

2.2.11.2.5. Treatment of test samples

All initial handling and treatment of test samples was carried out at 4°C. The following procedure was based on samples supplied in a 96-well flat bottomed microtitre plates: Samples were removed from storage at -20°C and allowed to thaw. Then, 40 µL of each sample was transferred to a clean well of a separate round-bottomed microtitre plate, Fluc-MeCN (120 µL) added to each well to give a volume

ratio of MeCN:sample of 3:1. Plate was capped and contents briefly mixed (600 rpm, 30 seconds). Then the plate was centrifuged (3000 rpm/1811 g, 4°C, 20 min). Thereafter, two separate aliquots of the treated sample were transferred to separate wells of a clean 2mL 96-deep well analysis block, one for analysis of parent drug and the other for analysis of metabolites, using the volumes tabulated below:

Analytes	**Overall dilution**	**Vol (µL)**						
		Sample extract	IS*	Fluc-IS	Water	diluent A	diluent B	total
Parent	500	10	25	10	0	595	625	1250
Metabolites	50	40	10.0	10	190	220	0	500

Diluent A = MeCN/water (50/50, v/v)
Diluent B = Diluent A containing FA (0.2%, v/v)
* IS = D_{11}-PHX for analysis of parent & D_{11}- Cis-Hydroxy-PHX for analysis of metabolites

Plate(s) were capped and contents were briefly mixed (600 rpm, 30 seconds), followed by centrifugation (3000 rpm/1811 g, 4°C, 10 min) and analysis by LC-MS/MS. Treated, un-diluted, samples were stored in sealed plates at 4°C for at least 1 week. For longer term storage this had to be at -20°C with the plates being tightly sealed to prevent entry of atmospheric water.

2.2.11.2.6. Preparation of Fluconazole reference samples

Two sets of references corresponding to the two different dilutions were prepared as described above. Blank, cell-free, Incubation medium samples (n=3) to test samples (n=3) of solutions were treated to give these samples. Alternatively, if extraction

recovery of fluconazole was quantitative, water was used instead of incubation medium.

2.2.11.2.7. LC-MS/MS conditions

Analyses were carried out with the following pieces of equipment: LC PUMP (QUATERNARY) (G1312B, Agilent Technologies UK Limited), (DEGASSER G1379B, Agilent Technologies UK Limited), COLUMN OVEN (G1316B, Agilent Technologies UK Limited), AUTOSAMPLER (HTS PAL, CTC Analytics), MASS SPECTROMETER (6500 Triple Quadrupole, AB Sciex), COMMUNICATIONS HUB, (Edgeport 8-port, Digi International), NITROGEN GENERATOR (Genius 3031, Peak Scientific).

2.2.11.2.8. HPLC conditions common to all analyses

HPLC Column: (Phenomenex)	50 x 2.1mm ID 2.6 µm Kinetex XBC18
Guard: (Sigma-Aldrich)	Upchurch pre-column filter with 0.5 µm frit
Temp. (°C):	40
Mobile Phase A:	H_2O +0.1% v/v FA
Mobile Phase B:	MeCN +0.1% v/v FA
Autosampler Wash Solvent 1:	H_2O: AcOH (99/1, v/v)
Autosampler Wash Solvent 2:	MeOH:ACE:IPA:AcOH (40/30/30/1, v/v)

Autosampler Washes:

Wash	No. of washes
Post Clean with Solvent 1	1
Post Clean with Solvent 2	2
Valve Clean with Solvent 1	1
Valve Clean with Solvent 2	2

2.2.11.2.9. MS parameters common to all analyses

IONISATION MODE:ELECTROSPRAY POSITIVE (ESI +ve)
CUR: 35
CAD: 9
IS: 5500
TEM: 500
GS1/GS2: 50/40

2.2.11.2.10. Analysis of Perhexiline

Volume (µL) injected: 10
Diverter valve timings (to MS): 0.6->1.9 minutes

HPLC Gradient:

Time (min)	Flow Rate(µL/min)	A (%)	B(%)
0	500	95	5
0.1	500	95	5
1.1	500	5	95
1.6	500	5	95
1.7	500	95	5
2.3	500	95	5

Analyte-Specific MS parameters:

Q1 Mass	Q3 mass	dwell time (ms)	Analyte ID	DP	EP	CE	CXP
278.3	95.2	30	PHX	60	10	40	10
289.3	95.2	30	D11-PHX IS	60	10	40	10
307.3	220.2	30	FLUCON OFF	60	10	40	10
311.3	223.2	30	D4-FLUCON OFF	60	10	40	10

2.2.11.2.11. Analysis of single hydroxy metabolite

Volume (µL) injected: 25
Diverter valve timings (to MS): 2->3.8 minutes

HPLC Gradient:

Time (min)	Flow Rate(µL/min)	A (%)	B(%)
0	500	95	5
0.1	500	95	5
4.1	500	50	50
4.2	500	5	95
4.7	500	5	95
4.8	500	95	5
5.4	500	95	5

Analyte-SpecIfic MS parameters:

Q1 Mass	Q3 mass	dwell time (ms)	Analyte ID	DP	EP	CE	CXP
305.2	96.1	20	D11-CIS-OH IS	60	10	40	10
294.2	95.1	20	CIS PHX-OH	60	10	40	10
294.2	95.101	20	TRANS PHX-OH	60	10	40	10
307.3	220.2	20	FLUCON*	60	10	40	10
311.3	223.2	20	D4-FLUCON*	60	10	40	10
294.201	95.1	20	CIS PHX-OH 2	60	10	40	10

* CE offset to avoid saturation of detector with high signal

2.2.11.2.12. Data processing and reporting of concentrations

Calibration lines were contructed using the area ratio of analyte to internal standard, a linear fit and and an appropriate weighting factor, typically $1/y^2$. The D_{11}-cis-hydroxy metabolite internal standard was used for measurements of all single hydroxyl metabolites. Also, the calibration standards were used to determine the concentrations of PHX and its two major single hydroxyl metabolites in the diluted sample extracts (C_{dil}) and then dilution was corrected for as follows:

$C_{fnd} = C_{dil}$ x dilution factor

Fluconazole reference samples were used to correct for losses of MeCN on storage of treated samples and for errors in the dilution stages by using the following formula:

$C_{corr} = C_{fnd}$ x ($Ref_{fluc}/Sample_{fluc}$)

Ref_{fluc} = Mean peak area ratio (n=3) of Fluc/D_4-Fluc for the reference samples at that particular dilution

$Sample_{fluc}$ = peak area ratio of Fluc/D_4-Fluc for the test sample at that particular dilution

The concentrations of the trans-hydroxy metabolites are subject to an extra correction to account for the presence of two diastereomers, e.g. for isomer A:

$C_{FINAL}(TOH_A) = C_{corr}(TOH_A)$ x Mean Ratio (Peak Area (T-OH_A)/(Peak-Area (T-OH_A)+ Peak Area (T-OH_B)))

The mean ratio was calculated over all the calibration standards.

2.2.11.2.13. Semi-quantitative measurements of total concentrations of metabolites

The metabolites were assumed to have identical MS responses to PHX-OH reference standards. A single-point calibration standard was used – based on the mean of the response from trans and cis-OH standards. The total peak areas across all peaks in the expected MRM channel were employed for each class of metabolite (single –OH, di-OH, etc.)

2.2 STATISTICAL ANALYSIS

Unless otherwise stated, numerical data are expressed as mean ± S.D from 3 independent experiments. Also, one way analysis of variance (ANOVA) followed by Dunnett's multiple comparison test to determine statistical significance between test groups. Statistical analysis was performed using GraphPad Prism® version 5.04 (GraphPad Prism Software Inc, CA, USA). The significance of differences between two groups was assessed with an unpaired student t-test. A p value of ≤ 0.05 was considered to be statistically significant.

CHAPTER THREE

CHARACTERISATION OF ISOLATED HUMAN LIVER SINUSOIDAL ENDOTHELIAL CELLS

3.1 INTRODUCTION

Liver sinusoidal endothelial cells (HLSEC) are a unique population of endothelial cells with features of vascular and lymphatic endothelial cells (Lalor *et al.*, 2006, Sorensen et al., 2015). They are the only endothelial cell population which lack an organised basement membrane and have transcytoplasmic pores termed fenestrations which are organised into groups of sieve plates (DeLeve, 2007, Stolz, 2011a). Liver sinusoidal endothelial cells were isolated from human volunteer liver using the immunomagnetic separation method with CD-31 conjugated beads described in chapter 2 (Lalor et al., 2002). This chapter deals with the validation of the isolated cells as authentic liver sinusoidal endothelial cells and different from endothelial cells from other vascular beds, specifically the dermis. Further, it shows the purity of the preparation by absence of other hepatic contaminants. Using a transcriptomic and bioinformatics approach, HLSEC will be compared with human dermal microvascular endothelial cells (HDMEC) and human dermal lymphatic endothelial cells (HDLEC). In addition to phenotypically characterising the isolated HLSEC for the expression of endothelial-cell-specific markers, this chapter shows the response of HLSEC to angiogenic factors which modulate endothelial cell physiology. This includes activation of growth factor receptors to induce intracellular signalling, cell proliferation, cell migration, and tubular morphogenesis. The chapter concludes with a comparative analysis of in-house isolated HLSEC with commercially-sourced ones. This shall set the stage for the assays in the subsequent experimental chapters that show the potential roles of HLSEC in drug-induced liver injury using single cell and multicellular liver microtissue systems.

3.2 RESULTS

3.2.1 Phenotypic characterisation of isolated human liver sinusoidal endothelial cells

3.2.1.1 Analysis of purity of the isolated liver sinusoidal endothelial cells

The process of isolating the human sinusoidal endothelial cells (HLSEC) used in the study entailed the enzymatic digestion of human liver tissue, followed by separation of constituent cells. HLSEC were separated using CD-31 conjugated magnetic beads as described in the materials and methods section. After separation of HLSEC and culture, there is likelihood of contamination by other hepatic cells. In order to evaluate the purity of the isolated cells, *mRNA* from the samples were analysed by qPCR for the expression of *albumin* and *collagen type-1* which are markers of hepatocyte and fibroblast respectively. As shown in figure 3.1, the expression of albumin in primary human hepatocyte (PHH) was significantly ($p < 0.001$) higher as compared with HLSEC, with an almost 200 million fold higher expression. Also, collagen type I was significantly ($p < 0.001$) highly expressed in human hepatic fibroblast (HHF) in comparison with HLSEC where there was almost no expression. This shows that that HLSEC thus isolated was pure and free from major hepatic contaminants.

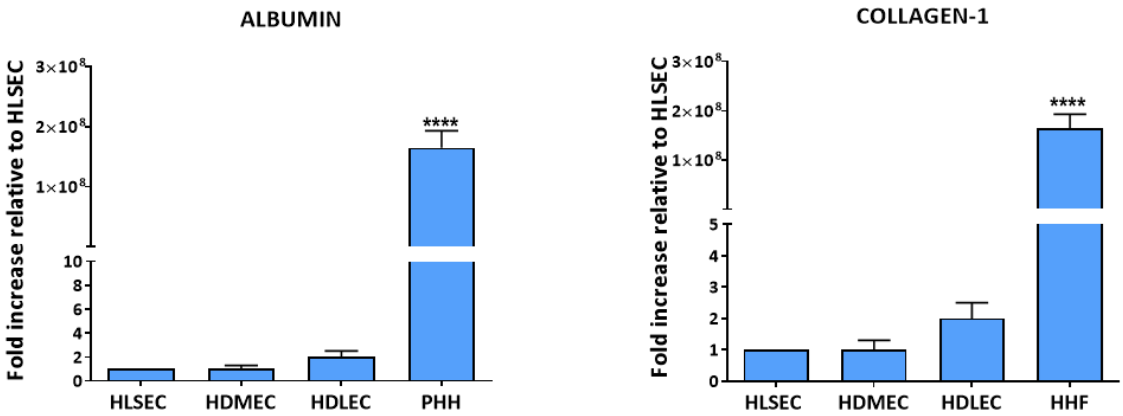

Figure 3.1: HLSEC do not express other hepatic markers
Relative expression of *albumin* and *collagen-1* in HLSEC and other liver cell types. HLSEC, HDMEC, HDLEC or HHF were cultured for 48 h or until 90% confluent. After removal of culture medium, cells were washed with ice-cold PBS twice and mRNA was extracted, cDNA synthesised and analysed for the expression of *albumin* or *collagen* by quantitative real-time PCR as described. Freshly isolated PHH was spun down at 80 g and lysed with buffer RLT to extract mRNA and processed as above. Results are expressed as mean ± SD, (n=3) from 3 separate experiments and analysed using one way analysis of variance ANOVA followed by Dunnett's multiple comparison test. Values are significant at ****p < 0.0001. HLSEC: human liver sinusoidal endothelial cells, HDMEC: Human dermal microvascular endothelial cells, HDLEC: Human dermal lymphatic endothelial cells, PHH: primary human hepatocyte, HHF: human hepatic fibroblast.

3.2.1.2 Liver sinusoidal endothelial cells are fenestrated

A hallmark of HLSEC is the presence of fenestrations that enable the transfer of substances between the blood circulating in the sinusoids and the underlying hepatocytes. In order to show that HLSEC maintained this primary characteristic following isolation and culture, they were processed for imaging by scanning electron microscopy. Figure 3.2 below shows an electron micrograph which compares the surface characteristics of liver sinusoidal endothelial cells with those of the human dermal microvascular endothelial cells (HDMEC). The electron micrograph shows that on HLSEC, there were fenestrations grouped into a cluster referred to as sieve plates

(circled in red) which were absent on HDMEC.

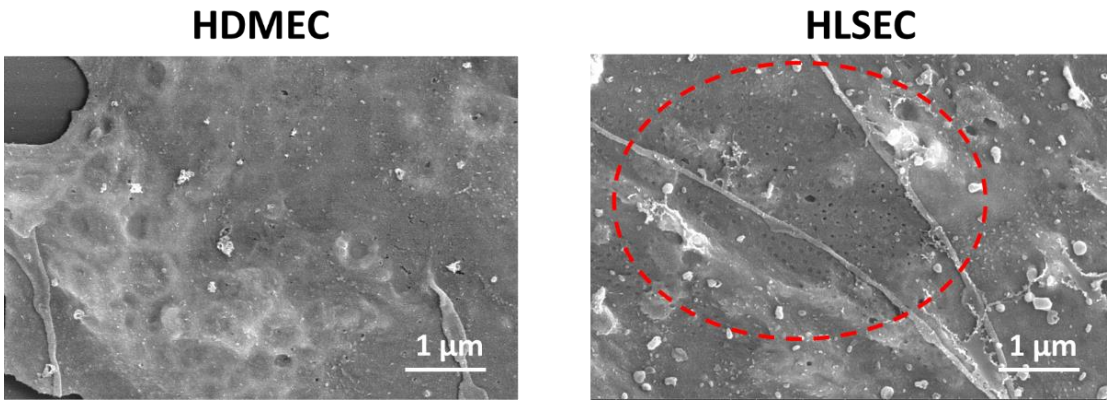

Figure 3.2: Scanning electron micrograph of HLSEC and HDMEC
Human dermal microvascular endothelial cells (HDMEC) or human liver sinusoidal endothelial cells (HLSEC) were plated out at a density of 2.6 X 10^4 cells/cm^2 on a collagen coated glass coverslip for 72 h. HDMEC and HLSEC were both cultured in the same medium. Cells on cover slips were then processed for scanning electron microscopy as described in materials and methods. Images above shows that fenestrations are absent on HDMEC but present on HLSEC.

3.2.1.3 Expression of endothelial markers on HLSEC and other endothelial cell types

In order to show that the isolated HLSEC expressed endothelial cell-specific genes, mRNA from HLSEC was analysed for platelet-endothelial adhesion molecule or *CD-31, VEGFR-1 and VEGFR-2*. Figure 3.3 shows the relative expression of endothelial markers on HLSEC, HDMEC and HDLEC. While all cells expressed the endothelial cell markers, HLSEC had a significantly higher expression of *VEGFR-1* and *CD-31* in comparison with HDLEC and a significantly ($p < 0.0001$) higher expression of *VEGFR-2* when compared with HDMEC. While this is an indication of the endothelial nature of the HLSEC that were isolated, it also shows that HLSEC better preserve these markers than the tested endothelial cell populations.

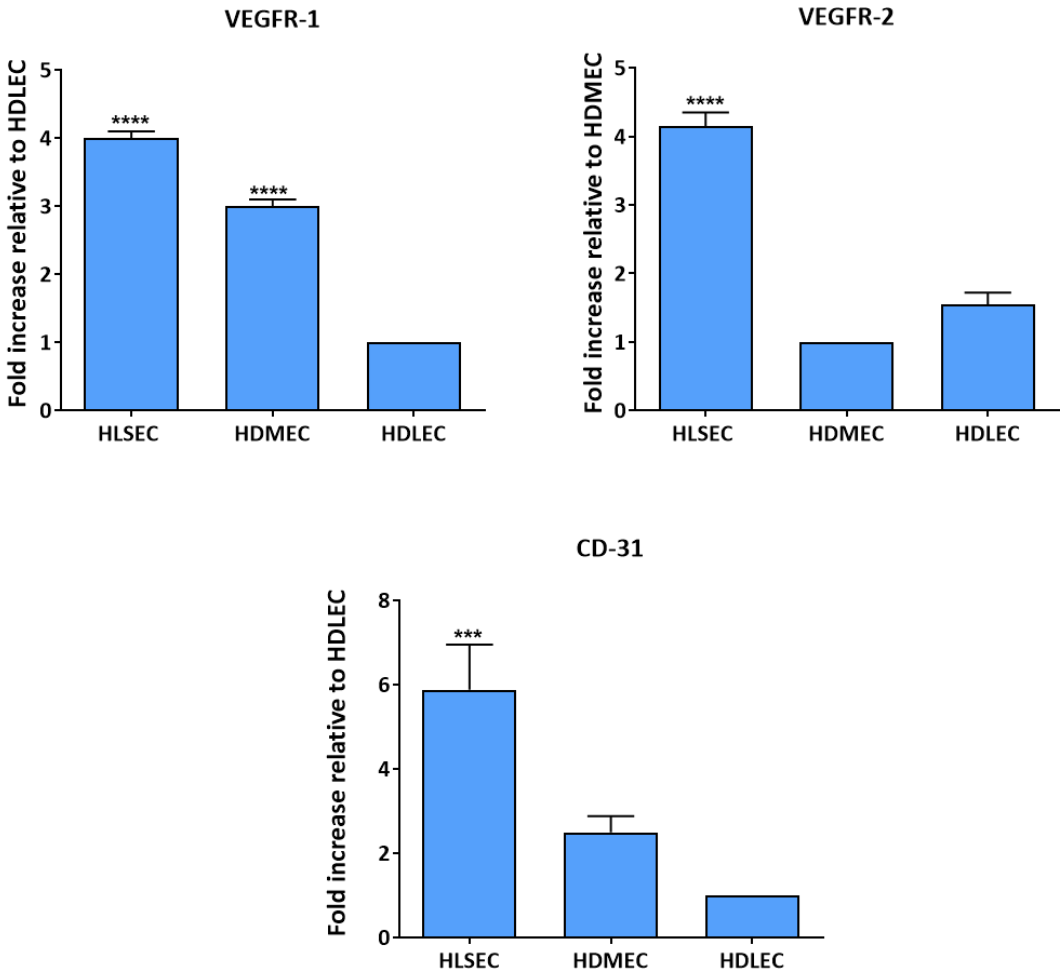

Figure 3.3: Expression of endothelial markers on HLSEC

Relative expression of *VEGFR-1, VEGFR-2* and *CD-31* in HLSEC and other endothelial cell types. HLSEC, HDMEC, HDLEC were cultured for 48 h or until 90% confluent. After removal of culture medium, cells were washed with ice-cold PBS twice and *mRNA* was extracted, cDNA synthesised and analysed for the expression of *VEGFR-1, VEGFR-2* and *CD-31* by quantitative real-time PCR as described. Results are expressed as mean ± SD, (n=3, three separate donor liver) and analysed using one way analysis of variance ANOVA followed by Dunnett's multiple comparison test. Values are significant at ****p < 0.0001 HLSEC: liver sinusoidal endothelial cells, HDMEC: Human dermal microvascular endothelial cells, HDLEC: Human dermal lymphatic endothelial cells. VEGFR-1, vascular endothelial growth factor receptor 1; VEGFR-2, vascular endothelial growth factor receptor 2.

3.2.1.4 Expression of lymphatic markers on HLSEC

To confirm reports in literature that HLSEC express markers of lymphatic endothelium (Mouta Carreira *et al.*, 2001, Nonaka *et al.*, 2007), *mRNA* from HLSEC was analysed for the expression of *VEGFR-3, LYVE-1, PROX-1* and *podoplanin* – classic lymphatic endothelial markers (Salven *et al.*, 2003, Lalor et al., 2006). Figure 3.4 shows the relative expression of *VEGFR-3, LYVE-1, PROX-1* and *podoplanin* in HLSEC, HDMEC and HDLEC. *VEGFR-3* was significantly ($p < 0.0001$) and highly expressed in HLSEC and HDLEC in comparison with HDMEC. HLSEC had a significantly ($p < 0.0001$) higher expression of *LYVE-1* in comparison with HDLEC. There was no difference in the expression of *LYVE-1* between HDMEC and HDLEC. On the other hand, podoplanin and *PROX-1* were significantly highly expressed in the lymphatic endothelium positive control, HDLEC, in comparison with HLSEC. This data agrees with literature (Dudas *et al.*, 2004) that, while HLSEC expressed some lymphatic markers, it did not express others. Figure 3.5 further confirms the expression of the lymphatic marker, *VEGFR-3*, in HLSEC at the protein level using immunofluorescent staining.

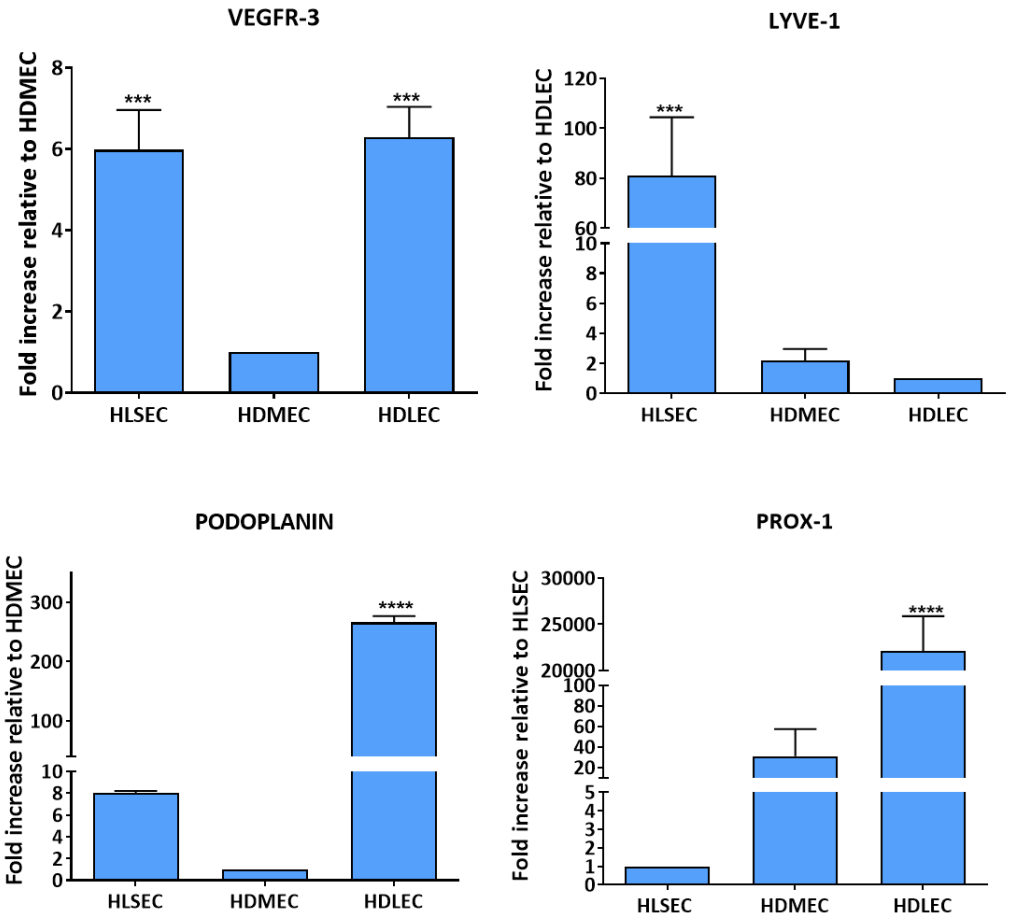

Figure 3.4: Expression of lymphatic endothelial markers on HLSEC

Relative expression of *VEGFR-3, LYVE-1, PROX-1* and *podoplanin* on HLSEC and other endothelial cell types. HLSEC, HDMEC, HDLEC were cultured for 48 h or until 90% confluent. After removal of culture medium, cells were washed with ice-cold PBS twice and mRNA was extracted, cDNA synthesised and analysed for the expression of *VEGFR-3, LYVE-1, PROX-1* and *podoplanin* by quantitative real-time PCR as described. Results are expressed as mean ± SD, (n=3, three separate donor liver) and analysed using one way analysis of variance ANOVA followed by Dunnett's multiple comparison test. Values are significant at ***$p < 0.001$ and ****$p < 0.0001$. HLSEC: liver sinusoidal endothelial cells, HDMEC: Human dermal microvascular endothelial cells, HDLEC: Human dermal lymphatic endothelial cells. PROX-1, Prospero homeobox protein 1; LYVE-1, Lymphatic vessel endothelial hyaluronan receptor 1.

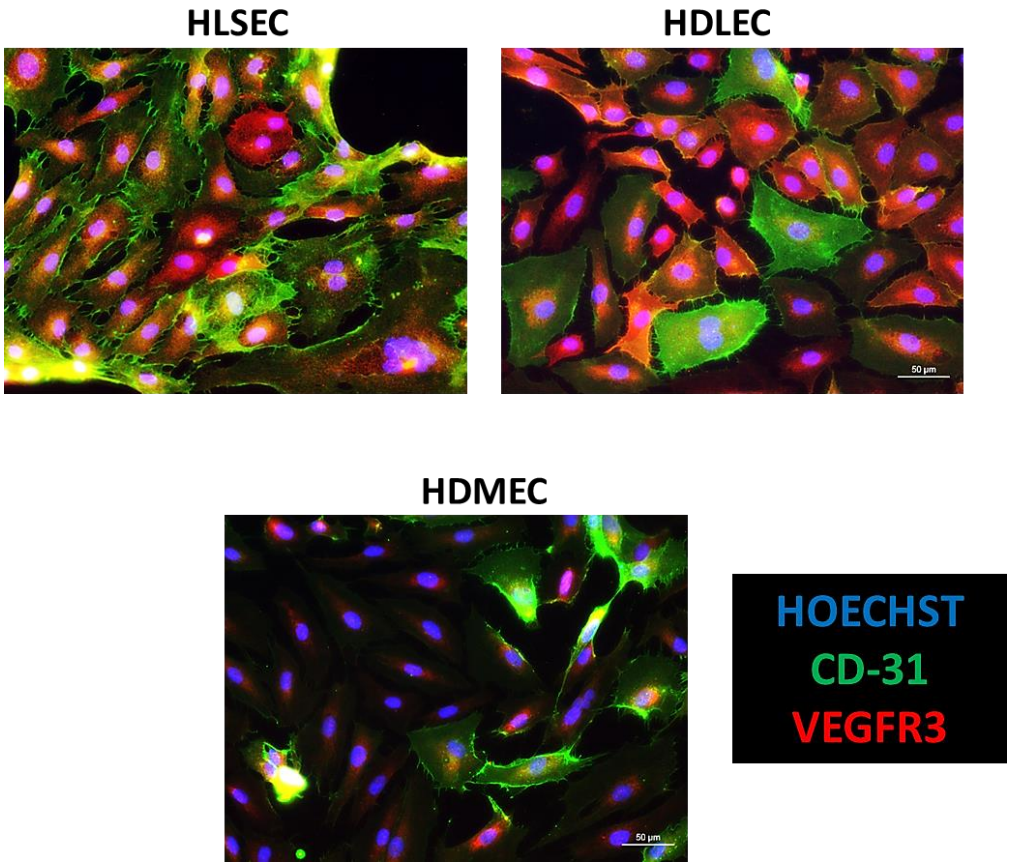

Figure 3.5: Immunofluorescent micrograph of HLSEC and HDMEC showing the expression of VEGFR-3
Cells were seeded on collagen-coated glass coverslips until they were at least 60 % confluent. They were fixed in 2 % paraformaldehyde for 15 min after removal of medium and two-time PBS washes. This was followed by processing for immunofluorescent microscopy as earlier described in materials and methods. Cells on coverslips were stained for VEGFR-3 [red] (lymphatic endothelial marker) and CD-31 [green] (vascular endothelial marker) and Hoechst [blue] (nuclear stain). VEGFR-3, vascular endothelial growth factor receptor 3.

3.2.1.5 Expression of HLSEC specific markers

The genes analysed above are vascular and/or lymphatic endothelium-specific. However, other genes have been reported in literature to be more specific to HLSEC. An example is the *blood coagulation factor VIII* otherwise known as anti-haemophilic factor (Do *et al.*, 1999). Others include *Stabilin-2* and *L-SIGN* which are involved in the scavenging and immunological functions of HLSEC (Cormier *et al.*, 2004, Nonaka et

al., 2007). Figure 3.6 below shows that while *factor VIII, L-SIGN, stabilin-1 and stabilin-2* were significantly ($p < 0.0001$) highly expressed in HLSEC in comparison with HDMEC. HDLEC also had a significantly high expression of *Stabilin-2* in comparison with *L-SIGN*.

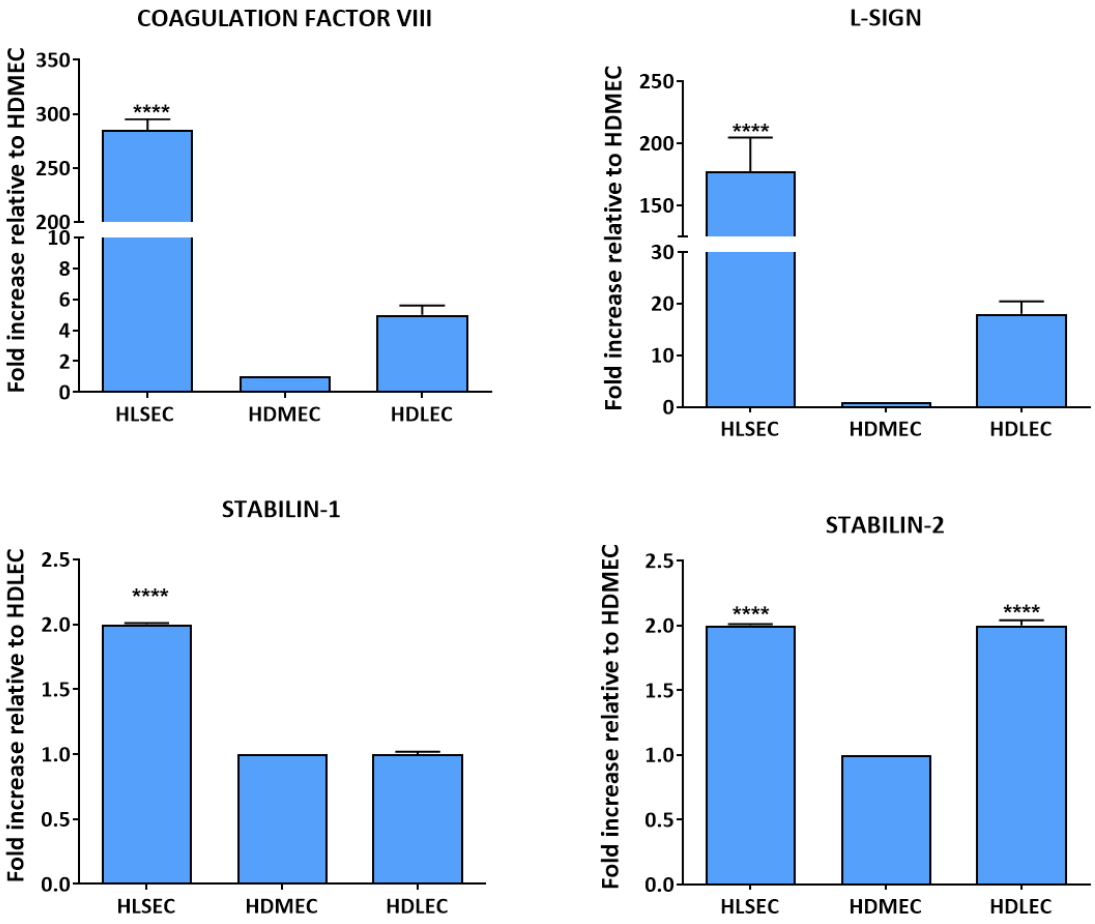

Figure 3.6: Expression of HLSEC-specific markers

Expression of *coagulation Factor VIII* and *L-SIGN* and *Stabilin-2* on HLSEC and other endothelial cell types. HLSEC, HDMEC, HDLEC were cultured for 48 h or until 90% confluent. After removal of culture medium, cells were washed with ice-cold PBS twice and mRNA was extracted, cDNA synthesised and analysed for the expression of *coagulation Factor VIII* and *L-SIGN* and *Stabilin-2* by quantitative real-time PCR as described. Results are expressed as mean ± SD, (n=3, three separate donor liver) and analysed using one way analysis of variance ANOVA followed by Dunnett's multiple comparison test. Values are significant at ****$p < 0.001$. HLSEC: liver sinusoidal endothelial cells, HDMEC: Human dermal microvascular endothelial cells, HDLEC: Human dermal lymphatic endothelial cells

3.2.1.6 Transcriptomic Analysis

In order to comprehensively compare liver sinusoidal endothelial cells with cells from other vascular beds, a whole transcriptome analysis was carried out on the mRNA extracted from liver sinusoidal endothelial cells, human dermal microvascular endothelial cells (HDMEC) and human dermal lymphatic endothelial cells (HDLEC) using GeneChip® Human Transcriptome Array 2.0 (HTA 2.0) (Affymetrix, UK). Experiments were carried out on endothelial cells from three different donors for each group. After the quality and integrity of the mRNA extracted from these samples were ascertained, they were analysed for differentially expressed genes to show the difference within and between the groups.

3.2.1.6.1 Principal component analysis

Signal intensity data generated from the GeneChip® Human Transcriptome Array, expression profiles were analysed using the Expression Console software (Affymetrix, UK). By means of a mathematical algorithm, principal component analysis (PCA) plots were generated to identify components with largest of variations and these were plotted against a second component which were independent of and uncorrelated with the first components, but show the largest variation (Ringner, 2008). This mathematical approach enables the separation of the individual samples analysed in directions that represent the overall variation in them based on their gene expression pattern, and to graphically show the level at which they compare with other samples in the overall analysis. Figure 3.7 below shows the principal component analysis (PCA)

of the samples from the three endothelial cell groups. While the plot shows a clear distinction between the three different endothelial cells groups, it shows a similar clustering pattern within each group. This is an indication of the homogeneity in gene expression within each of the groups.

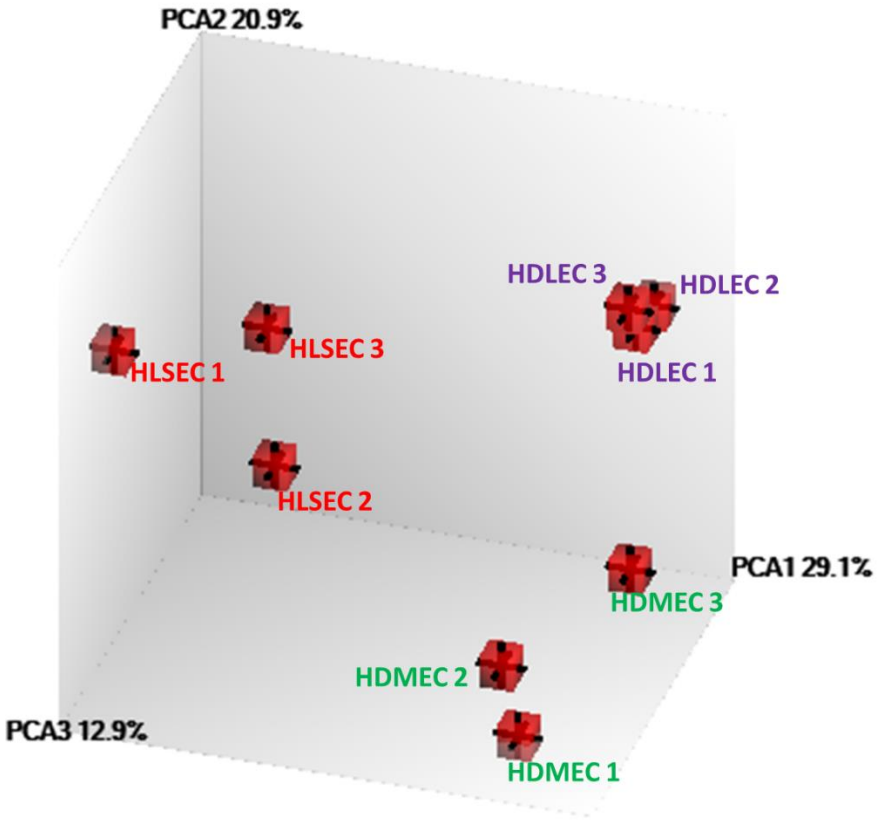

Figure 3.7: Principal component analysis of HLSEC, HDMEC and HDLEC.
Cells (HLSEC, HDMEC and HDLEC) were grown to 90% confluency, mRNA extracted and quantified as earlier described in materials and methods section. Then, mRNA samples were hybridised onto Affymetrix Human transcriptome (HTA 2.0) arrays and scanned using the Genechip Scanner 3000 7G. The resulting gene expression intensity data was analysed with the Expression Console® software (Affymetrix, UK) which was used to effect a quality control of the experiment as well as generate the principal component analysis (PCA) plot as shown in the figure above. The PCA plot helps to separate the samples into components with the largest amount of variation which is a function of the pattern of gene expression in the samples. The three-dimensional PCA plot reveals that 3 samples groups can be clearly separated, implying the existence of DE (Differentially Expressed) genes.

3.2.1.6.2 Analysis of differentially-expressed genes

In order to have a clearer picture of the difference between the three endothelial cell populations, each group was compared with every other group to show the pattern of gene expression. Figure 3.9 below is an MA plot showing the amount of variation between each matched pairs of cells. In comparison with HDMEC there were 371 upregulated genes in HLSEC, while there were 451 downregulated genes. Also there were 502 upregulated genes in HLSEC when compared with HDLEC. By contrast, there were 430 genes more highly expressed in HLSEC as against HDLEC. Comparing HDMEC with HDLEC, there were 265 upregulated genes while 328 genes were downregulated. Table 3.1 below shows 19 of the genes upregulated in HLSEC in comparison with HDMEC. Notable among these are coagulation factor VIII and lymphatic vessel endothelial hyaluronan receptor 1 (LYVE1) which have both been reported to be expressed in LSEC. Others genes upregulated in HLSEC versus HDMEC include mannose receptor C 1, C-type lectin domain receptor 1B both of which are scavenger receptors reviewed in chapter 1 of this thesis. Also, in the differential expression of HLSEC relative to HDLEC, similar genes were upregulated in HLSEC (Table 3.3). On the other hand, among the genes downregulated in HLSEC relative to HDMEC were transforming growth factor beta 2 (TGFB2), fibroblast growth factor 16, claudin 1. Of particular interest are genes downregulated in HLSEC relative to HDLEC (Table 3.4). These include the lymphatic markers, podoplanin and PROX-1**.** Claudin 1 was also downregulated in the comparison with HDMEC (Table 3.2).

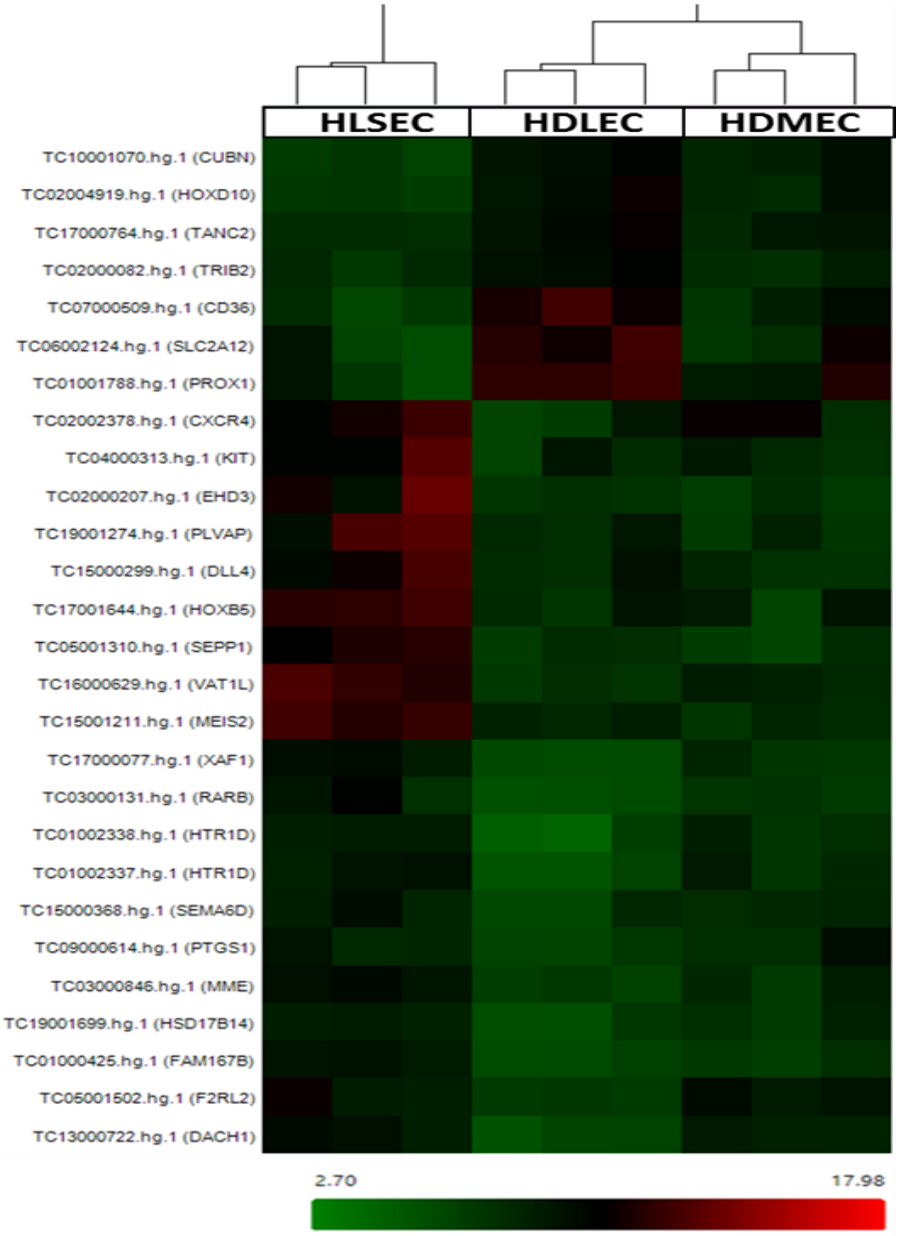

Figure 3.8: Heatmap showing expression of some of 5000 most highly expressed genes in the three groups of endothelial cells.

Cells (HLSEC, HDMEC and HDLEC) were grown to 90% confluency, mRNA extracted and quantified as earlier described in materials and methods section. Then, mRNA samples were hybridised onto Affymetrix Human transcriptome (HTA 2.0) arrays and scanned using the Genechip Scanner 3000 7G. The resulting gene expression intensity data was analysed with the Expression Console® software (Affymetrix, UK) which was used to effect a quality control of the experiment as well as estimate the expression of the genes of interest into $\log_2$ expression. The output from this analysis was further analysed using the Transcriptome Analysis Console (TAC) software (Affymetrix, UK). TAC was used to determine identify the differentially-expressed genes, the signal intensities of any particular gene in the sample of interest. The signal intensity data was then sorted by the 5000 most highly expressed genes, which were then visualised using hierarchical clustering to generate a heatmap. The heatmap above shows a general profile of gene expression indicated by signal intensity graphically depicted in colours, with green being the samples with the lowest gene expression while red are samples with highest gene expression.

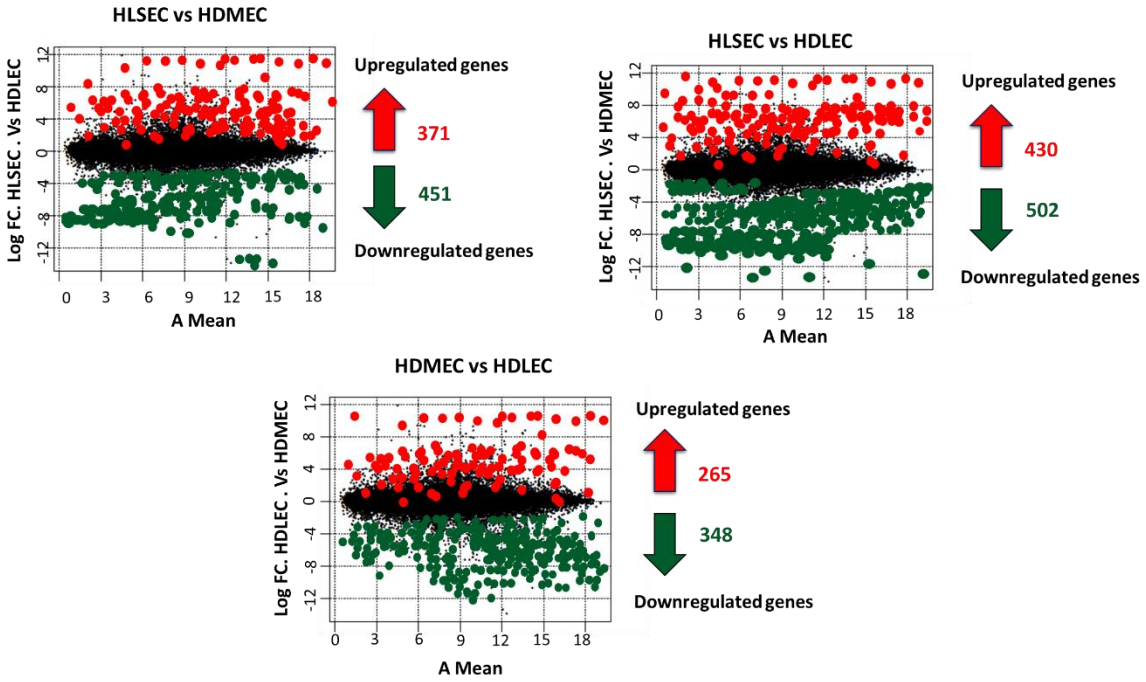

Figure 3.9: MA plot showing differentially-expressed genes between the groups of endothelial cells.
Cells (HLSEC, HDMEC and HDLEC) were grown to 90% confluency, mRNA extracted and quantified as earlier described in materials and methods section. Then, mRNA samples were hybridised onto Affymetrix Human transcriptome (HTA 2.0) arrays and scanned using the Genechip Scanner 3000 7G. The resulting gene expression intensity data was analysed with the Expression Console® software (Affymetrix, UK) which was used to effect a quality control of the experiment as well as estimate the expression of the genes of interest into $\log_2$ expression. The output from this analysis was further analysed using the Transcriptome Analysis Console (TAC) software (Affymetrix, UK). TAC was used to determine identify the differentially-expressed genes, the signal intensities of any particular gene in the sample of interest. Using signal intensity data generated, each group was compared with the other to generate the linear fold change (FC) in gene expression relative to the other. The estimated $\log_2$ fold change (logFC) in the genes of interest were compared between the groups of interest using t-test. The estimated p-values for each logFC values were adjusted for multiple testing using the False Discovery Rate (FDR) method. Significantly differential expression were those whose FDR had adjusted p-value < 0.05. The number of differentially-expressed genes in each paired comparison and the direction of the expression were plotted into an MA plot shown; M = log fold change, A= log expression.

Table 3.1: Most upregulated genes in HLSEC vs HDMEC

Gene Description	Fold Change
Ectonucleotide pyrophosphatase/phosphodiesterase 2 (ENPP2)	49.14
plasmalemma vesicle associated protein (PLVAP)	46.27
regulator of G-protein signaling 7 binding protein (RGS7BP)	38.67
placenta specific 8 (PLAC8)	35.64
tissue factor pathway inhibitor 2 (TFPI2)	30.55
tissue factor pathway inhibitor 2 (TFPI2)	29.4
protocadherin 17(PCDH17)	28.69
nitric oxide synthase trafficking (NOSTRIN)	28.17
guanylate binding protein 4 (GBP4)	22.74
EH domain containing 3 (EHD3)	19.58
acyl-CoA synthetase medium-chain family member 3 (ACSM3)	19.34
selenoprotein P, plasma, 1 (SEPP1)	19.28
SH3 and cysteine rich domain(STAC)	18.39
Meis homeobox 2(MEIS2)	17.56
acyl-CoA synthetase medium-chain family member 3 (ACSM3)	15.14
coagulation factor VIII, procoagulant component (F8)	14.69
lymphatic vessel endothelial hyaluronan receptor 1 (LYVE1)	14.15
neural cell adhesion molecule 2 (NCAM2)	11.47
junctional adhesion molecule 2 (JAM2)	11.43

Table 3.2: Most down-regulated genes in HLSEC vs HDMEC

Description	Fold change
cholinergic receptor, nicotinic alpha 1 (CHRNA1)	-17.79
RAB3B, member RAS oncogene family (RAB3B)	-19.66
transforming growth factor beta 2 (TGFB2)	-19.67
ADAM metallopeptidase domain 23 (ADAM23)	-21.13
chemokine (C-X-C motif) ligand 6 (CXCL6)	-21.9
chemokine (C-X3-C motif) ligand 1 (CX3CL1)	-23.34
matrix metallopeptidase 10 (MMP10)	-26.92
cholinergic receptor, nicotinic alpha 1 (CHRNA1)	-44.22
Transgelin (TAGLN)	-55.49
sparc/osteonectin, cwcv and kazal-like domains proteoglycan (testican) 1 (SPOCK1)	-56.53

Table 3.3: Most upregulated genes in HLSEC vs HDLEC

Description	Fold Change
ectonucleotide pyrophosphatase/phosphodiesterase 2 (ENPP2)	79.42
interferon, alpha-inducible protein 27 (IFI27)	77.62
interferon, alpha-inducible protein 27 (IFI27)	74.54
lymphatic vessel endothelial hyaluronan receptor 1 (LYVE1)	47.22
nitric oxide synthase trafficking (NOSTRIN)	43.46
regulator of G-protein signaling 7 binding protein (RGS7BP)	37.96
guanylate binding protein 4 (GBP4)	30.55
placenta specific 8 (PLAC8)	26.2
plasmalemma vesicle associated protein (PLVAP)	25.51
vesicle amine transport 1-like (VAT1L)	23
acyl-CoA synthetase medium-chain family member 3 (ACSM3)	21.89
acyl-CoA synthetase medium-chain family member 3 (ACSM3)	21.8
chemokine (C-X-C motif) receptor 4 (CXCR4)	21.44
CAP, adenylate cyclase-associated protein, 2 (yeast) (CAP2)	21.42
protocadherin 17 (PCDH17)	19.68
epithelial membrane protein 3 (EMP3)	18.91
bone marrow stromal cell antigen 2 (BST2)	18.46
SPARC like 1 (SPARCL1)	18.21
5-hydroxytryptamine (serotonin) receptor 1D, G protein-coupled (HTR1D)	17.86
junctional adhesion molecule 2 (JAM2)	17.05

Table 3.4: Most down-regulated genes in HLSEC vs HDLEC

Description	Fold Change
prospero homeobox 1 (PROX1)	-19.37
carcinoembryonic antigen-related cell adhesion molecule 1 (biliary glycoprotein) (CEACAM1)	-21.89
sulfotransferase family 1C member 4 (SULT1C4)	-23.33
transient receptor potential cation channel, subfamily C, member 6 (TRPC6)	-25.4
protein tyrosine phosphatase, receptor type, S (PTPRS)	-26.75
reelin(RELN)	-29.92
deltex 4, E3 ubiquitin ligase (DTX4)	-30.81
podoplanin(PDPN)	-34.5
solute carrier family 2 (facilitated glucose transporter), member 12 (SLC2A12)	-39.62
cholinergic receptor, nicotinic alpha 1(CHRNA1)	-108.66

3.2.2 Functional characterisation of HLSEC

In addition to validating HLSEC for the expression of endothelial cell-specific genes, it is important to functionally characterise them; namely evaluating their response to growth factors that are important in their physiology. This sub-section focusses on the response of HLSEC to VEGF-A and VEGF-C to elicit endothelial-specific responses – activation of cell surface receptors to induce intracellular signalling that result in cell proliferation, migration and ultimately formation of vasculature. The effect of growth factors on HLSEC fenestrations was also investigated.

3.2.2.1 Effect of growth factor stimulation on HSLEC fenestrations

Following reports that fenestrations on HLSEC are regulated by VEGF-A, HLSEC was cultured in the presence of VEGF-A as well as VEGF-C to see their effect on the fenestration in HLSEC. Scanning electron micrographs in figure 3.10 shows that upon stimulation with VEGF-A, there was a significant ($p<0.01$) increase in the number of the fenestration on HLSEC, whereas stimulation with VEGF-C did not induce any significant difference when compared with basal. Also, fenestral porosity was increased in the VEGF-A group.

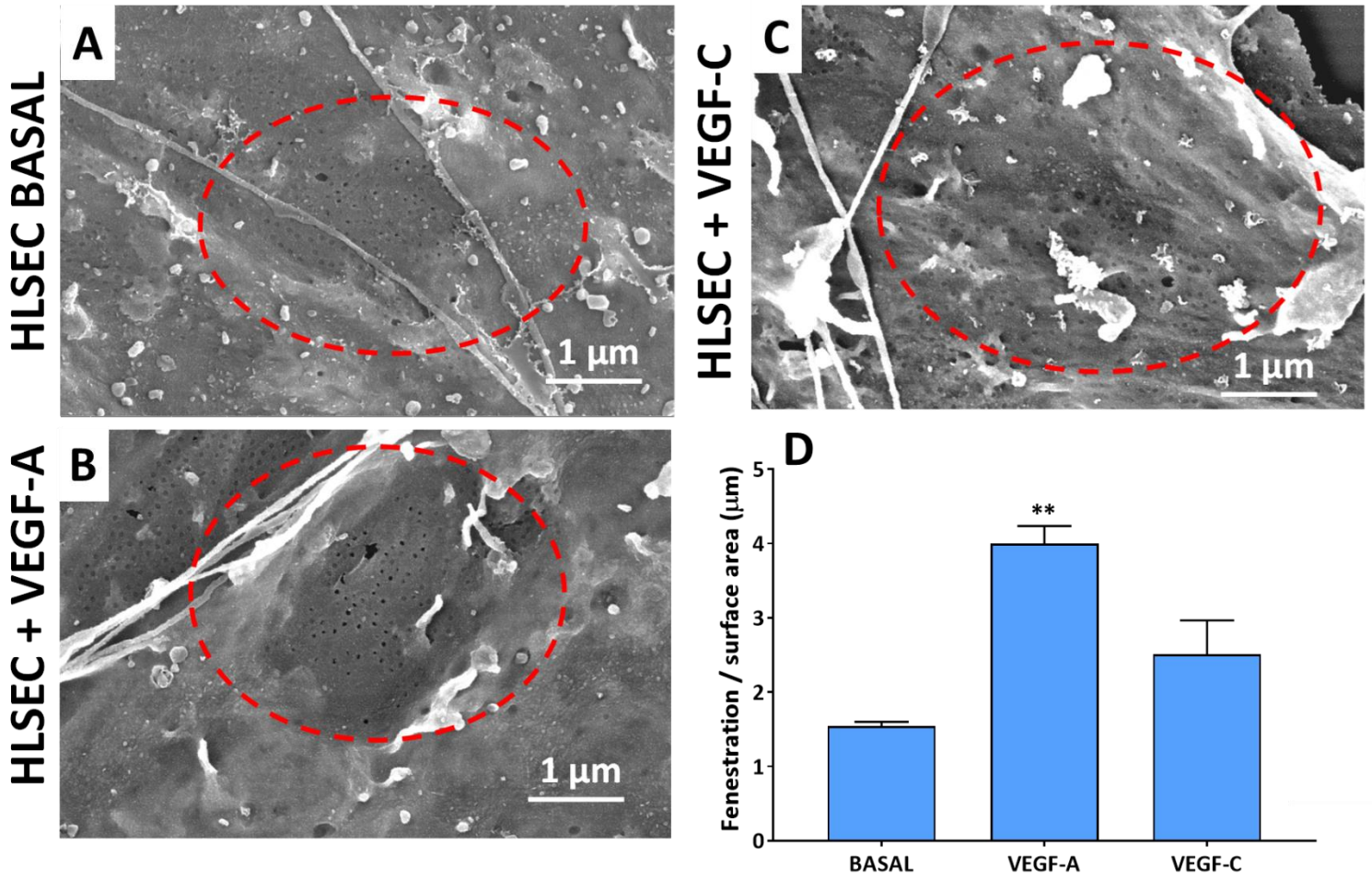

Figure 3.10: Scanning electron micrograph showing effect of growth factor on HLSEC

Cells were plated out at a density of 2.6 X 10^4 cells/cm^2 on a collagen coated glass coverslip for 24 h after which they medium was replaced with full growth medium supplemented with growth factor (B,C) or full growth medium alone (A) for 48 h. Cells on cover slips were then processed for scanning electron microscopy as described in materials and methods. Fenestrations are circled in dotted red lines. Fenestrations were counted from 4 randomly-selected images and represented mean ± SD (n=4). Groups were compared using ANOVA followed by Dunnett's multiple comparison test. Values are significant at **p < 0.01

3.2.2.2 Activation of intracellular signalling by growth factor stimulation

As shown above, HLSEC express VEGFR-1, VEGFR-2 and VEGFR-3. In order to assess the activation of these and any other similar receptors they might express, HLSEC, HDMEC and HDLEC were screened with a range of growth factors. Figure 3.11 shows that VEGFR-2 was activated by the two VEGF-A isoforms (VEGF-A_{121} and VEGF-A_{165}), and by VEGF-E in all three cell types. This was accompanied by a corresponding activation of ERK 1/2 (regulator of cell proliferation) and AKT (regulator of endothelial cell survival). VEGF-B and VEGF-C did not activate VEGFR-2 at the concentration used. AKT and ERK 1/2 were phosphorylated in response to FGF, EGF and HGF, but not by PDGF. In HDLEC there was a strong activation of AKT following VEGF-C stimulation.

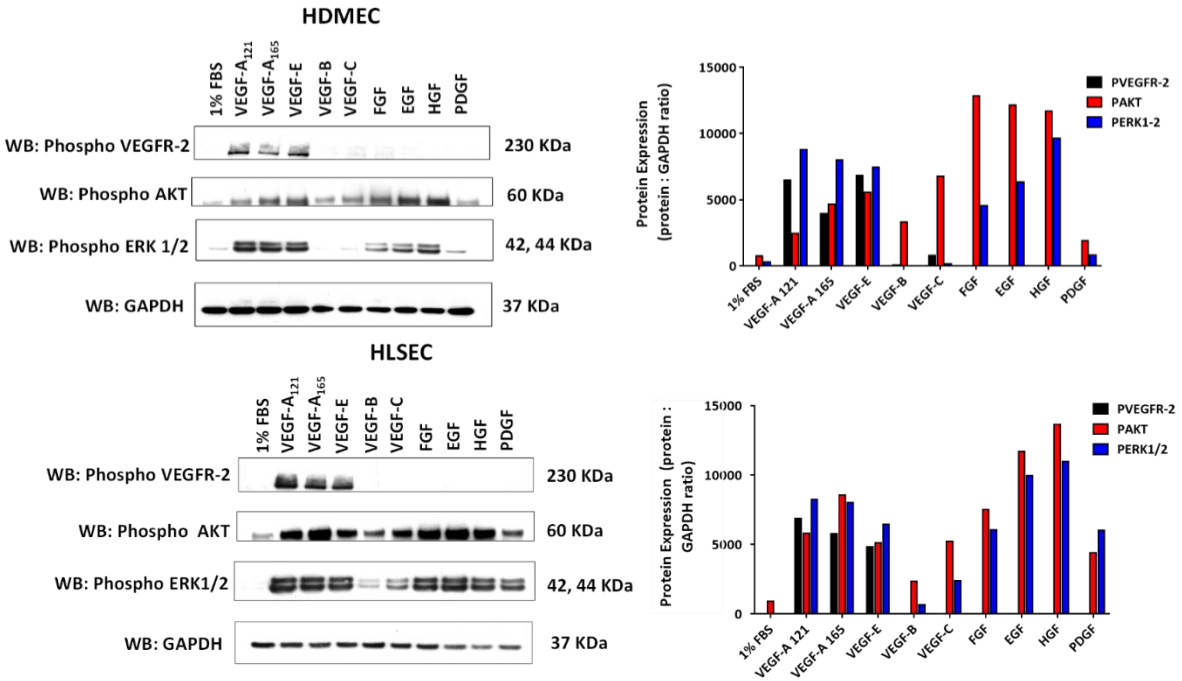

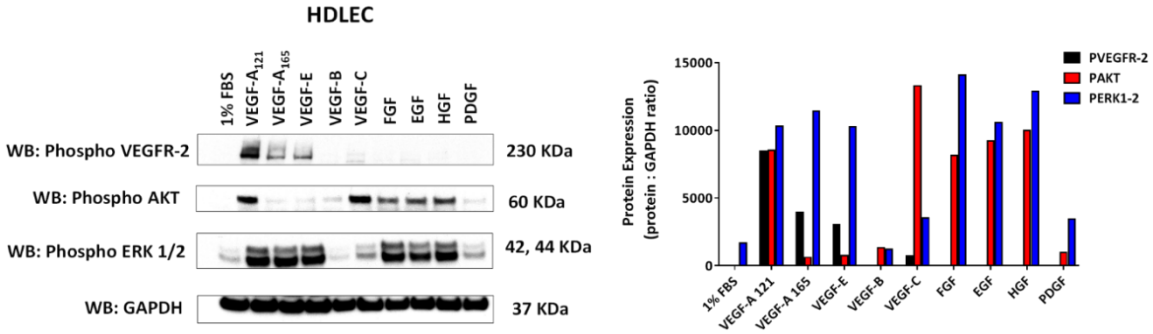

Figure 3.11: Activation of intracellular signalling pathway in endothelial cells
Cells were cultured until 90% confluent, kept on medium containing 1% FBS for 16 hours and then stimulated with 50 ng/ml of growth factors for 10 min. Cells were lysed for total protein contents using modified RIPA buffer, solubilised in LDS sample buffer, denatured at 90 ^{o}C. Protein was separated using SDS PAGE for 45 min., transferred unto nitrocellulose membrane for 2 h. and blocked with 5% BSA. Membranes were then probed with respective antibodies for phosphorylated VEGFR-2, total VEGFR-2, phosphorylated AKT, phosphorylated ERK 1/2 and GAPDH. FBS: foetal bovine serum, VEGF-A: vascular endothelial growth factor A, VEGF-B: vascular endothelial growth factor B, VEGF-C: vascular endothelial growth factor C, VEGF-E: vascular endothelial growth factor E, FGF: fibroblast growth factor, EGF: epidermal growth factor, PDGF: platelet-derived growth factor.

3.2.2.3 Cell proliferation

A downstream effect of the activation of these intracellular signalling pathway following phosphorylation of VEGFR-2 is cell proliferation. In order to show this, HLSEC, HDMEC, and HDLEC were incubated with the same range of growth factors used to activate the growth factor receptors. Figure 3.12 shows the proliferation of HLSEC, HDMEC, and HDLEC in response to a range of growth factors. Hepatocyte growth factor and growth factors of the VEGF family, except VEGF-B induced a highly significant ($p < 0.001$) increase in cell proliferation in HLSEC compared to basal. The trend was similar in HDMEC and HDLEC with a highly significant ($p<0.01$) increase in cell proliferation in comparison with the basal. Fibroblast growth factor and hepatocyte growth factor induced a highly significant ($p<0.01$) increase in cell proliferation in HLSEC while only HDMEC but not HDLEC had a highly significant ($p < 0.01$) increase in cell proliferation in response to FGF.

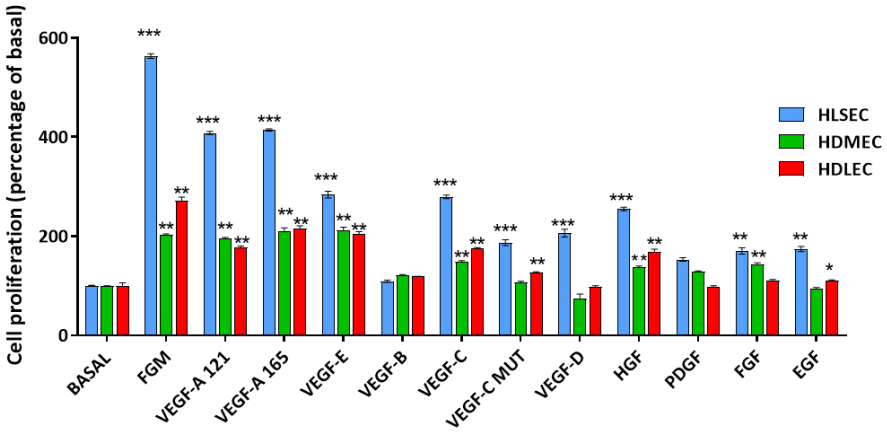

Figure 3.12: Cell proliferation assay
Cell proliferation in HLSEC and endothelial cells from other vascular beds. Cells were plated at 1.5 X 10^4 cells/ cm^3 on a collagen-coated plate for 48 h after which they were washed and placed on a culture medium containing 1% FBS for 16 h. Cell were stimulated with 50 ng/ml of growth factor in culture medium containing 1% FBS for 72h. Cells were thereafter washed with ice-cold PBS twice and lysed with Cell Titer Glo reagent and assayed for ATP content as described in methods. Results are expressed as mean ± SD, (n=3) and analysed using one way analysis of variance ANOVA followed by Dunnett's multiple comparison test, with growth factor stimulated groups compared against. Values are significant at *p<0.05, **p<0.01, ***P<0.001.

Also, while HDLEC experienced a significant ($p<0.05$) increase in cell proliferation in response to EGF, this was not observed in HDMEC. Platelet-derived growth factor did not induce any significant effect on cell proliferation in any cell type.

3.2.2.4 Cell migration

Cell migration represents a critical component of angiogenesis as endothelial cells migrate in response to growth factor stimulation. In order to confirm the ability of HLSEC to migrate in response to angiogenic growth factors, HLSEC, HDMEC and HDLEC were stimulated with VEGF-A or VEGF-C after the introduction of scratch unto endothelial cells grown to confluence in tissue-culture plates. Figure 3.13 below shows the effect of VEGF-A and VEGF-C on cell migration in endothelial cells. After 16 h of exposure to VEGF-A and VEGF-C, there was a highly significant ($p< 0.0001$) increase in wound closure in HLSEC and HDMEC when compared with unstimulated control. As for HDLEC, VEGF-A induced a highly significant ($p<0.001$) increase in wound closure when compared with basal, while a significant ($p<0.01$) increase in wound closure was obtained in response to VEGF-C.

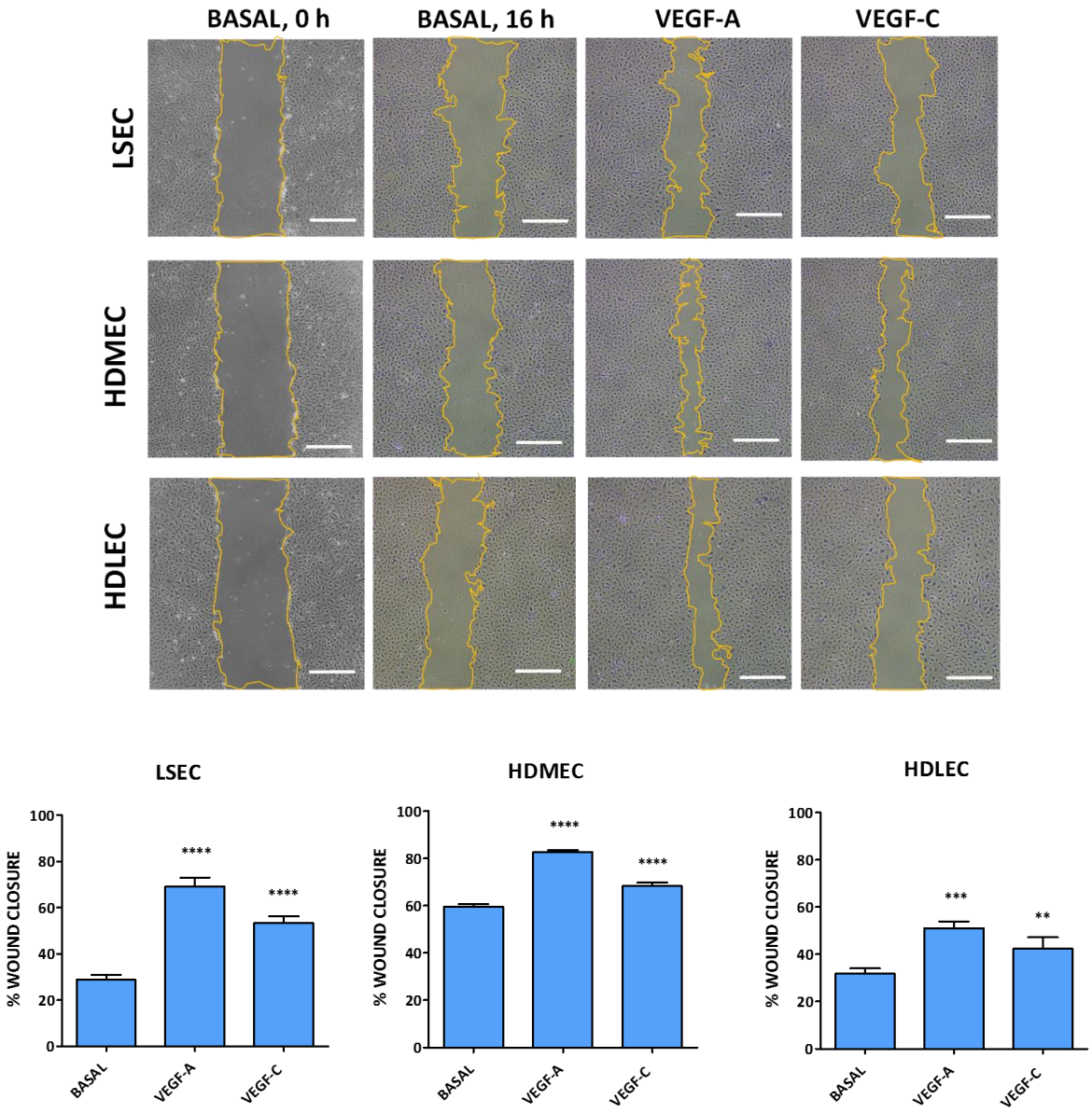

Figure 3.13: Cell Migration

Cell migration in HLSEC. HLSEC, HDMEC or HDLEC were plated on a collagen-coated 12-well tissue culture plate at 2.1 X 10^4 cells/cm^2 until fully confluent. Medium was removed; cells washed twice with PBS and then place on medium containing 1% FBS for 16 hours after which straight-line scratches were introduced with a sterile 200 µl pipette tip. Cells were washed with PBS after removal of culture medium to remove floating cells and 50 ng/ml of VEGF-A, VEGF-C or basal medium was added unto the cells. Pictures of the scratch-wounds were taken (mag X4) Cells were incubated at 37° C for 16 h after which there washed twice with PBS at room temperature, and fixed with 2% PFA for 15 minutes, washed twice again with PBS twice and further processed as earlier described. Images of scratch wounds were taken (t=16 h) and compared with those taken at an earlier time point (t= 0 h). Cell migration was calculated as percentage wound closure (area covered by growth factor stimulated compared with unstimulated at t= 0 h). Wound areas were measured using the scratch wound plugin of the Image-J software Results are expressed as mean ± SD, (n=3, three independent experiments) and analysed using one way analysis of variance ANOVA followed by Dunnett's multiple comparison test, with growth factor stimulated groups compared against. Values are significant at **p<0.01, ***P<0.001, ****p<0.00001. VEGF-A: Vascular endothelial growth factor A, VEGF-C: Vascular endothelial growth factor C. scale bars= 100 µm.

3.2.2.5 Tube formation

Upon activation of VEGF receptors to induce phosphorylation of intracellular signalling which effect cell proliferation and migration, an additional effect is cell permeability. This is required to enable the cells to reorganise to form new vasculature or new vasculature from pre-existing ones. In order to assess this in HLSEC, an *in vitro* angiogenesis assay which incorporates endothelial cells seeded upon a 'lawn' of confluent fibroblasts was carried out. Figure 3.14 shows the effect of VEGF-A and VEGF-C on the formation of tubular network in an *in vitro* angiogenesis assay in HLSEC and HDMEC. VEGF-A induced a highly significant ($p<0.01$) increase in tube formation in HLSEC and HDMEC in comparison to control. Also, VEGF-C induced a significant effect on both HLSEC and HDMEC when compared with the basal control.

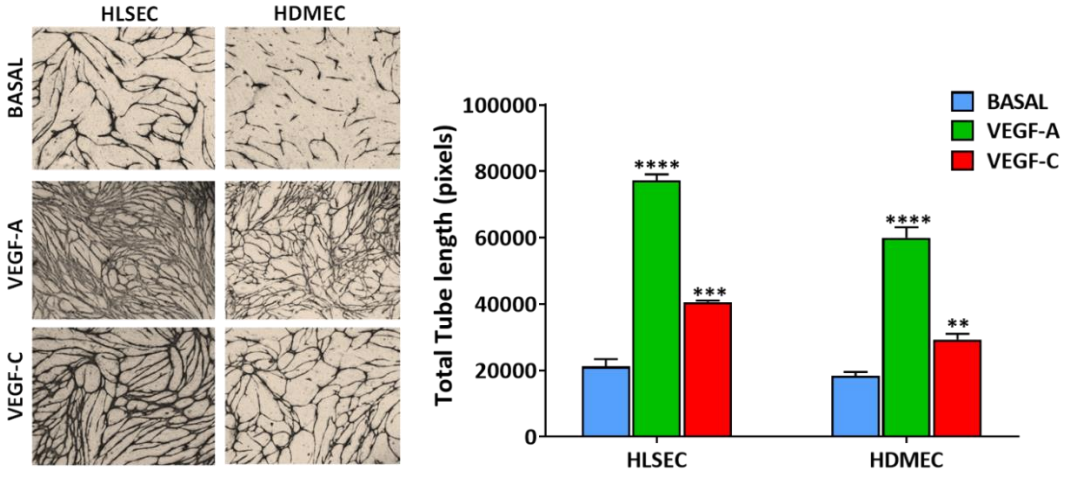

Figure 3.14: Tube formation assay
In vitro angiogenesis assay in HLSEC**.** Juvenile NHDF were cultured at 7.9 X 10 cells/ cm^2 for 3 days in a collagen coated glass 24-well plates for 72 h when the cells are fully confluent, after which HLSEC were plated on top at a density of 21 X 10^3 cells/ cm^2 for 24 h. Then cells were treated with growth medium containing 1% FBS and/ or 50 ng/ml of VEGF-A, VEGF-C for 72 h and then re-exposed to same for another 48 h. Cells were then washed in PBS at room temperature and fixed with 2% PFA for 15 min., washed twice with PBS and then stained for CD-31 following the colorimetric immunocytochemical methods already described. Angiogenesis was quantified using Angioquant (NIH, USA) which quantifies number of branches and tube lengths. Bars represent mean ± SD (n=3, three independent experiments) and basal state compared with growth-factor stimulated state by Student t-test. Data are significant at **p<0.01.

3.2.3 Comparative study between in-house HLSEC and commercially sourced HLSEC

Commercially-available cells are a viable source of liver sinusoidal endothelial cells. The potential advantage they confer is easy availability and the time saved from cell isolation. In order to assess the viability of commercially-sourced HLSEC, HLSEC procured from two commercial sources were compared with in-house isolated HLSEC. Cells were cultured till they were 90 % confluent and were analysed for key endothelial, lymphatic and LSEC marker genes by quantitative real-time PCR.

3.2.3.1 Commercially-sourced HLSEC express key endothelial and lymphatic makers at a very low level

In order to validate the endothelial identity of the commercial HLSEC, they were assessed by PCR for the expression of endothelial cell-specific genes. Also, they were assessed for the expression of lymphatic markers *VEGFR-3, LYVE-1, PROX-1* and *podoplanin*. Figure 3.15 below shows relatively low levels of all endothelial marker genes in commercial HLSEC in comparison with in-house isolated HLSEC. The relative expression of *VEGFR-1* in the group marked HLSEC SC (LM) was significantly lower than in their in-house isolated contemporary (HLSEC D141). The expression of *VEGFR-2* in the in-house isolated HLSEC was significantly higher than the HLSEC SC (PM) group. The trend is similar for *CD-31*, which is another

important endothelial cell marker. Although there was a relatively-low expression of the above genes in comparison with HLSEC 141, the HLSEC MED group has a significantly higher expression of the endothelial-specific genes in comparison with the HLSEC SC group. A similar trend can also be seen for the lymphatic markers, *VEGFR-3, PROX-1 and LYVE-1*. Nevertheless, the expression of podoplanin was relatively higher in HLSEC SC when compared with HLSEC 141 (figure 3.16).

3.2.3.2 Commercial HLSEC had relatively low expression of LSEC-specific genes

In order to further investigate the possibility of the commercial HLSEC expressing genes that are LSEC-specific, *mRNA* extracted from these were evaluated for the expression of coagulation *factor VIII*, *stabilin-1, stabilin-2* as well as *L-SIGN*. Similar to findings with regards to the expression of endothelial genes, figure 3.17 shows that the in-house isolated HLSEC had a significantly higher expression of coagulation *factor VIII* and *L-SIGN* in comparison with HLSEC SC (PM) and the other commercial samples. The expression of *stabilin-1* and *stabilin-2* were highly expressed in HLSEC D141 in comparison to the HLSEC SC groups.

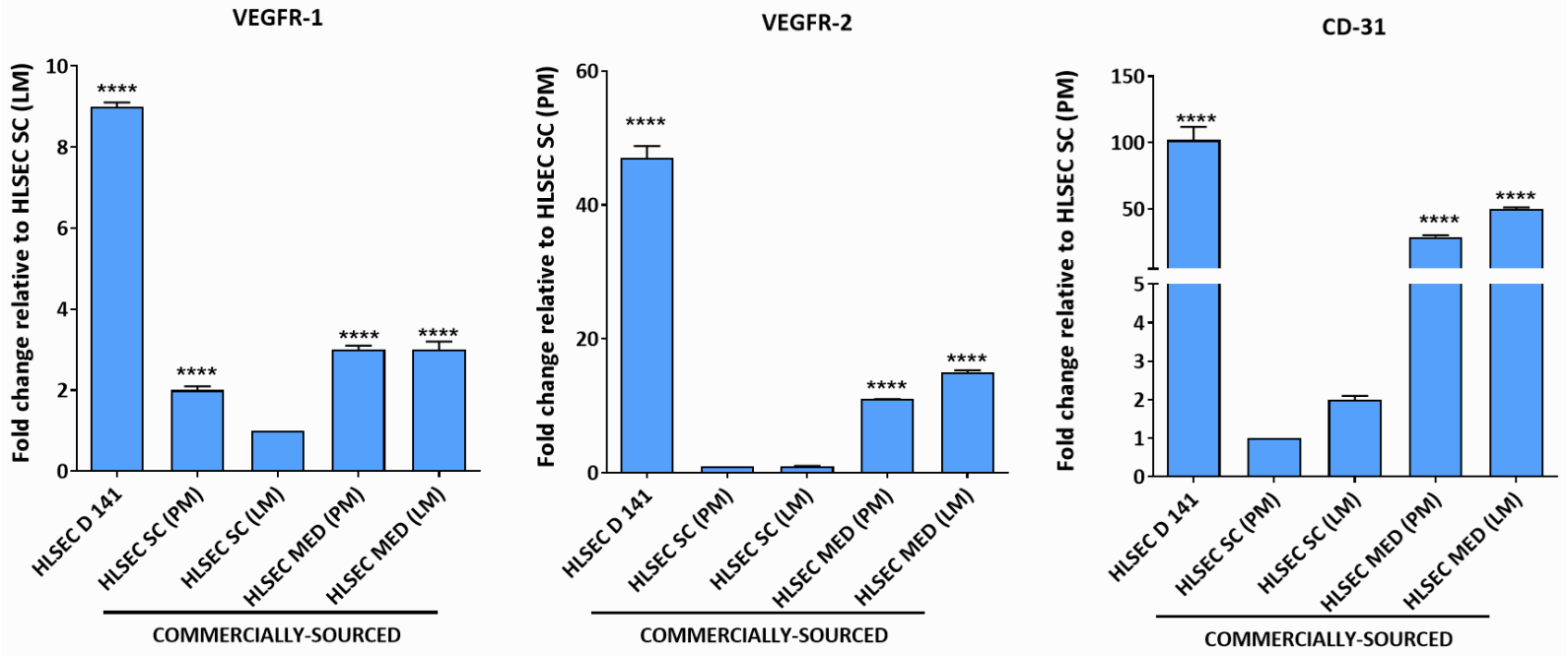

Figure 3.15: Expression of endothelial markers on HLSEC

Relative expression of VEGFR-1, VEGFR-2 AND CD-31 in in-house HLSEC and commercially-sourced ones. Cells were cultured for 48 h or until 90% confluent. After removal of culture medium, cells were washed with ice-cold PBS twice and mRNA was extracted, cDNA synthesised and analysed for the expression of the respective genes by qPCR as described. Freshly isolated PHH was spun down at 80 g and lysed with buffer RLT to extract mRNA and processed as above. Results are expressed as mean ± SD, (n=3, three independent experiments). HLSEC D141: in-house isolated human liver sinusoidal endothelial cell, LSEC SC (PM): Commercially-sourced liver sinusoidal endothelial cell from Sciencell cultured on their proprietary medium, HLSEC SC (LM): Commercially-sourced liver sinusoidal endothelial cells from Sciencell cultured on LSEC medium. Commercially-sourced liver sinusoidal endothelial cell from Medicyte cultured on their proprietary medium, HLSEC SC (LM): Commercially-sourced liver sinusoidal endothelial cell from Medicyte cultured on HLSEC medium

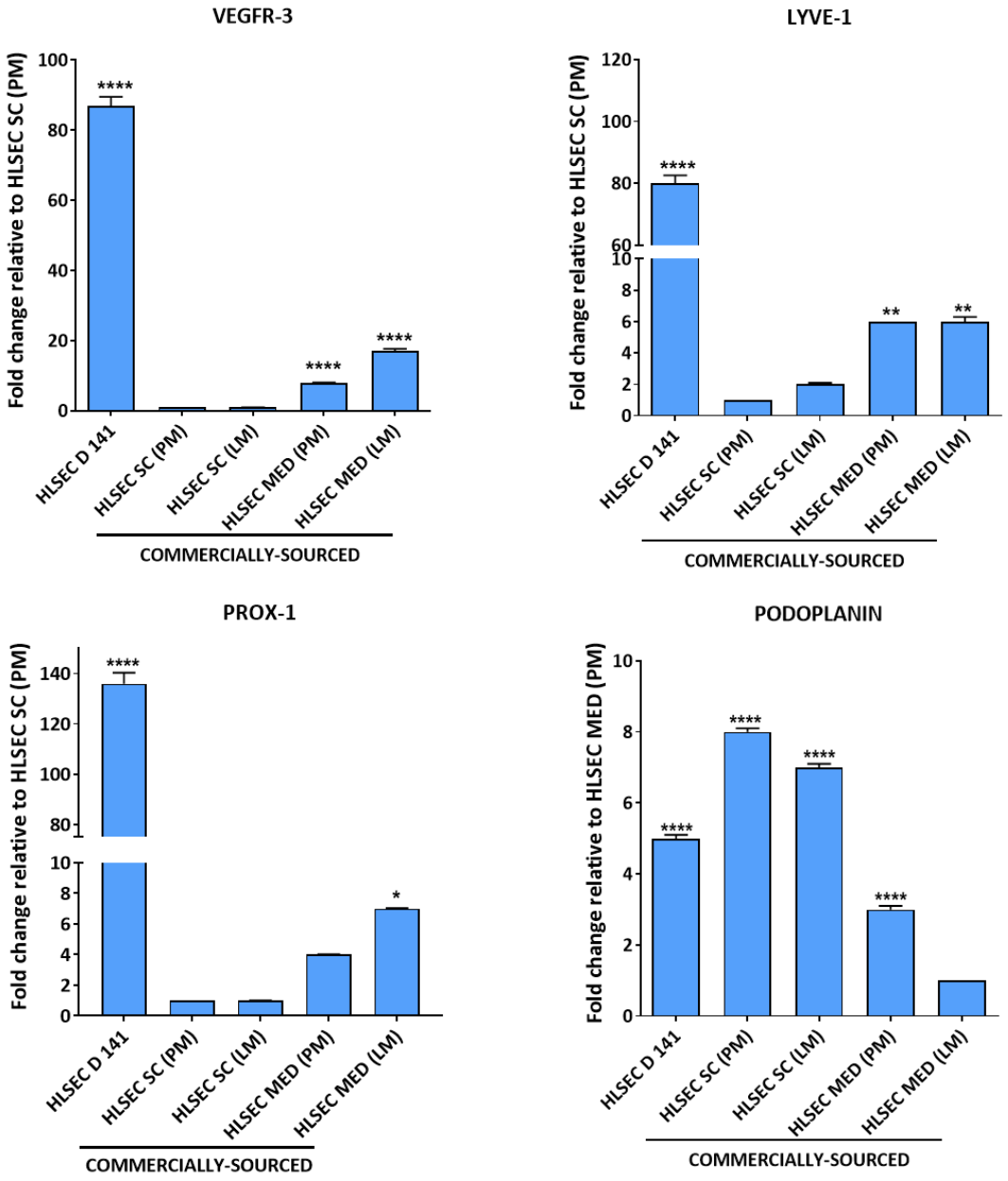

Figure 3.16: Expression of lymphatic markers on commercial HLSEC

Relative expression of coagulation VEGFR-3, LYVE-1, PROX-1 and podoplanin in in-house isolated and commercial HLSEC. Cells were cultured for 48 h or until 90% confluent. After removal of culture medium, cells were washed with ice-cold PBS twice and mRNA was extracted, cDNA synthesised and analysed for the expression of the respective genes by qPCR as described. Freshly isolated PHH was spun down at 80 g and lysed with buffer RLT to extract mRNA and processed as above. Results are expressed as mean ± SD (n=3, three independent experiments). HLSEC D141: in-house isolated human liver sinusoidal endothelial cell, LSEC SC (PM): Commercially-sourced liver sinusoidal endothelial cell from Sciencell cultured on their proprietary medium, HLSEC SC (LM): Commercially-sourced liver sinusoidal endothelial cells from Sciencell cultured on LSEC medium. Commercially-sourced liver sinusoidal endothelial cell from Medicyte cultured on their proprietary medium, HLSEC SC (LM): Commercially-sourced liver sinusoidal endothelial cell from Medicyte cultured on HLSEC medium.

3.2.3.3 Commercial HLSEC express fibroblast and pericyte markers

Since the commercially-sourced cells did not have reliable levels of expression of markers of vascular or lymphatic endothelium, they were further probed for the expression of markers of some other hepatic components namely, *collagen -1* (marker of fibroblasts) and *PDGFR* (marker of pericytes). Figure 3.18 below shows that the commercial HLSEC had a significantly higher expression of collagen-1 when compared with HLSEC D141. It is noteworthy that while there was an almost 2000 fold expression in PDGFR in HLSEC SC, the level of expression differed in the different medium conditions of the HLSEC MED groups. The HLSEC MED cultured in their proprietary medium had a 500 fold expression of PDGFR relative to HLSEC D141, while those cultured in the in-house HLSEC medium had only about 2-fold higher level of PDGR.

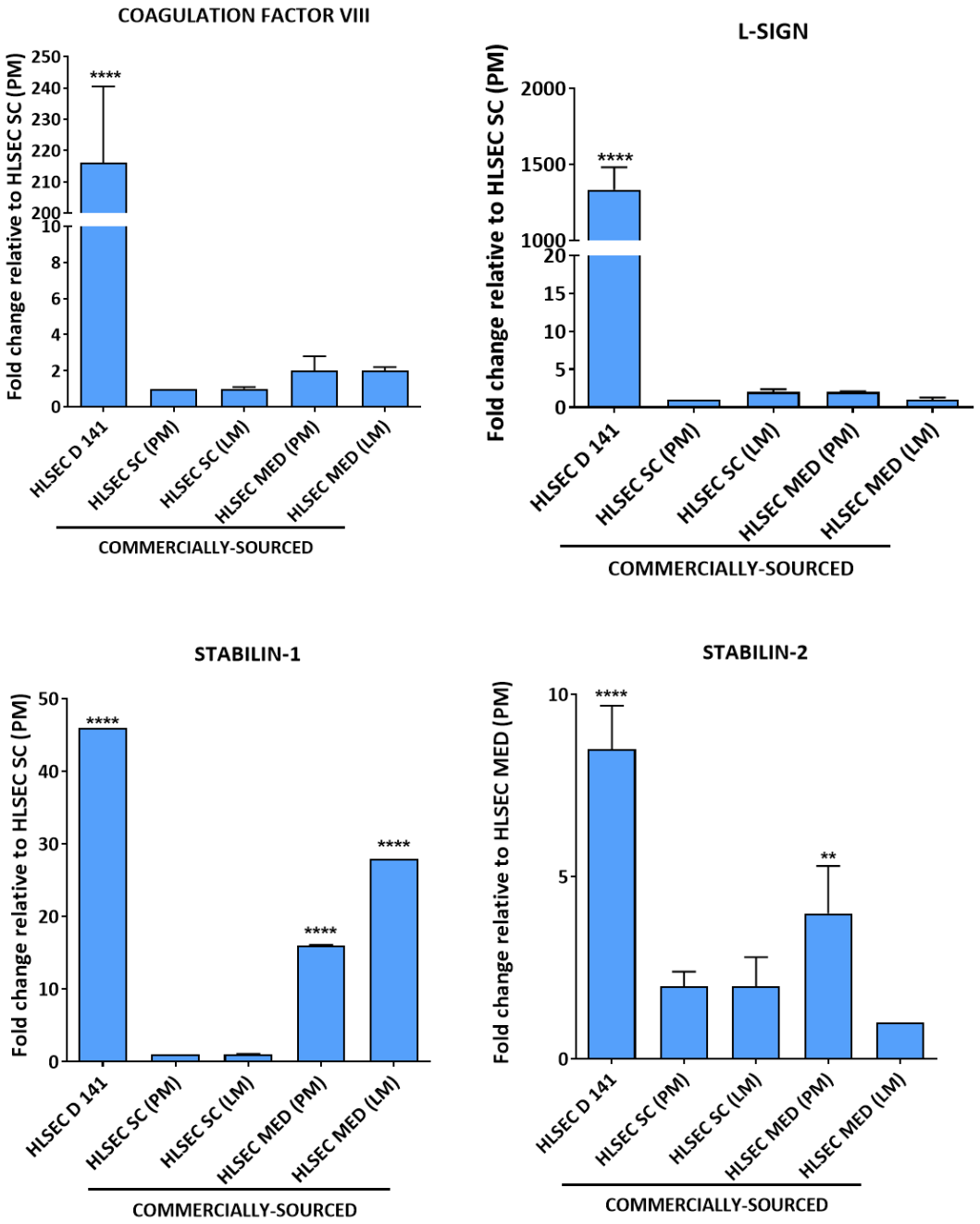

Figure 3.17: Expression of LSEC specific markers

Relative expression of coagulation factor VIII, stabilins-1 and -2 and L-SIGN in in-house isolated and commercial HLSEC. Cells were cultured for 48 h or until 90% confluent. After removal of culture medium, cells were washed with ice-cold PBS twice and mRNA was extracted, cDNA synthesised and analysed for the expression of the respective genes by qPCR as described. Results are expressed as mean ± SD, (n=3, three independent experiments). HLSEC D141: in-house isolated human liver sinusoidal endothelial cell, LSEC SC (PM): Commercially-sourced liver sinusoidal endothelial cell from Sciencell cultured on their proprietary medium, HLSEC SC (LM): Commercially-sourced liver sinusoidal endothelial cells from Sciencell cultured on LSEC medium. Commercially-sourced liver sinusoidal endothelial cell from Medicyte cultured on their proprietary medium, HLSEC SC (LM): Commercially-sourced liver sinusoidal endothelial cell from Medicyte cultured on HLSEC medium. HHF: human hepatic fibroblast.

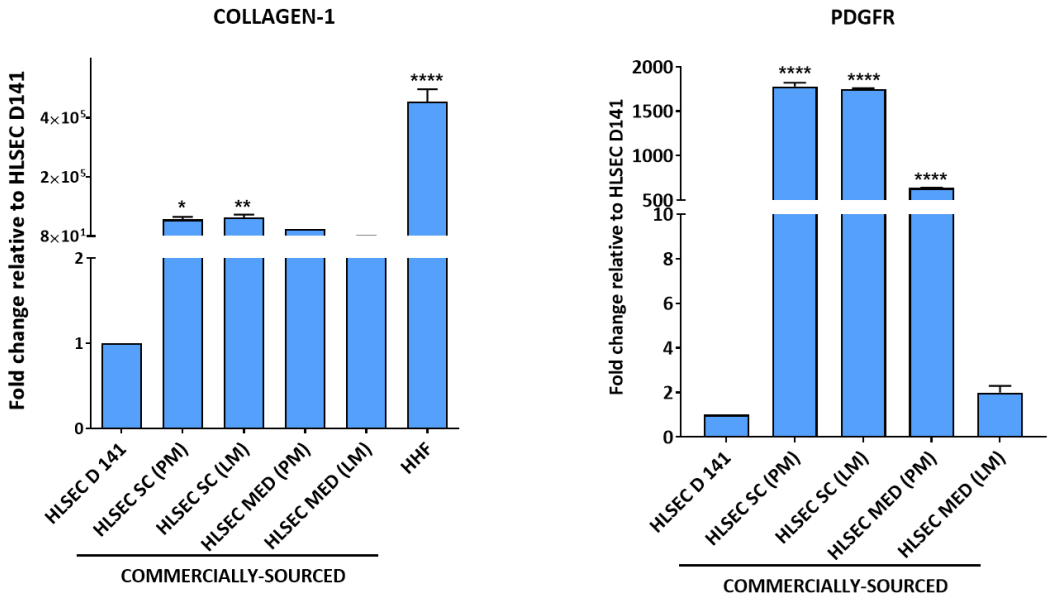

Figure 3.18: Commercial HLSEC express fibroblast markers

Relative expression of collagen-1 and PDGFR in in-house isolated and commercial HLSEC. Cells were cultured for 48 h or until 90% confluent. After removal of culture medium, cells were washed with ice-cold PBS twice and mRNA was extracted, cDNA synthesised and analysed for the expression of collagen or PDGFR by qPCR as described. Freshly isolated PHH was spun down at 80 g and lysed with buffer RLT to extract mRNA and processed as above. Results are expressed as mean ± SD, (n=3, three independent experiments). HLSEC D141: in-house isolated human liver sinusoidal endothelial cell, LSEC SC (PM): Commercially-sourced liver sinusoidal endothelial cell from Sciencell cultured on their proprietary medium, HLSEC SC (LM): Commercially-sourced liver sinusoidal endothelial cells from Sciencell cultured on LSEC medium. Commercially-sourced liver sinusoidal endothelial cell from Medicyte cultured on their proprietary medium, HLSEC SC (LM): Commercially-sourced liver sinusoidal endothelial cell from Medicyte cultured on HLSEC medium. HHF: human hepatic fibroblast. PDGFR: platelet-derived growth factor receptor.

3.3 DISCUSSION

There are a number of methods for the isolation of liver sinusoidal endothelial cells. These include immunomagnetic separation (Lalor et al., 2002) and density-gradient centrifugation (Braet *et al.*, 1994, Stolz, 2011a). There have been conflicting ideas as to the usefulness of immunomagnetic separation using CD-31 conjugated magnetic beads. Studies have shown that since CD-31 is upregulated in capillarised LSEC, the use of CD-31 in their isolation would result in a population enriched in capillarised LSEC (DeLeve et al., 2004, DeLeve *et al.*, 2006). These studies have suggested that HLSEC thus isolated would lack the hallmark of HLSEC—fenestrations. While this might be valid in preparations involving murine livers, the data obtained in this study shows that human HLSEC isolated using CD-31 immuno-sorting are fenestrated (figure 3.2). Further, the porosity of these fenestrations were improved in the presence of VEGF-A (figure 3.10). This is in agreement with reports showing similar effects (Xie *et al.*, 2012). The regulation of fenestral porosity and diameter has been reviewed in Chapter 1 of this thesis.

3.3.1 Validation of liver sinusoidal endothelial cells isolated from human liver

The definitive identification of liver sinusoidal cells is the presence of fenestrations which have been shown by electron microscopy. Aside structural features, it is important to show the expression of genes and proteins that are crucial to endothelial cell physiology. Consequently, as seen in figure 3.3, HLSEC that were

isolated expressed VEGFR-1, VEGFR-2 and CD-31. The level of expression is comparable with that in HDMEC and HDLEC. As shown in Chapter One, VEGFR-1 and VEGFR-2 are important for the physiology of endothelial cells (Zhuang & Ferrara, 2015). The expression of these, especially VEGFR-2 both at the mRNA and protein levels shows that the cells isolated were valid endothelial cells. In addition to these, the expression of VEGFR-3 in HLSEC, which is known as a marker of the lymphatic endothelium has been previously reported (Lalor et al., 2006, Ding et al., 2010a, Sorensen et al., 2015). This is further confirmed by the expression of the lymphatic marker, lymphatic vessel endothelial hyaluronan receptor 1 (LYVE-1). LYVE1 is involved in the endocytosis of hyaluronan in the course of its metabolism (Jackson, 2003). While LYVE-1 is expressed in lymphatic endothelial cells, its mere presence on an endothelial cell has been shown not to be a definitive marker of the lymphatic endothelium as other markers are required (Gordon *et al.*, 2008). Accordingly, PROX-1 and podoplanin, which are definitive lymphatic marker have been demonstrated (Salven et al., 2003). Figure 3.4 also shows that HLSEC does not express podoplanin and expresses only a very low level of PROX-1 compared to HDLEC. PROX-1 is a transcription factor involved in the embryonic formation of lymphatic endothelium and in the specification of the fate of the lymphatic endothelial cell (Wigle *et al.*, 2002, Hong *et al.*, 2002). Another lymphatic marker, VEGFR-3, was expressed in HLSEC as earlier reported (Ding et al., 2010a). VEGFR-3 is required for lymphangiogenesis (Zhang et al., 2010). This shows the uniqueness of LSEC as a 'hybrid' endothelial cell population – a vascular endothelial cells with features of lymphatic endothelial cells. It would be informative to understand the physiologic basis for this. Perhaps the most convincing indication of the identity of

the isolated cells as liver sinusoidal endothelial cells is the expression of coagulation factor VIII, stabilin-1 and L-SIGN (figure 3.6). Coagulation factor VIII (antihaemophilic factor) has been shown to be synthesised in the murine LSEC (Do et al., 1999) and an engraftment of human LSEC into murine model of haemophilia restored expression of factor VIII (Fomin *et al.*, 2013). L-SIGN is a transmembrane receptor involved in cell adhesion and in pathogen recognition (Khoo *et al.*, 2008). It is involved in capturing HIV-1, hepatitis C and Ebola viruses (Pohlmann *et al.*, 2001, Alvarez *et al.*, 2002, Cormier et al., 2004). All three – coagulation factor VIII, stabilin-1 and L-SIGN – have been used as LSEC markers (Lalor et al., 2006, Nonaka et al., 2007).

3.3.2 Human liver sinusoidal endothelial cells respond to growth factors which modulate endothelial cell physiology

In addition to expressing specific endothelial cell markers, it is important for endothelial cells to respond to growth factors involved in their physiology. As earlier reviewed in Chapter One of this thesis, endothelial cells respond to their requisite growth factors to effect their main functions – cell proliferation, migration, survival and permeability—in order to maintain the vascular structure or to produce new vessels when needed (Koch & Claesson-Welsh, 2012). Accordingly, when the isolated HLSEC were stimulated with a range of growth factors, they responded with a phosphorylation of the VEGFR-2 which is upstream of the pathway (s) involved in the physiology of endothelial cells (figure 3.11). Activation

of the VEGFR-2 results in the phosphorylation of extracellular signal-regulated protein kinases 1 and 2 (ERK 1/2) and AKT which are involved in cell survival, proliferation and migration (Mebratu & Tesfaigzi, 2009). As shown in figure 3.11 ERK 1/2 and AKT were phosphorylated by growth factors which induced the phosphorylation of VEGFR-2, further confirming phosphorylation of AKT and ERK 1/2 are downstream of VEGFR-2 (Holmes et al., 2007). Interestingly, other growth factors – EGF, FGF and HGF—also induced a phosphorylation of ERK 1/2 and AKT. Correspondingly, there was a significant increase in proliferation in cells incubated with VEGF-A, VEGF-E, VEGF-C, EGF, FGF and HGF (figure 3.12). This is indicative of the involvement of these growth factors in the proliferation of endothelial cells. Since VEGFR-2 and VEGFR-3 are intimately involved in angiogenesis, their ligands, VEGF-A and VEGF-C were used to study cell migration as shown in figure 3.13. After stimulating endothelial cells with VEGF-A or VEGF-C, there was a significant closure of the wound created 16 h beforehand. As earlier described in Chapter One, endothelial cells migrate in response to injury to the vascular endothelium and during angiogenesis (Michaelis, 2014a). Closely linked to endothelial cell migration is their ability to self-organise in the presence of extra cellular matrix (ECM)-secreting fibroblasts to form a tubular network. This was recapitulated in an *in vitro* angiogenesis assay earlier described (Hetheridge et al., 2011, Richards & Mellor, 2016). The assay comprises a co-culture of normal human dermal fibroblasts (NHDF) grown to confluence with endothelial cells. The fibroblast secrete growth factors and ECM components including collagen I and fibronectin (Sorrell *et al.*, 2007). This enables the endothelial cells to proliferate and self-organise in response to exogenously-supplemented VEGF-A or those secreted by the

fibroblasts. The pattern of endothelial cell could be in the form of a cluster, or sprouts along the cords of the fibroblasts resulting in elongations, thickening and formation of anastomosing structures (Hetheridge et al., 2011, Mavria *et al.*, 2006). To induce further branching, endothelial cells might secrete ECM-degrading enzymes (particularly matrix metalloproteinases; MMP-2 or MMP-9) which enable them to invade the ECM (Taraboletti *et al.*, 2002). The tubular structures formed by endothelial cells can then be detected by the use of endothelial-specific markers such as CD-31 used in this study, where significant induction of tube formation has been demonstrated.

3.3.3 Transcriptomic analysis shows a distinctive difference between HLSEC and other endothelial cell populations

The data from the transcriptomic analysis of the three endothelial cell types showed distinction between liver sinusoidal endothelial cells and dermal vascular and lymphatic endothelial cell population studied. As already reported in literature and reviewed in the introductory chapter of this thesis, LSEC possess scavenger functions, mediated by a range of scavenger and endocytic receptors. Prominent among these are the mannose receptor C1 and the C-lectin domain receptor 1B. In addition, some other genes earlier reported to be highly expressed in LSEC include the coagulation factor VIII which has been shown to be synthesised primarily in the LSEC (Everett *et al.*, 2014, Shahani *et al.*, 2014).This harmonises with real-time PCR data (figure 3.6). Further, the lymphatic marker *LYVE-1* was upregulated in HLSEC in comparison with HDMEC and even HDLEC

which is a dedicated lymphatic endothelial cell population. However, genes that were downregulated in the HLSEC in comparison with HDLEC included *PROX-1* and *podoplanin* which are key lymphatic markers. There were also genes directly linked with LSEC physiology, further distinguishing them as a unique population. One of these is the gene coding for plasmalemma vesicle associated protein (PLVAP). PLVAP is an endothelial-cell specific protein that forms part of the fenestral diaphragm, stomatal diaphragms of caveolae and diaphragms of transendothelial channels (Herrnberger *et al.*, 2012). This integral membrane glycoprotein is required for the formation of LSEC fenestrae as indicated in a study by Herrnberger *et al.* (2014) where Plvap $^{-/-}$ mice had a significantly low number of fenestrations. Further, their data correlated this low level of LSEC fenestration with hyperlipoproteinaemia accompanied by lipid and chylomicron deposition in renal and hepatic capillaries, as well as 'cloudy' plasma. Other important genes upregulated in the HLSEC samples and which are linked to the regulation of fenestration are nitric oxide synthase trafficking (NOSTRIN) and serotonin (5-hydroxytryptamine [5-HT]) receptor 2B. The link between 5-HT and regulation of fenestral diameter has been reviewed in chapter 1 of this thesis. Among the differentially upregulated genes in the HLSEC samples are ectonucleotide pyrophosphatase/phosphodiesterase 2 (ENPP2), tissue factor pathway inhibitor 2 (TFPI2), placenta specific 8 (PLAC8), protocadherin 17 (PCH17) which are either tumour suppressor genes or oncogenes (Hu *et al.*, 2013, Mourtada-Maarabouni *et al.*, 2013, Zhu *et al.*, 2013). This might be connected to the origin of the liver from which the HLSEC were isolated. The HLSEC were generally isolated from resections from liver of patients who have had some form

of hepatocellular carcinomas. Although the samples used for isolation were those without tumours, the fact that tumour-associated genes were detected in the HLSEC might be a reflection of the overall tissue they were isolated from. Of the downregulated genes in the HLSEC groups, claudin 1 is distinct. Claudin 1 belongs to a family of tight junctional proteins involved in the regulation of permeability of epithelial cells to ions and other small molecules. They are particularly important for the barrier function of the skin (Kirschner *et al.*, 2013). This is an important distinguishing factor between the structure of the hepatic sinusoidal endothelium and the dermal microvascular endothelium. While a tight junction is required for a normal skin endothelium, in order to create access for blood-borne drugs, lipids and other substances to the hepatocytes, the liver sinusoid is relatively 'porous', partly by the presence of fenestrations on their membranes, and low expression of tight junction proteins.

3.3.4 Commercially-sourced HLSEC need validation before use in experiments

Results from this chapter also indicate that a thorough validation process is required whenever cells are procured from external sources. This was demonstrated by the comparison performed between HLSEC isolated in-house and those obtained from commercial sources. In order to remove any confounding effect of culture media, both commercial HSLEC samples were cultured in their proprietary media or in the medium generally used for culturing

HLSEC in-house. The fact that one of the commercial HLSEC did not express any of the vascular or lymphatic endothelial cell markers, but rather markers of fibroblasts and pericytes shows that they might have contained a high level of contaminants. This observation may betray an inadequate quality control process.

A major limitation of this analysis is the fact that the liver from which HLSEC was isolated was from cancer patients. The experiments would have been more robust if liver samples from patient with no underlying liver pathology had been used. This could be sourced from implant rejection.

In conclusion, liver sinusoidal endothelial cells are a population of endothelial cells with features of lymphatic and vascular endothelia. They also have unique features that distinguish them from other endothelial cell populations. They can respond to a variety of growth factors to elicit endothelial-cell specific functions which promote formation of vasculature. A comparative study of in-house isolated HLSEC with commercially-sourced ones shows the need to adequately validate cells that are externally-sourced before use in any experiments. Although commercial HLSEC could save time and effort invested into isolating the cells, the data from this chapter showed in-house isolated HLSEC using CD-31-based immunomagnetic separation to be better suited for subsequent studies in this thesis. Hence, the next chapter will examine the response of human liver sinusoidal endothelial cells to a range of hepatotoxic drugs.

CHAPTER FOUR

EFFECTS OF HEPATOTOXIC DRUGS ON HUMAN LIVER SINUSOIDAL ENDOTHELIAL CELLS *IN VITRO*

4.1 INTRODUCTION

Results from the previous chapter showed the phenotypic and functional validation of HLSEC isolated from donor human liver. It was shown that VEGF-A plays a very important role in the physiology of HLSEC, in agreement with literature, as is true for endothelial cells from other vascular beds (Holmes et al., 2007, Guangqi *et al.*, 2012). This includes its ability to form tubular networks reminiscent of *in vivo* vasculature (Zeng *et al.*, 2015), cell proliferation in response to growth factors, activation of intracellular signalling that ultimately initiates cell survival and proliferation and cell migration. Activation of VEGFR-2 on HLSEC is also an important aspect of liver regeneration following partial hepatectomy and/ or exposure to hepatotoxic drugs (Ding et al., 2010a, Ding et al., 2014).

For this chapter, it was hypothesised that known small-molecule receptor tyrosine kinase inhibitors (TKIs) that cause liver damage can adversely affect the physiology of HLSEC. With focus on regorafenib, a TKI which has been extensively reported to cause liver injury in the clinic (Sacré *et al.*, 2016, Takahashi *et al.*, 2016b, Iacovelli *et al.*, 2014), it was proposed that TKIs could inhibit the activation of the VEGFR-2 receptor on the HLSEC thereby blocking the pathways that lead to cell survival and proliferation, and ultimately angiogenesis. Building on the fact that regorafenib could adversely affect the physiology of the HLSEC, it was proposed that this could also lead to toxicity to the HLSEC by causing cell death by apoptosis, abrogation of the cytoskeletal structure of the HLSEC and inhibition of the signalling pathway that promotes liver regeneration. In addition to TKIs, a comparative toxicity analysis was

performed to determine the sensitivity of HLSEC (vis-à-vis other hepatic and non-liver-derived endothelial cells) to a wide range of known liver toxins.

Therefore the overall aim of data described in this chapter was to show the effect of known hepatotoxins on HLSEC and how this possibly links with the known anti-angiogenic effect of small-molecule TKIs.

4.2 RESULTS

4.2.1 Comparative toxicity of liver toxins on HLSEC as against other hepatic cells and non-hepatic endothelial cells

Since HLSEC, which is a hepatic cell population, has been shown to possess features of lymphatic and vascular endothelial cells, it has become necessary to analyse its sensitivity to a broad range of hepatotoxic drugs in comparison with other vascular endothelial and lymphatic cell populations. Also, it would also be informative to compare the sensitivity of HLSEC to these drugs and in other hepatic cells.

4.2.1.1 HLSEC is preferentially more sensitive to a series of hepatotoxic tyrosine kinase inhibitors

In order to compare the sensitivities of HLSEC with other hepatic and endothelial cells to a range of small molecule TKI, primary human hepatocytes (PHH), human hepatic fibroblasts (HHF), human liver sinusoidal endothelial cells (HLSEC), human

dermal microvascular endothelial cells (HDMEC) and human dermal lymphatic endothelial cells (HDLEC) were incubated with regorafenib, pazopanib, axinitib and sunitinib for 72 h. Figure 4.1 shows the dose-response plot of regorafenib, pazopanib, axinitib and sunitinib on primary human hepatocyte (PHH), human hepatic fibroblasts (HHF), liver sinusoidal endothelial cells (HLSEC), human dermal microvascular endothelial cells (HDMEC) and human dermal lymphatic endothelial cells (HDLEC). An overall trend observed is that the IC_{50} of HLSEC is lowest for all TKIs in comparison with the other cells, except for sunitinib where HHF had the lowest IC_{50} value.

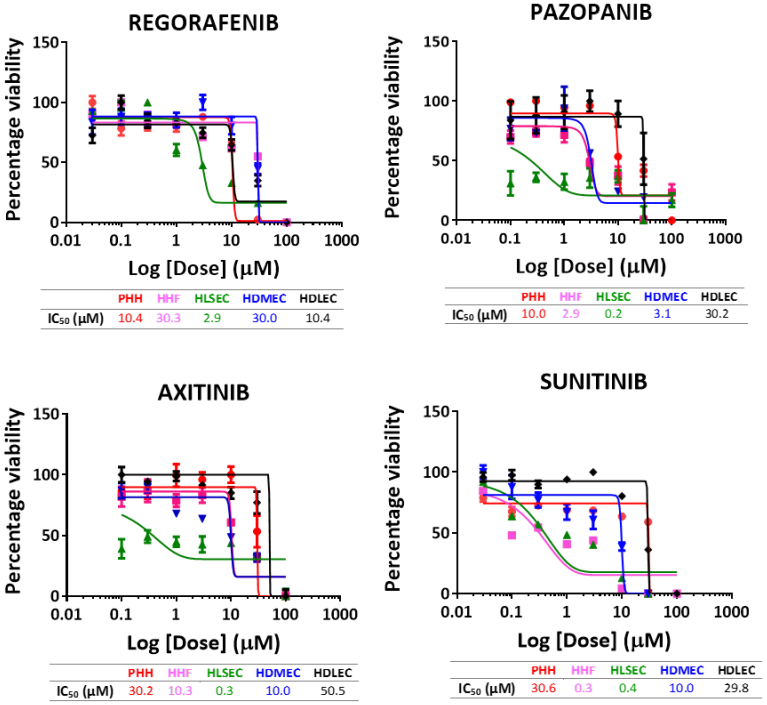

Figure 4.1: HLSEC is preferentially more sensitive to a series of tyrosine kinase inhibitors:

Dose-response curve showing effect of tyrosine-kinase inhibitors on hepatic cells and endothelial cells from different vascular beds. Cells were plated at 15.6 X 10^3 cells/ cm^2 (3.13 X 15^5 for PHH) in a collagen-coated 96-well plate for 48 h after which they were dosed with graded concentrations of tyrosine-kinase inhibitors originally constituted in DMSO. Final dosing concentrations or blank DMSO was made in medium to a uniform concentration of 0.1 % DMSO. Cells were dosed for 72 h after which they were washed with ice-cold PBS twice and lysed with Cell Titer Glo reagent and assayed for ATP content as described in the method section. IC_{50} values were determined and dose-response curve generated using GraphPad Prism 5. PHH; primary human hepatocytes, HHF: human hepatic fibroblasts, HLSEC: liver sinusoidal endothelial cells, HDMEC: human dermal microvascular endothelial cells, HDLEC: human dermal lymphatic endothelial cells.

The median inhibitory concentration (IC_{50}) of HLSEC was lowest for pazopanib. On the other hand, HDLEC was least sensitive to this range of TKIs; it has the highest IC_{50} values. With the exception of regorafenib and pazopanib, of the liver-derived cells PHH was most resistant to the toxic effect of the TKIs.

4.2.1.2 Effect of hepatotoxic drugs on hepatic and endothelial cells

Aside drugs that are known to directly affect the physiology of endothelial cells, other drugs that cause liver toxicity by other known mechanisms might also be toxic to HLSEC. Figure 4.2 shows the relative sensitivity of PHH, HHF, HLSEC, HDMEC and HDLEC to paracetamol, aflatoxin, benzbromarone, perhexiline and desipramine. All cells tested were sensitive to paracetamol at the same level, with an IC_{50} of ≈ 3 mM, which suggests that paracetamol toxicity might be non-metabolism related. Median inhibitory concentration of aflatoxin was similar for all endothelial cells, at ≈ 10 µM, while PHH and HHF had a similar IC_{50} at ≈ 2 µM. A similar trend can be observed for benzbromarone, whereby IC_{50} of the endothelial cells was about 5-fold of those in PHH and HHF. The only recognisable pattern that can be observed for perhexiline was in HDMEC and HDLEC where there was a similar IC_{50} of ≈ 30 µM, but HLSEC was most sensitive to (IC_{50}: 3.4 µM). Finally, HLSEC and PHH were equally sensitive to desipramine (IC_{50}: ≈ 6 µM) whereas HHF, HDMEC and HDLEC were some 5-fold less sensitive to the toxic effect of this liver toxin. Therefore this observation implies that there is a likelihood that the toxicities of these drugs are due to different

factors ranging from direct cell lysis as might be the case for paracetamol, to metabolic bioactivation or detoxification.

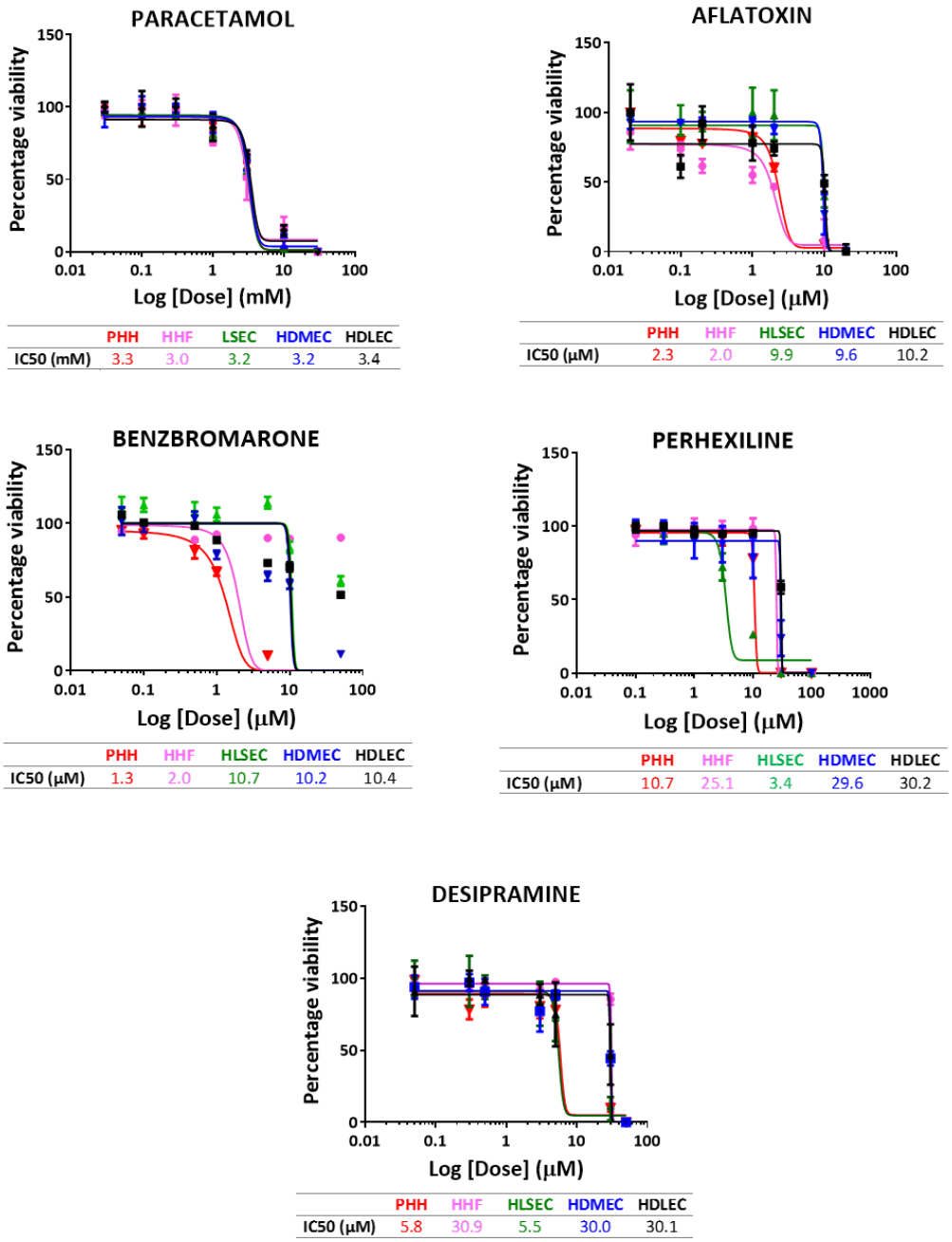

Figure 4.2: Effect of hepatotoxic drugs on hepatic and endothelial cells.

Dose-response curve showing effect of hepatotoxic drugs on hepatic cells and endothelial cells from different vascular beds. Cells were plated at 15.6 X 10^3 cells/ cm^2 (3.13 X 15^5 for PHH) in a collagen-coated 96-well plate for 48 h after which they were dosed with graded concentrations of tyrosine-kinase inhibitors originally constituted in DMSO. Final dosing concentrations or blank DMSO was made in medium to a uniform concentration of 0.1 % DMSO. Cells were dosed for 72 h after which they were washed with ice-cold PBS twice and lysed with Cell Titer Glo reagent and assayed for ATP content as described in the method section. IC50 values were determined and dose-response curve generated using GraphPad Prism 5. PHH; primary human hepatocyte, HHF: human hepatic fibroblasts, HLSEC: liver sinusoidal endothelial cells, HDMEC: human dermal microvascular endothelial cells, HDLEC: human dermal lymphatic endothelial cells.

4.2.2 Effect of small-molecule tyrosine kinase inhibitors on HLSEC physiology

4.2.2.1 Determination of the median inhibitory concentration (IC_{50}) of tyrosine kinase inhibitors

A dose-response curve was extracted from figure 4.1 above in order to determine the working concentration of the TKIs to be used in the subsequent series of experiments involving HLSEC. Figure 4.3 shows regorafenib to cause a 50% cell death at a dose of 2.9 µM while pazopanib, axitinib and sunitinib seem to be more potent at 0.2, 0.3 and 0.7 µM respectively.

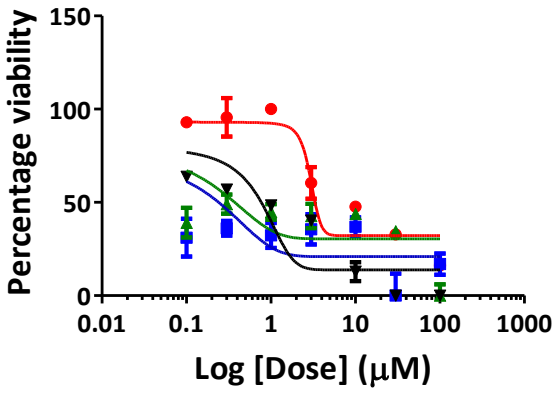

	REGORAFENIB	PAZOPANIB	AXITINIB	SUNITINIB
IC_{50} (µM)	2.9	0.2	0.3	0.7

Figure 4.3: Effect of Selected small molecule tyrosine kinase inhibitors on viability of HLSEC

Dose-response curve showing effect of tyrosine-kinase inhibitors on HLSEC. Cells were plated at 15.6 X 10^3 cells/ cm^2 in a collagen-coated 96-well plate for 48 h after which they were dosed with graded concentrations of tyrosine-kinase inhibitors originally constituted in DMSO. Final dosing concentrations or blank DMSO was made in HLSEC medium to a uniform concentration of 0.1 % DMSO. Cells were dosed for 72 h after which they were washed with ice-cold PBS twice and lysed with Cell Titer Glo reagent and assayed for ATP content as described in methods. IC50 values were estimated and dose-response curve generated using GraphPad Prism 5.

4.2.2.2 A range of selected TKIs inhibits the activation of VEGFR-2 on the HLSEC

In order to validate the ability of the selected TKIs to block the activation of VEGFR-2 and to determine the minimum concentration to use in subsequent experiments, HLSECs were dosed with drugs at a concentration of 0.01, 0.1, 1 and 10 μM for 30 min before being stimulated with VEGF-A for 10 min. Figure 4.4 shows the effect of regorafenib, pazopanib, axitinib and sunitinib on the activation of VEGFR-2 on HLSEC. While regorafenib completely inhibited the activation of VEGFR-2 at 1 μM, pazopanib did not seem to completely block this effect even at the highest concentration of 10 μM. Sunitinib completely blocked this effect at 10 μM, while axitinib was most potent—inhibiting the activation of VEGFR-2 at 10 nM. A similar trend can be seen for activation of the downstream proteins AKT and ERK 1/2, especially in regorafenib axitinib and sunitinib where there was a concentration-dependent inhibition.

REGORAFENIB

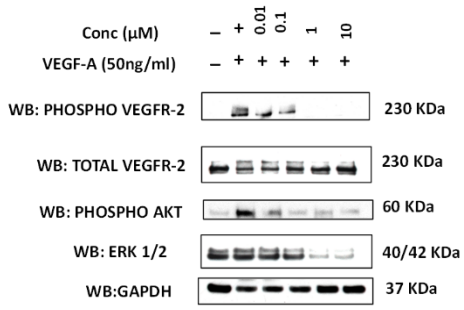

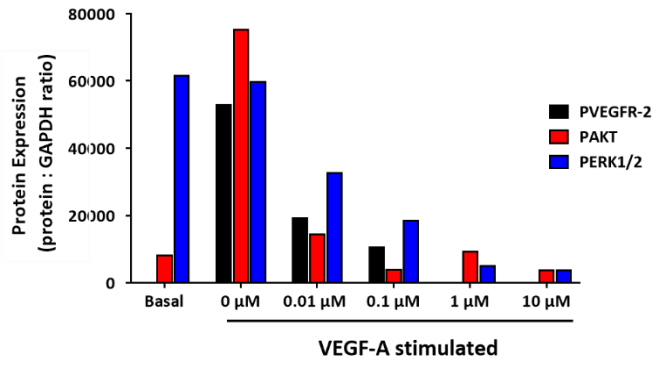

PAZOPANIB

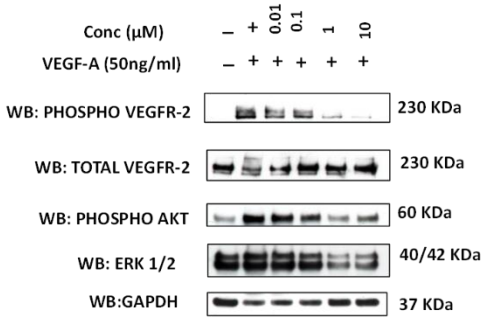

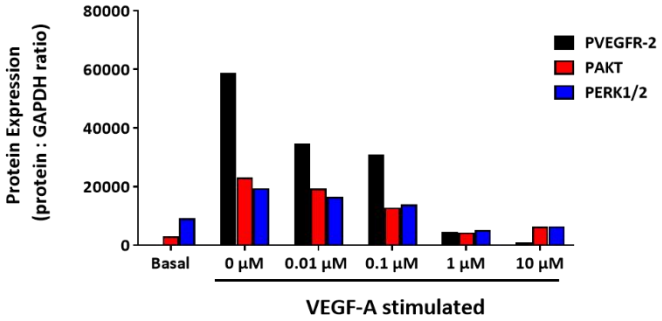

AXITINIB

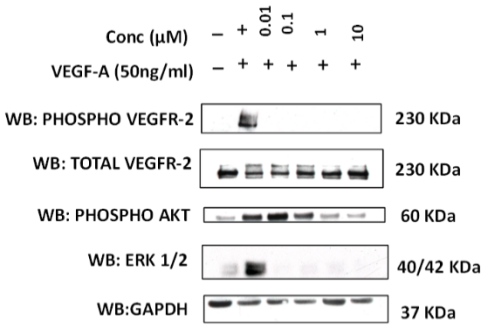

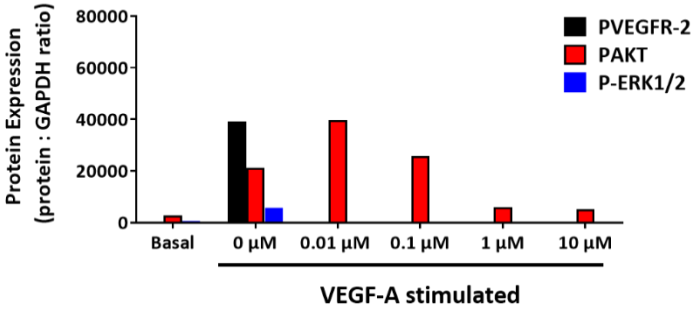

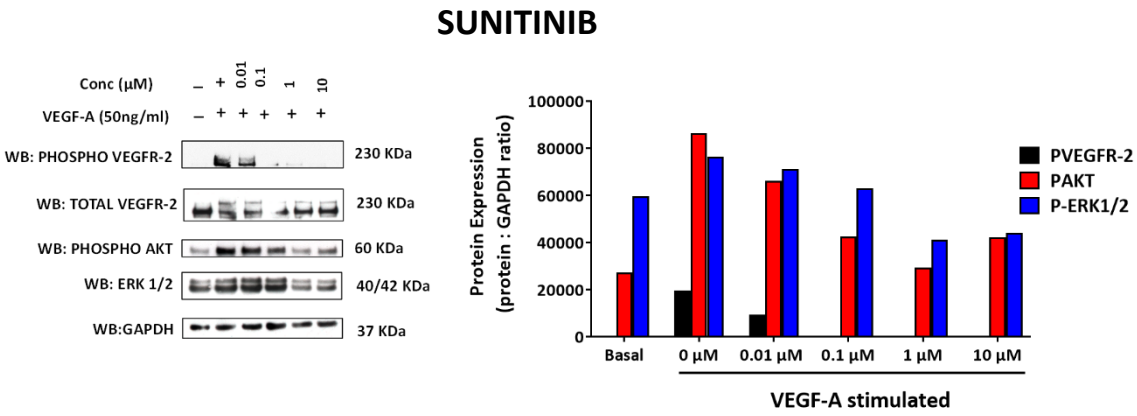

Figure 4.4: A range of selected tyrosine kinase inhibitors inhibits the activation of VEGFR-2 on the HLSEC

HLSEC were cultured until 90% confluent, kept on medium containing 1% FBS for 16 hours and then pre-treated with 0.01, 0.1, 1, 10 µM of TKI or medium containing 1 % FBS for 30 minutes. Then, cells were washed and stimulated with 50 ng/ml of VEGF-A for 10 min. Cells were lysed for total protein contents using modified RIPA buffer, solubilised in LDS sample buffer, denatured at 90 ^{o}C. Protein was separated using SDS PAGE for 45 min., transferred unto nitrocellulose membrane for 2 h. and blocked with 5% BSA. Membranes were then probed with respective antibodies for phosphorylated VEGFR-2, total VEGFR-2, phosphorylated AKT, phosphorylated ERK 1/2 and GAPDH.

4.2.2.3 Effect of regorafenib on VEGF-A and VEGF-C-mediated cell migration in HLSEC

Once it was established that 1 µM concentration of regorafenib was sufficient to cause an inhibition of the intracellular signalling in the HLSEC, experiments were set up to test this dose on cell migration. Figure 4.5 shows the effect of regorafenib on cell migration in HLSEC. VEGF-A and VEGF-C induced a highly significant ($p < 0.01$) increase in cell migration compared with basal control. This trend was reversed by another highly significant ($p < 0.01$) reduction in cell migration in the presence of 1 µM regorafenib.

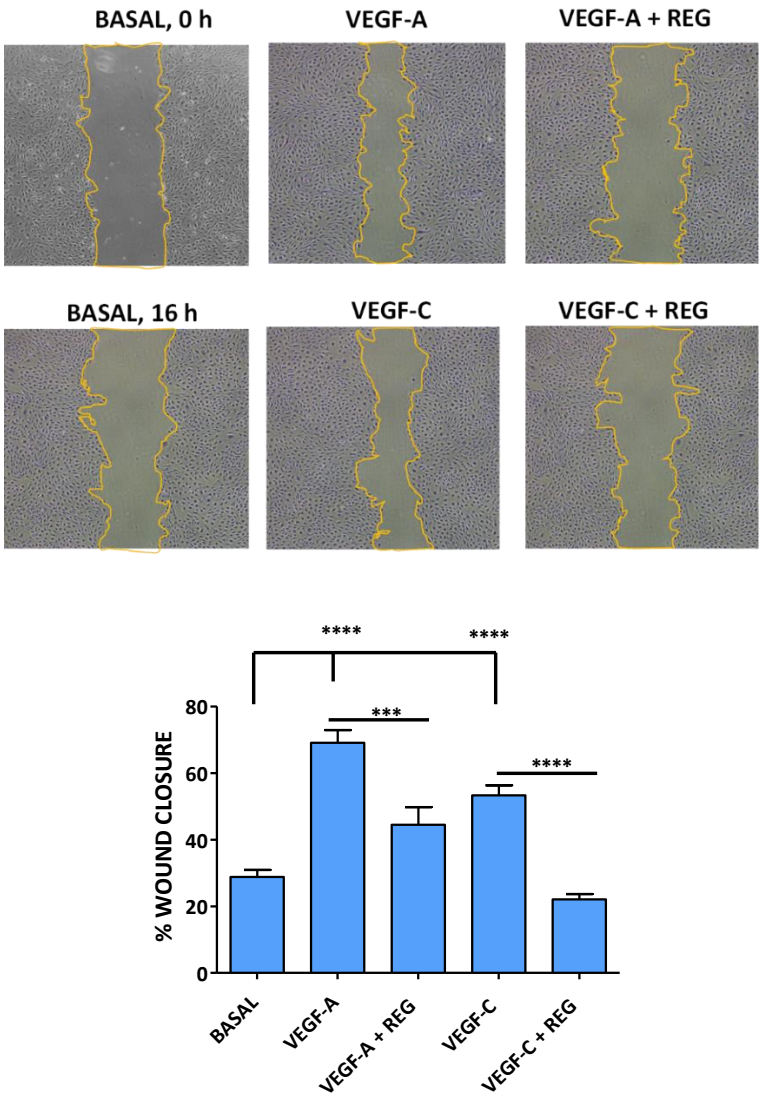

Figure 4.5: Effect of regorafenib on VEGF-A and VEGF-C- mediated cell migration in HLSEC

HLSEC were plated on a collagen-coated 12-well tissue culture plate at 2.63 X 10^4 cells/cm^2 until fully confluent. Cell culture medium was removed; cells washed twice with PBS and then place on medium containing 1% FBS for 16 hours after which straight-line scratches were introduced with a sterile 200 µl pipette tip. Cells were washed with PBS after removal of culture medium to remove floating cells and were pre-treated with regorafenib (1 µM) or 1 % FBS for 30 minutes. Cells were washed with PBS twice at room temperature. Then 50 ng/ml of VEGF-A, VEGF-C or basal medium was added unto the cells. Pictures of the scratch-wounds were taken (mag X4) using an inverted light microscope. Cells were incubated at 37° C for 16 h after which there washed twice with PBS at room temperature, and fixed with 2% PFA for 15 minutes, washed twice again with PBS twice and further processed as earlier described. Images of scratch wounds were taken (t=16 h) and compared with those taken at an earlier time point (t= 0 h). Cell migration was calculated as percentage wound closure (area covered by growth factor stimulated compared with unstimulated at t= 0 h). Wound areas were measured using the scratch wound plugin of the Image-J software. Data are represented as mean ± SD (n=3, three independent experiments). They were compared analysed using one way analysis of variance ANOVA followed by Dunnett's multiple comparison test. Values are significant at **p<0.01, ***p<0.001, ****p<0.0001. VEGF-A: Vascular endothelial growth factor A, VEGF-C: Vascular endothelial growth factor C, REG: regorafenib.

4.2.2.4 Regorafenib inhibits *in vitro* angiogenesis in HLSEC

Angiogenesis consists of the proliferation and coordinated migration of endothelial cells to form lumen-containing vessels. An *in vitro* angiogenesis assay was performed according to the method earlier described by Hetheridge et al. (2011), and Richards and Mellor (2016). In order to see the effect of regorafenib on the ability of HLSEC to form vascular network upon stimulation with VEGF-A and VEGF-C, HLSEC stimulated with VEGF-A or VEGF-C were treated with 1 µM of regorafenib.

Figure 4.6 shows the effect of 1 µM regorafenib on the ability of HLSEC to form vascular network in an *in vitro* angiogenesis assay.

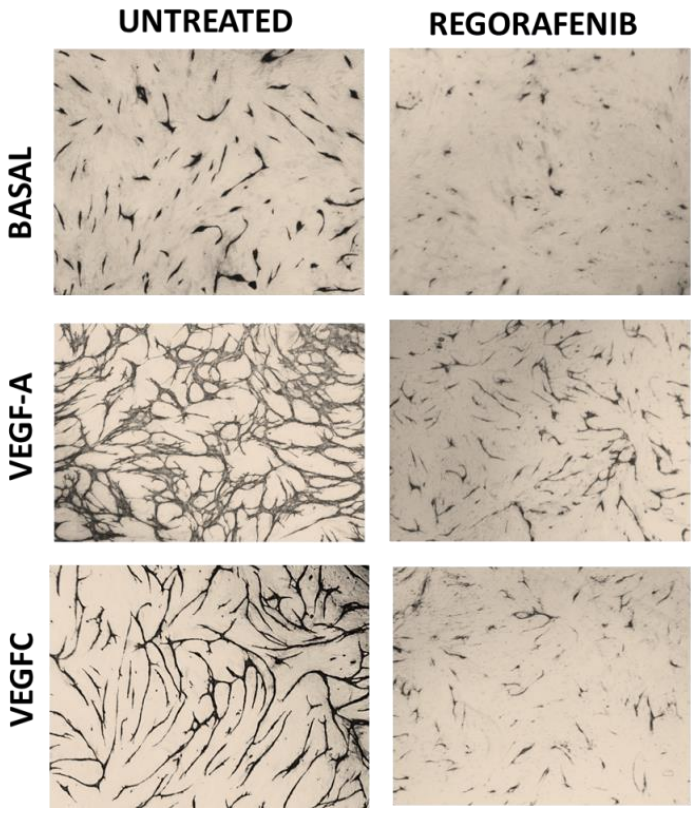

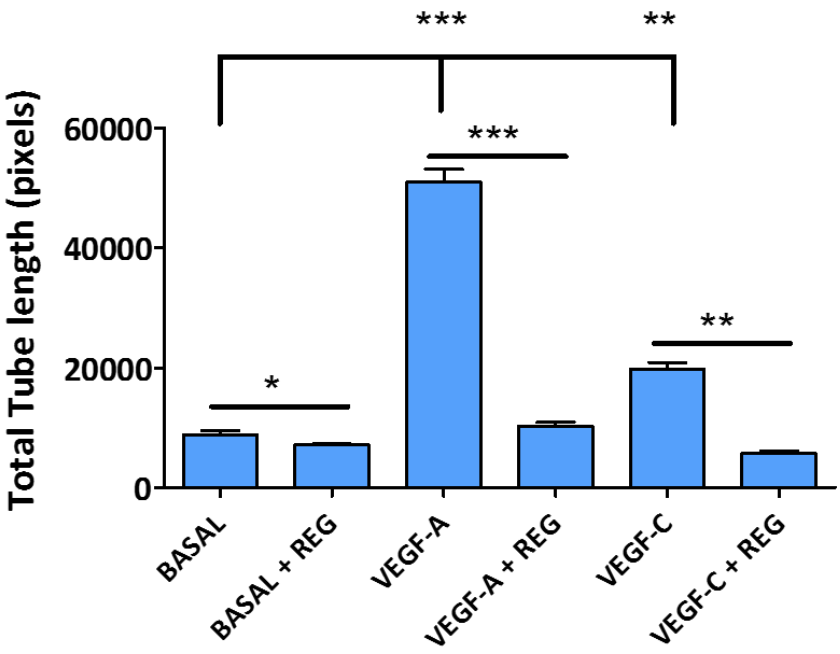

Figure 4.6: Regorafenib inhibits in-vitro angiogenesis in HLSEC

Juvenile NHDF were cultured at 7.9 X 10 cells/ cm^2 for 3 days in a collagen coated glass coverslips in 24-well plates after which HLSEC were plated on top at a density of 21 X 10^3 cells/ cm^2 for 24 h. Then cells were treated with growth medium containing 1% FBS and/ or 50 ng/ml of VEGF-A and VEGF-C for 72 h and then re-exposed to same for another 48 h. Cells were then washed in PBS at room temperature and fixed with 2% PFA for 15 min., washed twice with PBS and then stained for CD-31 following the colorimetric immunocytochemical methods already described in the result section. Angiogenesis was quantified using Angioquant. Bars represent mean ± SD (n=3, three independent experiments). Basal state compared with growth-factor stimulated state and analysed using one way analysis of variance ANOVA followed by Dunnett's multiple comparison test. Data are significant at * $p < 0.05$, ** $p < 0.01$, ***$p < 0.001$

While VEGF-A stimulation resulted in a highly significant ($p < 0.001$) increase in tube length when compared to basal control, VEGF-C exerted a lower level of significant ($p < 0.01$) increase in tube length. On the other hand, regorafenib caused a highly significant ($p < 0.001$) reduction in VEGF-A-induced tube formation and a significant ($p < 0.01$) reduction in VEGF-C-induced tube formation.

4.2.2.5 Regorafenib inhibits upregulation of angiocrine factors involved in liver regeneration

A physiological response to liver injury is liver repair and regeneration. Since activation of VEGFR-2 on HLSEC has been shown to be involved in this process, the effect of regorafenib on the upregulation of the angiocrine factors involved was investigated by quantitative real-time polymerase chain reaction (qRT-PCR). Figure 4.7 shows the effect of regorafenib on the upregulation of *Id1, Wnt-2* and *HGF* following VEGF-A, VEGF-c or SDF-1 stimulation. VEGF-A, VEGF-C, and SDF-1 significantly upregulated Id1 only after 1 h of stimulation. In the presence of 1 μM regorafenib, the level of Id1 mRNA was significantly ($p < 0.01$) reduced in VEGF-A and VEGF-C- stimulated HLSEC whereas, regorafenib had no significant effect on the level of *Id1*. There were significant increases in levels of *Wnt2* after 1h and 6 h of VEGF-A, VEGF-C and SDF-1 stimulation. However, this was significantly reduced in the presence of regorafenib, except for SDF-1 where levels remained unchanged. A similar trend can be observed for *HGF* whereby VEGF-A and VEGF-C significantly upregulated the expression of *HGF* after 1 h and 6 h of stimulation, but SDF-1 only effected a significant ($p < 0.05$) upregulation in *HGF* after 6 h of HLSEC stimulation. As was seen in *Wnt2*, regorafenib significantly reversed the upregulation of the level of *HGF* at 1h and 6 h post VEGF-A and VEGF-C stimulation; but no significant effect was seen for regorafenib in SDF-1-stimulated cells.

Id1

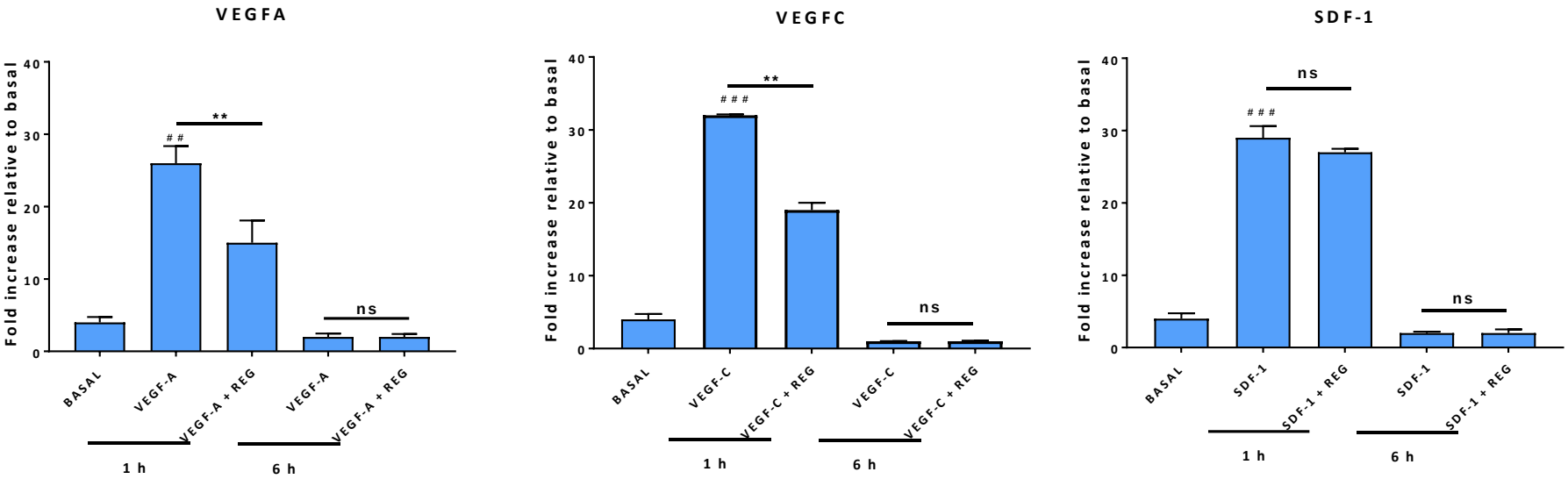
VEGFA
Fold increase relative to basal
40
30
20
10
0
##
**
ns
BASAL
VEGF-A
VEGF-A + REG
VEGF-A
VEGF-A + REG
1 h
6 h
VEGFC
Fold increase relative to basal
###
**
ns
BASAL
VEGF-C
VEGF-C + REG
VEGF-C
VEGF-C + REG
1 h
6 h
SDF-1
Fold increase relative to basal
###
ns
ns
BASAL
SDF-1
SDF-1 + REG
SDF-1
SDF-1 + REG
1 h
6 h

Wnt2

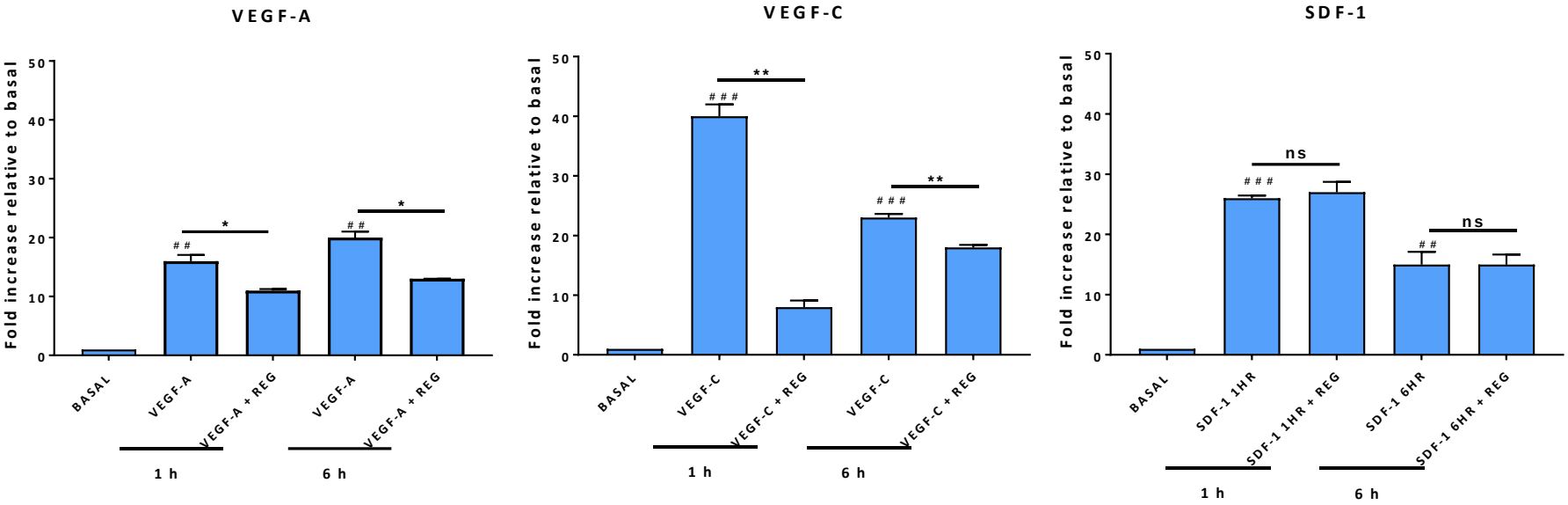
VEGF-A
Fold increase relative to basal
50
40
30
20
10
0
##
*
##
*
BASAL
VEGF-A
VEGF-A + REG
VEGF-A
VEGF-A + REG
1 h
6 h
VEGF-C
Fold increase relative to basal
50
40
30
20
10
0
###
**
###
**
BASAL
VEGF-C
VEGF-C + REG
VEGF-C
VEGF-C + REG
1 h
6 h
SDF-1
Fold increase relative to basal
50
40
30
20
10
0
###
ns
##
ns
BASAL
SDF-1 1HR
SDF-1 1HR + REG
SDF-1 6HR
SDF-1 6HR + REG
1 h
6 h

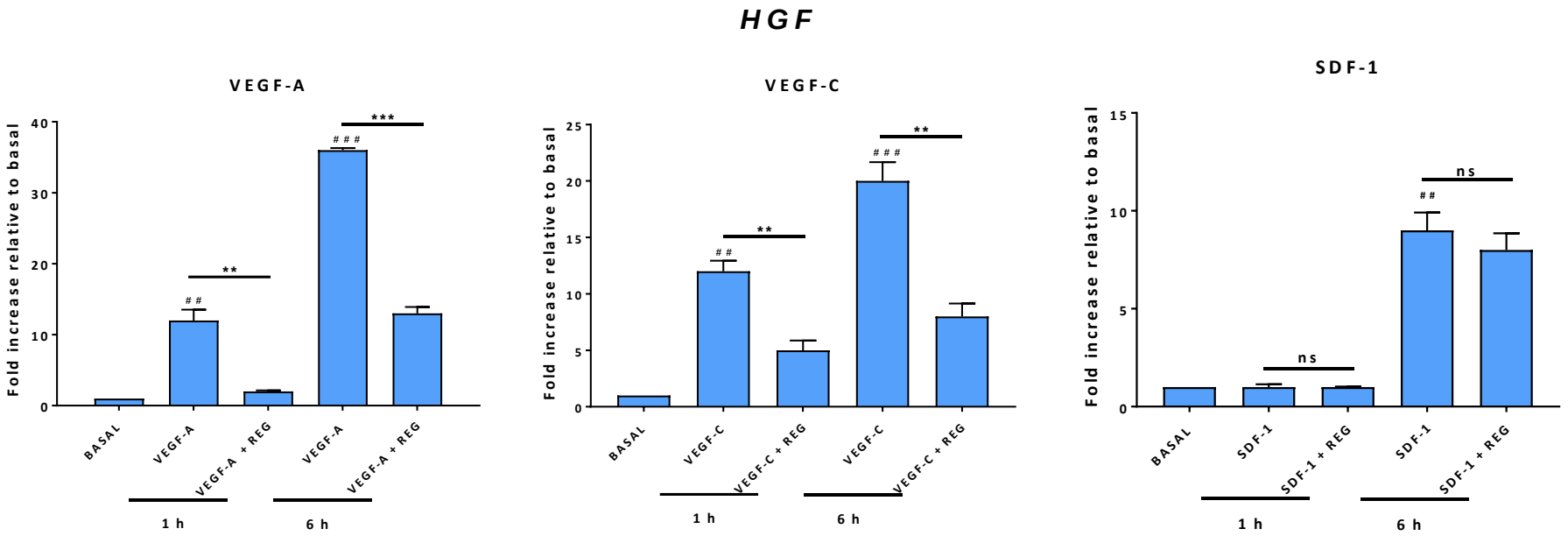

Figure 4.7: Regorafenib inhibits upregulation of angiocrine factors involved in liver regeneration

Relative expression of factors involved in liver regeneration. HLSEC were cultured until 90% confluent, kept on 1% FBS for 16 hours and then pre-treated with 1 µM regorafenib or 1 % FBS for 30 min. Then, cells were washed and stimulated with 50 ng/ml of VEGF-A, or VEGF-C or 10 ng/ml of SDF-1α for 1 or 6 h. mRNA was extracted, cDNA synthesised and analysed for the expression of ID1, HGF and Wnt2 by qPCR. Results are expressed as mean ± SD, (n=3, three independent experiments) and analysed using one way analysis of variance ANOVA followed by Dunnett's multiple comparison test. VEGF-A: vascular endothelial growth factor A, VEGF-C: vascular endothelial growth factor C, SDF-1: stromal cell-derived factor 1, REG: regorafenib (1 µM), Id1: inhibitor of DNA binding 1, wnt2: Wingless-type MMTV integration site family, member 2, HGF: hepatocyte growth factor.

4.2.3 Toxicity of regorafenib on HLSEC

As shown above, regorafenib inhibits the physiological functions of HLSEC; this is a potential for toxicity. Since an activation of the VEGFR-2 activates the pathways that lead to cell proliferation, migration and survival, inhibition of which prevents the ability of HLSEC to self-repair following injuries. Therefore, this section focuses on the ability of regorafenib to cause induction of apoptosis in HLSEC as well as the structural effect it has on the cytoskeleton of HLSEC.

4.2.3.1 Regorafenib but not paracetamol induces apoptosis in HLSEC by activation of caspase 3

Figure 4.8 compares the ability of regorafenib and paracetamol to induce apoptosis in HLSEC in a time- and dose-dependent fashion. Regorafenib did not induce the activation of caspase 3 at lower concentrations of 0.3 and 3 µM; it did this at a higher concentration of 30 µM and at 6 and 24 h time points. However, APAP did not induce apoptosis in HLSEC even at the highest dose of 30 mM and maximum time point where there was complete cell death and with no expression of actin.

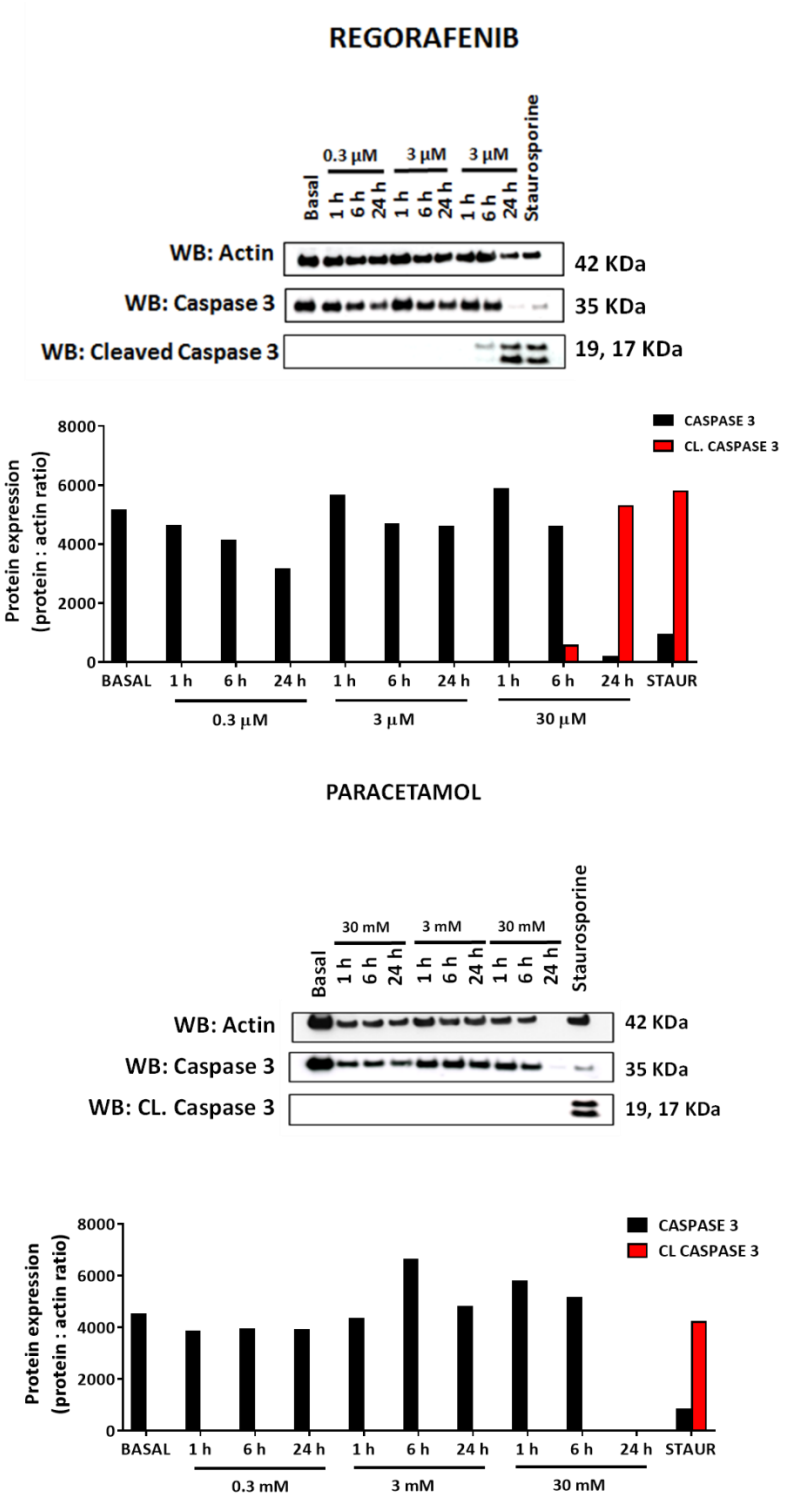

Figure 4.8: Regorafenib induces apoptosis in HLSEC

HLSEC were cultured until 90% confluent, kept on medium containing 1% FBS for 16 hours and then treated with 0.3, 3 or 30 µM regorafenib or 0.3, 3, or 30 mM APAP or 1 µM staurosporine or medium containing 1% FBS for 1, 6 or 24 h. Cells were lysed for total protein contents using modified RIPA buffer, solubilised in LDS sample buffer, denatured at 90 ^{o}C. Protein was separated using SDS PAGE for 45 min., transferred unto a nitrocellulose membrane for 2 h. and blocked with 5% BSA. Membranes were then probed with antibodies for caspase 3 and actin.

4.2.3.2 Regorafenib and paracetamol both induce apoptosis in primary human hepatocytes

Since Regorafenib induced apoptosis in HLSEC, it was important to investigate whether the same could be observed in freshly-isolated primary human hepatocytes. Figure 4.9 shows the effect of regorafenib and APAP on primary human hepatocytes. There is a hint of induction of cleavage of caspase 3 following every dose of regorafenib. Also, paracetamol induced caspase 3 cleavage at 24 h time point for 0.3 and 3mM dose levels, and because there was complete cell death at 30 mM, protein level in lysate was at an undetectable level.

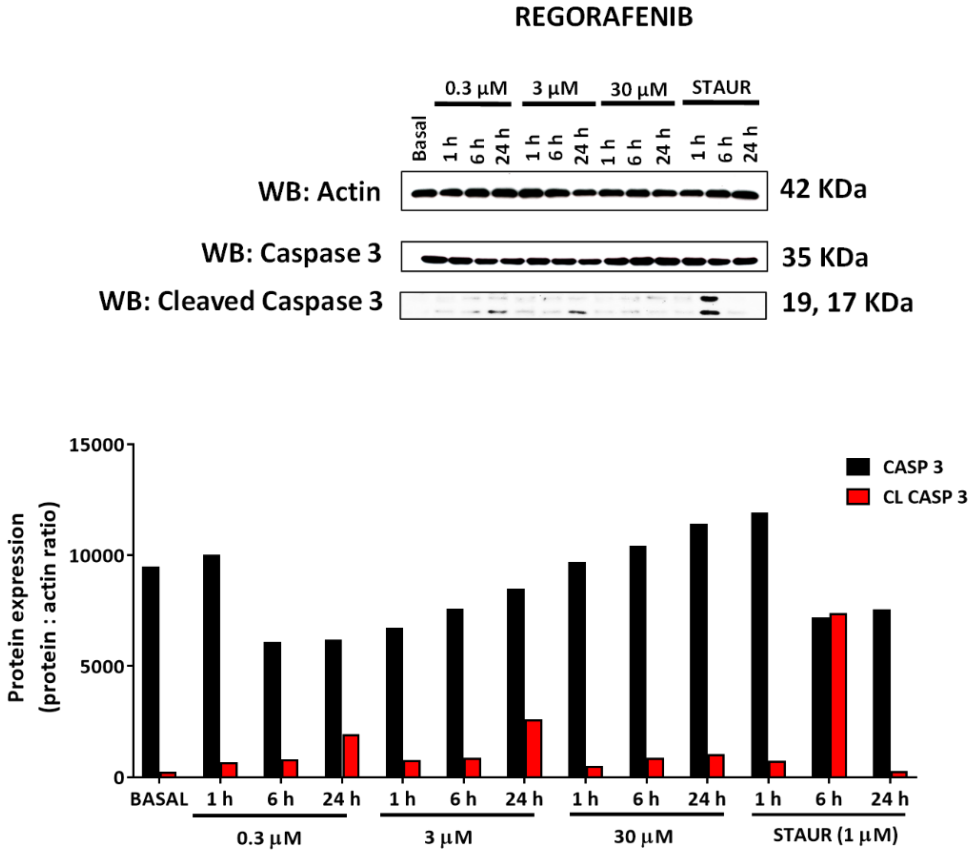

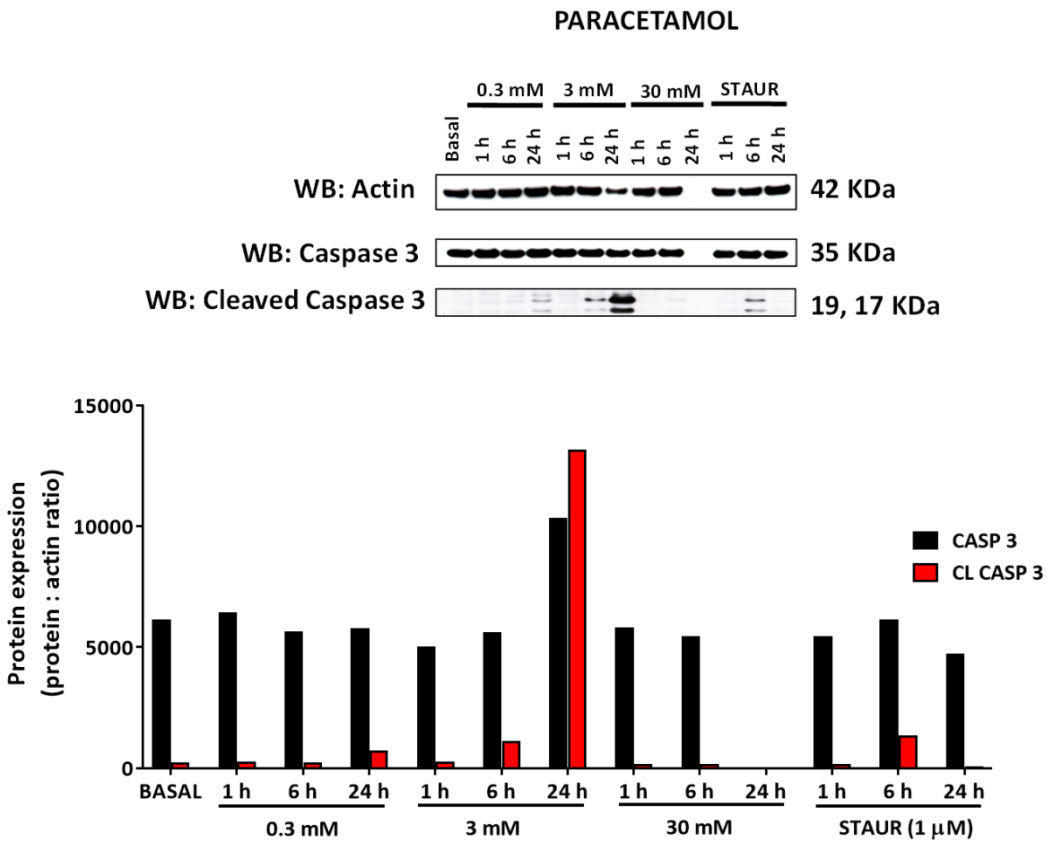

Figure 4.9: Regorafenib and paracetamol both induce apoptosis in primary human hepatocytes

Freshly-isolated primary human hepatocytes were treated with 0.3, 3 or 30 µM regorafenib or 0.3, 3, or 30 mM APAP or 1 µM staurosporine complete primary human hepatocyte medium for 1, 6 or 24 h. Cells were lysed for total protein contents using modified RIPA buffer, solubilised in LDS sample buffer, denatured at 90 ^{o}C. Protein was separated using SDS PAGE for 45 min., transferred unto a nitrocellulose membrane for 2 h. and blocked with 5% BSA. Membranes were then probed with antibodies for caspase 3, and actin. APAP: paracetamol, STAUR: 1 µM Staurosporine. CL casp 3, cleaved caspase 3.

4.2.3.3 Regorafenib causes a disruption in tight junction and cytoskeleton in a time-dependent manner

Following reports that regorafenib induced an effect similar to sinusoidal obstruction syndrome (reviewed in chapter 1) in the clinic (Takahashi et al., 2016a), the effect of regorafenib on the cytoskeleton and tight junction of HLSEC was investigated. Fully confluent HLSEC were treated with regorafenib at similar

concentration range and time points as above. Figure 4.10 and figure 4.11 show the effect of regorafenib on the tight junctional *(ZO-1*) and the cytoskeletal (*actin*) cell components. Figure 4.10 reveals that regorafenib adversely affects the cytoskeleton and the tight junction of HLSEC in a time- and concentration-dependent manner, the highest reduction being observed at the highest concentration of 30 µM. Further, figure 4.11 shows that regorafenib induced a significant ($p < 0.05$) reduction in the mRNA level of ZO-1 after 6 and 24 h of treatment with 0.3 and 3 µM concentrations. At a concentration of 30 µM, regorafenib caused a highly significant ($p < 0.01$) reduction in the expression of ZO-1. As for the cytoskeletal cellular component, actin, regorafenib only induced a significant ($p < 0.05$) reduction at 24 h for 0.3 µM and 6 h for 3 µM, and a highly significant ($p < 0.01$) reduction at 24 h for 3 µM. Whereas a much more highly significant ($p < 0.001$) reduction in actin was observed after 24 h in 30-µM-regorafenib-treated cells.

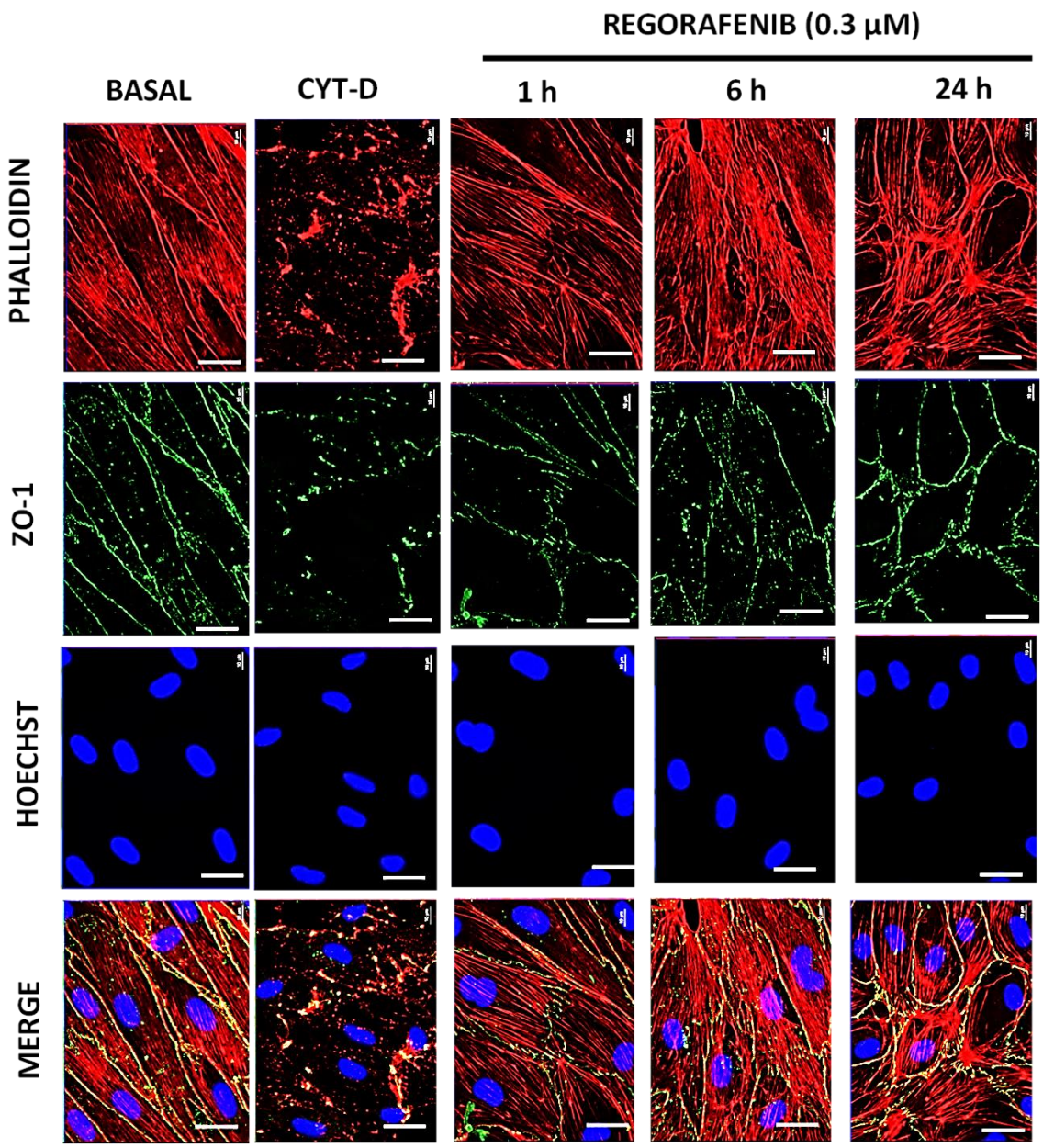
REGORAFENIB (0.3 µM)
BASAL
CYT-D
1 h
6 h
24 h
PHALLOIDIN
ZO-1
HOECHST
MERGE

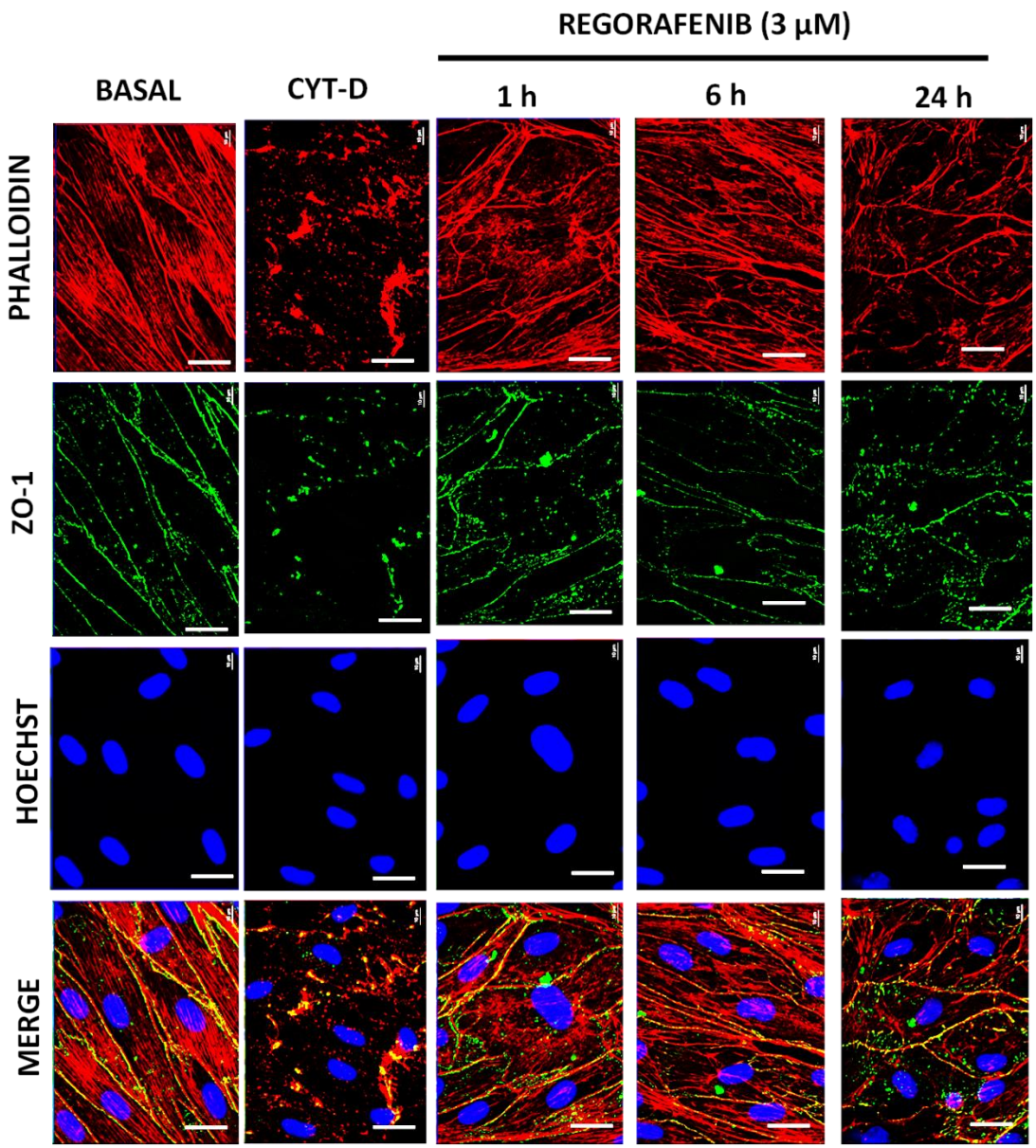
REGORAFENIB (3 µM)
BASAL
CYT-D
1 h
6 h
24 h
PHALLOIDIN
ZO-1
HOECHST
MERGE

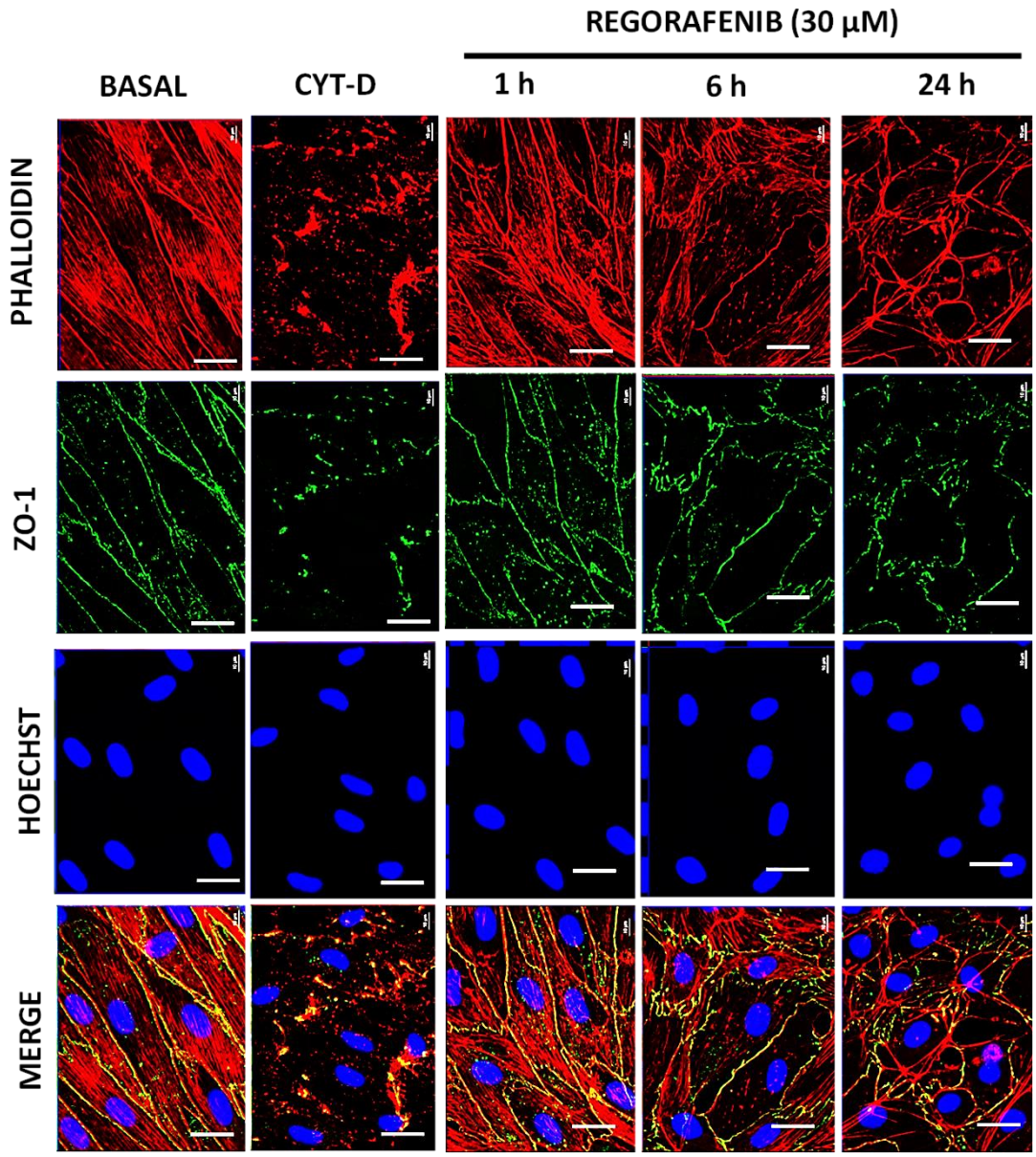

Figure 4.10: Regorafenib causes a reduction in tight junction and cytoskeleton in a time-dependent manner

Immunofluorescent micrographs showing expression of tight junctional (ZO-1) and cytoskeletal cellular structures in HLSEC. HLSEC were cultured to full confluency over 7 days after which they were treated with (A) basal medium, 1 µM cytochalasin D (Cyt D), 0.3 regorafenib, (B) 3 µM regorafenib or (C) 30 µM regorafenib for 1, 6 and 24 h. Then, cells were washed in PBS at room temperature, fixed with 2% PFA for 15 min and washed twice with PBS. Then cells were stained for ZO-1 and phalloidin following the methods earlier described for immunofluorescent staining. ZO-1, *zonas occludens*. Scale bars: 10 µM

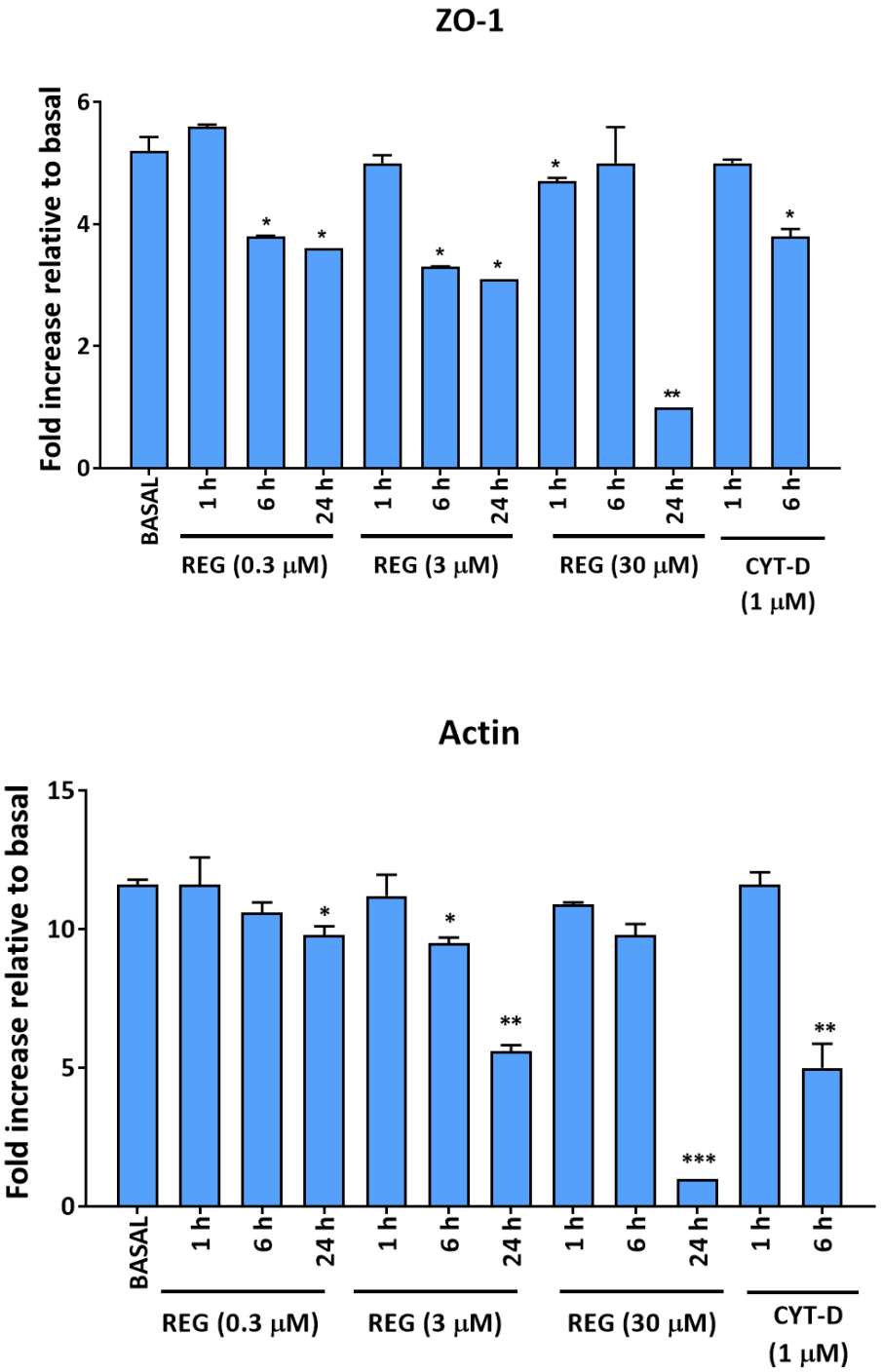

Figure 4.11: Regorafenib causes a reduction in tight junction and cytoskeleton in a time-dependent manner

Relative expression of tight junctional and cytoskeletal genes in HLSEC. HLSEC were cultured to full confluency over 7 days after which they were treated with 0.3, 3 and 30 μM regorafenib or 1 μM cytochalasin D or medium for 1, 6 and 24 h. Then, cells were washed and mRNA extracted using RLT buffer. cDNA was synthesised and analysed for the expression of ZO-1 and actin by qPCR. Results are expressed as mean ± SD, (n=3 of 3 independent experiments) and analysed using one way analysis of variance ANOVA followed by Dunnett's multiple comparison test. Data are significant at *p<0.05, **p<0.01, ***p<0.001. REG: regorafenib

4.3 DISCUSSION

4.3.1 Effect of tyrosine kinase inhibitors on HLSEC physiology

The aim of this chapter was to examine the effect of hepatotoxic drugs on HLSEC and to investigate the link between the ability of TKIs to inhibit endothelial cell physiology of HLSEC and their toxicity. This is to link with the overall aim of this project to explore the involvement of HLSEC in drug-induced liver injury. It is established that some small-molecule receptor tyrosine kinase inhibitors used in cancer chemotherapy are primarily anti-angiogenic drugs which block the formation of new blood vessels from pre-existing ones by inhibiting the activation of the receptors tyrosine kinase on endothelial cells (Folkman, 2007, Gotink & Verheul, 2010b, Kerbel, 2008). Principal among these is the VEGFR family, with VEGFR-2 and VEGFR-3 expressed mainly on vascular and lymphatic endothelial cells respectively. Blocking the activation of these receptors leads to an inhibition of the cellular processes that are hallmarks of endothelial cells and ultimately cancer progression; as VEGFR-3 is also expressed in tumour cells (Su *et al.*, 2007).

The results from the initial part of this chapter show the ability of four TKIs to inhibit the activation of VEGFR-2, a crucial angiogenesis mediator (Fig. 4.4). All the TKIs tested induced a dose-dependent inhibition of VEGFR-2 phosphorylation as well as downstream pathways involving ERK 1/2 and AKT. AKT and ERK 1/2 are involved in cell survival and cell proliferation upon activation in response to a wide rage of chemical biological stimuli (Lu & Xu, 2006, Liao & Hung, 2010). Axitinib was

most potent in its inhibition of the phosphorylation of VEGFR-2. Axitinib has previously been reported to be more a selective and more potent TKI against VEGFR-1, VEGFR-2 and VEGFR-3 than sunitinib and sorafenib in *in vitro* studies (van Geel *et al.*, 2012, Rini *et al.*, 2011). This specificity might be related to its relative toxicity to HLSEC compared to other TKIs tested (fig. 4.1).

The selection of regorafenib as the drug to carry forward in the remaining studies was due to its clinical use and reported toxicity profile (Krishnamoorthy *et al.*, 2015, Sacré et al., 2016). Regorafenib inhibited cell migration and *in vitro* tube formation at a sub-toxic concentration (figs. 4.5 and 4.6). These are two interrelated processes as endothelial cells migrate in the course of vasculogenesis and angiogenesis (Michaelis, 2014b, Lamalice et al., 2007). Results described above (fig 4.5 and fig 4.6) are similar to published data by Schmieder *et al.* (2014a) where regorafenib was reported to inhibit the intracellular signalling and cell migration in VEGF-C and VEGF-A stimulated lymphatic endothelial cells. Also, since regorafenib is known to be a potent inhibitor of VEGFR-3, inhibition of VEGF-C-induced vascular network formation shown in figure 4.6 confirms earlier reports that blocking VEGFR-3 is an important anti-angiogenic mechanism (Tammela *et al.*, 2008). This is beneficial in cancer chemotherapy where regorafenib has been reported to induce anti-migratory effect and abolishment of VEGF-A secretion and tube formation in a breast cancer cell line (Su *et al.*, 2016). However, the fact that a sub-toxic dose induced an inhibition of cell migration – which could be a physiologic response to a compromise in blood vessel integrity (Michaelis, 2014b) – poses a toxicological question. This is aptly illustrated by the ability of regorafenib to inhibit the upregulation of the angiocrine factors that play a key role in liver regeneration (fig.

4.7). Angiogenesis of the HLSEC has been reportedly involved in liver regeneration (Hu *et al.*, 2014). As earlier described in the introduction, this is preceded by activation of the VEGFR-2 by its ligand, VEGF-A; this initiates a cascade of events which involves the upregulation of the endothelial cell-specific transcription factor Id1 which in turn activates Wnt2 and HGF, resulting in hepatocyte proliferation (Ding et al., 2010a, Rafii et al., 2016). Although this experiment was done in a single culture system, the upregulation of these angiocrine factors were demonstrated in the presence of VEGF-A and VEGF-C. Pre-treatment with regorafenib significantly inhibited this process at every step involved in liver regeneration along the VEGFR-2-Id1 signalling pathway. This also hints at a likely involvement of VEGFR-3 in this process. As an indication that the significant reduction observed in this experiment was VEGF-2 and/ or VEGFR-3-dependent, regorafenib had no significant effect on the expression of these genes in the stromal cell-derived factor 1 (SDF-1)-stimulated cells. SDF-1 is a ligand for CXC chemokine receptor 7 (CXCR7) which is widely expressed in the brain, kidney, heart, haematopoietic cells and the vascular endothelial cells (Dai *et al.*, 2011). It has been shown that CXCR7 is involved in cell proliferation, adhesion, and activation of cell survival cell signalling molecules ERK 1/2 and/ or Akt (Burns *et al.*, 2006) and angiogenesis (Dai et al., 2011). It is also pro-regenerative as previously reported in an *in vitro* study where SDF-1 stimulation of human HLSEC effected an upregulation of Id1 which resulted in the production of hepatic-active angiocrine factors Wnt2 and HGF (Ding et al., 2014). The fact that regorafenib did not significantly affect the expression of the any of the angiocrine factors involved in liver regeneration in cells stimulated with SDF-1 suggests that regorafenib specifically targets VEGFR-2 and / or VEGFR-3 to effect this.

4.3.2 Relative toxicity of hepatotoxic drugs on HLSEC and other hepatic and endothelial cells

When compared with other hepatic and endothelial cells, HLSEC were generally more sensitive to TKIs tested in this study (fig. 4.1). More importantly, while compared with other hepatic cell types—primary human hepatocyte and human hepatic fibroblast—the relatively higher sensitivity of HLSEC may be another insight into the possibility of HLSEC as the primary target of this group of drugs in the liver. This might suggest their direct involvement in drug induced liver injury caused by this class of drugs (Karczmarek-Borowska & Sałek-Zań, 2015).

On the other hand, known hepatotoxins belonging to other groups showed a different pattern of toxicity to the cell types tested (fig. 4.2). For example, paracetamol was equitoxic to all the cell types tested. This is a novel finding considering what has been published to date on paracetamol toxicity. Published studies have linked paracetamol toxicity mainly to metabolic bioactivation whereby its electrophilic metabolite N-acetyl *p*-benzoquinone imine (NAPQI) causes a depletion of glutathione as a result of oxidative stress, resulting in hepatocellular necrosis (Hinson *et al.*, 1990, Hinson *et al.*, 2010). However, the uniform IC_{50} seen in metabolically-competent and non-metabolically competent cells suggests that another mechanism of toxicity must be predominant in paracetamol toxicity, including mitochondrial damage (Jaeschke *et al.*, 2012, McGill *et al.*, 2012). Indeed,

it has been shown that paracetamol targets the HLSEC with a resultant collapse of the sinusoidal structure (DeLeve et al., 1997)

4.3.3 Toxic effect of regorafenib on HLSEC

To further show that regorafenib targets the HLSEC in liver toxicity, HLSEC were incubated with varying doses of with regorafenib over a 24-hour period. Figure 4.6 shows that at 30 µM, regorafenib induces the cleavage of caspase 3 after 6 h while this was not the case with 30 mM paracetamol. In addition, lower doses of regorafenib induced caspase 3 cleavage in primary human hepatocytes (fig. 4.8). This is different from reports from a recent study by Weng et al. (2015) where regorafenib, at a maximum concentration of 15 µM, did not induce the activation of caspase 3 in rat hepatocytes *in vitro*. This might be due to species difference in drug response. For example Lu and Li (2001) reported that the CYP 3A family is induced differently in human and rat hepatocytes. Since regorafenib is metabolised by CYP3A4 in humans (FDA, 2012), the difference in biotransformation which might lead to metabolic bioactivation in a species and detoxification in another might be an explanation for this observation. This requires further investigation.

Regorafenib caused a significant reduction of cytoskeletal cellular components (actin) of HLSEC as seen both at mRNA level and by immunofluorescence in a time- and dose-dependent manner (fig 4.10 and fig 4.11). This might be an indication of the structural effect of regorafenib on HLSEC. This is important in view of the fact that regorafenib has recently been linked to sinusoidal obstruction syndrome

(Takahashi et al., 2016b), which involves the polymerisation of F-actin on the cytoskeleton of HLSEC, activation of increased synthesis of matrix metalloproteinase-9 (MMP-9) which digests the extracellular matrix components. This culminates in a rounding up of the HLSEC, gap formation in the endothelial barrier in the hepatic sinusoid, obstruction of the hepatic microcirculation and hepatocyte necrosis (DeLeve, 2008b). This has been fully described in chapter 1. Also, since, actin fibres are involved in cell migration—a feature of cell repair and wound healing—the effect of regorafenib on the cytoskeletal structure must have a far-reaching consequence (Lamalice et al., 2007).

The drawback from this section is the fact that data were derived from *in vitro* experiments. *In vivo* experiments would be required to ascertain these. Also, the experiments on the effects of the TKIs on the physiology of HLSEC were conducted only on regorafenib. Given the fact that other TKIs do not have exactly the same molecular targets as regorafenib, the response of HLSEC to these might be different from what was obtained. Also, the cytotoxicity assays carried out were only ATP-based, which were a measure of viable cells. Such other measures of toxicity as LDH leakage, MTT assay and other would have been more robust, while further creating a better picture of mechanism of toxicity of all the drugs tested.

Taken together, the data from this chapter shows that regorafenib causes a disruption in the physiology of human liver sinusoidal endothelial cells which might partly explain its toxicity. Also, HLSEC appear to be direct targets of TKIs, particularly regorafenib which results in apoptosis, and a potential polymerisation of cytoskeletal cellular components—a feature of sinusoidal obstruction syndrome.

Finally, the propensity of regorafenib to inhibit the homeostatic process of liver regeneration may further exacerbate any direct toxicity that it might have initiated both on HLSEC and the parenchymal cells of the liver.

CHAPTER FIVE

LIVER SINUSODIAL ENDOTHELIAL CELLS IN A CO-CULTURE LIVER MICROTISSUE SYSTEM

5.1 INTRODUCTION

Data from the previous chapter demonstrated that human liver sinusoidal endothelial cells (HLSEC) are potential targets of hepatotoxic drugs, particularly small molecule tyrosine kinase inhibitors that have an established profile of inducing liver toxicity in the clinic.

The focus of this chapter is the use of HLSEC in multicellular liver microtissue. As reviewed in the introduction to this thesis, studies have shown that liver microtissues, which are a 3D cell aggregation that allows for a more efficient cell-cell contact and interaction, constitute a better model for investigation liver pathophysiology compared to hepatocytes in a monolayer, as they preserve and better reconstitute liver functions (Bell et al., 2016). Furthermore, it has been shown that inclusion of non-parenchymal cells, such as endothelial cells, have proven more physiologically relevant in liver microtissues (Takebe et al., 2013, Takebe et al., 2014). Since most of the studies carried out were performed on non-microvascular and non-hepatic endothelial cells, it would be interesting to investigate some of the findings using primary liver sinusoidal endothelial cells. Following observation that vascular endothelial growth factor (VEGF-A) was secreted from hepatocytes following exposure of rats to hepatotoxic doses of paracetamol and that exogenous administration of VEGF-A offered protection against paracetamol toxicity (Donahower et al., 2006, Donahower et al., 2010a), it was hypothesised that inclusion of VEGF-A or VEGF-C could offer protection to the liver microtissues following exposure to hepatotoxic drugs. Finally, since activation of VEGFR-2 on HLSEC has been shown to induce liver regeneration *in vivo*, it was

hypothesised that growth factor stimulation of triculture microtissues could improve drug-metabolising capability of liver microtissues.

5.2 RESULTS

5.2.1 Triculture human liver microtissues enables recapitulation of the vascularisation of the liver sinusoids

Figure 5.1 shows the relative position of different cellular components of the human liver microtissues, as well as the differing degrees of details that can be revealed by different imaging methods. Figure 5.1 A is an image of liver tissue section revealing the vascularisation of the liver sinusoids. Figure 5.1 B which shows Haematoxylin and Eosin staining of a triculture liver microtissue only reveals details of nucleus and cytoplasm of the constituent cells. Figure 5.1 C shows the actin fibre of the fluorescently stained microtissue revealing the actin as a common feature of all cellular components. Figure 5.1 D shows the expression of albumin, a hepatocyte marker, on a primary human hepatocyte-only microtissue. On the other hand, figures 5.1 E & F reveal more structural details as they show the relative position of HLSEC in the microtissue environment. Liver sinusoidal endothelial cells self-organise to form a vascular-like structure reminiscent of the native liver sinusoidal environment as seen in figure 5.1 A.

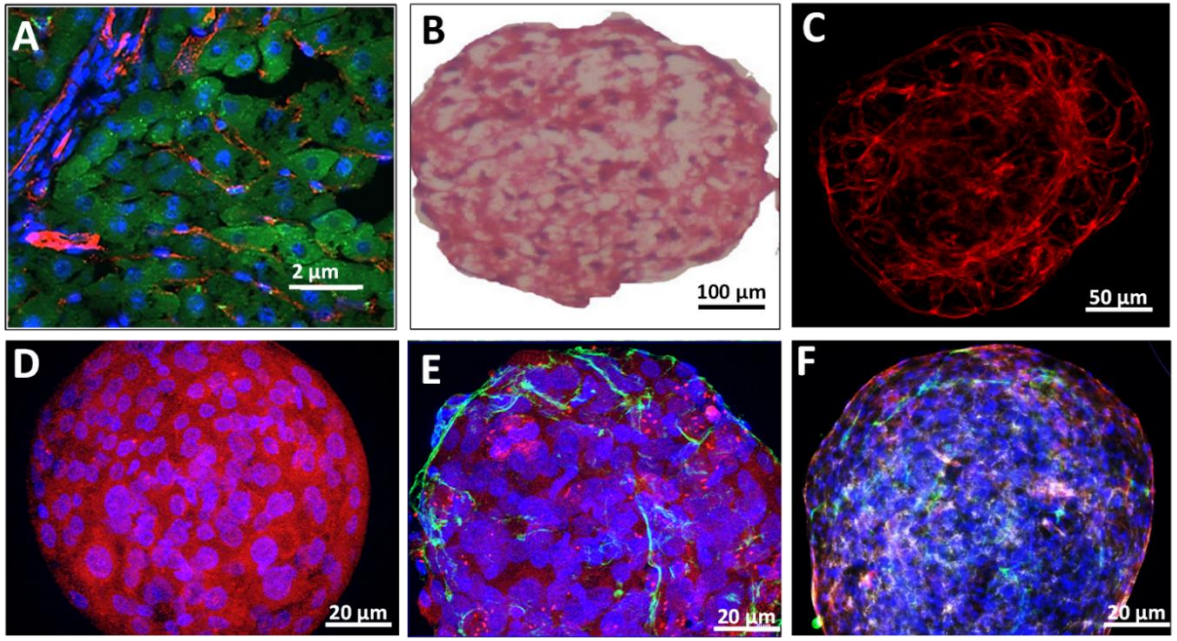

Figure 5.1: Structure of triculture human liver microtissues-
(A) Immunofluorescent image of human liver section **(B)** Light microscopy of the Haematoxylin and Eosin stained triculture human liver microtissue (C) immunofluorescent image of triculture liver microtissue stained for actin fibre, (Phalloidin in red) **(D)** immunofluorescent image of liver microtissue stained for albumin, in red **(E)** immunofluorescent image of liver microtissue, comprising primary human hepatocyte and liver sinusoidal endothelial cells stained for albumin (in red) and CD-31 (green) and nucleus (blue) **(F)** immunofluorescent image of liver microtissue, comprising primary human hepatocyte, liver sinusoidal endothelial cells and human hepatic fibroblasts stained for albumin (in red), CD-31 (green), collagen type 1 (white) and nucleus (blue). A total of 1500 cells were seeded on ultra-low attachment plates, centrifuged and incubated at 37°C for 7 d to allow cells to self-aggregate into microtissues as described in the methods section. On day 7, microtissues were harvested, medium removed and processed for immunoflourescent staining as previously described in the method section for Immunofluorescent staining for liver microtissues. Microtissues were stained for albumin (red), CD-31 (green), and nucleus (blue). Image A was taken using light microscope at a magnification of X100 while images (C-E) were taken at a magnification of X10 using an immunofluorescent microscope. (B) microtissues were harvested and processed histologically using as described in the methods section for haematoxylin and Eosin staining (C) PHH: microtissues comprising 1500 freshly-isolated primary human hepatocytes (D) PHH + HLSEC: microtissues comprising freshly isolated primary human hepatocytes and liver sinusoidal endothelial cells at a ratio of 2:1 to a total of 1500 cells, (B, E) PHH + HLSEC+ HHF: Microtissues comprising primary human hepatocytes, liver sinusoidal endothelial cells and human hepatic fibroblasts in a ratio of 8:2:2 to a total of 1500 cells. As for the human liver tissue sections, sections were prepared as described in material and methods and immunofluorescently stained for albumin (hepatocyte marker in green) and CD-31 (endothelial cell marker in red) as described in methods section.

5.2.2 Effect of growth factor stimulation on vascularisation pattern of human liver micro-tissues

Since LSEC have been shown to self-organise into vascular-like structure in the micro-tissue environment, triculture liver micro-tissues were stimulated with VEGF-A and VEGF-C to see the effect of these growth factors on the formation pf these vascular structures. The fact that these receptors are neither expressed in primary human hepatocytes nor human hepatic fibroblast makes HLSEC a specific of these growth factors. Figure 5.2 shows the effect of growth factor stimulation on the vascular structure of HLSEC in the triculture liver microtissue. CD-31 (green stain) is was used to reveal vascular structures. In the presence of VEGF-A, the vasculature formed resembled sprouting angiogenesis. On the other hand, VEGF-C induced formation of vascular structures round the hepatocytes in a manner similar to the liver sinusoids. This observation might suggest that VEGF-A and VEGF-C play different roles during organogenesis.

5.2.3 Expression of drug-metabolising enzymes in liver microtissues

In order to functionally validate the liver microtissues, they were assayed for the expression of oxidative (phase I) and conjugative (phase II) drug-metabolising enzymes. Figure 5.3 shows the expression of CYP 3A4, CYP 2D6, CYP 2E1 (phase I) and UGT 1A1 (phase II) in liver microtissues in comparison with cells grown in

monolayer. Protein expression had been corrected for in the quantification to accurately reflect the difference in expression profile between monoculture and multiculture systems. After 7 days in culture, the cells in monolayer lost their expression of CYPs 3A4 and 2E1 while the level of CYP 2D6 and UGT 1A1 were highly reduced in comparison with that in freshly-isolated hepatocytes. As regards the liver microtissues, the triculture system had a lower expression of CYPs 3A4, 2D6 and UGT 1A1 in comparison with the hepatocyte-only microtissues.

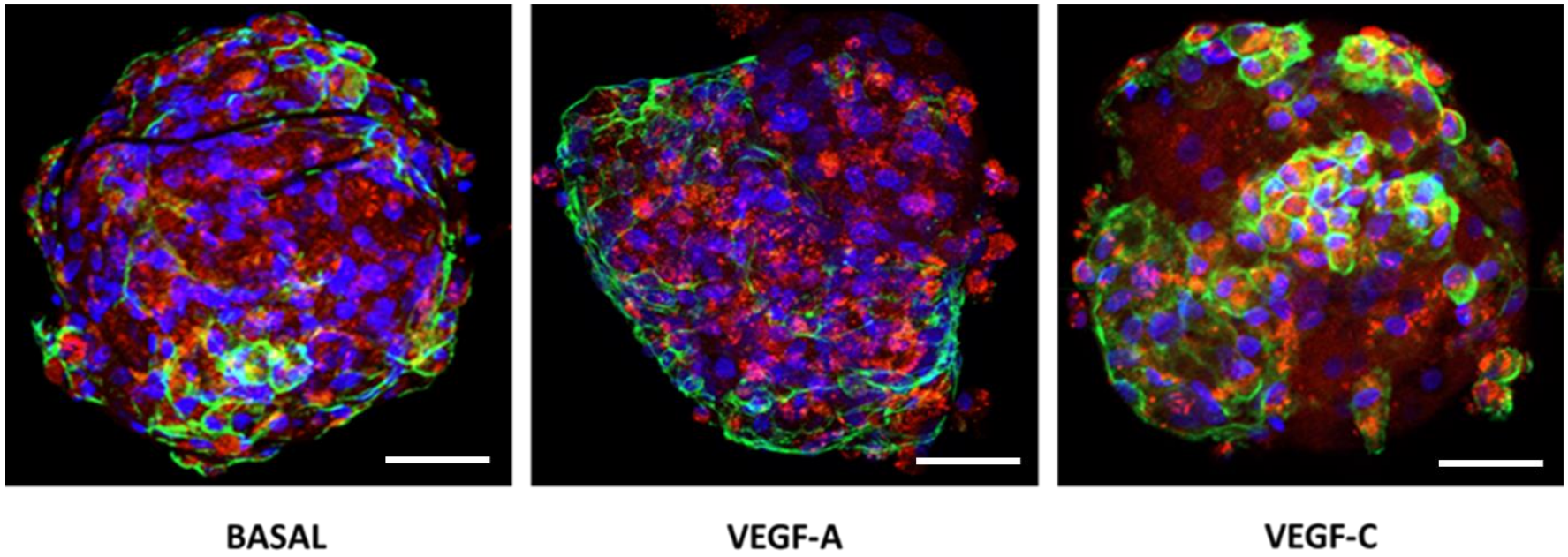

Figure 5.2: Effect of growth factor stimulation on vascularisation pattern of human liver microtissues

A total of 1500 cells were seeded on ultra-low attachment plates, centrifuged and incubated at 37°C for 7 d to allow cells to self-aggregate into microtissues as described in the Method section. On day 7, microtissues were harvested, medium removed and processed for immunofluorescent staining as previously described in the method section for Immunofluorescent staining for liver microtissues. Microtissues were stained for albumin (red), CD-31 (green), and nucleus (blue). Images were taken at a magnification of X100 using an immunofluorescent microscope. Microtissues comprised primary human hepatocytes, liver sinusoidal endothelial cells and human hepatic fibroblasts in a ratio of 8:2:2 to a total of 1500 cells. BASAL, VEGF-A, and VEGF-C: microtissue incubated with culture medium, culture medium supplemented with 50 ng/ml VEGF-A, culture medium supplemented with 50 ng/ml VEGF-C respectively.

Also, the level of expression of these enzymes was the same in the triculture microtissues system regardless of whether the constituent HLSEC were stimulated with vascular endothelial growth factors or not.

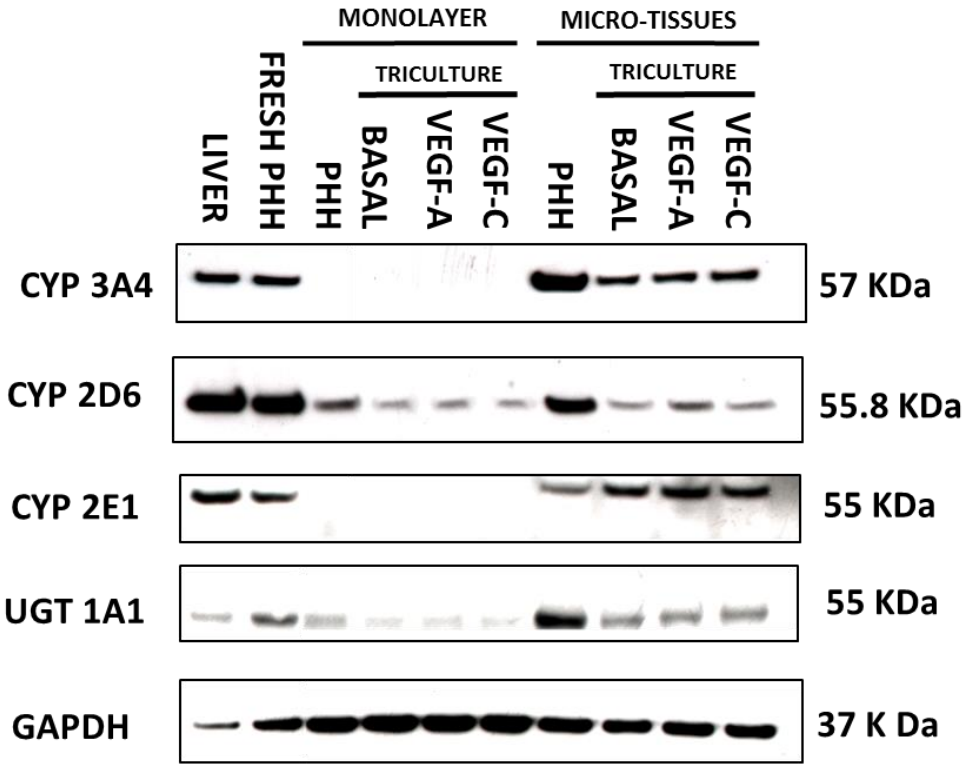

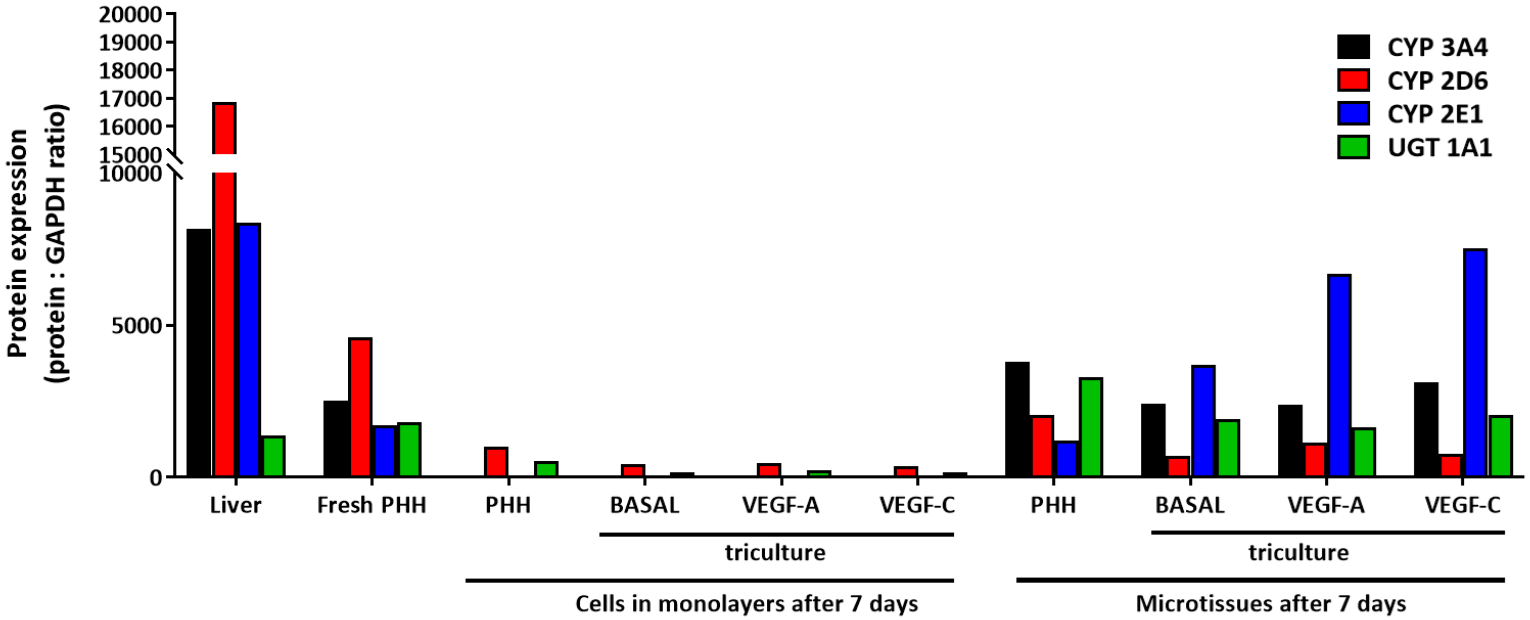

Figure 5.3: Expression of drug-metabolising enzymes in the liver microtissues-

A total of 1500 cells were seeded on ultra-low attachment plates, centrifuged and incubated at 37°C for 7 d to allow cells to self-aggregate into microtissues as described in the Method section. On day 7, microtissues were harvested, sonicated, centrifuged and quantified for total protein as previously described in methods section. Total protein from liver tissues, freshly isolated human hepatocytes and cells cultured in monolayer were prepared as earlier described in the methods section. Protein lysates were solubilised in LDS sample buffer, denatured at 90 ^{o}C. Protein was separated using SDS PAGE for 45 min., transferred unto nitrocellulose membrane for 2 h. and blocked with 10 % milk. Membranes were then probed with respective antibodies CYP 3A4, CYP 2D6, CYP 2E1, UGT 1A1 and GAPDH. Band intensity was quantified using Image J version 1.48v. Data is representative of three independent experiments. Differences in hepatocyte number between the monoculture and triculture systems were corrected for by multiplying the band intensities of UGT protein in the triculture system by a factor of 1.5. PHH; primary human hepatocyte, HHF: human hepatic fibroblasts, HLSEC: liver sinusoidal endothelial cells.

5.2.4 Drug metabolism in tri-culture liver microtissues.

In order to determine whether the microtissues analysed for the expression of drug-metabolising enzymes were metabolically competent, a drug-metabolism study was conducted. This follows the observation that the tri-culture microtissues showed a lower expression of certain drug-metabolising enzymes. The metabolism of drugs known to be oxidatively metabolised by CYPs 2D6 and 2E1 and conjugated by UGT 1A1 was investigated.

5.2.4.1 Paracetamol metabolism is reduced in triculture liver microtissues

Paracetamol is principally metabolised by CYP 2E1 and CYP 3A4 to form N-acetyl *p*-benzoquinone imine (NAPQI) which is unstable, highly reactive and not readily detectable experimentally (Trettin *et al.*, 2014). NAPQI readily reacts with glutathione, which after a series of steps form cysteine and mercapturic acid conjugates, which are detectable using mass spectrometry. In addition, paracetamol is glucuronidated and sulphated to form glucuronide and sulphate conjugates respectively. Liver microtissues in monoculture or triculture were incubated with 1 mM of paracetamol for 24 h after which culture medium (containing parental drug and metabolites) were analysed for the presence of oxidative and conjugative metabolites. Figure 5.5 is a chromatogram showing the levels of metabolites of paracetamol in mono-culture and triculture liver microtissues after analysis by mass spectrometry. Retention time (on x-axis)

identified the peaks obtained to be metabolites of paracetamol. While the intensities of the peaks showed amount of the metabolite of interest. The intensities of the peaks on the chromatograms show that the levels of the metabolites formed in the triculture microtissues were lower than in their monoculture counterparts. This is further confirmed in figure 5.4 which shows the amount of metabolites of paracetamol produced per hepatocyte in the mono-cellular and tri-culture liver microtissues. There were significantly ($p < 0.001$) lower levels of the cysteine and glucuronide conjugates of paracetamol in the tri-culture microtissue system in comparison to the PHH-only microtissues. A similar trend was also seen for the sulphated paracetamol metabolite whereby there was a highly significant ($p < 0.01$) lower level of the sulphate metabolite in the tri-culture microtissue than in the mono-culture system.

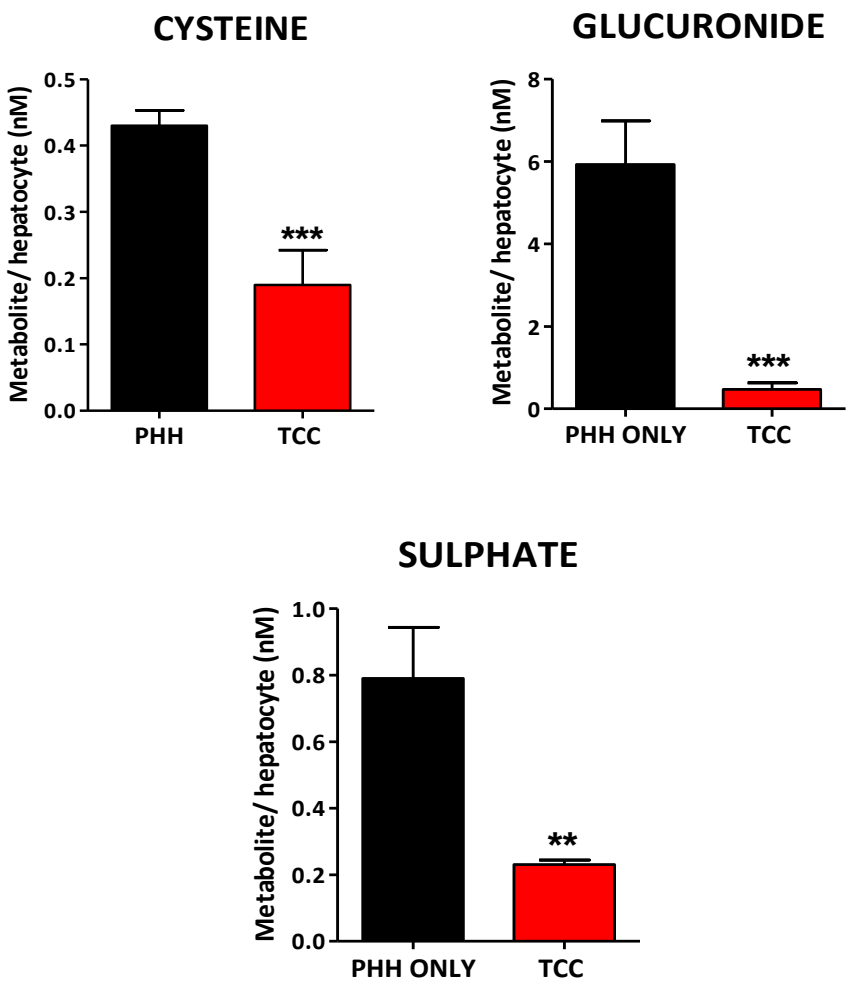

Figure 5.4: Paracetamol metabolism in liver microtissues

A total of 1500 cells were seeded on an ultra-low attachment plate, centrifuged and incubated at 37°C for 7 d to allow cells to self-aggregate into microtissues as described in the Method section. On day 7, microtissues were incubated with 1 mM of paracetamol for 24 h after which samples were snap frozen and stored at -20C before analysis. Samples were analysed for LC/MS/MS for identification of metabolites of paracetamol as described in the method section. Amount of metabolites produced in the samples were corrected for the number of hepatocytes in liver microtissues. Concentration of metabolites were compared using Student t-test. Values are significant at **p < 0.01, ***p < 0.001. (n=3, from three different donors). PHH only: Microtissues containing a total of 1500 freshly-isolated primary human hepatocytes, TCC: triculture microtissues comprising primary human hepatocytes, liver sinusoidal endothelial cells and human hepatic fibroblasts in a ratio of 8:2:2 to a total of 1500 cells.

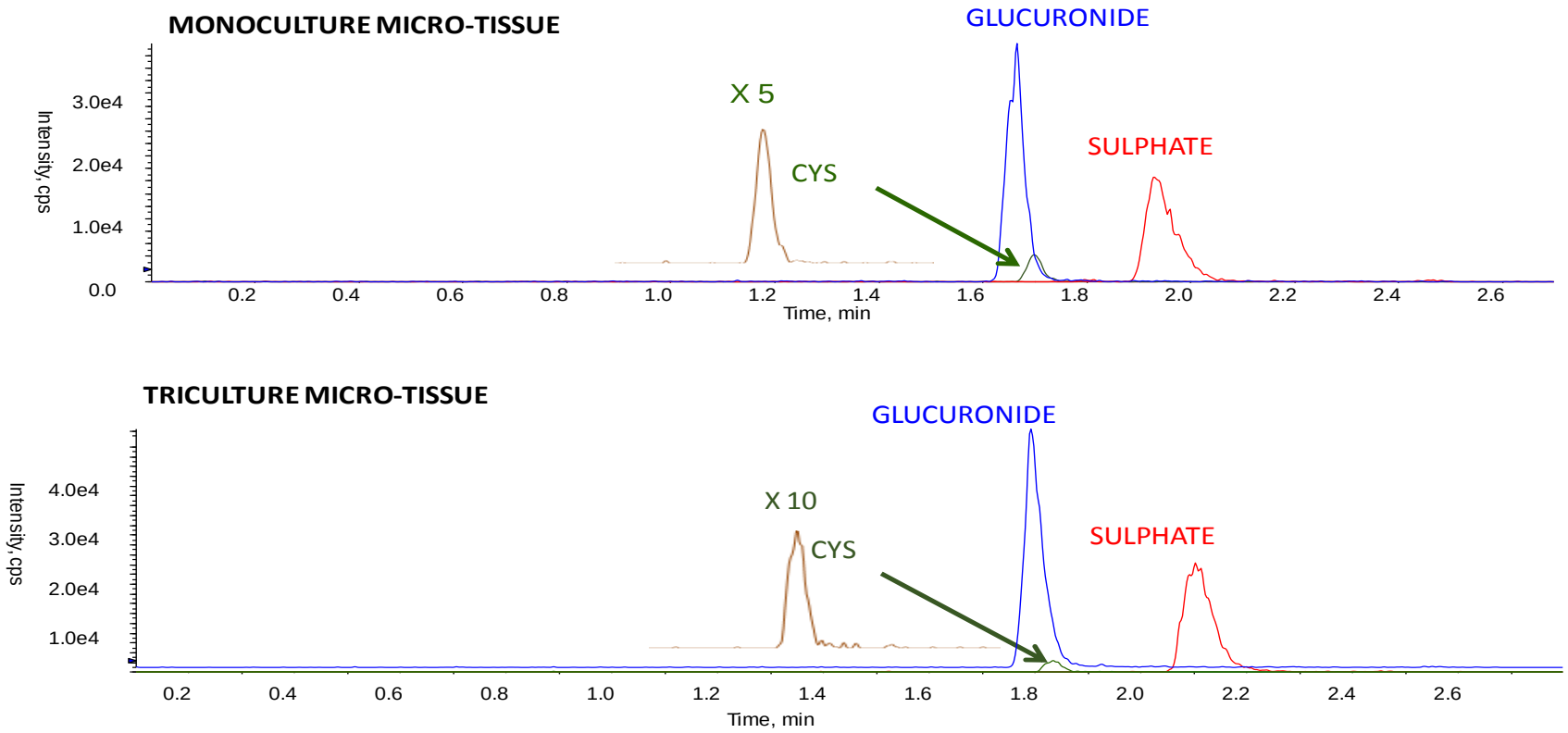

Figure 5.5: Chromatogram of paracetamol metabolism-

A total of 1500 cells were seeded on an ultra-low attachment plate, centrifuged and incubated at 37°C for 7 d to allow cells to self-aggregate into microtissues as described in the Method section. On day 7, microtissues were incubated with 1 mM of paracetamol for 24 h after which samples were snap frozen and stored at -20C before analysis. Samples were analysed for LC/MS/MS for identification of metabolites of paracetamol as described in the method section. Amount of metabolites produced in the samples were corrected for the number of hepatocytes in liver microtissues. CYS, Cysteine conjugate of paracetamol.

5.2.4.2 Paracetamol metabolism at varying cell ratios in human liver microtissues

To further determine the effect of cell number and age on the metabolism of paracetamol, liver microtissues were prepared with PHH, HLSEC and HHF at different ratios of 2:1:1, 4:1:1, 8:1:1 and 10:7:2. Microtissues were incubated with 1 mM paracetamol for 24 h on days 7, 14 and 28 after they were formed. As shown in figure 5.6, there was significant reduction in the amount of phase I and phase II metabolites across the different cell ratios of triculture microtissues when compared with the PHH-only liver microtissues. In the liver microtissues formed at a ratio of 2:1:1, there were significant reductions in the levels of all metabolites in 14- and 28-day old microtissues when compared with their 7-day old counterparts. However, the levels of the cysteine conjugate of paracetamol in microtissues formed at ratios of 4:1:1, 8:1:1 and 10:7:2 remained stable over the course of 21 days. Also the levels of the glucuronide of paracetamol remained unchanged in the liver microtissues of the 8:1:1 configuration over the course of 21 days, while there was a significant ($p < 0.05$) reduction in the level of this metabolite in the 28-day, 4:1:1 and 10:7:2 microtissues. The amount of sulphated paracetamol produced was significantly ($p < 0.05$) reduced in the 14- and 28-day old microtissues produced at the ratio of 10:7:2 when compared with their 7-day old counterparts. While there was no significant difference in the level of paracetamol sulphate in the 14-day old microtissues made at the ratios of 4:1:1 and 8:1:1 as against the 7-day old microtissues, their levels significantly declined after 28 days.

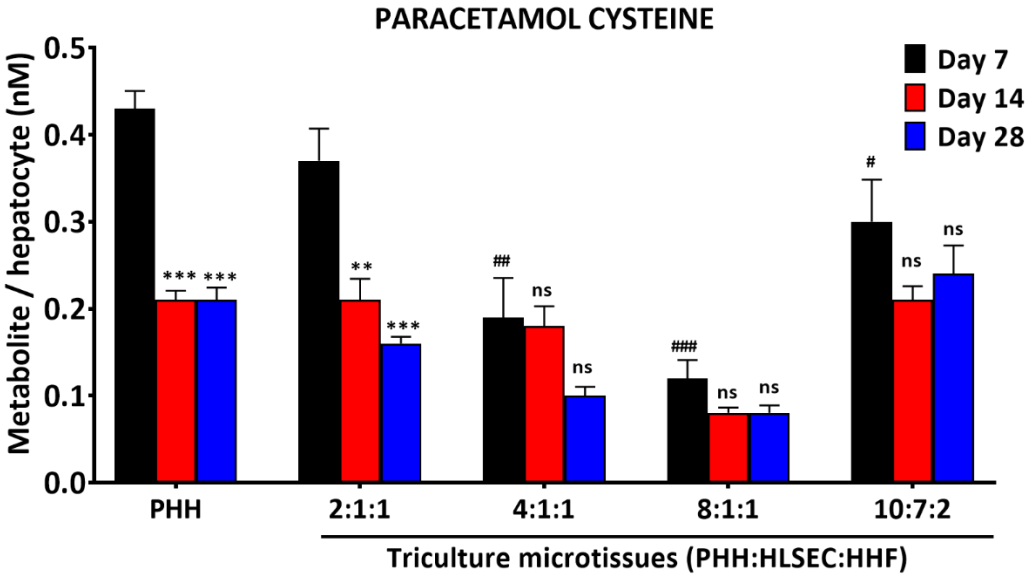
PARACETAMOL CYSTEINE
Metabolite / hepatocyte (nM)
0.5
0.4
0.3
0.2
0.1
0.0
Day 7
Day 14
Day 28
*** ***
**
***
##
ns
ns
###
ns
ns
#
ns
ns
PHH
2:1:1
4:1:1
8:1:1
10:7:2
Triculture microtissues (PHH:HLSEC:HHF)

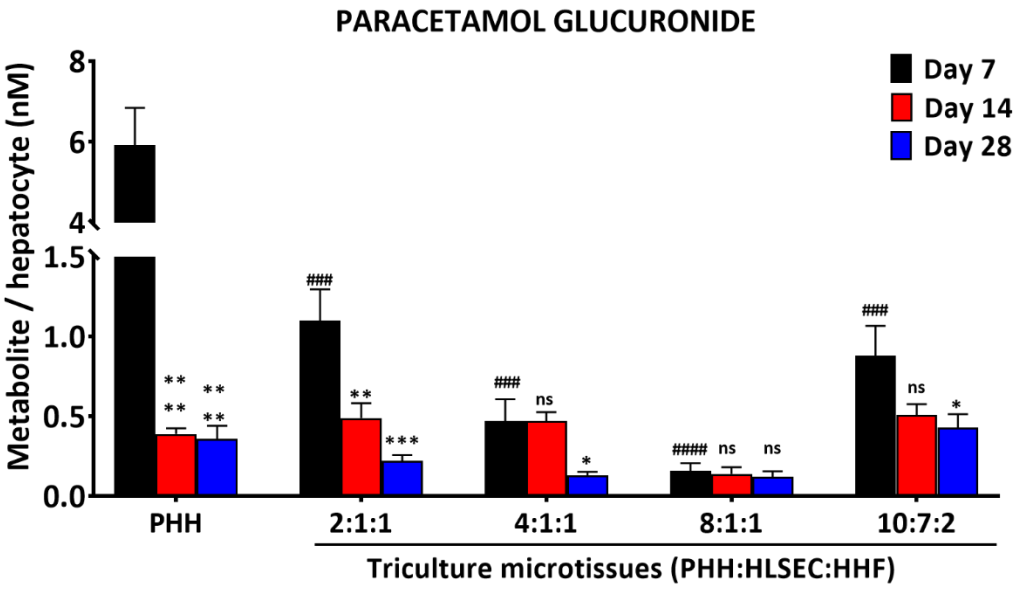
PARACETAMOL GLUCURONIDE
Metabolite / hepatocyte (nM)
8
6
4
1.5
1.0
0.5
0.0
Day 7
Day 14
Day 28
** **
** **
###
**
***
###
ns
*
####
ns
ns
###
ns
*
PHH
2:1:1
4:1:1
8:1:1
10:7:2
Triculture microtissues (PHH:HLSEC:HHF)

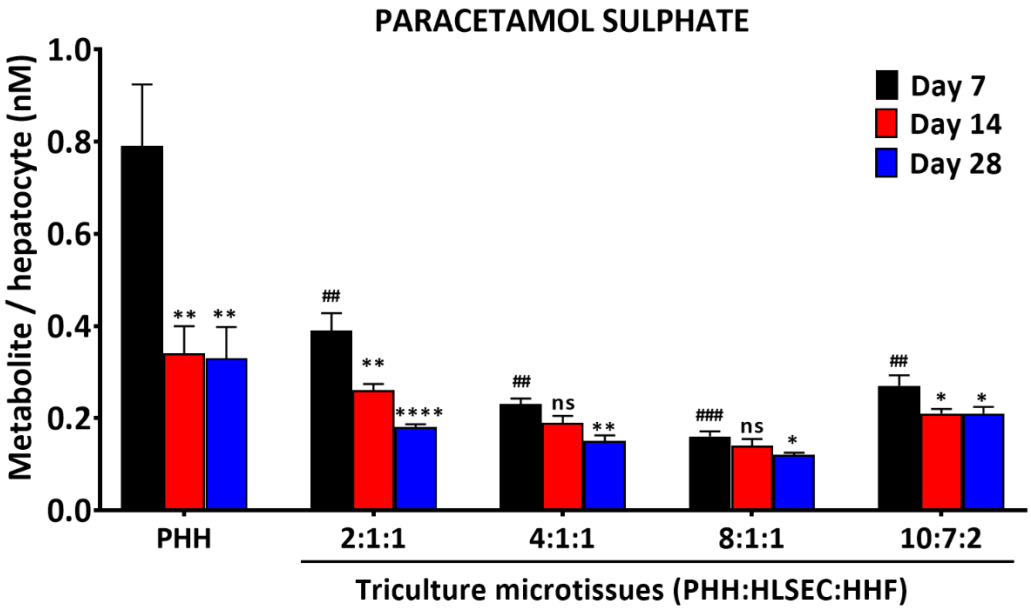

Figure 5.6: Paracetamol metabolism at varying cell ratios in liver microtissues-

A total of 1500 cells were seeded on an ultra-low attachment plate, centrifuged and incubated at 37°C for 7 d to allow cells to self-aggregate into microtissues as described in the Method section. On days 7, 14 or 28, microtissues were incubated with 1 mM of paracetamol for 24 h after which samples were snap frozen and stored at -20C before analysis. Samples were analysed for LC/MS/MS for identification of metabolites of paracetamol as described in the method section. Amount of metabolites produced in the samples were corrected for the number of hepatocytes in liver microtissues. Concentration of metabolites were compared using one way analysis of variance (ANOVA) followed by Dunnett's multiple comparison. Values are significant at **$p < 0.01$, ***$p < 0.001$ and ****$p<0.0001$ (vs corresponding cell ratio at 7 days); $^{\#}p < 0.05$, $^{\#\#}p<0.01$, and $^{\#\#\#}p < 0.001$ (7-day old microtissues in PHH vs triculture groups). (n=8, from eight different microtissues). PHH only: Microtissues containing a total of 1500 freshly-isolated primary human hepatocytes, triculture microtissues comprise primary human hepatocytes (PHH), human liver sinusoidal endothelial cells (HLSEC) and human hepatic fibroblasts (HHF) at ratios of 2:1:1, 4:1:1, 8:1:1 and 10:7:2 to a total of 1500 cells.

5.2.4.3 Metabolism of Perhexiline

Perhexiline is primarily metabolised by CYP 2D6 to form a mixture of trans- and cis-hydroxylated metabolites (Davies et al., 2007). Figure 5.8 is a chromatogram showing the oxidative metabolites of perhexiline formed after incubation with 5 µM of the parent compound. Perhexiline was metabolised to form two trans- and two cis- hydroxyl perhexiline metabolites. After correction for cell number in the

liver microtissues, there was significantly ($p < 0.05$) low level of cis-hydroxy perhexiline 1 formed in the unstimulated liver microtissues compared to the PHH-only group (Fig. 5.7). There was also a significantly ($p < 0.01$) low level of cis-hydroxy perhexiline 1 in the VEGF-A and VEGF-C-stimulated microtissues in comparison with the PHH-only microtissues. The same trend is also true for the formation of cis-hydroxy perhexiline 2 in the tri-culture microtissues. Similarly, the triculture microtissues formed significantly ($p < 0.01$) lower levels of trans-hydroxy perhexiline 1 and 2. This might suggest that the presence of HLSEC and HHF in a liver microtissue does not improve metabolic competence.

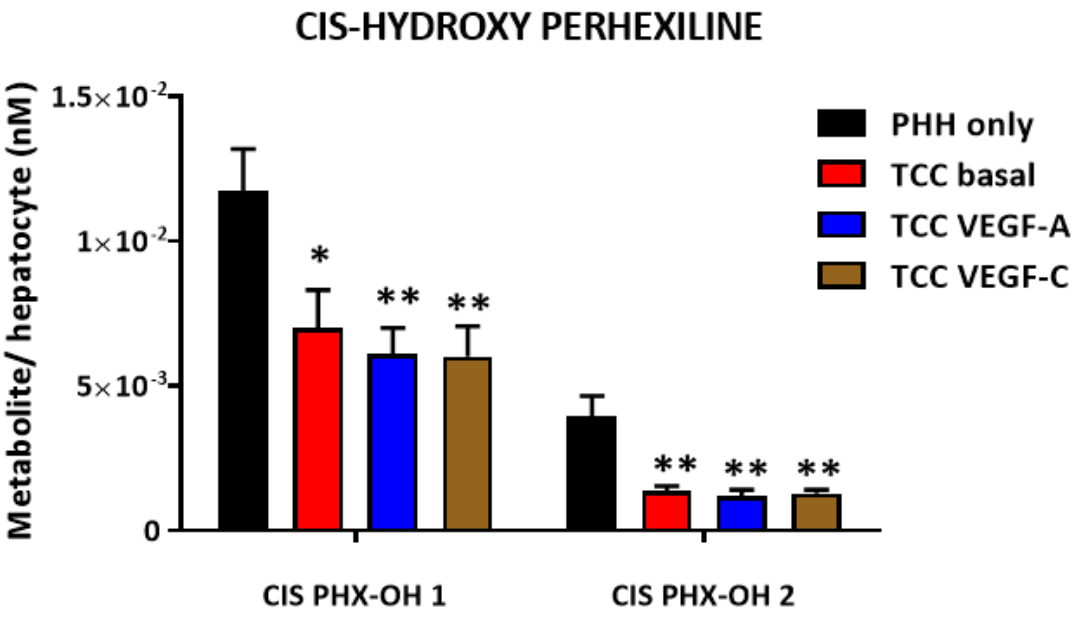

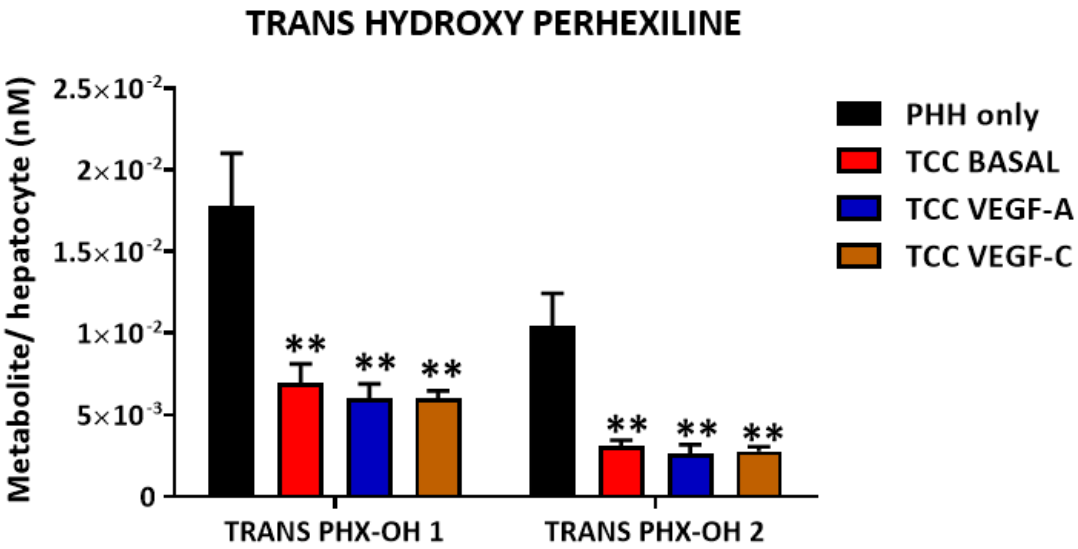

Figure 5.7: Inclusion of non-parenchymal cells inhibits the metabolism of perhexiline in human liver microtissues-

A total of 1500 cells were seeded on an ultra-low attachment plate, centrifuged and incubated at 37°C for 7 d to allow cells to self-aggregate into microtissues as described in the Method section. On day 7, microtissues were incubated with 5 µM of perhexiline for 24 h after which samples were snap frozen and stored at -20C before analysis. Samples were analysed for LC/MS/MS for identification of metabolites of perhexiline as described in the method section. Amount of metabolites produced in the samples were corrected for the number of hepatocytes in liver microtissues. Concentration of metabolites analysed and compared using one way analysis of variance ANOVA followed by Dunnett's multiple comparison test. Values are significant at *$p < 0.05$, **$p < 0.01$. (n=6). PHH only: Microtissues containing a total of 1500 freshly-isolated primary human hepatocytes, TCC: triculture microtissues comprising primary human hepatocytes, liver sinusoidal endothelial cells and human hepatic fibroblasts in a ratio of 8:2:2 to a total of 1500 cells. BASAL, VEGF-A, and VEGF-C: microtissue incubated with culture medium, culture medium supplemented with 50 ng/ml VEGF-A, culture medium supplemented with 50 ng/ml VEGF-C respectively. PHX-OH: hydroxy perhexiline.

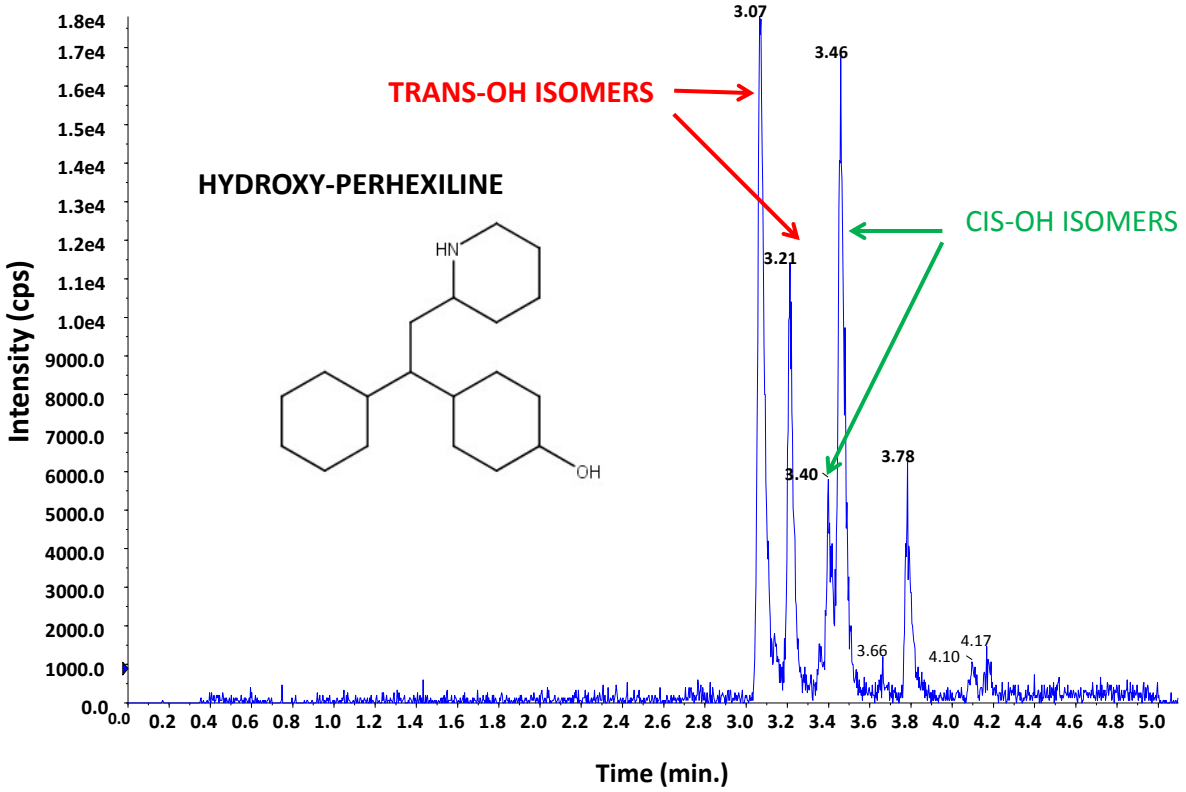

Figure 5.8: Chromatogram of perhexiline metabolism-

A total of 1500 cells were seeded on a ultra-low attachment plate, centrifuged and incubated at 37°C for 7 d to allow cells to self-aggregate into microtissues as described in the Method section. On day 7, microtissues were incubated with 5 µM of perhexiline for 24 h after which samples were snap frozen and stored at -20C before analysis. Samples were analysed for LC/MS/MS for identification of metabolites of perhexiline as described in the method section. Amount of metabolites produced in the samples were corrected for the number of hepatocytes in liver microtissues. PHH only: Microtissues containing a total of 1500 freshly-isolated primary human hepatocytes, TCC: triculture microtissues comprising primary human hepatocytes, liver sinusoidal endothelial cells and human hepatic fibroblasts in a ratio of 8:2:2 to a total of 1500 cells. BASAL, VEGF-A, and VEGF-C: microtissues incubated with culture medium, culture medium supplemented with 50 ng/ml VEGF-A, culture medium supplemented with 50 ng/ml VEGF-C respectively.

5.2.5 Sensitivity of liver microtissues to hepatotoxic drugs

Having observed a significant difference in the expression and activity of drug metabolising enzymes in mono-culture and tri-culture liver microtissues, their relative sensitivity to a range of hepatotoxic drugs was investigated. This was done in order to explore the possibility of a correlation between the metabolism and toxicity. Also, since VEGF-A and VEGF-C were shown in chapter 4 above to induce the factors responsible for liver regeneration, and that exogenous administration of VEGF-A significantly reduced paracetamol-induced liver toxicity in rats (Donahower et al., 2010a), it was hypothesised that VEGF-A and VEGF-C might confer a protective effect on the liver microtissues.

5.2.5.1 Paracetamol toxicity

The sensitivity of primary human hepatocyte in monolayer was compared to that in a microtissue configuration. Figure 5.9 shows that paracetamol is more toxic to PHH in monolayer than in the microtissue configuration. While the IC_{50} value for paracetamol in the monolayer was 3.3 mM, it was approximately 10 mM in microtissues. This represents a 3-fold difference in sensitivity. The presence of other cell types in the microtissues did not make any difference in this respect. Figure 5.10 shows a different trend in the presence of growth factors. Neither VEGF-A nor VEGF-C protected the liver microtissues against paracetamol toxicity as

the IC_{50} was constant in all the systems. This shows that growth factors do not confer any protection to liver microtissues.

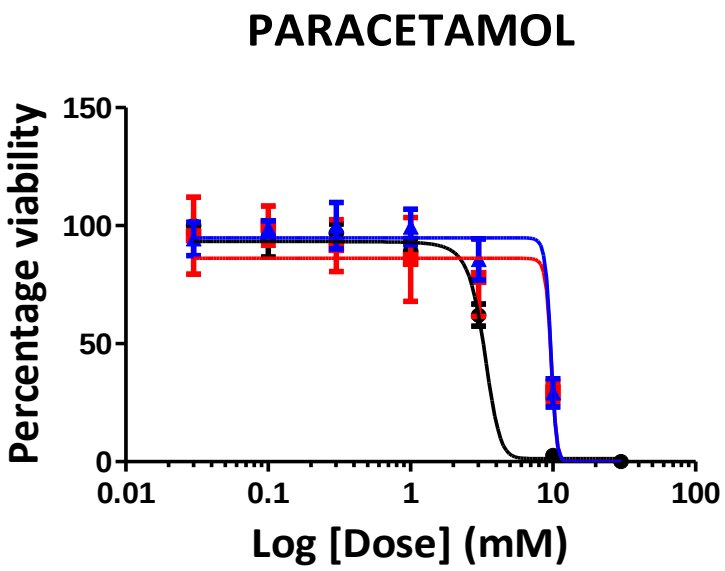

	PHH MONOLAYER	PHH MICRO-TISSUE	TRICULTURE MICRO-TISSUE
IC_{50} (mM)	3.3	9.7	9.6

Figure 5.9: Primary human hepatocytes in monolayer are more sensitive than liver microtissues to paracetamol toxicity-

Dose-response curve comparing toxicity of paracetamol on liver microtissues with primary human hepatocytes in monolayer. For liver microtissues, a total of 1500 cells were seeded on ultra-low attachment plates, centrifuged and incubated at 37°C for 7 d to allow cells to self-aggregate into microtissues as described in the Method section. On day 7, serial doses of paracetamol were prepared in culture medium. Microtissues were dosed for 72 h with 100 µl of drugs or medium, after which an equal volume of 3D Cell Titer Glo® reagent was added and assayed for ATP content as described in methods. Primary human hepatocytes in monolayers were plated, incubated, treated and assayed for ATP as previously described. IC_{50} values were estimated and dose-response curve generated using GraphPad Prism 5. (n=3, three independent experiments). PHH monolayer: Primary human hepatocytes seeded out in a monolayer configuration, PHH microtissue: microtissue containing primary human hepatocytes only. Triculture microtissue: microtissue comprising primary human hepatocytes, liver sinusoidal endothelial cells and human hepatic fibroblasts in a ratio of 8:2:2 to a total of 1500 cells.

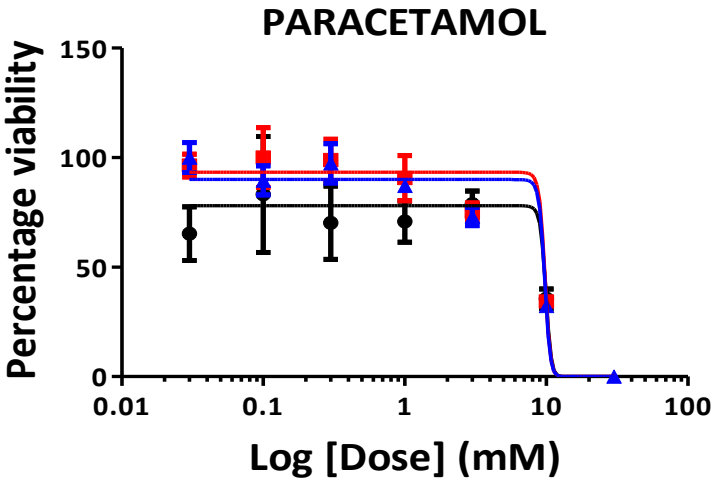

	BASAL	VEGF-A	VEGF-C
IC_{50} (mM)	9.9	9.8	9.7

Figure 5.10: Growth factor supplementation does not impact on the toxicity of paracetamol on liver microtissues-

Dose-response curve showing effect of paracetamol on liver microtissues. A total of 1500 cells were seeded on ultra-low attachment plates, centrifuged and incubated at 37°C for 7 d to allow cells to self-aggregate into microtissues as described in the Method section. On day 7, serial doses of paracetamol were prepared in culture medium. Microtissues were dosed for 72 h with 100 µl of drugs or medium, after which an equal volume of 3D Cell Titer Glo® reagent was added and assayed for ATP content as described in methods. IC_{50} values were estimated and dose-response curve generated using GraphPad Prism 5. (n=3, three independent experiments). VEGF-A: triculture microtissues comprising primary human hepatocytes, liver sinusoidal endothelial cells and human hepatic fibroblasts in a ratio of 8:2:2 to a total of 1500 cells and supplemented with 50 ng/ml of VEGF-A, VEGF-C: triculture microtissues comprising primary human hepatocytes, liver sinusoidal endothelial cells and human hepatic fibroblasts in a ratio of 8:2:2 to a total of 1500 cells and supplemented with 50 ng/ml of VEGF-C.

5.2.5.2 Regorafenib toxicity

To test whether the effect seen above was specific to paracetamol, and to investigate if growth factor administration could protect against TKI-induced toxicity, the experiments were repeated using regorafenib. Figure 5.11 shows a different trend. It reveals that in addition to growth factor stimulation not influencing the IC_{50} of regorafenib, the toxicity of regorafenib was the same in

monolayer (monoculture and triculture) and well as in microtissues (monoculture, tri-culture, agonist stimulated or basal).

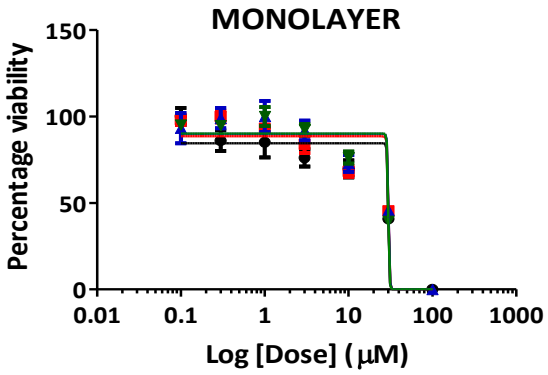

	PHH	TCC BASAL	TCC VEGF-A	TCC VEGF-C
IC50 (µM)	30.0	30.0	30.0	29.9

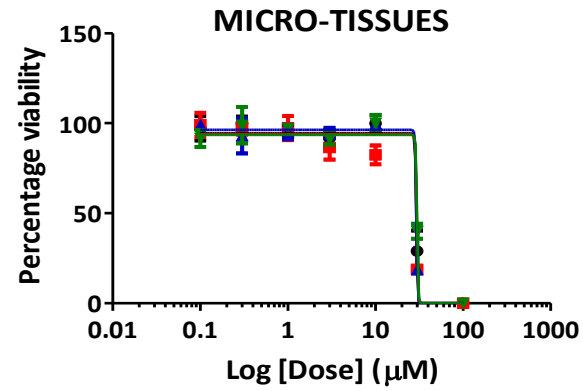

	PHH	TCC BASAL	TCC VEGF-A	TCC VEGF-C
IC50 (µM)	29.7	29.4	29.4	29.9

Figure 5.11: Regorafenib is equitoxic to hepatic cells in monolayer and in microtissue configuration-

Dose-response curve showing effect of regorafenib on liver monoculture and triculture liver microtissue and in monolayer system. A total of 1500 cells were seeded on an ultra-low attachment plate, centrifuged and incubated at 37°C for 7 d to allow cells to self-aggregate into microtissues as described in the Method section. On day 7, serial doses of the regorafenib originally constituted in DMSO were prepared. Final dosing concentrations or blank DMSO was made in HLSEC medium to a uniform concentration of 0.1 % DMSO. Microtissues were dosed for 72 h with 100 µl of drugs or medium containing 0.1 % DMSO, after which an equal volume of 3D Cell Titer Glo® reagent was added and assayed for ATP content as described in methods. Primary human hepatocytes in monolayers (monoculture and triculture) were plated, incubated, treated and assayed for ATP as previously described. IC_{50} values were estimated and dose-response curve generated using GraphPad Prism 5. (n=3). PHH; microtissues containing a total of 1500 freshly-isolated primary human hepatocytes, TCC: triculture microtissues comprising primary human hepatocytes, liver sinusoidal endothelial cells and human hepatic fibroblasts in a ratio of 8:2:2 to a total of 1500 cells. BASAL, VEGF-A, and VEGF-C: microtissue incubated with culture medium, culture medium supplemented with 50 ng/ml VEGF-A, culture medium supplemented with 50 ng/ml VEGF-C respectively.

5.2.5.3 Toxicities of other liver toxins

In order to extend the observations made with paracetamol and regorafenib, liver microtissues were dosed with aflatoxin, benzbromarone, desipramine and perhexiline. These drugs have been reported to induce liver injury via different mechanisms, including generation of reactive metabolites, mitotoxicity and induction of apoptosis. Figure 5.12 shows the toxicities of benzbromarone, desipramine and perhexiline in monoculture liver microtissues relative to microtissues with or without growth factor supplementation. The IC_{50} of aflatoxin was less than 1 µM in all systems whereas benzbromarone had similar IC_{50} in the range of 95-108 µM in all the conditions. A different trend was seen for desipramine and perhexiline. As for desipramine, the monoculture and unstimulated triculture microtissues had a similar IC_{50} at approximately 18 µM. On the other hand, the VEGF-A and VEGF-C- stimulated microtissues were less sensitive, with 50 % cell death at 31 and 32.6 µM respectively. Primary human hepatocyte-only microtissues were more than 5-fold less sensitive to perhexiline compared to triculture microtissues. This observation suggests that the presence of non-parenchymal cell makes liver microtissues more sensitive to perhexiline toxicity irrespective of growth factor stimulation.

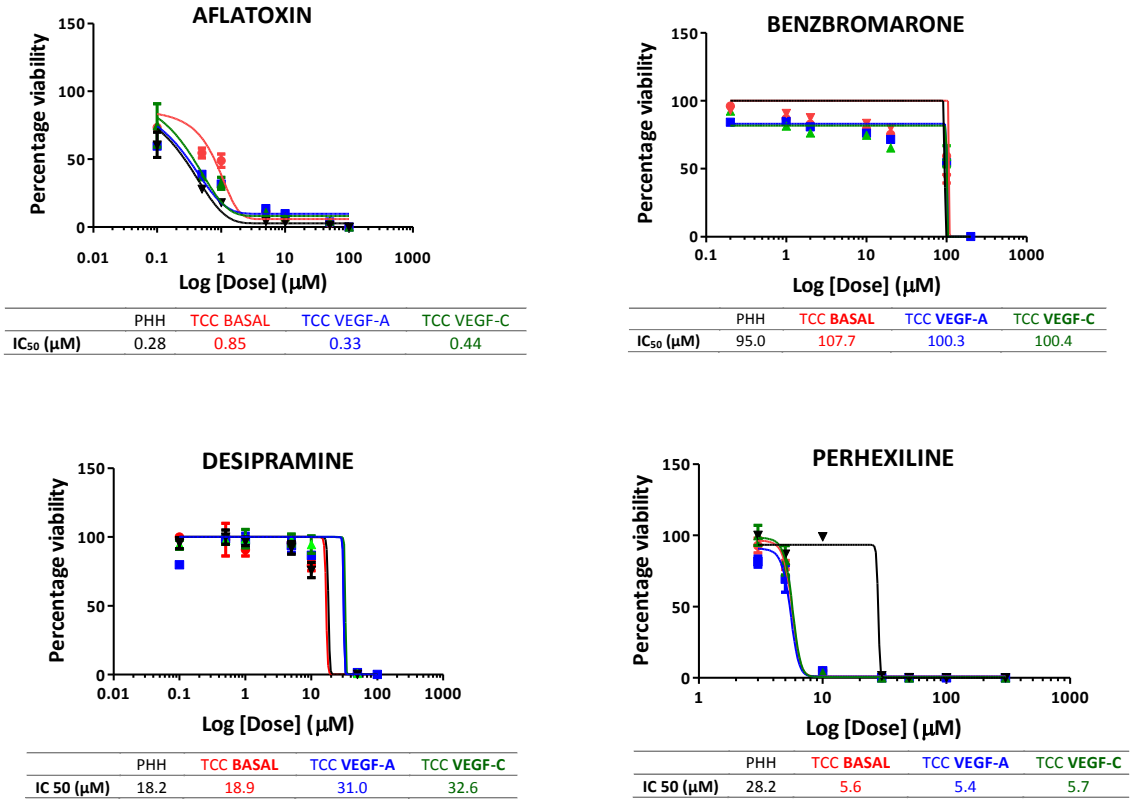

	PHH	TCC BASAL	TCC VEGF-A	TCC VEGF-C
IC_{50} (µM)	0.28	0.85	0.33	0.44

	PHH	TCC BASAL	TCC VEGF-A	TCC VEGF-C
IC_{50} (µM)	95.0	107.7	100.3	100.4

	PHH	TCC BASAL	TCC VEGF-A	TCC VEGF-C
IC 50 (µM)	18.2	18.9	31.0	32.6

	PHH	TCC BASAL	TCC VEGF-A	TCC VEGF-C
IC 50 (µM)	28.2	5.6	5.4	5.7

Figure 5.12: Effect of hepatotoxic drugs on liver microtissues-

Dose-response curve showing effect of hepatotoxic drugs on liver monoculture and triculture liver microtissue. A total of 1500 cells were seeded on an ultra-low attachment plate, centrifuged and incubated at 37°C for 7 d to allow cells to self-aggregate into microtissues as described in the Method section. On day 7, serial doses of the drugs originally constituted in DMSO were prepared. Final dosing concentrations or blank DMSO was made in HLSEC medium to a uniform concentration of 0.1 % DMSO. Microtissues were dosed for 72 h with 100 µl of drugs or medium containing 0.1 % DMSO, after which an equal volume of 3D Cell Titer Glo® reagent was added and assayed for ATP content as described in methods. IC_{50} values were estimated and dose-response curve generated using GraphPad Prism 5. (n=3). PHH; microtissues containing a total of 1500 freshly-isolated primary human hepatocytes, TCC: triculture microtissues comprising primary human hepatocytes, liver sinusoidal endothelial cells and human hepatic fibroblasts in a ratio of 8:2:2 to a total of 1500 cells. BASAL, VEGF-A, and VEGF-C: microtissues incubated with culture medium, culture medium supplemented with 50 ng/ml VEGF-A, culture medium supplemented with 50 ng/ml VEGF-C respectively.

5.3 DISCUSSION

Liver sinusoidal endothelial cells self-organise in liver microtissues to form a network that can take different appearances depending on the predominant growth factor environment. This can be very important while studying the cell-specific toxic effect of drugs in a multicellular liver microtissue system. As reviewed in the introductory section, the VEGF-A/ VEGFR-2 signalling pathway plays a key role in organogenesis whereby the nascent HLSEC create a pattern for the formation of lobular organisation of the liver by directing the liver into cords (Matsumoto et al., 2001, McLin & Yazigi, 2011). The observation made in figure 5.2 whereby VEGF-A and VEGF-C formed different patterns of HLSEC growth within the liver microtissue might suggest different roles of these angiogenic factors. It stands to reason that during hepatogenesis, VEGF-A may be responsible for proliferation of the primordial HLSEC while VEGF-C helps direct the pattern of growth to form the sinusoid. This might involve the VEGF-C/VEGFR-3 axis as VEGFR-3 is essential during embryonic angiogenesis (Paavonen et al., 2000), and a knockout of the VEGFR-3 has been shown to be embryonically lethal (Dumont et al., 1998). It would be informative to investigate the role of VEGF-C/VEGFR-3 in hepatogenesis.

5.3.1 Expression and activity of drug-metabolising enzymes in liver microtissues

There was a dramatically low level of drug-metabolising enzymes in the cells cultured as monolayers over a period of 7 d (Fig. 5.3). This is in agreement with previously published data that showed that hepatocytes de-differentiate in culture (Heslop et al., 2016). This shows that presence of other non-parenchymal cells does not improve the expression of these enzymes. On the other hand PHH-only microtissues maintained a level of CYPs 3A4 and 2D6 as well as UGT 1A1 comparable to what was observed in freshly-isolated PHH and whole liver tissue. Takahashi *et al.* (2015) and Gaskell *et al.* (2016) have reported an improved hepatic phenotype in 3D liver spheroids compared with cells cultured as a monolayer. While these were performed on HepaRG and HepG2 cells, Bell et al. (2016) have shown that PHH microtissues exhibit a remarkably improved maintenance of hepatocyte-specific functions including drug metabolism. However, none of these studies have included primary HLSEC and/ or HHF. The finding that inclusion of non-parenchymal cells (HLSEC and HHF) reduced the protein expression of these enzymes in tri-culture microtissues (figs. 5.3, 5.4, 5.6 and 5.7) is indicative of the possibility of an enzyme inhibitory activity in the presence of these cells. This 'inhibitory' effect was also seen in the drug metabolism studies wherein the triculture microtissues effected a significant reduction in the metabolites – oxidative and conjugative— formed in paracetamol and perhexiline (figs. 5.4, 5.6 and 5.7). This shows that presence of non-parenchymal cells (HLSEC and HHF) not only affected the protein expression of these enzymes, it also affected their catalytic activities.

5.3.2 Sensitivities of liver microtissues to hepatotoxic drugs

As shown in the previous chapter, paracetamol was equitoxic to all the monolayer-grown cells tested in the comparative toxicological analysis. However, microtissues were 3-fold less sensitive to this toxic effect regardless of presence of non-parenchymal cells or growth factor supplementation. Previous studies have shown that paracetamol causes LDH leakage—an indication of loss of plasma membrane integrity in hepatocytes (Bajt *et al.*, 2004). This observation may be indicative of the possibility that the microtissues provide a protective layer against this effect as constituent cells in microtissues are held together by adhesion molecules and the formation of extracellular matrix (Lin *et al.*, 2006). The inability of growth factor supplementation to confer protection on the triculture liver microtissue may suggest that the effect reported by Donahower et al. (2010a), that administration of recombinant VEGF-A protected against a mouse model of paracetamol toxicity, cannot yet be replicated *in vitro* using this model of human liver microtissues. This might also be suggestive of species difference in sensitivity to hepatotoxic drugs. A more relevant direct comparison would probably require an experiment with liver microtissues using hepatic cells derived from mice. On the other hand, regorafenib was toxic to liver microtissues at the same concentration as hepatocytes in monolayer. The fact that regorafenib targets both hepatocytes and HLSEC as shown in the previous chapter might explain the result obtained with the liver microtissue, in which the presence or absence of HLSEC did not offer any protection. This was

different in the case of perhexiline where the presence of non-parenchymal cells resulted in liver microtissues being 5-fold more sensitive to perhexiline. Perhexiline is metabolised by CYP 2D6 (Davies et al., 2007) which is polymorphic in expression wherein about 5-10% of Caucasians are poor metabolisers with two non-functional allelic variants of the CYP 2D6 gene (Zhou, 2009). An early study associated perhexiline-induced liver injury with impaired debrisoquine metabolism (Morgan *et al.*, 1984); and debrisoquine is a probe drug for CYP 2D6 activity. Since the elimination of perhexiline is dependent on its oxidative metabolism to its hydroxy derivatives which make it more hydrophilic and so more excretable, a deficiency in this would increase the plasma half-life of the parental compound up to 30 days compared to 3-12 days in normal metabolisers (Wright *et al.*, 1973, Ashrafian et al., 2007). This increases the time of exposure to perhexiline which increases the likelihood of its toxicity among the poor metabolisers. As reviewed in Chapter 1 of this thesis, the amphiphilic nature of the perhexiline molecule predisposes it to be rapidly accumulated in the mitochondrion at high concentrations where it uncouples mitochondrial oxidative phosphorylation by inhibiting complexes I and II, resulting in decreased ATP formation (Deschamps *et al.*, 1994, Fromenty & Pessayre, 1995). Although it was not a case of genetic polymorphism, a direct link can be established between the CYP expression data (fig. 5.3), the metabolism data (figure 5.7) and the toxicity data (fig. 5.12) wherein the low expression of CYP 2D6 in the triculture liver microtissue led to a significantly low metabolism in comparison with the PHH-only microtissues. The relatively poor metabolism of perhexiline in the triculture microtissues explains the low IC_{50} seen as a high level of the parental would have accumulated in the cells, leading to increased toxicity.

A major limitation of the experimental setup in this chapter was the inability to utilise cells from same donor for the triculture microtissues. This emanated from the fact that primary human hepatocytes needed to be used freshly after isolation while HLSEC and HHF used required time to expand before being ready for experiments. If the primary human hepatocytes had been cryopreservable, then it would have been possible to donor-match all the cells in every triculture liver microtissue experiments. This would have possibly improved the expression of hepatocyte specific markers.

In conclusion, the data in this chapter has shown that HLSEC have the propensity to form a vascular-like network in a triculture liver microtissue environment which opens up the possibility to study the effect of growth factor stimulation on these. This could be further developed to enable the evaluation of cell-specific effects of xenobiotics in a multicellular system. While the microtissues had a higher expression of key metabolic enzymes compared to cells in monolayer configuration, the triculture liver microtissue system seems to inhibit this. Metabolism studies also support this as CYP 2D6 and CYP 2E1-dependent metabolisms were significantly lower in the triculture liver microtissues. Finally, the low metabolic competence of the tri-culture liver microtissue may explain the high toxicity of perhexiline in triculture liver microtissue as hydroxylation is an important detoxification and elimination pathway for perhexiline.

CHAPTER SIX

OVERALL DISCUSSION

6.1 INTRODUCTION

Drug-induced liver injury (DILI) remains a leading cause of drug withdrawal and attrition at different stages of development (Laverty *et al.*, 2011, Haque *et al.*, 2016), resulting in loss of time and other resources invested into drug development, hence a loss of potentially efficacious therapeutic agents. Reasons for withdrawal range from mild elevation of liver transaminases to chronic liver failure (Akingbasote *et al.*, 2016). As a result of these, there remains the need for an *in vitro* model system that can detect hepatotoxicity earlier on during pre-clinical development. To date, most preclinical studies have primarily employed the use of hepatocytes aimed at understanding and preventing DILI due to their overall abundance within the hepatic lobule as they make up over 60% of hepatic cell population (Rogers & Dintzis, 2012). Nevertheless, other resident cell types of the liver can and do play a role in DILI. This was the aim of this thesis—specifically to investigate the role of liver sinusoidal endothelial cells (LSEC) in DILI. The data shown and discussed in the previous chapters have highlighted the uniqueness of LSEC especially in comparison with endothelial cells from other vascular beds. It shows the response of HLSEC to hepatotoxic drugs of different classes, with emphasis on small-molecule receptor tyrosine kinase inhibitors. The result chapters also addressed the inclusion of HLSEC in a multicellular liver microtissue system. This final chapter is a summary of the findings from this study— new findings, potentials and future directions.

6.1.1 Liver sinusoidal endothelial cells are a unique endothelial cell population and differ from other endothelial cell populations

Results obtained from this thesis further confirms liver sinusoidal endothelial cells as a unique endothelial cell population. In addition to the expression of markers – CD-31, VEGFR-1, and VEGFR-2 which indicates their identity as endothelial cells (Zhuang & Ferrara, 2015), they also responded to a range of relevant growth factors that mediate their physiologic functions of proliferation, migration and tubular morphogenesis (Holmes et al., 2007, Koch & Claesson-Welsh, 2012). Data in Chapter 3 shows that HLSEC have a higher expression of VEGFR-2 relative to HDMEC and HDLEC. Being a liver-resident cell population and the first point of contact with xenobiotics and other pathogenic substances, LSEC might have been well adapted to this environment by the expression of this cell-survival mediating receptor, since VEGFR-2 is key to the activation of the intracellular signalling pathways that mediate endothelial cell survival, proliferation, and migration culminating in angiogenesis. Another important scenario that makes the high expression of VEGFR-2 on LSEC very important to liver physiology is in liver regeneration. In a ground-breaking research by Ding and co-workers, it was demonstrated that during liver injury or partial hepatectomy in mice, hepatocytes released VEGF-A (Ding et al., 2010a, Ding et al., 2014). LSEC respond to this via a cascade of events that results in the release of hepatocyte growth factor (HGF) which then stimulate hepatocyte proliferation and consequent liver regeneration. During this process, there is also a high rate of LSEC proliferation which help create the vasculature that guide the arrangement of the hepatocytes into cords and in

the perfusion of the regenerated liver. It is therefore conceivable that a high expression of VEGFR-2 on LSEC would be key to this process. VEGFR-3 is expressed on HLSEC as shown in Chapter 3. Whilst the experiments carried out focussed primarily on the activation of VEGFR-2 on HLSEC upon exposure to VEGF-A and VEGF-C, the importance of the formation of VEGFR-2/VEGFR-3 heterodimer might need investigating. By employing *in situ* proximity ligation assay (PLA), Nilsson *et al.* (2010) have demonstrated that VEGF-C or VEGF-A could form VEGFR-2/VEGFR-3 heterodimers in primary human saphenous endothelial cells. They further showed that neutralising VEGFR-3 and preventing the formation of VEGFR-2/ VEGFR-3 heterodimers in an embryoid body model of angiogenesis prevented angiogenic sprouting. Since HLSEC express VEGFR-3, the formation of such heterodimers is likely; that might provide new insight into the regulation of the sinusoidal vasculature. Other important aspects of the uniqueness of the LSEC is the expression of L-SIGN, stabilin-1, stabilin-2, mannose receptor C1, which play key roles in scavenging and endocytosis of foreign substances (Politz *et al.*, 2002, Gardner *et al.*, 2003, Cormier et al., 2004, Malovic et al., 2007).

As shown in chapter 3, the presence of fenestration on the surface of LSEC by scanning electron microscopy and the high expression of plasmalemma vesicle associated protein (PLVAP) and serotonin (5-hydroxytryptamine [5-HT]) receptor 2B detected by whole transcriptome analysis is another indication of the uniqueness of LSEC as an endothelial cell population. As already reviewed in chapter 1 and discussed in chapter 3, liver sinusoidal endothelial cells are the only endothelial cell population that are fenestrated and they lack an organised basement membrane; glomerular endothelial cells are also fenestrated, but they

do have an organised basement membrane (DeLeve, 2007). A basement membrane is a thin layer of fibrous tissue or extracellular matrix material that separates the endothelium from the underlying tissue (Kierszenbaum & Tres, 2015). In the kidney, glomerular basement membrane (Miner, 2012) is an important component of the glomerular filtration system, which separates the glomerular vasculature from the urinary space. It is important to note that the fenestrations on the glomerular endothelial cells are 'plugged' by a glycocalyx-like material which further imparts a barrier function to the endothelium (Haraldsson & Jeansson, 2009). On the contrary, LSEC lack a basement membrane, but an interstitial space referred to as space of Disse (SD) is present between the endothelial compartment and the underlying hepatocytes. As reviewed in Chapter 1, the fenestration on LSEC permits the movement of xenobiotics and chylomicrons of diameters less than those of the fenestrations to gain access to hepatocyte in order to effect their metabolism (Wisse et al., 1996). Any process that causes the reduction of these 'transcellular windows' is termed capillarisation or pseudocapillarisation and is deleterious to both LSEC function and obviously liver physiology (DeLeve et al., 2004), resulting in hyperlipidaemia and atherosclerosis (Stolz, 2011a). An important finding in this study was the high expression of the plasmalemma vesicle associated protein (PLVAP) on HLSEC which has been shown to be important in the regulation of fenestrations. As discussed in chapter 3, a knock out of *PLVAP* results in hyperlipoproteinaemia (Herrnberger et al., 2012). A study identified PLVAP as a molecular target in hepatocellular carcinoma due to the high expression of PLVAP in this cancer type (Wang *et al.*, 2014), without regard for its role in LSEC physiology. A monoclonal

antibody directed against PLVAP was shown to reduce tumour size in a mouse model of hepatocellular carcinoma. The problem with this strategy is the fact that this target is present on normal cells and are needed for their physiology. In fact, it is possible that the high expression of PLVAP in hepatocellular carcinoma was due to angiogenesis-derived LSEC which evidently would also express this gene. Therefore, should this anti-PLVAP monoclonal antibody be carried forward into development, there is all likelihood of patients being later diagnosed with hyperlipidaemia. Another important aspect relating to the uniqueness of LSEC and their possession of fenestration is the result obtained in Chapter 3 which shows a significant increase in fenestration in VEGF-A stimulated cells in comparison with unstimulated control. A link can be established here with PLVAP expression on the LSEC. Strickland *et al.* (2005) demonstrated that VEGF-A, in a time dependent manner, produced an increase in the expression of PLVAP via VEGFR-2-AKT signalling pathway. Hence, the findings that PLVAP was highly expressed on HLSEC and that VEGF-A induced a significant increase in HLSEC fenestration may be related.

As reviewed in chapter 1, fenestration on LSEC is regulated via serotonin receptor 2 (5-HT_2) activation (Gatmaitan et al., 1996). Some antidepressant drugs are known to induce liver injury among which is desipramine which acts by inhibiting the uptake of serotonin in the post synaptic cleft (Peppin & Raffa, 2015). It has been shown that desipramine treatment induced a downregulation of the 5-HT_2 receptor in the brains of rodents (Yatham *et al.*, 1999). There is a high possibility of desipramine inducing this effect on the liver sinusoidal endothelial cells, being the first group of cells to come in contact with the drug as it enters into the liver

via hepatic portal vein. That being the case, a downregulation of the 5-HT_2 receptor would indeed impact on the regulation of the fenestration on the LSEC, thereby reducing its contractile ability and enabling the entry of larger substances into the SD and the hepatocyte. The relative sensitivity of HLSEC to desipramine in an *in vitro* cell viability assay as shown in Chapter 4 might be an indication of this possibility. Further, transcriptomic analysis has shown the expression of other genes like nitric oxide synthase trafficking (NOSTRIN) which is involved in the regulation of the synthesis of NO by lowering the activity of eNOS (Xu *et al.*, 2013). Since LSEC is a major site of NO production (Perri & Shah, 2005b), the relatively high expression of NOSTRIN might be required to control the amount of NO produced so as to regulate local vascular dilation in the liver sinusoid.

6.1.2 Liver sinusoidal endothelial cells are direct targets of hepatotoxic drugs

Data from Chapter 4 of this thesis shows the relative sensitivity of HLSEC to a range of hepatotoxic drugs in comparison with dermal vascular and lymphatic endothelial cells, human hepatic fibroblasts and primary human hepatocytes. HLSEC was relatively more sensitive to the small molecule receptor tyrosine kinase inhibitors (TKIs) screened. These TKIs inhibited the activation of VEGFR-2 with the subsequent inhibition of the downstream signalling pathways. The different TKIs inhibited the VEGFR-2 activation to different extents and at different concentrations. Regorafenib was chosen as the representative TKI due to its well-reported liver

toxicity in the clinic (Grothey et al., 2013, Demetri et al., 2013). Regorafenib induced an inhibition of VEGFR-2 mediated cell migration, tubular morphogenesis and upregulation of angiocrine factors involved in liver regeneration following stimulation with VEGF-A or VEGF-C. It also induced apoptosis by activation of caspase 3 in HLSEC as well as in hepatocytes. It caused a disruption of the actin cytoskeleton in HLSEC. Put together, this set of data shows that the HLSEC is a direct target in TKI toxicity. Effects of regorafenib on HLSEC could be summed up into functional and structural toxicity. The fact that anti-angiogenic drugs mainly target the mechanisms involved in the formation and maintenance of vasculature increases the chances of vascular toxicity; the same molecular targets are also required for normal endothelial cell physiology (Widakowich et al., 2007, Gotink & Verheul, 2010a). This shows the need to discover more tumour-vasculature-specific molecular targets to address this problem. One way this can be done is to isolate the endothelial cells from tumours and profile their gene expression pattern with that of normal vasculature from the same organ. This should make it possible to avoid these on-target toxic effects. Secondly, the finding that HLSEC are selectively more sensitive to hepatotoxic drugs than primary human hepatocytes or human hepatic fibroblasts, as shown in this study, is an indication of their potential as early targets of DILI compounds as confirmed in previous studies (McCuskey *et al.*, 2001, McCuskey et al., 2005, McCuskey, 2006). Ito et al. (2003) demonstrated that injury to LSEC occurred before hepatocytes during paracetamol toxicity. This is not surprising as any substances entering the liver would first interact with LSEC before gaining access to the hepatocyte either for metabolic bioactivation or detoxification. From this perspective, it seems urgent to discover an LSEC specific

liver biomarker of DILI. This may not be far-fetched as is evidenced in the discovery of MiR-122 as a liver- and hepatocyte-specific biomarker of drug-induced liver injury (Wang *et al.*, 2009, Antoine *et al.*, 2013). A paracetamol model of liver injury might also be explored as a pilot study in this regard. Briefly, LSEC from normal control and paracetamol-treated mouse livers could be isolated and profiled for miRNA.

Another indication of LSEC being a direct target of hepatotoxic drugs is the structural effect seen with regorafenib as shown in Chapter 4. Regorafenib induced a time- and dose-dependent disruption in the cytoskeletal structure of HLSEC. This is in agreement with recent data by Wilkinson *et al.* (2016) who showed that the cardiotoxic anticancer drug, doxorubicin, does cause a disruption in the endothelium by interfering with the cytoskeletal structure of the human cardiac microvascular endothelial cells. Recent data shows that targeting the microvasculature with VEGF-B can protect against doxorubicin-induced cardiovascular injury (Räsänen *et al.*, 2016). A similar strategy could be adopted to protect against DILI.

Perhaps the novel finding in this aspect of the study is the data showing the inhibitory effect of regorafenib on one of the pathways required for liver regeneration. A physiologic response to liver injury is the activation of VEGFR-2 on LSEC by VEGF-A secreted by hepatocytes thereby starting a cascade that result in secretion of HGF which informs hepatocyte proliferation (Discussed in details in Chapter 1). The fact that regorafenib blocked this process is an indication of another likely mechanism of its mode of contribution to DILI. This is because if after exposure to hepatotoxic drugs, the homeostatic response of liver repair and

regeneration is disrupted, the initial insult would be exacerbated resulting in more severe damage to the liver. In the future, it would be informative to test this in an *in vivo* model.

6.1.3 Human liver sinusoidal endothelial cells in a triculture microtissue system

Chapter 5 showed the inclusion of HLSEC in a 3-cell liver microtissue system. This is perhaps the first time triculture liver microtissue has been generated using freshly-isolated primary human hepatocytes, primary human liver sinusoidal endothelial cells and primary human hepatic fibroblasts. Previous studies have relied upon immortalised cells as the source of one or all of the constituent cells (Gaskell et al., 2016). Some studies have also used non-liver derived endothelial cells including HUVEC (Takebe et al., 2013, Nelson et al., 2015). While the studies claimed improvement in liver function in comparison with hepatocytes or hepatocyte-like cells in monolayer, the results could not be directly related to what would have been obtained if primary liver cells were used. This was the case as reported by Ravenscroft *et al.* (2016) who demonstrated that contractile function of the cardiac microtissue depended on a triculture system comprising stem cell derived cardiomyocytes, cardiac microvascular endothelial cells and cardiac fibroblasts. They further showed that inclusion of non-cardiac fibroblast or non-cardiac endothelial cells did not impart functionality on the microtissues generated. This supports the strategy employed in the development of the liver microtissues presented in this thesis. Data in the initial part of Chapter 5 shows the ability of

HLSEC to vascularise the liver microtissues as demonstrated by immunofluorescence microscopy. This could be developed to create a novel model for the study of liver-specific angiogenesis. Also, as seen in chapter 4, HLSEC are selectively more sensitive to a range of hepatotoxic drugs especially small molecule tyrosine kinase inhibitors. This could be further explored in a multicellular microtissue system such that, with the use of imaging techniques that enable the visualisation of different constituent cell types, structural effect of drugs in these could be explored.

Chapter 5 also highlighted the advantage of 3D liver microtissue over hepatocytes in monolayer. Results confirmed previous findings that the 3D system better reconstitutes the *in vivo* environment wherein constituent cells are able to interact and communicate, thus enabling improved viability and functionality (Achilli et al., 2012, Takebe et al., 2013). In order to further this result, HLSEC, and human hepatic fibroblasts were included in the liver microtissues to recreate a more *in vivo*-relevant environment. Structurally, LSECs form the conduit that convey oxygen and nutrient into the liver while fibroblasts secrete extracellular matrix materials like collagen thereby enabling the organ to maintain its structure. In the experiments performed, it took hepatocyte-only microtissues almost twice the time it took triculture liver organoid to mature (data not shown). It was easier to handle triculture liver microtissues than their monoculture counterparts during the rigorous process of histological processing, as the inclusion of these other cell types conferred structure to the microtissues. This structural stability was expected to be translated into functionality. Surprisingly, the expression of drug-metabolising enzymes –CYP2D6, CYP3A4 and UGT1A1—was lower in the triculture liver

microtissues. These effects were further observed in drug metabolism studies using paracetamol (a CYP 2E1 and UGT 1A1 substrate) and perhexiline (a CYP 2D6 and UGT 1A1 substrate). After correcting for the cell number (for hepatocytes) in the liver microtissues, drug metabolism was significantly lower in the triculture microtissues than in their monoculture equivalent. Following this, the triculture liver microtissues were supplemented with VEGF-A and VEGF-C to stimulate the HLSEC to investigate if they (HLSEC) could produce factors that might ultimately improve function in hepatocytes. This was attempted since activation of VEGFR-2 on LSEC was an important first step in liver regeneration (Ding et al., 2010a, Ding et al., 2014). However, growth factor supplementation did not induce any improvement in expression and activities of these oxidative and conjugative enzymes. This raises questions as to why an opposite effect of hypothesised outcome was produced. This might have been a direct result of the isolation process that involved the use of collagenase which might have contributed to the rapid de-differentiation process of the hepatocytes *in vitro* (Bell et al., 2016, Heslop et al., 2016). Another highly likely explanation for this observation was the possibility of HLSEC and HHF producing cytokines with inhibitory effect on the expression of these liver enzymes. This line of argument may be worth examining as Abdel-Razzak *et al.* (1993) and Muntane-Relat *et al.* (1995) have demonstrated that such pro-inflammatory cytokines as interleukin-6 (Il-6), interleukin-1 alpha (Il-1 alpha), interferon gamma (IF-γ) and tumour necrosis factor-alpha (TNF-alpha) induced a suppression of CYP1A2, CYP2C, CYP2E1 and CYP3A mRNA and proteins in primary human hepatocyte culture. In studies carried out by Pascussi *et al.* (2000), and Ding and Staudinger (2005), it was suggested that these inflammatory

mediators, especially Il-6, repressed the phosphorylation of pregnane-X receptor (PXR) via the protein kinase C pathway which occurs in inflammation. PXR is the nuclear receptor involved in the transcription of the CYP3A family of genes (Bertilsson *et al.*, 1998). The fact that endothelial cells and fibroblast have been shown to produce Il-6 might partly explain the significant reduction in expression and activity of some of these drug-metabolising enzymes (Shalaby *et al.*, 1989, Tiggelman *et al.*, 1995). The regulation of CYP activity by inflammation mediators and by protein-protein interactions has been reviewed by Morgan (2001) and Oladimeji *et al.* (2016). Further work is required to establish this link in the triculture liver microtissue model. Another likely explanation for the observed reduction in the expression of these drug-metabolising enzymes is the 'zonation effect'. It is known that the expression and activity of drug-metabolising enzymes vary along the gradient of the zones of the liver as shown in Chapter 1; metabolism increases from periportal to centrilobular regions of the liver (Lindros, 1997) such that centrilobular hepatocytes are more metabolically competent. It has been shown that expressions of CYP 2E1 and CYP 3A4 are highest at the centrilobular zone of the liver (LeCluyse et al., 2012a). Whether the inclusion of HLSEC and HHF induced a zonation effect on the liver microtissues is a question that requires answering. It is worth noting, however, that liver zonation has been suggested to be regulated by cytokines (Gebhardt & Matz-Soja, 2014). As the metabolic gradient increases, the oxygen tension decreases along the periportal to centrilobular gradient (Colnot & Perret, 2011), implying that oxygen tension may have a direct bearing on the metabolic capabilities of hepatocytes. Traditionally, and as in this study, cell culture was carried out at the atmospheric oxygen tension of 20 % while

oxygen level in the centrilobular zone of the liver is usually at around 6.7% (Martinez *et al.*, 2008). Consequently, a future experiment would ideally perform all procedures at the physiologically-relevant oxygen tension of 5-6.7 % as this might make a difference in metabolic competence of the hepatocytes in the microtissues. Further, liver microtissues in this study were prepared with only HLSEC and HHF in addition to PHH. Stellate cells and Kupffer cells might be included in a 'complete' liver microtissue.

6.2 CONCLUSION AND FUTURE DIRECTION

The data from this thesis shows that human liver sinusoidal endothelial cells constitute a unique population that makes them well-suited to their vascular bed and a potential source of a liver specific marker of early–onset vascular toxicity. Its unique expression of lymphatic endothelial cell markers – VEGFR-3 and LYVE-1—also need to be further explored in order to uncover a unique role of LSEC in liver physiology which is as at yet not fully understood (Tanaka & Iwakiri, 2016). As transcriptomic data has shown, the high expression of oncogenes and tumour suppressor genes in HLSEC which might be a reflection of the tissue environment where the cells where isolated, it would be ideal to isolate HLSEC from liver of non-cancer patients (possibly from rejected liver transplants).

Human liver sinusoidal endothelial cells are a direct target of hepatotoxic drugs, especially small molecule receptor tyrosine kinase inhibitors as these inhibit endothelial cell physiology. In addition to inhibiting angiogenic mechanisms, regorafenib induced apoptosis in HLSEC via caspase 3 activation, caused a

disruption of cytoskeletal structure and blocked one of the important pathways required for liver regeneration via inhibition of VEGFR-2 activation. These *in vitro* outcomes – disruption of cytoskeletal structure of the HLSEC and inhibition of the VEGF-A/ VEGFR-2-mediated liver regeneration – need to be tested *in vivo*. While the exact molecular mechanism of the disruption of the cytoskeletal structure need to be elucidated, it would be imperative to employ the murine monocrotaline model of sinusoidal obstruction syndrome (SOS) to better understand this *in vivo* (DeLeve et al., 2003, Wang et al., 2005).

Finally, while liver microtissues are an improvement over hepatocytes cultured in monolayer in terms of expression of drug-metabolising enzymes, triculture liver microtissues had no advantage over their monocellular counterparts. Future work would need to address the hypothesis involving the release of proinflammatory cytokines which inhibit the activation of the nuclear receptors responsible for transcription of the genes coding for the cytochromes P450 proteins. In addition, an ideal multicellular microtissue should include other hepatic cells comprising primary human hepatocytes and additional non-parenchymal cells like stellate and Kupffer cells.

This study has demonstrated the uniqueness of liver sinusoidal endothelial cells and serves as a confirmation that any biological, pharmacological or toxicological research intended to study liver sinusoidal endothelial cells must indeed utilise liver sinusoidal endothelial cells. This has become clear as shown in this study because several published articles that purported to investigate LSEC utilised endothelial cells from other vascular beds. Only when LSEC is used can any study carried out

reflect LSEC-specific effect. Also, this study has shown that while LSEC is a direct target of hepatotoxic drugs and exhibit relatively higher sensitivity to hepatotoxic drugs, there is need to further develop experimental models that can specifically and directly elucidate the contribution of LSEC to DILI especially in a multicellular system. By means of this study, the potential role of liver sinusoidal endothelial cells in drug induced liver injury (by tyrosine kinase inhibitors) has been elucidated to be by blockage of the physiology of LSEC, structural damage by cytoskeletal disruption, and cell death by apoptosis via activation of caspase 3.

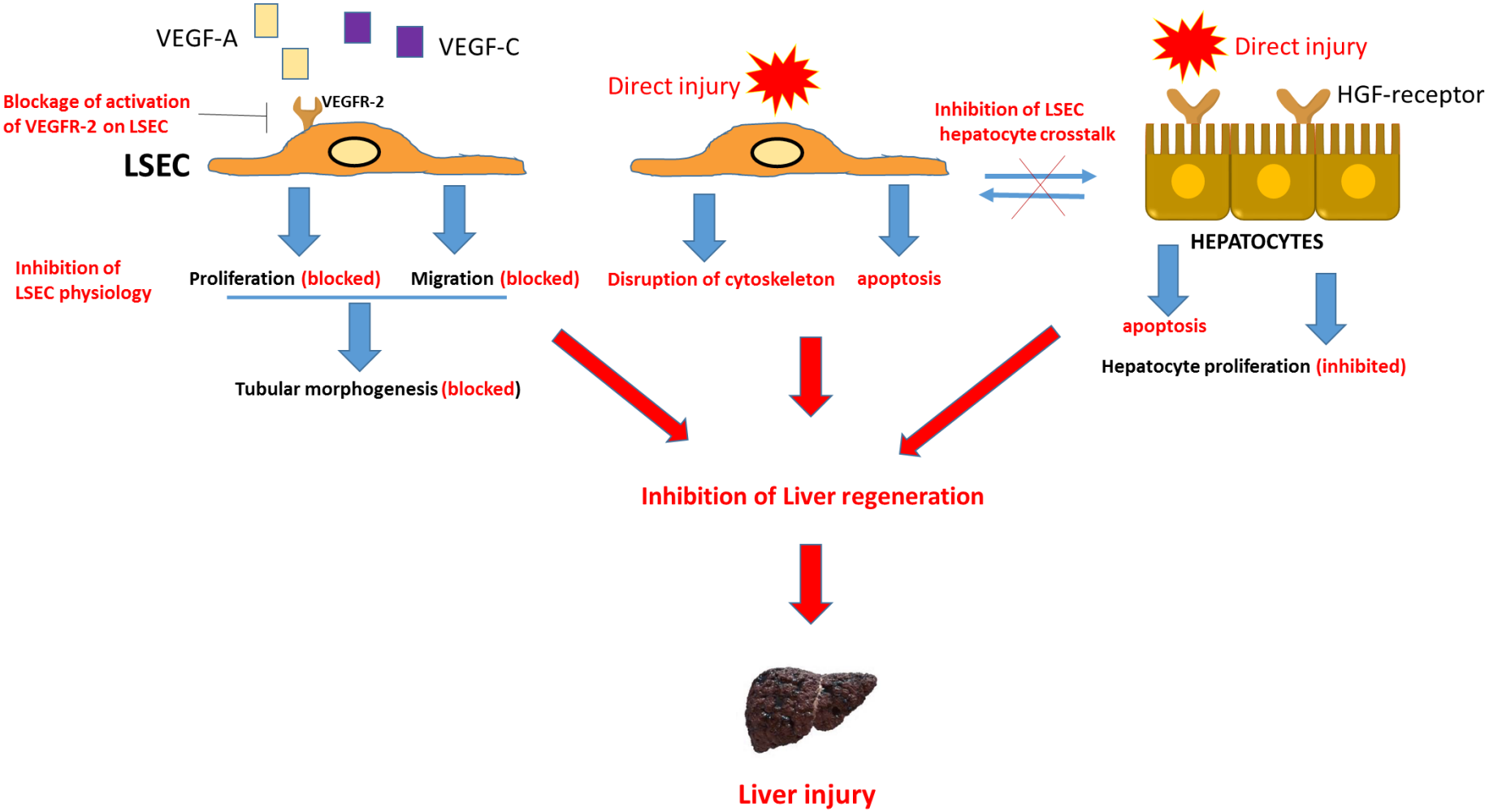

Figure 6.1: Summary figure of the role of liver sinusoidal endothelial cells in regorafenib-mediated drug-induced liver injury.
Regorafenib induces an inhibition of the activation of the VEGFR-2 receptor which normally initiates a series of cellular event including cell proliferation, migration and tubular morphogenesis. All these process were blocked in the presence of regorafenib. It causes a disruption of cytoskeletal structure of the LSEC. Regorafenib further blocks the process of liver regeneration and rather initiates apoptosis both on hepatocytes and the LSEC.

BIBLIOGRAPHY

Aase, K., von Euler, G., Li, X., Ponten, A., Thoren, P., Cao, R., Cao, Y., Olofsson, B., Gebre-Medhin, S., Pekny, M., Alitalo, K., Betsholtz, C. & Eriksson, U. 2001. Vascular endothelial growth factor-B-deficient mice display an atrial conduction defect. *Circulation* **104**:358-64.

Abdel-Razzak, Z., Loyer, P., Fautrel, A., Gautier, J. C., Corcos, L., Turlin, B., Beaune, P. & Guillouzo, A. 1993. Cytokines down-regulate expression of major cytochrome P-450 enzymes in adult human hepatocytes in primary culture. *Molecular pharmacology* **44**:707-15.

Abrams, T. J., Lee, L. B., Murray, L. J., Pryer, N. K. & Cherrington, J. M. 2003. SU11248 inhibits KIT and platelet-derived growth factor receptor beta in preclinical models of human small cell lung cancer. *Molecular cancer therapeutics* **2**:471-8.

Achilli, T. M., Meyer, J. & Morgan, J. R. 2012. Advances in the formation, use and understanding of multi-cellular spheroids. *Expert opinion on biological therapy* **12**:1347-60.

Akingbasote, J., Foster, A. J., Jones, H. B., David, R. M., Gooderham, N., Wilson, I. D. & Kenna, G. 2016. Improved hepatic physiology in hepatic cytochrome P450 reductase null (HRN[trade mark sign]) mice dosed orally with fenclozic acid. *Toxicology Research*.

Alvarez, C. P., Lasala, F., Carrillo, J., Muniz, O., Corbi, A. L. & Delgado, R. 2002. C-type lectins DC-SIGN and L-SIGN mediate cellular entry by Ebola virus in cis and in trans. *Journal of virology* **76**:6841-4.

Amali, M. O., Sullivan, A., Jenkins, R. E., Farrell, J., Meng, X., Faulkner, L., Whitaker, P., Peckham, D., Park, B. K. & Naisbitt, D. J. 2016. Detection of drug-responsive B lymphocytes and antidrug IgG in patients with beta-lactam hypersensitivity. *Allergy*.

Angulo, P. & Lindor, K. D. 2002. Non-alcoholic fatty liver disease. *Journal of gastroenterology and hepatology* **17**:S186-S90.

Antoine, D. J., Dear, J. W., Lewis, P. S., Platt, V., Coyle, J., Masson, M., Thanacoody, R. H., Gray, A. J., Webb, D. J. & Moggs, J. G. 2013. Mechanistic biomarkers provide early and sensitive detection of acetaminophen-induced acute liver injury at first presentation to hospital. *Hepatology* **58**:777-87.

Ashrafian, H., Horowitz, J. D. & Frenneaux, M. P. 2007. Perhexiline. *Cardiovascular Drug Reviews* **25**:76-97.

Ashtari, S., Pourhoseingholi, M. A. & Zali, M. R. 2015. Non-alcohol fatty liver disease in Asia: Prevention and planning. *World journal of hepatology* **7**:1788-96.

Badmann, A., Langsch, S., Keogh, A., Brunner, T., Kaufmann, T. & Corazza, N. 2012. TRAIL enhances paracetamol-induced liver sinusoidal endothelial cell death in a Bim- and Bid-dependent manner. *Cell death & disease* **3**:e447.

Bajt, M. L., Knight, T. R., Lemasters, J. J. & Jaeschke, H. 2004. Acetaminophen-induced oxidant stress and cell injury in cultured mouse hepatocytes: protection by N-acetyl cysteine. *Toxicological sciences* **80**:343-49.

Baldwin, M. E., Halford, M. M., Roufail, S., Williams, R. A., Hibbs, M. L., Grail, D., Kubo, H., Stacker, S. A. & Achen, M. G. 2005. Vascular endothelial growth factor D is dispensable for development of the lymphatic system. *Molecular and cellular biology* **25**:2441-9.

Bale, S. S., Vernetti, L., Senutovitch, N., Jindal, R., Hegde, M., Gough, A., McCarty, W. J., Bakan, A., Bhushan, A., Shun, T. Y., Golberg, I., DeBiasio, R., Usta, B. O., Taylor, D. L. & Yarmush, M. L. 2014. In Vitro Platforms for Evaluating Liver Toxicity. *Experimental biology and medicine (Maywood, N.J.)* **239**:1180-91.

Bates, D. O. & Harper, S. J. 2002. Regulation of vascular permeability by vascular endothelial growth factors. *Vascular pharmacology* **39**:225-37.

Baydar, T., Engin, A. B., Girgin, G., Aydin, S. & Sahin, G. 2005. Aflatoxin and ochratoxin in various types of commonly consumed retail ground samples in Ankara, Turkey. *Annals of agricultural and environmental medicine : AAEM* **12**:193-7.

Beath, S. 2003. hepatic function and physiology in the newborn. *Seminars in Neonatology* **8**:337-46.

Becker, M. A., Schumacher, H. R., Jr., Wortmann, R. L., MacDonald, P. A., Eustace, D., Palo, W. A., Streit, J. & Joseph-Ridge, N. 2005. Febuxostat compared with allopurinol in patients with hyperuricemia and gout. *N Engl J Med* **353**:2450-61.

Bell, C. C., Hendriks, D. F., Moro, S. M., Ellis, E., Walsh, J., Renblom, A., Fredriksson Puigvert, L., Dankers, A. C., Jacobs, F., Snoeys, J., Sison-Young, R. L., Jenkins, R. E., Nordling, A., Mkrtchian, S., Park, B. K., Kitteringham, N. R., Goldring, C. E., Lauschke, V. M. & Ingelman-Sundberg, M. 2016. Characterization of primary human hepatocyte spheroids as a model system for drug-induced liver injury, liver function and disease. *Scientific reports* **6**:25187.

Bellentani, S., Scaglioni, F., Marino, M. & Bedogni, G. 2010. Epidemiology of non-alcoholic fatty liver disease. *Digestive diseases (Basel, Switzerland)* **28**:155-61.

Bergers, G. & Benjamin, L. E. 2003. Tumorigenesis and the angiogenic switch. *Nature reviews. Cancer* **3**:401-10.

Berrocoso, E., Sanchez-Blazquez, P., Garzon, J. & Mico, J. A. 2009. Opiates as antidepressants. *Current pharmaceutical design* **15**:1612-22.

Bertilsson, G., Heidrich, J., Svensson, K., Åsman, M., Jendeberg, L., Sydow-Bäckman, M., Ohlsson, R., Postlind, H., Blomquist, P. & Berkenstam, A. 1998. Identification of a human nuclear receptor defines a new signaling pathway for CYP3A induction. *Proceedings of the National Academy of Sciences* **95**:12208-13.

Bhatia, S. N., Balis, U. J., Yarmush, M. L. & Toner, M. 1999. Effect of cell-cell interactions in preservation of cellular phenotype: Cocultivation of hepatocytes and nonparenchymal cells. *FASEB Journal* **13**:1883-900.

Blomhoff, R., Drevon, C. A., Eskild, W., Helgerud, P., Norum, K. R. & Berg, T. 1984. Clearance of acetyl low density lipoprotein by rat liver endothelial cells. Implications for hepatic cholesterol metabolism. *The Journal of biological chemistry* **259**:8898-903.

Bosch, J. 2007. Vascular deterioration in cirrhosis: the big picture. *Journal of clinical gastroenterology* **41 Suppl 3**:S247-53.

Botham, K. M. & Wheeler-Jones, C. P. 2007. Introduction to the Biochemical Society Focused Meeting on Diet and Cardiovascular Health: chylomicron remnants and their emerging roles in vascular dysfunction in atherosclerosis. *Biochemical Society transactions* **35**:437-9.

Braet, F., De Zanger, R., Jans, D., Spector, I. & Wisse, E. 1996. Microfilament-disrupting agent latrunculin A induces and increased number of fenestrae in rat liver sinusoidal endothelial cells: comparison with cytochalasin B. *Hepatology* **24**:627-35.

Braet, F., De Zanger, R., Sasaoki, T., Baekeland, M., Janssens, P., Smedsrod, B. & Wisse, E. 1994. Assessment of a method of isolation, purification, and cultivation of rat liver sinusoidal endothelial cells. *Laboratory investigation; a journal of technical methods and pathology* **70**:944-52.

Braet, F., Muller, M., Vekemans, K., Wisse, E. & Le Couteur, D. G. 2003. Antimycin A-induced defenestration in rat hepatic sinusoidal endothelial cells. *Hepatology* **38**:394-402.

Braet, F. & Wisse, E. 2002. Structural and functional aspects of liver sinusoidal endothelial cell fenestrae: a review. *Comparative hepatology* **1**:1.

Burns, J. M., Summers, B. C., Wang, Y., Melikian, A., Berahovich, R., Miao, Z., Penfold, M. E. T., Sunshine, M. J., Littman, D. R., Kuo, C. J., Wei, K., McMaster, B. E., Wright, K., Howard, M. C. & Schall, T. J. 2006. A novel chemokine receptor for SDF-1 and I-TAC involved in cell survival, cell adhesion, and tumor development. *The Journal of experimental medicine* **203**:2201-13.

Cantley, L. C. 2002. The phosphoinositide 3-kinase pathway. *Science* **296**:1655-7.

Cardone, M. H., Roy, N., Stennicke, H. R., Salvesen, G. S., Franke, T. F., Stanbridge, E., Frisch, S. & Reed, J. C. 1998. Regulation of cell death protease caspase-9 by phosphorylation. *Science* **282**:1318-21.

Carmeliet, P., Ferreira, V., Breier, G., Pollefeyt, S., Kieckens, L., Gertsenstein, M., Fahrig, M., Vandenhoeck, A., Harpal, K., Eberhardt, C., Declercq, C., Pawling, J., Moons, L., Collen, D., Risau, W. & Nagy, A. 1996. Abnormal blood vessel development and lethality in embryos lacking a single VEGF allele. *Nature* **380**:435-9.

Cattley, R. C. & Cullen, J. M. 2013. Chapter 45 - Liver and Gall Bladder. *In*: Wanda, M. H., Colin, G. R., Matthew, A. W., Brad, B., Ricardo OchoaA2 - Wanda M. Haschek, C. G. R. M. A. W. B. B. & Ricardo, O. [Eds.] *Haschek and Rousseaux's Handbook of Toxicologic Pathology (Third Edition).* Academic Press, Boston, pp. 1509-66.

Chan, H. F., Zhang, Y. & Leong, K. W. 2016. Efficient One-Step Production of Microencapsulated Hepatocyte Spheroids with Enhanced Functions. *Small* **12**:2720-30.

Chen, Y., Tortorici, M. A., Garrett, M., Hee, B., Klamerus, K. J. & Pithavala, Y. K. 2013. Clinical Pharmacology of Axitinib. *Clinical Pharmacokinetics* **52**:713-25.

Christensen, J. 2007. A preclinical review of sunitinib, a multitargeted receptor tyrosine kinase inhibitor with anti-angiogenic and antitumour activities. *Annals of Oncology* **18**:x3-x10.

Chung, A. S., Lee, J. & Ferrara, N. 2010. Targeting the tumour vasculature: insights from physiological angiogenesis. *Nature reviews. Cancer* **10**:505-14.

Cogger, V. C., Muller, M., Fraser, R., McLean, A. J., Khan, J. & Le Couteur, D. G. 2004. The effects of oxidative stress on the liver sieve. *J Hepatol* **41**:370-6.

Cohen, E. E. W., Rosen, L. S., Vokes, E. E., Kies, M. S., Forastiere, A. A., Worden, F. P., Kane, M. A., Sherman, E., Kim, S., Bycott, P., Tortorici, M., Shalinsky, D. R., Liau, K. F. & Cohen, R. B. 2008. Axitinib Is an Active Treatment for All Histologic Subtypes of Advanced Thyroid Cancer: Results From a Phase II Study. *Journal of Clinical Oncology* **26**:4708-13.

Collardeau-Frachon, S. & Scoazec, J. Y. 2008. Vascular development and differentiation during human liver organogenesis. *Anat Rec (Hoboken)* **291**:614-27.

Colnot, S. & Perret, C. 2011. Liver zonation. *Molecular pathology of liver diseases.* Springer, pp. 7-16.

Cormier, E. G., Durso, R. J., Tsamis, F., Boussemart, L., Manix, C., Olson, W. C., Gardner, J. P. & Dragic, T. 2004. L-SIGN (CD209L) and DC-SIGN (CD209) mediate transinfection of liver cells by hepatitis C virus. *Proceedings of the National Academy of Sciences of the United States of America* **101**:14067-72.

Couvelard, A., Scoazec, J. Y., Dauge, M. C., Bringuier, A. F., Potet, F. & Feldmann, G. 1996. Structural and functional differentiation of sinusoidal endothelial cells during liver organogenesis in humans. *Blood* **87**:4568-80.

Cross, T. J., Bagot, C., Portmann, B., Wendon, J. & Gillett, D. 2006. Imatinib mesylate as a cause of acute liver failure. *American journal of hematology* **81**:189-92.

Dahlin, D. C., Miwa, G. T., Lu, A. Y. & Nelson, S. D. 1984. N-acetyl-p-benzoquinone imine: a cytochrome P-450-mediated oxidation product of acetaminophen. *Proceedings of the National Academy of Sciences of the United States of America* **81**:1327-31.

Dai, X., Tan, Y., Cai, S., Xiong, X., Wang, L., Ye, Q., Yan, X., Ma, K. & Cai, L. 2011. The role of CXCR7 on the adhesion, proliferation and angiogenesis of endothelial progenitor cells. *Journal of Cellular and Molecular Medicine* **15**:1299-309.

Daskalopoulou, S. S., Tzovaras, V., Mikhailidis, D. P. & Elisaf, M. 2005. Effect on serum uric acid levels of drugs prescribed for indications other than treating hyperuricaemia. *Current pharmaceutical design* **11**:4161-75.

Davies, B. J., Coller, J. K., Somogyi, A. A., Milne, R. W. & Sallustio, B. C. 2007. CYP2B6, CYP2D6, and CYP3A4 catalyze the primary oxidative metabolism of perhexiline enantiomers by human liver microsomes. *Drug metabolism and disposition: the biological fate of chemicals* **35**:128-38.

Dejana, E., Orsenigo, F. & Lampugnani, M. G. 2008. The role of adherens junctions and VE-cadherin in the control of vascular permeability. *Journal of cell science* **121**:2115-22.

DeLeve, L. D. 2007. Hepatic microvasculature in liver injury. *Seminars in liver disease* **27**:390-400.

Deleve, L. D. 2008. Sinusoidal obstruction syndrome. *Gastroenterology & hepatology* **4**:101-3.

DeLeve, L. D. 2011. Vascular liver disease and the liver sinusoidal endothelial cells. *In*: Garcia-Tsao, L. D. a. G. [Ed.] *Vascular Liver Disease: Mechanisms and Management.* Springer Science + Business Media, USA, pp. 25-40.

DeLeve, L. D. 2013. Liver sinusoidal endothelial cells and liver regeneration. *The Journal of clinical investigation* **123**:1861-6.

DeLeve, L. D. 2015. Liver sinusoidal endothelial cells in hepatic fibrosis. *Hepatology* **61**:1740-6.

DeLeve, L. D., Ito, Y., Bethea, N. W., McCuskey, M. K., Wang, X. & McCuskey, R. S. 2003. Embolization by sinusoidal lining cells obstructs the microcirculation in rat sinusoidal obstruction syndrome. *American journal of physiology. Gastrointestinal and liver physiology* **284**:G1045-52.

Deleve, L. D., Wang, X. & Guo, Y. 2008. Sinusoidal endothelial cells prevent rat stellate cell activation and promote reversion to quiescence. *Hepatology* **48**:920-30.

DeLeve, L. D., Wang, X., Hu, L., McCuskey, M. K. & McCuskey, R. S. 2004. Rat liver sinusoidal endothelial cell phenotype is maintained by paracrine and autocrine regulation. *American journal of physiology. Gastrointestinal and liver physiology* **287**:G757-63.

DeLeve, L. D., Wang, X., Kaplowitz, N., Shulman, H. M., Bart, J. A. & van der Hoek, A. 1997. Sinusoidal endothelial cells as a target for acetaminophen toxicity. Direct action versus requirement for hepatocyte activation in different mouse strains. *Biochemical pharmacology* **53**:1339-45.

DeLeve, L. D., Wang, X., McCuskey, M. K. & McCuskey, R. S. 2006. Rat liver endothelial cells isolated by anti-CD31 immunomagnetic separation lack fenestrae and sieve plates. *American journal of physiology. Gastrointestinal and liver physiology* **291**:G1187-9.

Demetri, G. D., Reichardt, P., Kang, Y. K., Blay, J. Y., Rutkowski, P., Gelderblom, H., Hohenberger, P., Leahy, M., von Mehren, M., Joensuu, H., Badalamenti, G., Blackstein, M., Le Cesne, A., Schoffski, P., Maki, R. G., Bauer, S., Nguyen, B. B., Xu, J., Nishida, T., Chung, J., Kappeler, C., Kuss, I., Laurent, D. & Casali, P. G. 2013. Efficacy and safety of regorafenib for advanced gastrointestinal stromal tumours after failure of imatinib and sunitinib (GRID): an international, multicentre, randomised, placebo-controlled, phase 3 trial. *Lancet* **381**:295-302.

Demetri, G. D., van Oosterom, A. T., Garrett, C. R., Blackstein, M. E., Shah, M. H., Verweij, J., McArthur, G., Judson, I. R., Heinrich, M. C., Morgan, J. A., Desai, J., Fletcher, C. D., George, S., Bello, C. L., Huang, X., Baum, C. M. & Casali, P. G. 2006. Efficacy and safety of sunitinib in patients with advanced gastrointestinal stromal tumour after failure of imatinib: a randomised controlled trial. *Lancet* **368**:1329-38.

Deng, Y., Sychterz, C., Suttle, A. B., Dar, M. M., Bershas, D., Negash, K., Qian, Y., Chen, E. P., Gorycki, P. D. & Ho, M. Y. 2013. Bioavailability, metabolism and disposition of oral pazopanib in patients with advanced cancer. *Xenobiotica; the fate of foreign compounds in biological systems* **43**:443-53.

Deschamps, D., DeBeco, V., Fisch, C., Fromenty, B., Guillouzo, A. & Pessayre, D. 1994. Inhibition by perhexiline of oxidative phosphorylation and the β-oxidation of fatty acids: Possible role in pseudoalcoholic liver lesions. *Hepatology* **19**:948-61.

Deveraux, Q. L., Roy, N., Stennicke, H. R., Van Arsdale, T., Zhou, Q., Srinivasula, S. M., Alnemri, E. S., Salvesen, G. S. & Reed, J. C. 1998. IAPs block apoptotic events induced by caspase-8 and cytochrome c by direct inhibition of distinct caspases. *The EMBO journal* **17**:2215-23.

Dikov, M. M., Ohm, J. E., Ray, N., Tchekneva, E. E., Burlison, J., Moghanaki, D., Nadaf, S. & Carbone, D. P. 2005. Differential roles of vascular endothelial growth factor receptors 1 and 2 in dendritic cell differentiation. *Journal of immunology* **174**:215-22.

Ding, B.-S., Cao, Z., Lis, R., Nolan, D. J., Guo, P., Simons, M., Penfold, M. E., Shido, K., Rabbany, S. Y. & Rafii, S. 2014. Divergent angiocrine signals from vascular niche balance liver regeneration and fibrosis. *Nature* **505**:97-102.

Ding, B.-S., Nolan, D. J., Butler, J. M., James, D., Babazadeh, A. O., Rosenwaks, Z., Mittal, V., Kobayashi, H., Shido, K., Lyden, D., Sato, T. N., Rabbany, S. Y. & Rafii, S. 2010a. Inductive angiocrine signals from sinusoidal endothelium are required for liver regeneration. *Nature* **468**:310-15.

Ding, B. S., Nolan, D. J., Butler, J. M., James, D., Babazadeh, A. O., Rosenwaks, Z., Mittal, V., Kobayashi, H., Shido, K., Lyden, D., Sato, T. N., Rabbany, S. Y. & Rafii, S. 2010b. Inductive angiocrine signals from sinusoidal endothelium are required for liver regeneration. *Nature* **468**:310-5.

Ding, X. & Staudinger, J. L. 2005. Repression of PXR-mediated induction of hepatic CYP3A gene expression by protein kinase C. *Biochemical pharmacology* **69**:867-73.

Do, H., Healey, J. F., Waller, E. K. & Lollar, P. 1999. Expression of factor VIII by murine liver sinusoidal endothelial cells. *The Journal of biological chemistry* **274**:19587-92.

Donahower, B., McCullough, S. S., Kurten, R., Lamps, L. W., Simpson, P., Hinson, J. A. & James, L. P. 2006. Vascular endothelial growth factor and hepatocyte regeneration in acetaminophen toxicity. *American journal of physiology. Gastrointestinal and liver physiology* **291**:G102-9.

Donahower, B. C., McCullough, S. S., Hennings, L., Simpson, P. M., Stowe, C. D., Saad, A. G., Kurten, R. C., Hinson, J. A. & James, L. P. 2010a. Human Recombinant Vascular Endothelial Growth Factor Reduces Necrosis and Enhances Hepatocyte Regeneration in a Mouse Model of Acetaminophen Toxicity. *The Journal of pharmacology and experimental therapeutics* **334**:33-43.

Donahower, B. C., McCullough, S. S., Hennings, L., Simpson, P. M., Stowe, C. D., Saad, A. G., Kurten, R. C., Hinson, J. A. & James, L. P. 2010b. Human recombinant vascular endothelial growth factor reduces necrosis and enhances hepatocyte regeneration in a mouse model of acetaminophen toxicity. *J Pharmacol Exp Ther* **334**:33-43.

Drixler, T. A., Vogten, M. J., Ritchie, E. D., van Vroonhoven, T. J., Gebbink, M. F., Voest, E. E. & Borel Rinkes, I. H. 2002. Liver regeneration is an angiogenesis-associated phenomenon. *Annals of surgery* **236**:703-11; discussion 11-2.

Du, C., Narayanan, K., Leong, M. F. & Wan, A. C. A. 2014. Induced pluripotent stem cell-derived hepatocytes and endothelial cells in multi-component hydrogel fibers for liver tissue engineering. *Biomaterials* **35**:6006-14.

Dudas, J., Papoutsi, M., Hecht, M., Elmaouhoub, A., Saile, B., Christ, B., Tomarev, S. I., von Kaisenberg, C. S., Schweigerer, L., Ramadori, G. & Wilting, J. 2004. The homeobox transcription factor Prox1 is highly conserved in embryonic hepatoblasts and in adult and transformed hepatocytes, but is absent from bile duct epithelium. *Anatomy and embryology* **208**:359-66.

Dumont, D. J., Jussila, L., Taipale, J., Lymboussaki, A., Mustonen, T., Pajusola, K., Breitman, M. & Alitalo, K. 1998. Cardiovascular Failure in Mouse Embryos Deficient in VEGF Receptor-3. *Science* **282**:946-49.

Edwards, I. R. & Aronson, J. K. 2000. Adverse drug reactions: definitions, diagnosis, and management. *The Lancet* **356**:1255-59.

Eggebeen, A. T. 2007. Gout: an update. *American family physician* **76**:801-8.

Elvevold, K., Smedsrod, B. & Martinez, I. 2008. The liver sinusoidal endothelial cell: a cell type of controversial and confusing identity. *American journal of physiology. Gastrointestinal and liver physiology* **294**:G391-400.

Essop, M. F. & Opie, L. H. 2004. Metabolic therapy for heart failure. *European heart journal* **25**:1765-8.

Everett, L. A., Cleuren, A. C. A., Khoriaty, R. N. & Ginsburg, D. 2014. Murine coagulation factor VIII is synthesized in endothelial cells. *Blood* **123**:3697-705.

FDA 2012. Label for STIVARGA (regorafenib). pp. Label for STIVARGA (regorafenib) approved on 27 September 2012.

FDA 2013. FDA approves Stivarga for advanced gastrointestinal stromal tumors. *In*: Yao, S. [Ed.] *FDA NEWS RELEASE.* FDA, 10903 New Hampshire Avenue Silver Spring, MD 20993.

Feher, J. & Lengyel, G. 2012. Silymarin in the prevention and treatment of liver diseases and primary liver cancer. *Current pharmaceutical biotechnology* **13**:210-7.

Felser, A., Lindinger, P. W., Schnell, D., Kratschmar, D. V., Odermatt, A., Mies, S., Jeno, P. & Krahenbuhl, S. 2014. Hepatocellular toxicity of benzbromarone: effects on mitochondrial function and structure. *Toxicology* **324**:136-46.

Ferrara, N., Gerber, H. P. & LeCouter, J. 2003. The biology of VEGF and its receptors. *Nature medicine* **9**:669-76.

Folkman, J. 2007. Angiogenesis: an organizing principle for drug discovery? *Nature reviews. Drug discovery* **6**:273-86.

Fomin, M. E., Zhou, Y., Beyer, A. I., Publicover, J., Baron, J. L. & Muench, M. O. 2013. Production of Factor VIII by Human Liver Sinusoidal Endothelial Cells Transplanted in Immunodeficient uPA Mice. *PloS one* **8**:e77255.

Fong, G. H., Rossant, J., Gertsenstein, M. & Breitman, M. L. 1995. Role of the Flt-1 receptor tyrosine kinase in regulating the assembly of vascular endothelium. *Nature* **376**:66-70.

Forbes, S. J. & Parola, M. 2011. Liver fibrogenic cells. *Best Practice & Research Clinical Gastroenterology* **25**:207-17.

Forbes, S. J. & Rosenthal, N. 2014. Preparing the ground for tissue regeneration: from mechanism to therapy. *Nat Med* **20**:857-69.

Fraser, R., Dobbs, B. R. & Rogers, G. W. 1995. Lipoproteins and the liver sieve: the role of the fenestrated sinusoidal endothelium in lipoprotein metabolism, atherosclerosis, and cirrhosis. *Hepatology* **21**:863-74.

Fromenty, B. & Pessayre, D. 1995. Inhibition of mitochondrial beta-oxidation as a mechanism of hepatotoxicity. *Pharmacology & therapeutics* **67**:101-54.

Fulton, D., Gratton, J. P. & Sessa, W. C. 2001. Post-translational control of endothelial nitric oxide synthase: why isn't calcium/calmodulin enough? *J Pharmacol Exp Ther* **299**:818-24.

Gahr, M., Zeiss, R., Lang, D., Connemann, B. J., Hiemke, C. & Schonfeldt-Lecuona, C. 2016. Drug-Induced Liver Injury Associated With Antidepressive Psychopharmacotherapy: An Explorative Assessment Based on Quantitative Signal Detection Using Different MedDRA Terms. *Journal of clinical pharmacology* **56**:769-78.

Ganesan, L. P., Mates, J. M., Cheplowitz, A. M., Avila, C. L., Zimmerer, J. M., Yao, Z., Maiseyeu, A., Rajaram, M. V., Robinson, J. M. & Anderson, C. L. 2016. Scavenger receptor B1, the HDL receptor, is expressed abundantly in liver sinusoidal endothelial cells. *Sci Rep* **6**:20646.

Gardiner, S. J. & Begg, E. J. 2006. Pharmacogenetics, Drug-Metabolizing Enzymes, and Clinical Practice. *Pharmacological Reviews* **58**:521.

Gardner, J. P., Durso, R. J., Arrigale, R. R., Donovan, G. P., Maddon, P. J., Dragic, T. & Olson, W. C. 2003. L-SIGN (CD 209L) is a liver-specific capture receptor for hepatitis C virus. *Proceedings of the National Academy of Sciences of the United States of America* **100**:4498-503.

Garrido-Urbani, S., Bradfield, P. F., Lee, B. P. & Imhof, B. A. 2008. Vascular and epithelial junctions: a barrier for leucocyte migration. *Biochemical Society transactions* **36**:203-11.

Gaskell, H., Sharma, P., Colley, H. E., Murdoch, C., Williams, D. P. & Webb, S. D. 2016. Characterization of a Functional C3A Liver Spheroid Model. *Toxicology Research*.

Gatmaitan, Z., Varticovski, L., Ling, L., Mikkelsen, R., Steffan, A. M. & Arias, I. M. 1996. Studies on fenestral contraction in rat liver endothelial cells in culture. *Am J Pathol* **148**:2027-41.

Gebhardt, R. & Matz-Soja, M. 2014. Liver zonation: Novel aspects of its regulation and its impact on homeostasis. *World journal of gastroenterology : WJG* **20**:8491-504.

Gerber, H. P., McMurtrey, A., Kowalski, J., Yan, M., Keyt, B. A., Dixit, V. & Ferrara, N. 1998. Vascular endothelial growth factor regulates endothelial cell survival through the phosphatidylinositol 3'-kinase/Akt signal transduction pathway. Requirement for Flk-1/KDR activation. *The Journal of biological chemistry* **273**:30336-43.

Gerhardt, H. & Betsholtz, C. 2005. How do endothelial cells orientate? *Exs*:3-15.

Gharwan, H. & Groninger, H. 2016. Kinase inhibitors and monoclonal antibodies in oncology: clinical implications. *Nat Rev Clin Oncol* **13**:209-27.

Gocek, E., Moulas, A. N. & Studzinski, G. P. 2014. Non-receptor protein tyrosine kinases signaling pathways in normal and cancer cells. *Critical Reviews in Clinical Laboratory Sciences* **51**:125-37.

Godoy, P., Hewitt, N. J., Albrecht, U., Andersen, M. E., Ansari, N., Bhattacharya, S., Bode, J. G., Bolleyn, J., Borner, C., Bottger, J., Braeuning, A., Budinsky, R. A., Burkhardt, B., Cameron, N. R., Camussi, G., Cho, C. S., Choi, Y. J., Craig Rowlands, J., Dahmen, U., Damm, G., Dirsch, O., Donato, M. T., Dong, J., Dooley, S., Drasdo, D., Eakins, R., Ferreira, K. S., Fonsato, V., Fraczek, J., Gebhardt, R., Gibson, A., Glanemann, M., Goldring, C. E., Gomez-Lechon, M. J., Groothuis, G. M., Gustavsson, L., Guyot, C., Hallifax, D., Hammad, S., Hayward, A., Haussinger, D., Hellerbrand, C., Hewitt, P., Hoehme, S., Holzhutter, H. G., Houston, J. B., Hrach, J., Ito, K., Jaeschke, H., Keitel, V., Kelm, J. M., Kevin Park, B., Kordes, C., Kullak-Ublick, G. A., LeCluyse, E. L., Lu, P., Luebke-Wheeler, J., Lutz, A., Maltman, D. J., Matz-Soja, M., McMullen, P., Merfort, I., Messner, S., Meyer, C., Mwinyi, J., Naisbitt, D. J., Nussler, A. K., Olinga, P., Pampaloni, F., Pi, J., Pluta, L., Przyborski, S. A., Ramachandran, A., Rogiers, V., Rowe, C., Schelcher, C., Schmich, K., Schwarz, M., Singh, B., Stelzer, E. H., Stieger, B., Stober, R., Sugiyama, Y., Tetta, C., Thasler, W. E., Vanhaecke, T., Vinken, M., Weiss, T. S., Widera, A., Woods, C. G., Xu, J. J., Yarborough, K. M. & Hengstler, J. G. 2013. Recent advances in 2D and 3D in vitro systems using primary hepatocytes, alternative hepatocyte sources and non-parenchymal liver cells and their use in investigating mechanisms of hepatotoxicity, cell signaling and ADME. *Archives of toxicology* **87**:1315-530.

Gordon, E. J., Gale, N. W. & Harvey, N. L. 2008. Expression of the hyaluronan receptor LYVE-1 is not restricted to the lymphatic vasculature; LYVE-1 is also expressed on embryonic blood vessels. *Developmental Dynamics* **237**:1901-09.

Gotink, K. J. & Verheul, H. M. 2010. Anti-angiogenic tyrosine kinase inhibitors: what is their mechanism of action? *Angiogenesis* **13**:1-14.

Greene, A. K., Wiener, S., Puder, M., Yoshida, A., Shi, B., Perez-Atayde, A. R., Efstathiou, J. A., Holmgren, L., Adamis, A. P., Rupnick, M., Folkman, J. & O'Reilly, M. S. 2003. Endothelial-Directed Hepatic Regeneration After Partial Hepatectomy. *Annals of surgery* **237**:530-35.

Greuter, T. & Shah, V. H. 2016. Hepatic sinusoids in liver injury, inflammation, and fibrosis: new pathophysiological insights. *Journal of gastroenterology*.

Grothey, A., Van Cutsem, E., Sobrero, A., Siena, S., Falcone, A., Ychou, M., Humblet, Y., Bouche, O., Mineur, L., Barone, C., Adenis, A., Tabernero, J., Yoshino, T., Lenz, H. J., Goldberg, R. M., Sargent, D. J., Cihon, F., Cupit, L., Wagner, A. & Laurent, D. 2013. Regorafenib monotherapy for previously treated metastatic colorectal cancer (CORRECT): an international, multicentre, randomised, placebo-controlled, phase 3 trial. *Lancet* **381**:303-12.

Guangqi, E., Cao, Y., Bhattacharya, S., Dutta, S., Wang, E. & Mukhopadhyay, D. 2012. Endogenous Vascular Endothelial Growth Factor-A (VEGF-A) Maintains Endothelial Cell Homeostasis by Regulating VEGF Receptor-2 Transcription. *The Journal of biological chemistry* **287**:3029-41.

Guengerich, F. P., Johnson, W. W., Ueng, Y. F., Yamazaki, H. & Shimada, T. 1996. Involvement of cytochrome P450, glutathione S-transferase, and epoxide hydrolase in the metabolism of aflatoxin B1 and relevance to risk of human liver cancer. *Environmental Health Perspectives* **104**:557-62.

Ha, C. H., Wang, W., Jhun, B. S., Wong, C., Hausser, A., Pfizenmaier, K., McKinsey, T. A., Olson, E. N. & Jin, Z. G. 2008. Protein kinase D-dependent phosphorylation and nuclear export of histone deacetylase 5 mediates vascular endothelial growth factor-induced gene expression and angiogenesis. *The Journal of biological chemistry* **283**:14590-9.

Hamada, T., Ichida, K., Hosoyamada, M., Mizuta, E., Yanagihara, K., Sonoyama, K., Sugihara, S., Igawa, O., Hosoya, T., Ohtahara, A., Shigamasa, C., Yamamoto, Y., Ninomiya, H. & Hisatome, I. 2008. Uricosuric Action of Losartan via the Inhibition of Urate Transporter 1 (URAT 1) in Hypertensive Patients. *American Journal of Hypertension* **21**:1157-62.

Hamid, A. S., Tesfamariam, I. G., Zhang, Y. & Zhang, Z. G. 2013. Aflatoxin B1-induced hepatocellular carcinoma in developing countries: Geographical distribution, mechanism of action and prevention. *Oncology Letters* **5**:1087-92.

Hanahan, D. & Weinberg, R. A. 2000. The hallmarks of cancer. *Cell* **100**:57-70.

Handa, K., Matsubara, K., Fukumitsu, K., Guzman-Lepe, J., Watson, A. & Soto-Gutierrez, A. 2014. Assembly of human organs from stem cells to study liver disease. *The American journal of pathology* **184**:348-57.

Hang, T. C., Lauffenburger, D. A., Griffith, L. G. & Stolz, D. B. 2012. Lipids promote survival, proliferation, and maintenance of differentiation of rat liver sinusoidal endothelial cells in vitro. *American journal of physiology. Gastrointestinal and liver physiology* **302**:G375-88.

Haque, T., Sasatomi, E. & Hayashi, P. H. 2016. Drug-Induced Liver Injury: Pattern Recognition and Future Directions. *Gut and Liver* **10**:27-36.

Hara, Y., Nakajima, M., Miyamoto, K. I. & Yokoi, T. 2005. Inhibitory effects of psychotropic drugs on mexiletine metabolism in human liver microsomes: Prediction of in vivo drug interactions. *Xenobiotica; the fate of foreign compounds in biological systems* **35**:549-60.

Haraldsson, B. & Jeansson, M. 2009. Glomerular filtration barrier. *Current opinion in nephrology and hypertension* **18**:331-5.

Haschek, W. M., Rousseaux, C. G. & Wallig, M. A. 2010. Chapter 9 - The Liver. *Fundamentals of Toxicologic Pathology (Second edition).* Academic Press, San Diego, pp. 197-235.

Hawton, K., Bergen, H., Simkin, S., Dodd, S., Pocock, P., Bernal, W., Gunnell, D. & Kapur, N. 2013. Long term effect of reduced pack sizes of paracetamol on poisoning deaths and liver transplant activity in England and Wales: interrupted time series analyses. *BMJ (Clinical research ed.)* **346**:f403.

Herrnberger, L., Ebner, K., Junglas, B. & Tamm, E. R. 2012. The role of plasmalemma vesicle-associated protein (PLVAP) in endothelial cells of Schlemm's canal and ocular capillaries. *Experimental Eye Research* **105**:27-33.

Herrnberger, L., Hennig, R., Kremer, W., Hellerbrand, C., Goepferich, A., Kalbitzer, H. R. & Tamm, E. R. 2014. Formation of fenestrae in murine liver sinusoids depends on plasmalemma vesicle-associated protein and is required for lipoprotein passage. *PloS one* **9**:e115005.

Heslop, J. A., Rowe, C., Walsh, J., Sison-Young, R., Jenkins, R., Kamalian, L., Kia, R., Hay, D., Jones, R. P., Malik, H. Z., Fenwick, S., Chadwick, A. E., Mills, J., Kitteringham, N. R., Goldring, C. E. & Kevin Park, B. 2016. Mechanistic evaluation of primary human hepatocyte culture using global proteomic analysis reveals a selective dedifferentiation profile. *Archives of toxicology*.

Hetheridge, C., Mavria, G. & Mellor, H. 2011. Uses of the in vitro endothelial-fibroblast organotypic co-culture assay in angiogenesis research. *Biochemical Society transactions* **39**:1597-600.

Hickey, P. L., Angus, P. W., McLean, A. J. & Morgan, D. J. 1995. Oxygen supplementation restores theophylline clearance to normal in cirrhotic rats. *Gastroenterology* **108**:1504-09.

Hinson, J. A., Roberts, D. W., Benson, R. W., Dalhoff, K., Loft, S. & Poulsen, H. E. 1990. Mechanism of paracetamol toxicity. *Lancet* **335**:732.

Hinson, J. A., Roberts, D. W. & James, L. P. 2010. Mechanisms of Acetaminophen-Induced Liver Necrosis. *Handbook of experimental pharmacology*:369-405.

Hiratsuka, S., Minowa, O., Kuno, J., Noda, T. & Shibuya, M. 1998. Flt-1 lacking the tyrosine kinase domain is sufficient for normal development and angiogenesis in mice. *Proceedings of the National Academy of Sciences of the United States of America* **95**:9349-54.

Holmes, K., Roberts, O. L., Thomas, A. M. & Cross, M. J. 2007. Vascular endothelial growth factor receptor-2: structure, function, intracellular signalling and therapeutic inhibition. *Cellular signalling* **19**:2003-12.

Holmqvist, K., Cross, M. J., Rolny, C., Hagerkvist, R., Rahimi, N., Matsumoto, T., Claesson-Welsh, L. & Welsh, M. 2004. The adaptor protein shb binds to tyrosine 1175 in vascular endothelial growth factor (VEGF) receptor-2 and regulates VEGF-dependent cellular migration. *The Journal of biological chemistry* **279**:22267-75.

Holt, M. P., Yin, H. & Ju, C. 2010. Exacerbation of acetaminophen-induced disturbances of liver sinusoidal endothelial cells in the absence of Kupffer cells in mice. *Toxicology letters* **194**:34-41.

Hong, Y. K., Harvey, N., Noh, Y. H., Schacht, V., Hirakawa, S., Detmar, M. & Oliver, G. 2002. Prox1 is a master control gene in the program specifying lymphatic endothelial cell fate. *Developmental dynamics : an official publication of the American Association of Anatomists* **225**:351-7.

Hooser, S. B., Beasley, V. R., Waite, L. L., Kuhlenschmidt, M. S., Carmichael, W. W. & Haschek, W. M. 1991. Actin filament alterations in rat hepatocytes induced in vivo and in vitro by microcystin-LR, a hepatotoxin from the blue-green alga, Microcystis aeruginosa. *Veterinary pathology* **28**:259-66.

Hu, J., Srivastava, K., Wieland, M., Runge, A., Mogler, C., Besemfelder, E., Terhardt, D., Vogel, M. J., Cao, L., Korn, C., Bartels, S., Thomas, M. & Augustin, H. G. 2014. Endothelial cell-derived angiopoietin-2 controls liver regeneration as a spatiotemporal rheostat. *Science* **343**:416-9.

Hu, X., Sui, X., Li, L., Huang, X., Rong, R., Su, X., Shi, Q., Mo, L., Shu, X., Kuang, Y., Tao, Q. & He, C. 2013. Protocadherin 17 acts as a tumour suppressor inducing tumour cell apoptosis and autophagy, and is frequently methylated in gastric and colorectal cancers. *The Journal of pathology* **229**:62-73.

Hubbard, S. R. & Till, J. H. 2000. Protein tyrosine kinase structure and function. *Annual review of biochemistry* **69**:373-98.

Hung, M. J., Hu, P. & Hung, M. Y. 2014. Coronary artery spasm: review and update. *International journal of medical sciences* **11**:1161-71.

Hussain, M. M. 2000. A proposed model for the assembly of chylomicrons. *Atherosclerosis* **148**:1-15.

Iacovelli, R., Palazzo, A., Procopio, G., Santoni, M., Trenta, P., De Benedetto, A., Mezi, S. & Cortesi, E. 2014. Incidence and relative risk of hepatic toxicity in patients treated with anti-angiogenic tyrosine kinase inhibitors for malignancy. *British journal of clinical pharmacology* **77**:929-38.

Ichida, K., Hosoyamada, M., Hisatome, I., Enomoto, A., Hikita, M., Endou, H. & Hosoya, T. 2004. Clinical and molecular analysis of patients with renal hypouricemia in Japan-influence of URAT1 gene on urinary urate excretion. *Journal of the American Society of Nephrology : JASN* **15**:164-73.

Inai, T., Mancuso, M., Hashizume, H., Baffert, F., Haskell, A., Baluk, P., Hu-Lowe, D. D., Shalinsky, D. R., Thurston, G., Yancopoulos, G. D. & McDonald, D. M. 2004. Inhibition of Vascular Endothelial Growth Factor (VEGF) Signaling in Cancer Causes Loss of Endothelial Fenestrations, Regression of Tumor Vessels, and Appearance of Basement Membrane Ghosts. *The American journal of pathology* **165**:35-52.

Inamori, M., Mizumoto, H. & Kajiwara, T. 2009. An approach for formation of vascularized liver tissue by endothelial cell-covered hepatocyte spheroid integration. *Tissue engineering. Part A* **15**:2029-37.

Ito, Y., Bethea, N. W., Abril, E. R. & McCuskey, R. S. 2003. Early hepatic microvascular injury in response to acetaminophen toxicity. *Microcirculation* **10**:391-400.

Ito, Y., Machen, N. W., Abril, E. R. & McCuskey, R. S. 2004. Effects of acetaminophen on hepatic microcirculation in mice. *Comparative hepatology* **3 Suppl 1**:S33.

Ito, Y., Sorensen, K. K., Bethea, N. W., Svistounov, D., McCuskey, M. K., Smedsrod, B. H. & McCuskey, R. S. 2007. Age-related changes in the hepatic microcirculation in mice. *Experimental gerontology* **42**:789-97.

Iwakiri, Y. & Groszmann, R. J. 2007. Vascular endothelial dysfunction in cirrhosis. *J Hepatol* **46**:927-34.

Jackson, D. G. 2003. The lymphatics revisited: new perspectives from the hyaluronan receptor LYVE-1. *Trends in cardiovascular medicine* **13**:1-7.

Jaeschke, H., McGill, M. R. & Ramachandran, A. 2012. Oxidant stress, mitochondria, and cell death mechanisms in drug-induced liver injury: lessons learned from acetaminophen hepatotoxicity. *Drug metabolism reviews* **44**:88-106.

Jansen, T. L., Reinders, M. K., van Roon, E. N. & Brouwers, J. R. 2004. Benzbromarone withdrawn from the European market: another case of "absence of evidence is evidence of absence"? *Clinical and experimental rheumatology* **22**:651.

Joukov, V., Pajusola, K., Kaipainen, A., Chilov, D., Lahtinen, I., Kukk, E., Saksela, O., Kalkkinen, N. & Alitalo, K. 1996. A novel vascular endothelial growth factor, VEGF-C, is a ligand for the Flt4 (VEGFR-3) and KDR (VEGFR-2) receptor tyrosine kinases. *The EMBO journal* **15**:290-98.

Kang, Y. B., Sodunke, T. R., Lamontagne, J., Cirillo, J., Rajiv, C., Bouchard, M. J. & Noh, M. 2015. Liver sinusoid on a chip: Long-term layered co-culture of primary rat hepatocytes and endothelial cells in microfluidic platforms. *Biotechnology and Bioengineering* **112**:2571-82.

Kapadia, S., Hapani, S., Choueiri, T. K. & Wu, S. 2013. Risk of liver toxicity with the angiogenesis inhibitor pazopanib in cancer patients. *Acta Oncologica* **52**:1202-12.

Karczmarek-Borowska, B. & Sałek-Zań, A. 2015. Hepatotoxicity of molecular targeted therapy. *Contemporary Oncology* **19**:87-92.

Karkkainen, M. J., Haiko, P., Sainio, K., Partanen, J., Taipale, J., Petrova, T. V., Jeltsch, M., Jackson, D. G., Talikka, M., Rauvala, H., Betsholtz, C. & Alitalo, K. 2004. Vascular endothelial growth factor C is required for sprouting of the first lymphatic vessels from embryonic veins. *Nature immunology* **5**:74-80.

Kaufmann, P., Torok, M., Hanni, A., Roberts, P., Gasser, R. & Krahenbuhl, S. 2005. Mechanisms of benzarone and benzbromarone-induced hepatic toxicity. *Hepatology* **41**:925-35.

Kendall, R. L. & Thomas, K. A. 1993. Inhibition of vascular endothelial cell growth factor activity by an endogenously encoded soluble receptor. *Proceedings of the National Academy of Sciences of the United States of America* **90**:10705-9.

Kennedy, J. A., Unger, S. A. & Horowitz, J. D. 1996. Inhibition of carnitine palmitoyltransferase-1 in rat heart and liver by perhexiline and amiodarone. *Biochemical pharmacology* **52**:273-80.

Kerbel, R. S. 2008. Tumor Angiogenesis. *The New England journal of medicine* **358**:2039-49.

Khoo, U.-S., Chan, K. Y. K., Chan, V. S. F. & Lin, C. L. S. 2008. DC-SIGN and L-SIGN: the SIGNs for infection. *Journal of Molecular Medicine* **86**:861-74.

Kierszenbaum, A. L. & Tres, L. 2015. *Histology and cell biology: an introduction to pathology.* Elsevier Health Sciences,

Kim, K., Ohashi, K., Utoh, R., Kano, K. & Okano, T. 2012. Preserved liver-specific functions of hepatocytes in 3D co-culture with endothelial cell sheets. *Biomaterials* **33**:1406-13.

Kirschner, N., Rosenthal, R., Furuse, M., Moll, I., Fromm, M. & Brandner, J. M. 2013. Contribution of tight junction proteins to ion, macromolecule, and water barrier in keratinocytes. *The Journal of investigative dermatology* **133**:1161-9.

Klein, D., Demory, A., Peyre, F., Kroll, J., Augustin, H. G., Helfrich, W., Kzhyshkowska, J., Schledzewski, K., Arnold, B. & Goerdt, S. 2008. Wnt2 acts as a cell type-specific, autocrine growth factor in rat hepatic sinusoidal endothelial cells cross-stimulating the VEGF pathway. *Hepatology* **47**:1018-31.

Knook, D. L. & Sleyster, E. C. 1980. Isolated parenchymal, Kupffer and endothelial rat liver cells characterized by their lysosomal enzyme content. *Biochemical and biophysical research communications* **96**:250-57.

Koch, S. & Claesson-Welsh, L. 2012. Signal Transduction by Vascular Endothelial Growth Factor Receptors. *Cold Spring Harbor Perspectives in Medicine* **2**.

Kostadinova, R., Boess, F., Applegate, D., Suter, L., Weiser, T., Singer, T., Naughton, B. & Roth, A. 2013. A long-term three dimensional liver co-culture system for improved prediction of clinically relevant drug-induced hepatotoxicity. *Toxicology and applied pharmacology* **268**:1-16.

Koudelkova, P., Weber, G. & Mikulits, W. 2015. Liver Sinusoidal Endothelial Cells Escape Senescence by Loss of p19ARF. *PloS one* **10**:e0142134.

Krause , D. S. & Van Etten , R. A. 2005. Tyrosine Kinases as Targets for Cancer Therapy. *New England Journal of Medicine* **353**:172-87.

Krishnamoorthy, S. K., Relias, V., Sebastian, S., Jayaraman, V. & Saif, M. W. 2015. Management of regorafenib-related toxicities: a review. *Therapeutic Advances in Gastroenterology* **8**:285-97.

Kumar, R., Crouthamel, M. C., Rominger, D. H., Gontarek, R. R., Tummino, P. J., Levin, R. A. & King, A. G. 2009. Myelosuppression and kinase selectivity of multikinase angiogenesis inhibitors. *Br J Cancer* **101**:1717-23.

Kumar, R., Harrington, L., Hopper, T., Miller, C., Onori, J., Cheung, M., Stafford, J., Epperly, A. & Gilmer, T. 2005. Correlation of anti-tumor and anti-angiogenic activity of VEGFR inhibitors with inhibition of VEGFR2 phosphorylation in mice. *ASCO Annual Meeting Proceedings.* pp. 9537.

Kwak, E. L., Sordella, R., Bell, D. W., Godin-Heymann, N., Okimoto, R. A., Brannigan, B. W., Harris, P. L., Driscoll, D. R., Fidias, P., Lynch, T. J., Rabindran, S. K., McGinnis, J. P., Wissner, A., Sharma, S. V., Isselbacher, K. J., Settleman, J. & Haber, D. A. 2005. Irreversible inhibitors of the EGF receptor may circumvent acquired resistance to gefitinib. *Proceedings of the National Academy of Sciences of the United States of America* **102**:7665-70.

Kwekkeboom, D. J. 2015. Pazopanib: a new drug for pancreatic neuroendocrine tumours. *The Lancet. Oncology* **16**:606-7.

Lalor, P. F., Edwards, S., McNab, G., Salmi, M., Jalkanen, S. & Adams, D. H. 2002. Vascular adhesion protein-1 mediates adhesion and transmigration of lymphocytes on human hepatic endothelial cells. *Journal of immunology* **169**:983-92.

Lalor, P. F., Lai, W. K., Curbishley, S. M., Shetty, S. & Adams, D. H. 2006. Human hepatic sinusoidal endothelial cells can be distinguished by expression of phenotypic markers related to their specialised functions in vivo. *World journal of gastroenterology : WJG* **12**:5429-39.

Lamalice, L., Le Boeuf, F. & Huot, J. 2007. Endothelial cell migration during angiogenesis. *Circulation research* **100**:782-94.

Larson, A. M., Polson, J., Fontana, R. J., Davern, T. J., Lalani, E., Hynan, L. S., Reisch, J. S., Schiodt, F. V., Ostapowicz, G., Shakil, A. O. & Lee, W. M. 2005. Acetaminophen-induced acute liver failure: results of a United States multicenter, prospective study. *Hepatology* **42**:1364-72.

Laverty, H., Benson, C., Cartwright, E., Cross, M., Garland, C., Hammond, T., Holloway, C., McMahon, N., Milligan, J., Park, B., Pirmohamed, M., Pollard, C., Radford, J., Roome, N., Sager, P., Singh, S., Suter, T., Suter, W., Trafford, A., Volders, P., Wallis, R., Weaver, R., York, M. & Valentin, J. 2011. How can we improve our understanding of cardiovascular safety liabilities to develop safer medicines? *British journal of pharmacology* **163**:675-93.

Le Couteur, D. G., Cogger, V. C., Markus, A. M. A., Harvey, P. J., Yin, Z.-L., Ansselin, A. D. & McLean, A. J. 2001. Pseudocapillarization and associated energy limitation in the aged rat liver. *Hepatology* **33**:537-43.

Le Couteur, D. G., Hickey, H., Harvey, P. J., Gready, J. & McLean, A. J. 1999. Hepatic artery flow and propranolol metabolism in perfused cirrhotic rat liver. *The Journal of pharmacology and experimental therapeutics* **289**:1553-8.

LeCluyse, E. L., Alexandre, E., Hamilton, G. A., Viollon-Abadie, C., Coon, D. J., Jolley, S. & Richert, L. 2005. Isolation and culture of primary human hepatocytes. *Methods in molecular biology* **290**:207-29.

LeCluyse, E. L., Witek, R. P., Andersen, M. E. & Powers, M. J. 2012. Organotypic liver culture models: Meeting current challenges in toxicity testing. *Critical reviews in toxicology* **42**:501-48.

LeCouter, J., Moritz, D. R., Li, B., Phillips, G. L., Liang, X. H., Gerber, H.-P., Hillan, K. J. & Ferrara, N. 2003. Angiogenesis-Independent Endothelial Protection of Liver: Role of VEGFR-1. *Science* **299**:890.

Lee, M. H., Graham, G. G., Williams, K. M. & Day, R. O. 2008. A benefit-risk assessment of benzbromarone in the treatment of gout. Was its withdrawal from the market in the best interest of patients? *Drug safety* **31**:643-65.

Leise, M. D., Poterucha, J. J. & Talwalkar, J. A. 2014. Drug-induced liver injury. *Mayo Clinic proceedings. Mayo Clinic* **89**:95-106.

Lemoine, A., Gautier, J. C., Azoulay, D., Kiffel, L., Belloc, C., Guengerich, F. P., Maurel, P., Beaune, P. & Leroux, J. P. 1993. Major pathway of imipramine metabolism is catalyzed by cytochromes P-450 1A2 and P-450 3A4 in human liver. *Molecular pharmacology* **43**:827-32.

Li, F., Ambrosini, G., Chu, E. Y., Plescia, J., Tognin, S., Marchisio, P. C. & Altieri, D. C. 1998. Control of apoptosis and mitotic spindle checkpoint by survivin. *Nature* **396**:580-4.

Li, X., Lee, C., Tang, Z., Zhang, F., Arjunan, P., Li, Y., Hou, X., Kumar, A. & Dong, L. 2009. VEGF-B. *Cell Adhesion & Migration* **3**:322-27.

Liao, Y. & Hung, M.-C. 2010. Physiological regulation of Akt activity and stability. *American journal of translational research* **2**:19-42.

Lin, R.-Z., Chou, L.-F., Chien, C.-C. M. & Chang, H.-Y. 2006. Dynamic analysis of hepatoma spheroid formation: roles of E-cadherin and β1-integrin. *Cell and tissue research* **324**:411-22.

Lindros, K. O. 1997. Zonation of cytochrome P450 expression, drug metabolism and toxicity in liver. *General pharmacology* **28**:191-6.

Linnet, K. 2004. In vitro microsomal metabolism of imipramine under conditions mimicking the in vivo steady-state situation. *Human Psychopharmacology: Clinical and Experimental* **19**:31-36.

Livak, K. J. & Schmittgen, T. D. 2001. Analysis of relative gene expression data using real-time quantitative PCR and the 2(-Delta Delta C(T)) Method. *Methods (San Diego, Calif.)* **25**:402-8.

Lu, C. & Li, A. P. 2001. Species comparison in P450 induction: effects of dexamethasone, omeprazole, and rifampin on P450 isoforms 1A and 3A in primary cultured hepatocytes from man, Sprague-Dawley rat, minipig, and beagle dog. *Chem Biol Interact* **134**:271-81.

Lu, Z. & Xu, S. 2006. ERK1/2 MAP kinases in cell survival and apoptosis. *IUBMB Life* **58**:621-31.

MacPhee, P. J., Schmidt, E. E. & Groom, A. C. 1995. Intermittence of blood flow in liver sinusoids, studied by high-resolution in vivo microscopy. *The American journal of physiology* **269**:G692-8.

Malovic, I., Sorensen, K. K., Elvevold, K. H., Nedredal, G. I., Paulsen, S., Erofeev, A. V., Smedsrod, B. H. & McCourt, P. A. 2007. The mannose receptor on murine liver sinusoidal endothelial cells is the main denatured collagen clearance receptor. *Hepatology* **45**:1454-61.

March, S., Hui, E. E., Underhill, G. H., Khetani, S. & Bhatia, S. N. 2009. Microenvironmental regulation of the sinusoidal endothelial cell phenotype in vitro. *Hepatology* **50**:920-8.

Marion, M. J., Hantz, O. & Durantel, D. 2010. The HepaRG cell line: biological properties and relevance as a tool for cell biology, drug metabolism, and virology studies. *Methods in molecular biology* **640**:261-72.

Martinez, I., Nedredal, G. I., Oie, C. I., Warren, A., Johansen, O., Le Couteur, D. G. & Smedsrod, B. 2008. The influence of oxygen tension on the structure and function of isolated liver sinusoidal endothelial cells. *Comparative hepatology* **7**:4.

Matsumoto, K., Yoshitomi, H., Rossant, J. & Zaret, K. S. 2001. Liver Organogenesis Promoted by Endothelial Cells Prior to Vascular Function. *Science* **294**:559-63.

Mavria, G., Vercoulen, Y., Yeo, M., Paterson, H., Karasarides, M., Marais, R., Bird, D. & Marshall, C. J. 2006. ERK-MAPK signaling opposes Rho-kinase to promote endothelial cell survival and sprouting during angiogenesis. *Cancer cell* **9**:33-44.

McCuskey, R. 2012. Chapter 1 - Anatomy of the Liver. *Zakim and Boyer's Hepatology (Sixth Edition).* W.B. Saunders, Saint Louis, pp. 3-19.

McCuskey, R. S. 2006. Sinusoidal endothelial cells as an early target for hepatic toxicants. *Clinical hemorheology and microcirculation* **34**:5-10.

McCuskey, R. S., Bethea, N. W., Wong, J., McCuskey, M. K., Abril, E. R., Wang, X., Ito, Y. & DeLeve, L. D. 2005. Ethanol binging exacerbates sinusoidal endothelial and parenchymal injury elicited by acetaminophen. *Journal of hepatology* **42**:371-77.

McCuskey, R. S., Machen, N. W., Wang, X., McCuskey, M. K., Abril, E., Earnest, D. L. & DeLeve, L. D. 2001. A single ethanol binge exacerbates early acetaminophen-induced centrilobular injury to the sinusoidal endothelium and alters sinusoidal blood flow. *In*: Wisse, E., Knook, D., De, Z. a. n. g. e. r. & Arthur, M. J. P. [Eds.] *In: Cells of the Hepatic Sinusoid.* The Kupffer Cell Foundation, Leiden, The Netherlands.

McDonald, M. G. & Rettie, A. E. 2007. Sequential metabolism and bioactivation of the hepatotoxin benzbromarone: formation of glutathione adducts from a catechol intermediate. *Chemical research in toxicology* **20**:1833-42.

McGill, M. R., Sharpe, M. R., Williams, C. D., Taha, M., Curry, S. C. & Jaeschke, H. 2012. The mechanism underlying acetaminophen-induced hepatotoxicity in humans and mice involves mitochondrial damage and nuclear DNA fragmentation. *The Journal of clinical investigation* **122**:1574-83.

McLean, A. J., Cogger, V. C., Chong, G. C., Warren, A., Markus, A. M., Dahlstrom, J. E. & Le Couteur, D. G. 2003. Age-related pseudocapillarization of the human liver. *The Journal of pathology* **200**:112-7.

McLin, V. A. & Yazigi, N. 2011. 67 - Developmental Anatomy and Physiology of the Liver and Bile Ducts. *Pediatric Gastrointestinal and Liver Disease (Fourth Edition).* W.B. Saunders, Saint Louis, pp. 718-27.

Meadows, K. N., Bryant, P. & Pumiglia, K. 2001. Vascular endothelial growth factor induction of the angiogenic phenotype requires Ras activation. *The Journal of biological chemistry* **276**:49289-98.

Mebratu, Y. & Tesfaigzi, Y. 2009. How ERK1/2 Activation Controls Cell Proliferation and Cell Death Is Subcellular Localization the Answer? *Cell cycle (Georgetown, Tex.)* **8**:1168-75.

Mena, A. C., Pulido, E. G. & Guillen-Ponce, C. 2010. Understanding the molecular-based mechanism of action of the tyrosine kinase inhibitor: sunitinib. *Anti-cancer drugs* **21 Suppl 1**:S3-11.

Mendel, D. B., Laird, A. D., Xin, X., Louie, S. G., Christensen, J. G., Li, G., Schreck, R. E., Abrams, T. J., Ngai, T. J., Lee, L. B., Murray, L. J., Carver, J., Chan, E., Moss, K. G., Haznedar, J. O., Sukbuntherng, J., Blake, R. A., Sun, L., Tang, C., Miller, T., Shirazian, S., McMahon, G. & Cherrington, J. M. 2003. In vivo antitumor activity of SU11248, a novel tyrosine kinase inhibitor targeting vascular endothelial growth factor and platelet-derived growth factor receptors: determination of a pharmacokinetic/pharmacodynamic relationship. *Clinical cancer research : an official journal of the American Association for Cancer Research* **9**:327-37.

Meng, X., Earnshaw, C. J., Tailor, A., Jenkins, R. E., Waddington, J. C., Whitaker, P., French, N. S., Naisbitt, D. J. & Park, B. K. 2016. Amoxicillin and Clavulanate Form Chemically and Immunologically Distinct Multiple Haptenic Structures in Patients. *Chemical research in toxicology* **29**:1762-72.

Mereish, K. A., Bunner, D. L., Ragland, D. R. & Creasia, D. A. 1991. Protection against microcystin-LR-induced hepatotoxicity by Silymarin: biochemistry, histopathology, and lethality. *Pharmaceutical research* **8**:273-7.

Messner, S., Agarkova, I., Moritz, W. & Kelm, J. M. 2013. Multi-cell type human liver microtissues for hepatotoxicity testing. *Archives of toxicology* **87**:209-13.

Michaelis, U. R. 2014a. Mechanisms of endothelial cell migration. *Cellular and molecular life sciences : CMLS* **71**:4131-48.

Michaelis, U. R. 2014b. Mechanisms of endothelial cell migration. *Cellular and Molecular Life Sciences* **71**:4131-48.

Miller, C. M., Donner, A. J., Blank, E. E., Egger, A. W., Kellar, B. M., Østergaard, M. E., Seth, P. P. & Harris, E. N. 2016. Stabilin-1 and Stabilin-2 are specific receptors for the cellular internalization of phosphorothioate-modified antisense oligonucleotides (ASOs) in the liver. *Nucleic Acids Research*.

Miner, J. H. 2012. The Glomerular Basement Membrane. *Experimental cell research* **318**:973-78.

Miyamoto, Y., Ikeuchi, M., Noguchi, H., Yagi, T. & Hayashi, S. 2015. Spheroid Formation and Evaluation of Hepatic Cells in a Three-Dimensional Culture Device. *Cell medicine* **8**:47-56.

Miyao, M., Kotani, H., Ishida, T., Kawai, C., Manabe, S., Abiru, H. & Tamaki, K. 2015. Pivotal role of liver sinusoidal endothelial cells in NAFLD/NASH progression. *Laboratory investigation; a journal of technical methods and pathology* **95**:1130-44.

Morgan, E. T. 2001. Regulation of Cytochrome P450 by Inflammatory Mediators: Why and How? *Drug Metabolism and Disposition* **29**:207-12.

Morgan, M. Y., Reshef, R., Shah, R. R., Oates, N. S., Smith, R. L. & Sherlock, S. 1984. Impaired oxidation of debrisoquine in patients with perhexiline liver injury. *Gut* **25**:1057-64.

Motzer , R. J., Hutson , T. E., Cella , D., Reeves , J., Hawkins , R., Guo , J., Nathan , P., Staehler , M., de Souza , P., Merchan , J. R., Boleti , E., Fife , K., Jin , J., Jones , R., Uemura , H., De Giorgi , U., Harmenberg , U., Wang , J., Sternberg , C. N., Deen , K., McCann , L., Hackshaw , M. D., Crescenzo , R., Pandite , L. N. & Choueiri , T. K. 2013. Pazopanib versus Sunitinib in Metastatic Renal-Cell Carcinoma. *New England Journal of Medicine* **369**:722-31.

Mourtada-Maarabouni, M., Watson, D., Munir, M., Farzaneh, F. & Williams, G. T. 2013. Apoptosis suppression by candidate oncogene PLAC8 is reversed in other cell types. *Current cancer drug targets* **13**:80-91.

Mouta Carreira, C., Nasser, S. M., di Tomaso, E., Padera, T. P., Boucher, Y., Tomarev, S. I. & Jain, R. K. 2001. LYVE-1 is not restricted to the lymph vessels: expression in normal liver blood sinusoids and down-regulation in human liver cancer and cirrhosis. *Cancer research* **61**:8079-84.

Mueller, E. W., Rockey, M. L. & Rashkin, M. C. 2008. Sunitinib-related fulminant hepatic failure: case report and review of the literature. *Pharmacotherapy* **28**:1066-70.

Muntane-Relat, J., Ourlin, J. C., Domergue, J. & Maurel, P. 1995. Differential effects of cytokines on the inducible expression of CYP1A1, CYP1A2, and CYP3A4 in human hepatocytes in primary culture. *Hepatology* **22**:1143-53.

Muriel, P. 2009. Role of free radicals in liver diseases. *Hepatology International* **3**:526-36.

Nakamura, K., Hatano, E., Narita, M., Miyagawa-Hayashino, A., Koyama, Y., Nagata, H., Iwaisako, K., Taura, K. & Uemoto, S. 2012. Sorafenib attenuates monocrotaline-induced sinusoidal obstruction syndrome in rats through suppression of JNK and MMP-9. *J Hepatol* **57**:1037-43.

Nakatani, K., Kaneda, K., Seki, S. & Nakajima, Y. 2004. Pit cells as liver-associated natural killer cells: morphology and function. *Medical electron microscopy : official journal of the Clinical Electron Microscopy Society of Japan* **37**:29-36.

Neal, G. E., Eaton, D. L., Judah, D. J. & Verma, A. 1998. Metabolism and toxicity of aflatoxins M1 and B1 in human-derived in vitro systems. *Toxicology and applied pharmacology* **151**:152-8.

Nelson, D. L., Lehninger, A. L. & Cox, M. M. 2008. *Lehninger Principles of Biochemistry.* W.H. Freeman,

Nelson, L. J., Navarro, M., Treskes, P., Samuel, K., Tura-Ceide, O., Morley, S. D., Hayes, P. C. & Plevris, J. N. 2015. Acetaminophen cytotoxicity is ameliorated in a human liver organotypic co-culture model. *Scientific reports* **5**:17455.

Nilsson, I., Bahram, F., Li, X., Gualandi, L., Koch, S., Jarvius, M., Söderberg, O., Anisimov, A., Kholová, I., Pytowski, B., Baldwin, M., Ylä-Herttuala, S., Alitalo, K., Kreuger, J. & Claesson-Welsh, L. 2010. VEGF receptor 2/-3 heterodimers detected in situ by proximity ligation on angiogenic sprouts. *The EMBO journal* **29**:1377-88.

Nonaka, H., Tanaka, M., Suzuki, K. & Miyajima, A. 2007. Development of murine hepatic sinusoidal endothelial cells characterized by the expression of hyaluronan receptors. *Developmental dynamics : an official publication of the American Association of Anatomists* **236**:2258-67.

Ohyashiki, K., Kuriyama, Y., Nakajima, A., Tauchi, T., Ito, Y., Miyazawa, H., Kimura, Y., Serizawa, H. & Ebihara, Y. 2002. Imatinib mesylate-induced hepato-toxicity in chronic myeloid leukemia demonstrated focal necrosis resembling acute viral hepatitis. *Leukemia* **16**:2160-1.

Oladimeji, P., Cui, H., Zhang, C. & Chen, T. 2016. Regulation of PXR and CAR by protein-protein interaction and signaling crosstalk. *Expert opinion on drug metabolism & toxicology* **12**:997-1010.

Olofsson, B., Korpelainen, E., Pepper, M. S., Mandriota, S. J., Aase, K., Kumar, V., Gunji, Y., Jeltsch, M. M., Shibuya, M., Alitalo, K. & Eriksson, U. 1998. Vascular endothelial growth factor B (VEGF-B) binds to VEGF receptor-1 and regulates plasminogen activator activity in endothelial cells. *Proceedings of the National Academy of Sciences of the United States of America* **95**:11709-14.

Onali, P., Dedoni, S. & Olianas, M. C. 2009. Direct Agonist Activity of Tricyclic Antidepressants at Distinct Opioid Receptor Subtypes. *Journal of Pharmacology and Experimental Therapeutics* **332**:255.

Osusky, K. L., Hallahan, D. E., Fu, A., Ye, F., Shyr, Y. & Geng, L. 2004. The receptor tyrosine kinase inhibitor SU11248 impedes endothelial cell migration, tubule formation, and blood vessel formation in vivo, but has little effect on existing tumor vessels. *Angiogenesis* **7**:225-33.

Otsuka, H., Sasaki, K., Okimura, S., Nagamura, M. & Nakasone, Y. 2013. Micropatterned co-culture of hepatocyte spheroids layered on non-parenchymal cells to understand heterotypic cellular interactions. *Science and Technology of Advanced Materials* **14**:065003.

Paavonen, K., Puolakkainen, P., Jussila, L., Jahkola, T. & Alitalo, K. 2000. Vascular Endothelial Growth Factor Receptor-3 in Lymphangiogenesis in Wound Healing. *The American journal of pathology* **156**:1499-504.

Parker, W. B. 2009. Enzymology of Purine and Pyrimidine Antimetabolites Used in the Treatment of Cancer. *Chemical reviews* **109**:2880-93.

Parsons, J. T. 2003. Focal adhesion kinase: the first ten years. *Journal of cell science* **116**:1409-16.

Pascussi, J. M., Gerbal-Chaloin, S., Pichard-Garcia, L., Daujat, M., Fabre, J. M., Maurel, P. & Vilarem, M. J. 2000. Interleukin-6 negatively regulates the expression of pregnane X receptor and constitutively activated receptor in primary human hepatocytes. *Biochemical and biophysical research communications* **274**:707-13.

Pasvolsky, O., Leader, A., Iakobishvili, Z., Wasserstrum, Y., Kornowski, R. & Raanani, P. 2015. Tyrosine kinase inhibitor associated vascular toxicity in chronic myeloid leukemia. *Cardio-Oncology* **1**:1.

Patel, S. J., Milwid, J. M., King, K. R., Bohr, S., Iracheta-Vellve, A., Li, M., Vitalo, A., Parekkadan, B., Jindal, R. & Yarmush, M. L. 2012. Gap junction inhibition prevents drug-induced liver toxicity and fulminant hepatic failure. *Nat Biotech* **30**:179-83.

Paul, M. K. & Mukhopadhyay, A. K. 2004. Tyrosine kinase – Role and significance in Cancer. *International journal of medical sciences* **1**:101-15.

Pemovska, T., Johnson, E., Kontro, M., Repasky, G. A., Chen, J., Wells, P., Cronin, C. N., McTigue, M., Kallioniemi, O., Porkka, K., Murray, B. W. & Wennerberg, K. 2015. Axitinib effectively inhibits BCR-ABL1(T315I) with a distinct binding conformation. *Nature* **519**:102-05.

Peppin, J. F. & Raffa, R. B. 2015. Delta opioid agonists: a concise update on potential therapeutic applications. *Journal of clinical pharmacy and therapeutics* **40**:155-66.

Perez-Pomares, J. M., Carmona, R., Gonzalez-Iriarte, M., Macias, D., Guadix, J. A. & Munoz-Chapuli, R. 2004. Contribution of mesothelium-derived cells to liver sinusoids in avian embryos. *Developmental dynamics : an official publication of the American Association of Anatomists* **229**:465-74.

Perri, R. & Shah, V. 2005a. Hepatic Sinusoidal Endothelial Cells. *In*: Dufour, J.-F., Clavien, P.-A., Trautwein, C. & Graf, R. [Eds.] *Signaling Pathways in Liver Diseases.* Springer Berlin Heidelberg, pp. 53-62.

Perri, R. E. & Shah, V. 2005b. Hepatic Sinusoidal Endothelial Cells. *In*: Dufour, J.-F., Clavien, P.-A., Trautwein, C. & Graf, R. [Eds.] *Signaling Pathways in Liver Diseases.* Springer Berlin Heidelberg, Berlin, Heidelberg, pp. 53-62.

Phan, A. T., Halperin, D. M., Chan, J. A., Fogelman, D. R., Hess, K. R., Malinowski, P., Regan, E., Ng, C. S., Yao, J. C. & Kulke, M. H. 2015. Pazopanib and depot octreotide in advanced, well-differentiated neuroendocrine tumours: a multicentre, single-group, phase 2 study. *The Lancet. Oncology* **16**:695-703.

Podar, K., Tonon, G., Sattler, M., Tai, Y. T., Legouill, S., Yasui, H., Ishitsuka, K., Kumar, S., Kumar, R., Pandite, L. N., Hideshima, T., Chauhan, D. & Anderson, K. C. 2006. The small-molecule VEGF receptor inhibitor pazopanib (GW786034B) targets both tumor and endothelial cells in multiple myeloma. *Proceedings of the National Academy of Sciences of the United States of America* **103**:19478-83.

Pohlmann, S., Soilleux, E. J., Baribaud, F., Leslie, G. J., Morris, L. S., Trowsdale, J., Lee, B., Coleman, N. & Doms, R. W. 2001. DC-SIGNR, a DC-SIGN homologue expressed in endothelial cells, binds to human and simian immunodeficiency viruses and activates infection in trans. *Proceedings of the National Academy of Sciences of the United States of America* **98**:2670-5.

Politz, O., Gratchev, A., McCourt, P. A., Schledzewski, K., Guillot, P., Johansson, S., Svineng, G., Franke, P., Kannicht, C., Kzhyshkowska, J., Longati, P., Velten, F. W., Johansson, S. & Goerdt, S. 2002. Stabilin-1 and -2 constitute a novel family of fasciclin-like hyaluronan receptor homologues. *The Biochemical journal* **362**:155-64.

Powell, W., Jr, Koch-Weser, J. & Williams, R. A. 1968. LEthal hepatic necrosis after therapy with imipramine and desipramine. *JAMA* **206**:642-45.

PRICE, L. H., NELSON, J. C. & WALTRIP, R. W. 1983. Desipramine-associated hepatitis. *Journal of clinical psychopharmacology* **3**:243-45.

Rafii, S., Butler, J. M. & Ding, B. S. 2016. Angiocrine functions of organ-specific endothelial cells. *Nature* **529**:316-25.

Ramsdell, H. S., Parkinson, A., Eddy, A. C. & Eaton, D. L. 1991. Bioactivation of aflatoxin B1 by human liver microsomes: role of cytochrome P450 IIIA enzymes. *Toxicology and applied pharmacology* **108**:436-47.

Räsänen, M., Degerman, J., Nissinen, T. A., Miinalainen, I., Kerkelä, R., Siltanen, A., Backman, J. T., Mervaala, E., Hulmi, J. J., Kivelä, R. & Alitalo, K. 2016. VEGF-B gene therapy inhibits doxorubicin-induced cardiotoxicity by endothelial protection. *Proceedings of the National Academy of Sciences*.

Ravenscroft, S. M., Pointon, A., Williams, A. W., Cross, M. J. & Sidaway, J. E. 2016. Cardiac Non-myocyte Cells Show Enhanced Pharmacological Function Suggestive of Contractile Maturity in Stem Cell Derived Cardiomyocyte Microtissues. *Toxicological Sciences* **152**:99-112.

Reese, M. J., Wurm, R. M., Muir, K. T., Generaux, G. T., St. John-Williams, L. & McConn, D. J. 2008. An in Vitro Mechanistic Study to Elucidate the Desipramine/Bupropion Clinical Drug-Drug Interaction. *Drug Metabolism and Disposition* **36**:1198.

Richards, M. & Mellor, H. 2016. In Vitro Coculture Assays of Angiogenesis. *Methods in molecular biology* **1430**:159-66.

Rieder, H., Armbrust, T., Meyer zum Buschenfelde, K. H. & Ramadori, G. 1993. Contribution of sinusoidal endothelial liver cells to liver fibrosis: expression of transforming growth factor-beta 1 receptors and modulation of plasmin-generating enzymes by transforming growth factor-beta 1. *Hepatology* **18**:937-44.

Ringner, M. 2008. What is principal component analysis? *Nat Biotech* **26**:303-04.

Rini, B. I., Escudier, B., Tomczak, P., Kaprin, A., Szczylik, C., Hutson, T. E., Michaelson, M. D., Gorbunova, V. A., Gore, M. E., Rusakov, I. G., Negrier, S., Ou, Y. C., Castellano, D., Lim, H. Y., Uemura, H., Tarazi, J., Cella, D., Chen, C., Rosbrook, B., Kim, S. & Motzer, R. J. 2011. Comparative effectiveness of axitinib versus sorafenib in advanced renal cell carcinoma (AXIS): a randomised phase 3 trial. *Lancet* **378**:1931-9.

Rini, B. I., Melichar, B., Ueda, T., Grunwald, V., Fishman, M. N., Arranz, J. A., Bair, A. H., Pithavala, Y. K., Andrews, G. I., Pavlov, D., Kim, S. & Jonasch, E. 2013. Axitinib with or without dose titration for first-line metastatic renal-cell carcinoma: a randomised double-blind phase 2 trial. *The Lancet. Oncology* **14**:1233-42.

Roberts, D. W., Bucci, T. J., Benson, R. W., Warbritton, A. R., McRae, T. A., Pumford, N. R. & Hinson, J. A. 1991. Immunohistochemical localization and quantification of the 3-(cystein-S-yl)-acetaminophen protein adduct in acetaminophen hepatotoxicity. *The American journal of pathology* **138**:359-71.

Roberts, D. W., Lee, W. M., Hinson, J. A., Bai, S., Swearingen, C. J., Stravitz, R. T., Reuben, A., Letzig, L., Simpson, P. M., Rule, J., Fontana, R. J., Ganger, D., Reddy, K. R., Liou, I., Fix, O. & James, L. P. 2016. An Immunoassay to Rapidly Measure Acetaminophen Protein Adducts Accurately Identifies Patients with Acute Liver Injury or Failure. *Clinical Gastroenterology and Hepatology*.

Robinson, D. R., Wu, Y. M. & Lin, S. F. 2000. The protein tyrosine kinase family of the human genome. *Oncogene* **19**:5548-57.

Robinson, S. M., Mann, J., Vasilaki, A., Mathers, J., Burt, A. D., Oakley, F., White, S. A. & Mann, D. A. 2013. Pathogenesis of FOLFOX induced sinusoidal obstruction syndrome in a murine chemotherapy model. *J Hepatol* **59**:318-26.

Rockey, D. C. & Chung, J. J. 1996. Regulation of inducible nitric oxide synthase in hepatic sinusoidal endothelial cells. *The American journal of physiology* **271**:G260-7.

Rogers, A. B. & Dintzis, R. Z. 2012. 13 - Liver and Gallbladder. *In*: Piper, M. T., Suzanne, D., Denny, L., Charles W. FrevertA2 - Piper M. Treuting, S. D. D. L. & Charles, W. F. [Eds.] *Comparative Anatomy and Histology.* Academic Press, San Diego, pp. 193-201.

Ruch, C., Skiniotis, G., Steinmetz, M. O., Walz, T. & Ballmer-Hofer, K. 2007. Structure of a VEGF-VEGF receptor complex determined by electron microscopy. *Nature structural & molecular biology* **14**:249-50.

Rudmann, D. G. 2013. On-target and off-target-based toxicologic effects. *Toxicologic pathology* **41**:310-4.

Sacré, A., Lanthier, N., Dano, H., Aydin, S., Leggenhager, D., Weber, A., Dekairelle, A.-F., De Cuyper, A., Gala, J.-L., Humblet, Y., Sempoux, C. & Van den Eynde, M. 2016. Regorafenib induced severe toxic hepatitis: characterization and discussion. *Liver International*:n/a-n/a.

Sacre, A., Lanthier, N., Dano, H., Aydin, S., Leggenhager, D., Weber, A., Dekairelle, A. F., De Cuyper, A., Gala, J. L., Humblet, Y., Sempoux, C. & Van den Eynde, M. 2016. Regorafenib induced severe toxic hepatitis: characterization and discussion. *Liver international : official journal of the International Association for the Study of the Liver*.

Salven, P., Mustjoki, S., Alitalo, R., Alitalo, K. & Rafii, S. 2003. VEGFR-3 and CD133 identify a population of CD34+ lymphatic/vascular endothelial precursor cells. *Blood* **101**:168-72.

Sato, M., Suzuki, S. & Senoo, H. 2003. Hepatic stellate cells: unique characteristics in cell biology and phenotype. *Cell structure and function* **28**:105-12.

Sawano, A., Iwai, S., Sakurai, Y., Ito, M., Shitara, K., Nakahata, T. & Shibuya, M. 2001. Flt-1, vascular endothelial growth factor receptor 1, is a novel cell surface marker for the lineage of monocyte-macrophages in humans. *Blood* **97**:785-91.

Schlessinger, J. & Ullrich, A. 1992. Growth factor signaling by receptor tyrosine kinases. *Neuron* **9**:383-91.

Schmieder, R., Hoffmann, J., Becker, M., Bhargava, A., Müller, T., Kahmann, N., Ellinghaus, P., Adams, R., Rosenthal, A., Thierauch, K.-H., Scholz, A., Wilhelm, S. M. & Zopf, D. 2014a. Regorafenib (BAY 73-4506): Antitumor and antimetastatic activities in preclinical models of colorectal cancer. *International Journal of Cancer. Journal International du Cancer* **135**:1487-96.

Schmieder, R., Hoffmann, J., Becker, M., Bhargava, A., Muller, T., Kahmann, N., Ellinghaus, P., Adams, R., Rosenthal, A., Thierauch, K. H., Scholz, A., Wilhelm, S. M. & Zopf, D. 2014b. Regorafenib (BAY 73-4506): antitumor and antimetastatic activities in preclinical models of colorectal cancer. *International journal of cancer* **135**:1487-96.

Ségaliny, A. I., Tellez-Gabriel, M., Heymann, M.-F. & Heymann, D. 2015. Receptor tyrosine kinases: Characterisation, mechanism of action and therapeutic interests for bone cancers. *Journal of Bone Oncology* **4**:1-12.

Shah, R. R., Morganroth, J. & Shah, D. R. 2013. Hepatotoxicity of tyrosine kinase inhibitors: clinical and regulatory perspectives. *Drug safety* **36**:491-503.

Shah, V., Haddad, F. G., Garcia-Cardena, G., Frangos, J. A., Mennone, A., Groszmann, R. J. & Sessa, W. C. 1997. Liver sinusoidal endothelial cells are responsible for nitric oxide modulation of resistance in the hepatic sinusoids. *J Clin Invest* **100**:2923-30.

Shahani, T., Covens, K., Lavend'homme, R., Jazouli, N., Sokal, E., Peerlinck, K. & Jacquemin, M. 2014. Human liver sinusoidal endothelial cells but not hepatocytes contain factor VIII. *J Thromb Haemost* **12**:36-42.

Shalaby, F., Rossant, J., Yamaguchi, T. P., Gertsenstein, M., Wu, X.-F., Breitman, M. L. & Schuh, A. C. 1995. Failure of blood-island formation and vasculogenesis in Flk-1-deficient mice. *Nature* **376**:62-66.

Shalaby, M. R., Waage, A. & Espevik, T. 1989. Cytokine regulation of interleukin 6 production by human endothelial cells. *Cellular immunology* **121**:372-82.

Shin, J.-G., Park, J.-Y., Kim, M.-J., Shon, J.-H., Yoon, Y.-R., Cha, I.-J., Lee, S.-S., Oh, S.-W., Kim, S.-W. & Flockhart, D. A. 2002. Inhibitory Effects of Tricyclic Antidepressants (TCAs) on Human Cytochrome P450 Enzymes in Vitro: Mechanism of Drug Interaction between TCAs and Phenytoin. *Drug Metabolism and Disposition* **30**:1102.

Shiratori, Y., Tananka, M., Kawase, T., Shiina, S., Komatsu, Y. & Omata, M. 1993. Quantification of sinusoidal cell function in vivo. *Seminars in liver disease* **13**:39-49.

Si-Tayeb, K., Lemaigre, F. P. & Duncan, S. A. 2010. Organogenesis and development of the liver. *Developmental cell* **18**:175-89.

Sloan, B. & Scheinfeld, N. S. 2008. Pazopanib, a VEGF receptor tyrosine kinase inhibitor for cancer therapy. *Curr Opin Investig Drugs* **9**:1324-35.

Smedsrod, B., Pertoft, H., Gustafson, S. & Laurent, T. C. 1990. Scavenger functions of the liver endothelial cell. *The Biochemical journal* **266**:313-27.

Smith, B. J., Pithavala, Y., Bu, H. Z., Kang, P., Hee, B., Deese, A. J., Pool, W. F., Klamerus, K. J., Wu, E. Y. & Dalvie, D. K. 2014. Pharmacokinetics, metabolism, and excretion of [14C]axitinib, a vascular endothelial growth factor receptor tyrosine kinase inhibitor, in humans. *Drug metabolism and disposition: the biological fate of chemicals* **42**:918-31.

Smith, P. K., Krohn, R. I., Hermanson, G. T., Mallia, A. K., Gartner, F. H., Provenzano, M. D., Fujimoto, E. K., Goeke, N. M., Olson, B. J. & Klenk, D. C. 1985. Measurement of protein using bicinchoninic acid. *Analytical biochemistry* **150**:76-85.

Sorensen, K. K., McCourt, P., Berg, T., Crossley, C., Le Couteur, D., Wake, K. & Smedsrod, B. 2012. The scavenger endothelial cell: a new player in homeostasis and immunity. *American journal of physiology. Regulatory, integrative and comparative physiology* **303**:R1217-30.

Sorensen, K. K., Simon-Santamaria, J., McCuskey, R. S. & Smedsrod, B. 2015. Liver Sinusoidal Endothelial Cells. *Compr Physiol* **5**:1751-74.

Sørensen, L. B., Sørensen, R. N., Miners, J. O., Somogyi, A. A., Grgurinovich, N. & Birkett, D. J. 2003. Polymorphic hydroxylation of perhexiline in vitro. *British journal of clinical pharmacology* **55**:635-38.

Sorrell, J. M., Baber, M. A. & Caplan, A. I. 2007. A self-assembled fibroblast-endothelial cell co-culture system that supports in vitro vasculogenesis by both human umbilical vein endothelial cells and human dermal microvascular endothelial cells. *Cells, tissues, organs* **186**:157-68.

Spano, J.-P., Chodkiewicz, C., Maurel, J., Wong, R., Wasan, H., Barone, C., Létourneau, R., Bajetta, E., Pithavala, Y. & Bycott, P. 2008. Efficacy of gemcitabine plus axitinib compared with gemcitabine alone in patients with advanced pancreatic cancer: an open-label randomised phase II study. *The Lancet* **371**:2101-08.

Speed, B., Bu, H. Z., Pool, W. F., Peng, G. W., Wu, E. Y., Patyna, S., Bello, C. & Kang, P. 2012. Pharmacokinetics, distribution, and metabolism of [14C]sunitinib in rats, monkeys, and humans. *Drug metabolism and disposition: the biological fate of chemicals* **40**:539-55.

Stolz, D. B. 2011. Sinusoidal Endothelial Cells. *In*: Monga, S. P. S. [Ed.] *Molecular Pathology of Liver Diseases.* Springer US, Boston, MA, pp. 97-107.

Straub, A. C., Clark, K. A., Ross, M. A., Chandra, A. G., Li, S., Gao, X., Pagano, P. J., Stolz, D. B. & Barchowsky, A. 2008. Arsenic-stimulated liver sinusoidal capillarization in mice requires NADPH oxidase-generated superoxide. *J Clin Invest* **118**:3980-9.

Straub, A. C., Stolz, D. B., Ross, M. A., Hernandez-Zavala, A., Soucy, N. V., Klei, L. R. & Barchowsky, A. 2007. Arsenic stimulates sinusoidal endothelial cell capillarization and vessel remodeling in mouse liver. *Hepatology* **45**:205-12.

Strickland, L. A., Jubb, A. M., Hongo, J. A., Zhong, F., Burwick, J., Fu, L., Frantz, G. D. & Koeppen, H. 2005. Plasmalemmal vesicle-associated protein (PLVAP) is expressed by tumour endothelium and is upregulated by vascular endothelial growth factor-A (VEGF). *The Journal of pathology* **206**.

Strumberg, D., Scheulen, M. E., Schultheis, B., Richly, H., Frost, A., Büchert, M., Christensen, O., Jeffers, M., Heinig, R., Boix, O. & Mross, K. 2012. Regorafenib (BAY 73-4506) in advanced colorectal cancer: a phase I study. *British Journal of Cancer* **106**:1722-27.

Su, J.-C., Mar, A.-C., Wu, S.-H., Tai, W.-T., Chu, P.-Y., Wu, C.-Y., Tseng, L.-M., Lee, T.-C., Chen, K.-F., Liu, C.-Y., Chiu, H.-C. & Shiau, C.-W. 2016. Disrupting VEGF-A paracrine and autocrine loops by targeting SHP-1 suppresses triple negative breast cancer metastasis. *Scientific reports* **6**:28888.

Su, J. L., Yen, C. J., Chen, P. S., Chuang, S. E., Hong, C. C., Kuo, I. H., Chen, H. Y., Hung, M. C. & Kuo, M. L. 2007. The role of the VEGF-C/VEGFR-3 axis in cancer progression. *British journal of cancer* **96**:541-5.

Sun, Y., Jin, K., Childs, J. T., Xie, L., Mao, X. O. & Greenberg, D. A. 2006. Vascular endothelial growth factor-B (VEGFB) stimulates neurogenesis: Evidence from knockout mice and growth factor administration. *Developmental biology* **289**:329-35.

Svistounov, D., Warren, A., McNerney, G. P., Owen, D. M., Zencak, D., Zykova, S. N., Crane, H., Huser, T., Quinn, R. J., Smedsrod, B., Le Couteur, D. G. & Cogger, V. C. 2012. The Relationship between fenestrations, sieve plates and rafts in liver sinusoidal endothelial cells. *PloS one* **7**:e46134.

Takahashi, M., Harada, S., Suzuki, H., Yamashita, N., Orita, H., Kato, M. & Kotoh, K. 2016. Regorafenib could cause sinusoidal obstruction syndrome. *Journal of gastrointestinal oncology* **7**:E41-4.

Takahashi, T., Yamaguchi, S., Chida, K. & Shibuya, M. 2001. A single autophosphorylation site on KDR/Flk-1 is essential for VEGF-A-dependent activation of PLC-gamma and DNA synthesis in vascular endothelial cells. *The EMBO journal* **20**:2768-78.

Takahashi, Y., Hori, Y., Yamamoto, T., Urashima, T., Ohara, Y. & Tanaka, H. 2015. 3D spheroid cultures improve the metabolic gene expression profiles of HepaRG cells. *Bioscience Reports* **35**.

Takebe, T., Sekine, K., Enomura, M., Koike, H., Kimura, M., Ogaeri, T., Zhang, R. R., Ueno, Y., Zheng, Y. W., Koike, N., Aoyama, S., Adachi, Y. & Taniguchi, H. 2013. Vascularized and functional human liver from an iPSC-derived organ bud transplant. *Nature* **499**:481-4.

Takebe, T., Zhang, R. R., Koike, H., Kimura, M., Yoshizawa, E., Enomura, M., Koike, N., Sekine, K. & Taniguchi, H. 2014. Generation of a vascularized and functional human liver from an iPSC-derived organ bud transplant. *Nature protocols* **9**:396-409.

Takezawa, T., Yamazaki, M., Mori, Y., Yonaha, T. & Yoshizato, K. 1992. Morphological and immuno-cytochemical characterization of a hetero-spheroid composed of fibroblasts and hepatocytes. *Journal of cell science* **101 (Pt 3)**:495-501.

Tallman, M. S., McDonald, G. B., DeLeve, L. D., Baer, M. R., Cook, M. N., Graepel, G. J. & Kollmer, C. 2013. Incidence of sinusoidal obstruction syndrome following Mylotarg (gemtuzumab ozogamicin): a prospective observational study of 482 patients in routine clinical practice. *International journal of hematology* **97**:456-64.

Tammela, T., Zarkada, G., Wallgard, E., Murtomaki, A., Suchting, S., Wirzenius, M., Waltari, M., Hellstrom, M., Schomber, T., Peltonen, R., Freitas, C., Duarte, A., Isoniemi, H., Laakkonen, P., Christofori, G., Yla-Herttuala, S., Shibuya, M., Pytowski, B., Eichmann, A., Betsholtz, C. & Alitalo, K. 2008. Blocking VEGFR-3 suppresses angiogenic sprouting and vascular network formation. *Nature* **454**:656-60.

Tanaka, M. & Iwakiri, Y. 2016. The Hepatic Lymphatic Vascular System: Structure, Function, Markers, and Lymphangiogenesis. *Cellular and Molecular Gastroenterology and Hepatology* **2**:733-49.

Taniguchi, E., Sakisaka, S., Matsuo, K., Tanikawa, K. & Sata, M. 2001. Expression and role of vascular endothelial growth factor in liver regeneration after partial hepatectomy in rats. *The journal of histochemistry and cytochemistry : official journal of the Histochemistry Society* **49**:121-30.

Taraboletti, G., D'Ascenzo, S., Borsotti, P., Giavazzi, R., Pavan, A. & Dolo, V. 2002. Shedding of the Matrix Metalloproteinases MMP-2, MMP-9, and MT1-MMP as Membrane Vesicle-Associated Components by Endothelial Cells. *The American journal of pathology* **160**:673-80.

Thiele, G. M., Miller, J. A., Klassen, L. W. & Tuma, D. J. 1999. Chronic ethanol consumption impairs receptor-mediated endocytosis of formaldehyde-treated albumin by isolated rat liver endothelial cells. *Hepatology* **29**:1511-7.

Tiggelman, A. M. B. C., Boers, W., Linthorst, C., Brand, H. S., Sala, M. & Chamuleau, R. A. E. M. 1995. Interleukin-6 production by human liver (myo)fibroblasts in culture. Evidence for a regulatory role of LPS, IL-lβ and TNFα. *Journal of hepatology* **23**:295-306.

Tornavaca, O., Chia, M., Dufton, N., Almagro, L. O., Conway, D. E., Randi, A. M., Schwartz, M. A., Matter, K. & Balda, M. S. 2015. ZO-1 controls endothelial adherens junctions, cell–cell tension, angiogenesis, and barrier formation. *The Journal of cell biology* **208**:821-38.

Trettin, A., Batkai, S., Thum, T., Jordan, J. & Tsikas, D. 2014. Trapping of NAPQI, the intermediate toxic paracetamol metabolite, by aqueous sulfide (S(2)(-)) and analysis by GC-MS/MS. *Journal of chromatography. B, Analytical technologies in the biomedical and life sciences* **963**:99-105.

Triebskorn, R., Casper, H., Heyd, A., Eikemper, R., Köhler, H. R. & Schwaiger, J. 2004. Toxic effects of the non-steroidal anti-inflammatory drug diclofenac: Part II. Cytological effects in liver, kidney, gills and intestine of rainbow trout (Oncorhynchus mykiss). *Aquatic Toxicology* **68**:151-66.

Turner, R., Lozoya, O., Wang, Y., Cardinale, V., Gaudio, E., Alpini, G., Mendel, G., Wauthier, E., Barbier, C., Alvaro, D. & Reid, L. M. 2011. Human hepatic stem cell and maturational liver lineage biology. *Hepatology* **53**:1035-45.

Valent, P., Hadzijusufovic, E., Schernthaner, G. H., Wolf, D., Rea, D. & le Coutre, P. 2015. Vascular safety issues in CML patients treated with BCR/ABL1 kinase inhibitors. *Blood* **125**:901-6.

Valla, D. C. & Cazals-Hatem, D. 2016. Sinusoidal obstruction syndrome. *Clin Res Hepatol Gastroenterol*.

van Geel, R. M. J. M., Beijnen, J. H. & Schellens, J. H. M. 2012. Concise Drug Review: Pazopanib and Axitinib. *The Oncologist* **17**:1081-89.

Verheul, H. M., Voest, E. E. & Schlingemann, R. O. 2004. Are tumours angiogenesis-dependent? *The Journal of pathology* **202**:5-13.

Vestweber, D. 2008. VE-Cadherin. *Arteriosclerosis, thrombosis, and vascular biology* **28**:223.

Vreuls, C. P., Driessen, A., Olde Damink, S. W., Koek, G. H., Duimel, H., van den Broek, M. A., Dejong, C. H., Braet, F. & Wisse, E. 2016. Sinusoidal obstruction syndrome (SOS): A light and electron microscopy study in human liver. *Micron* **84**:17-22.

Wack, K. E., Ross, M. A., Zegarra, V., Sysko, L. R., Watkins, S. C. & Stolz, D. B. 2001. Sinusoidal ultrastructure evaluated during the revascularization of regenerating rat liver. *Hepatology* **33**:363-78.

Waddell, T. & Cunningham, D. Evaluation of regorafenib in colorectal cancer and GIST. *The Lancet* **381**:273-75.

Walker, R. M., Racz, W. J. & McElligott, T. F. 1983. Scanning electron microscopic examination of acetaminophen-induced hepatotoxicity and congestion in mice. *The American journal of pathology* **113**:321-30.

Wallez, Y. & Huber, P. 2008. Endothelial adherens and tight junctions in vascular homeostasis, inflammation and angiogenesis. *Biochimica et Biophysica Acta (BBA) - Biomembranes* **1778**:794-809.

Wan, H. T., Mruk, D. D., Tang, E. I., Xiao, X., Cheng, Y.-H., Wong, E. W. P., Wong, C. K. C. & Cheng, C. Y. 2014. Role of non-receptor protein tyrosine kinases in spermatid transport during spermatogenesis. *Seminars in Cell & Developmental Biology* **30**:65-74.

Wan, P. T. C., Garnett, M. J., Roe, S. M., Lee, S., Niculescu-Duvaz, D., Good, V. M., Project, C. G., Jones, C. M., Marshall, C. J., Springer, C. J., Barford, D. & Marais, R. 2004. Mechanism of Activation of the RAF-ERK Signaling Pathway by Oncogenic Mutations of B-RAF. *Cell* **116**:855-67.

Wang, K., Zhang, S., Marzolf, B., Troisch, P., Brightman, A., Hu, Z., Hood, L. E. & Galas, D. J. 2009. Circulating microRNAs, potential biomarkers for drug-induced liver injury. *Proceedings of the National Academy of Sciences* **106**:4402-07.

Wang, L., Wang, X., Wang, L., Chiu, J. D., van de Ven, G., Gaarde, W. A. & Deleve, L. D. 2012. Hepatic vascular endothelial growth factor regulates recruitment of rat liver sinusoidal endothelial cell progenitor cells. *Gastroenterology* **143**:1555-63.e2.

Wang, S., Li, X., Parra, M., Verdin, E., Bassel-Duby, R. & Olson, E. N. 2008. Control of endothelial cell proliferation and migration by VEGF signaling to histone deacetylase 7. *Proceedings of the National Academy of Sciences of the United States of America* **105**:7738-43.

Wang, Y.-H., Cheng, T.-Y., Chen, T.-Y., Chang, K.-M., Chuang, V. P. & Kao, K.-J. 2014. Plasmalemmal Vesicle Associated Protein (PLVAP) as a therapeutic target for treatment of hepatocellular carcinoma. *BMC Cancer* **14**:815.

Wang, Y.-P., Yan, J., Beger, R. D., Fu, P. P. & Chou, M. W. 2005. Metabolic activation of the tumorigenic pyrrolizidine alkaloid, monocrotaline, leading to DNA adduct formation in vivo. *Cancer letters* **226**:27-35.

Wei, Y., Weng, D., Li, F., Zou, X., Young, D. O., Ji, J. & Shen, P. 2008. Involvement of JNK regulation in oxidative stress-mediated murine liver injury by microcystin-LR. *Apoptosis* **13**:1031-42.

Wellner, M., Maasch, C., Kupprion, C., Lindschau, C., Luft, F. C. & Haller, H. 1999. The proliferative effect of vascular endothelial growth factor requires protein kinase C-alpha and protein kinase C-zeta. *Arteriosclerosis, thrombosis, and vascular biology* **19**:178-85.

Weng, Z., Luo, Y., Yang, X., Greenhaw, J. J., Li, H., Xie, L., Mattes, W. B. & Shi, Q. 2015. Regorafenib impairs mitochondrial functions, activates AMP-activated protein kinase, induces autophagy, and causes rat hepatocyte necrosis. *Toxicology* **327**:10-21.

Widakowich, C., de Castro, G., Jr., de Azambuja, E., Dinh, P. & Awada, A. 2007. Review: side effects of approved molecular targeted therapies in solid cancers. *The oncologist* **12**:1443-55.

Wigle, J. T., Harvey, N., Detmar, M., Lagutina, I., Grosveld, G., Gunn, M. D., Jackson, D. G. & Oliver, G. 2002. An essential role for Prox1 in the induction of the lymphatic endothelial cell phenotype. *The EMBO journal* **21**:1505-13.

Wilhelm, S. M., Dumas, J., Adnane, L., Lynch, M., Carter, C. A., Schutz, G., Thierauch, K. H. & Zopf, D. 2011. Regorafenib (BAY 73-4506): a new oral multikinase inhibitor of angiogenic, stromal and oncogenic receptor tyrosine kinases with potent preclinical antitumor activity. *International journal of cancer* **129**:245-55.

Wilkinson, E. L., Sidaway, J. E. & Cross, M. J. 2016. Cardiotoxic drugs Herceptin and doxorubicin inhibit cardiac microvascular endothelial cell barrier formation resulting in increased drug permeability. *Biology Open* **5**:1362-70.

Wisse, E. 1970. An electron microscopic study of the fenestrated endothelial lining of rat liver sinusoids. *Journal of ultrastructure research* **31**:125-50.

Wisse, E. 1972. An Ultrastructural Characterization of the Endothelial Cell in the Rat Liver Sinusoid under Normal and Various Experimental Conditions, as a Contribution to the Distinction between Endothelial and Kupffer Cells. *J. Ultrastruct. Res.* **38**:528-62.

Wisse, E., Braet, F., Luo, D., De Zanger, R., Jans, D., Crabbe, E. & Vermoesen, A. 1996. Structure and function of sinusoidal lining cells in the liver. *Toxicologic pathology* **24**:100-11.

Wisse, E. & Knook, D. L. 1977. *Kupffer cells and other liver sinusoidal cells : proceedings of the International Kupffer Cell Symposium held in Noordwijkerhout, the Netherlands, 4-7 September, 1977.* Elsevier/North-Holland Biomedical Press ;sole distributors for the USA and Canada, Elsevier North-Holland, Amsterdam ; New York New York, xii, 544 p.

Wright, G., Leeson, G., Zeiger, A. & Lang, J. 1973. Proceedings: The absorption, excretion and metabolism of perhexiline maleate by the human. *Postgraduate medical journal* **49**:Suppl 3: 8-15.

Xie, G., Wang, X., Wang, L., Wang, L., Atkinson, R. D., Kanel, G. C., Gaarde, W. A. & Deleve, L. D. 2012. Role of differentiation of liver sinusoidal endothelial cells in progression and regression of hepatic fibrosis in rats. *Gastroenterology* **142**:918-27.e6.

Xu, X.-y., Pang, W.-j., Wen, Z.-n. & Xiang, W.-p. 2013. Changes in human umbilical vein endothelial cells induced by endothelial nitric oxide synthase traffic inducer. *Journal of Huazhong University of Science and Technology [Medical Sciences]* **33**:272-76.

Yatham, L. N., Liddle, P. F., Dennie, J., Shiah, I. S., Adam, M. J., Lane, C. J., Lam, R. W. & Ruth, T. J. 1999. Decrease in brain serotonin 2 receptor binding in patients with major depression following desipramine treatment: a positron emission tomography study with fluorine-18-labeled setoperone. *Archives of general psychiatry* **56**:705-11.

Yin, C. Y., Evason, K. J., Asahina, K. & Stainier, D. Y. R. 2013. Hepatic stellate cells in liver development, regeneration, and cancer. *Journal of Clinical Investigation* **123**:1902-10.

Zeng, X. Q., Li, N., Pan, D. Y., Miao, Q., Ma, G. F., Liu, Y. M., Tseng, Y. J., Li, F., Xu, L. L. & Chen, S. Y. 2015. Kruppel-like factor 2 inhibit the angiogenesis of cultured human liver sinusoidal endothelial cells through the ERK1/2 signaling pathway. *Biochemical and biophysical research communications* **464**:1241-7.

Zhang, F., Tang, Z., Hou, X., Lennartsson, J., Li, Y., Koch, A. W., Scotney, P., Lee, C., Arjunan, P., Dong, L., Kumar, A., Rissanen, T. T., Wang, B., Nagai, N., Fons, P., Fariss, R., Zhang, Y., Wawrousek, E., Tansey, G., Raber, J., Fong, G.-H., Ding, H., Greenberg, D. A., Becker, K. G., Herbert, J.-M., Nash, A., Yla-Herttuala, S., Cao, Y., Watts, R. J. & Li, X. 2009a. VEGF-B is dispensable for blood vessel growth but critical for their survival, and VEGF-B targeting inhibits pathological angiogenesis. *Proceedings of the National Academy of Sciences* **106**:6152-57.

Zhang, J., Yang, P. L. & Gray, N. S. 2009b. Targeting cancer with small molecule kinase inhibitors. *Nature reviews. Cancer* **9**:28-39.

Zhang, L., Zhou, F., Han, W., Shen, B., Luo, J., Shibuya, M. & He, Y. 2010. VEGFR-3 ligand-binding and kinase activity are required for lymphangiogenesis but not for angiogenesis. *Cell research* **20**:1319-31.

Zhou, S. F. 2009. Polymorphism of human cytochrome P450 2D6 and its clinical significance: Part I. *Clin Pharmacokinet* **48**:689-723.

Zhu, B., Zhang, P., Zeng, P., Huang, Z., Dong, T. F., Gui, Y. K. & Zhang, G. W. 2013. Tissue factor pathway inhibitor-2 silencing promotes hepatocellular carcinoma cell invasion in vitro. *Anat Rec (Hoboken)* **296**:1708-16.

Zhu, K., Pino, M., Siefker-Radtke, A., Shalinsky, D., Hu-Lowe, D. & McConkey, D. 2006. AG-013736, a novel VEGF receptor and PDGF receptor inhibitor with potent activity against human bladder carcinoma in vitro and in vivo. *ASCO Annual Meeting Proceedings.* pp. 13109.

Zhuang, G. & Ferrara, N. 2015. The VEGF Receptor Family. *In*: Wheeler, L. D. & Yarden, Y. [Eds.] *Receptor Tyrosine Kinases: Family and Subfamilies.* Springer International Publishing, Cham, pp. 821-41.

Zivi, A., Cerbone, L., Recine, F. & Sternberg, C. N. 2012. Safety and tolerability of pazopanib in the treatment of renal cell carcinoma. *Expert Opinion on Drug Safety* **11**:851-59.

Zopf, D., Heinig, R., Thierauch, K.-H., Hirth-Dietrich, C., Hafner, F.-T., Christensen, O., Lin, T., Wilhelm, S. & Radtke, M. 2014. Abstract 1666: Regorafenib (BAY 73-4506): preclinical pharmacology and clinical identification and quantification of its major metabolites. *Cancer research* **70**:1666.